Politecnico di Torino

Master Course in ICT for Smart Societies

Academic Year 2021/2022

October 2022

Master's Degree Thesis

Control approaches for ventilative cooling and indoor air quality systems in a school demo-building in Torre Pellice

Advisor:
Prof. Chiesa Giacomo

Co-Advisor:
Eng. Fasano Francesca

Candidate:
Vigliotti Manuela

Acknowledgements

This thesis is my Master's Degree in ICT for Smart Societies' conclusion at the Politecnico di Torino. It was a challenging path, made lighter thanks to all the people who have always supported me and believed in me.

For this reason, I would like to sincerely thank my advisor Prof. **Giacomo Chiesa** and its collaborators, Engs. **Francesca Fasano** and **Paolo Grasso**, for all the help in the development and writing of the thesis and for their wide availability.

Moreover, I would like to express my deepest gratitude to my partner **Denis** without which I could not have undertaken and completed this journey, for all his support and suggestions.

Lastly, I would like to mention **my family and that of my partner**, which have always been present in moments of need.

This thesis is part of the **E-DYCE project** [24] under POLITO works. This project has received funding from the European Union's **Horizon 2020** research and innovation programme under grant agreement No 893930/06/ (E-DYCE)

Abstract

Indoor air quality and ventilative cooling for thermal comfort are critical to assure space comfort conditions. This thesis aims to implement a control solution to manage remotely different detached mechanical ventilation units installed in a school demo building in Torre Pellice that is part of the E-DYCE European project. The main objective is to control indoor air quality and ventilation for cooling with different control strategies. Control approaches can be monitored using SOAP to retrieve current conditions of rooms from sensors and Modbus to control the mechanical ventilation units or simulated with the Energy Management System of EnergyPlus. All different controls are compared by considering thermal and air quality indicators and energy consumption.

Keywords: EnergyPlus simulation, Energy Management System, E-DYCE project, mechanical ventilation, indoor air quality, thermal comfort, ventilative cooling, SOAP, Modbus, energy consumption.

Contents

1. Thesis Structure

In section 2, a general introduction of the topic is presented, also introducing the case study of this thesis. In section 3, state-of-the-art solutions are introduced, both for indoor air quality monitoring and ventilative cooling, and in section 4, used tools and methodologies are reported. In section 5, the modeling part of the thesis is described. In particular, it explains how classrooms' models with mechanical ventilation are obtained and how they are calibrated considering temperature, CO_2, electrical consumption, and the mechanical ventilation airflow. In section 6, the software used to modify IDFs for models' calibrations is presented, while in 7, the software structure used to retrieve and process data used in the calibration process is illustrated in detail. Then in 8, all strategies simulated through IDF models are described, and in 9, results are reported and commented. In chapter 10, the hardware structure that will be installed in Torre Pellice school to test strategies in real conditions is explained, and in 11 the relative software structure that will run on that hardware is presented in depth. Eventually, in 12, monitored strategies tested in the school are investigated, and corresponding results are shown and analyzed in 13. In 14, conclusions of the thesis obtained from results of both simulated and monitored strategies are outlined. The complete flow of the structure can be deepened in Fig. 1.1.

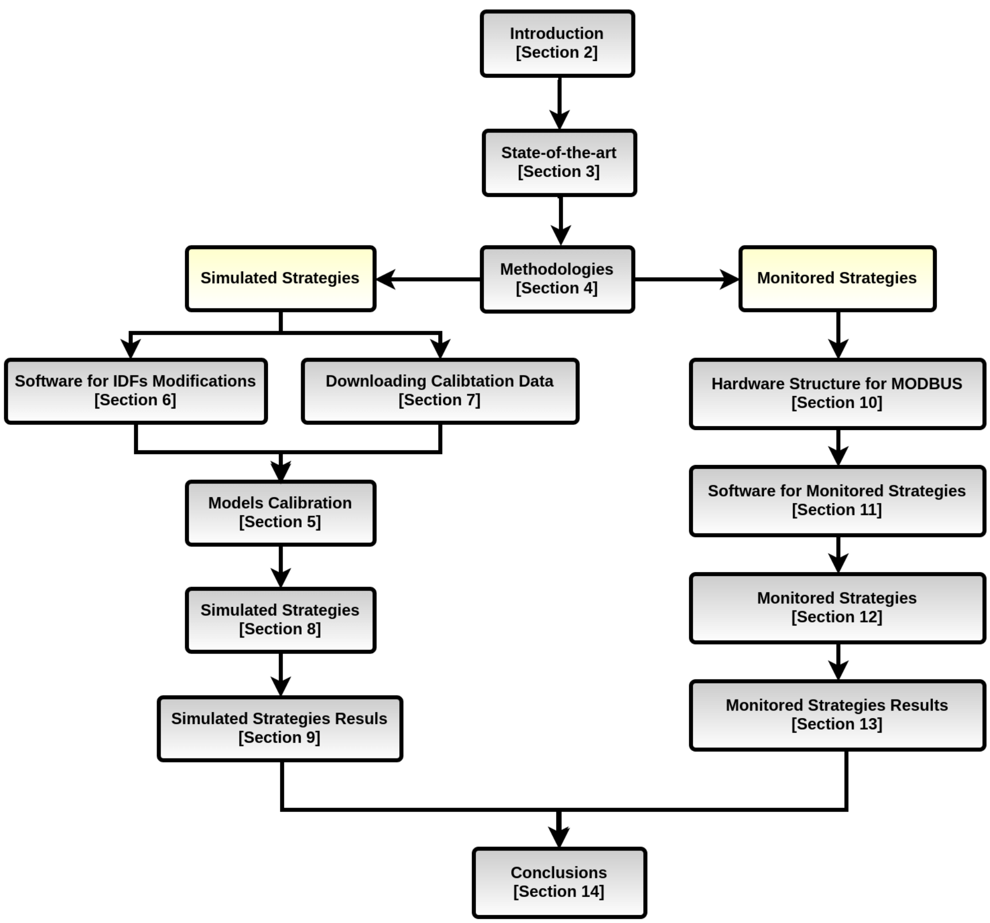

Figure 1.1: Thesis structure

2. Introduction

2.1 Overview of the topic and related issues

A well-ventilated indoor environment is a prerequisite for the building's occupants' health, as a high CO_2 concentration is related to a reduction in the occupants' attention and vigilance, negatively affecting memory and focus capacities [5, 20, 40]. Moreover, it has been proved that elevated indoor CO_2 levels are strictly related to the increasing of sick building syndrome symptomatology, which includes rash, headaches, fatigue, eye irritation, and respiratory disease [52, 69].

These effects are of crucial importance if it is considered that people spend more than 90% of their time indoors, and, if children are considered, the impact is even higher given that they also spend 30% of their life in schools [5, 20]. Therefore, it is increasingly important to ventilate schools correctly.

Besides CO_2, various contaminants need to be monitored to guarantee the healthiness of indoor spaces. Those pollutants can be generated from indoor sources or come from outside. Moreover, they can be divided into two main categories:

- bioeffluents that are generated by the human body, like CO_2, odor, particulates, water vapor, biological aerosols, and other pollutants,
- pollutants produced by buildings and materials, like VOCs and TVOCs, which are dangerous for the occupants' health because some are suspected or known carcinogens, while others are irritants or have an annoying smell.

If the building is crowded, like schools, offices, and commercial buildings, it has been proved that carbon dioxide is a good indicator of the overall air quality [51]. In fact, in these cases, people are the most relevant source of CO_2 production, so this gas can be considered a marker for all human-related contaminants as they are roughly correlated with CO_2 emissions by breathing. Building-produced pollutants are instead poorly correlated with it, so for most applications, minimum constant ventilation is kept for the whole occupation period. In other cases, CO_2-based ventilation is combined with a night purge to dilute all contaminants produced by buildings and materials before occupants come in the morning [16, 32, 52].

In addition, the need for healthy indoor air quality has started to attract more and more attention in recent years, especially because of the spreading of SARS-CoV-2, whose principal transmission mode is due to infectious respiratory droplets in indoor environments' air. These droplets can be considered air pollutants, so they can be removed through ventilation to ensure the environment's healthiness [23, 63]. Besides COVID-19, airborne transmission is among the most relevant transmission modes of several diseases spread between people in the same space. So, ventilation assumes a vital role in today's school buildings to avoid the spreading of respiratory illness among children, and as a consequence, to their families.

In addition to previous advantages, it has been proved by many studies that the use of mechanical ventilation with an appropriate control strategy can lead to energy savings of up to 38% [16, 51, 52, 65, 75], especially during the winter period since it avoids heat dispersion due to excessive ventilation. These savings in building consumption can lead to the reduction of global warming and energy waste because the building sector is accounted for 40% of the primary energy used worldwide [31, 35, 42, 65].

Another strategy that allows saving energy in buildings is ventilative cooling [12, 35, 62]. Ventilative cooling is a technique whose aim is to reduce the indoor environment's temperature to guarantee thermal comfort in order to decrease or completely prevent cooling energy consumption by using colder outdoor air for ventilation [19]. The hotter the weather, the higher can be the savings [63].

2.2 E-DYCE Project

E-DYCE [24] is a European project that is part of a larger group of projects called H2020 aimed to support and encourage research projects during the period from 2014 to 2020 [29]. The main aim of the E-DYCE project is to create an innovative approach to increase reliability, scalability, adaptability, and accuracy of the Energy Performance Certification, exploiting real-time optimization of building performances and comforts and considering the building's dynamic behavior to evaluate a Dynamic Energy Performance Certification. It provides, in addition, intuitive feedback to owners and professionals, to enhance the communication between them. In this way, benefits on both indoor environmental conditions and energy consumption can be achieved.

Another E-DYCE aim is to improve the energy performance assessment to include rules to evaluate the DEPC in free-running buildings and old cultural heritage ones.

The E-DYCE project has demo buildings in different locations over Europe [18]:

- Geneva (Switzerland);
- Torre Pellice (Italy), where demo buildings include both schools and residential buildings;
- Nicosia (Cyprus);
- Hånbæk Frederikshavn (Denmark);
- Aalborg (Denmark).

2.3 Thesis Objectives

This thesis aims to implement a control solution to manage remotely three different detached mechanical ventilation units installed in an E-DYCE school demo building in Torre Pellice. The main objective is to control indoor air quality and ventilation for cooling by comparing different control strategies that run in parallel over three units to find the optimal one, considering both environmental parameters and energy consumption. Control approaches for ventilative cooling are monitored by testing them in the school by using SOAP to retrieve the current conditions of rooms from Capetti sensors and Modbus to send control signals to mechanical ventilation units. Strategies related to indoor air quality control are instead both monitored and simulated with the Energy Management System of EnergyPlus using calibrated models of real rooms to obtain significant results.

Nomenclature

ACH Air Changes per Hour
ASCII American Standard Code for Information Interchange
ASHRAE American Society of Heating, Refrigerating and Air-Conditioning Engineers
CAV Constant Air Volume
CO_2 Carbon Dioxide
COVID-19 Coronavirus Disease 2019
CSV Comma-Separated Values
DB DesingBuilder
DEPC Dynamic Energy Performance Certification
E-DYCE Energy flexible DYnamic building CErtification
EMS Energy Management System
EPC Energy Performance Certification
EPW EnergyPlus Weather File
ERL EnergyPlus Runtime Language
GET Method used to retrieve information about the REST API resource

Nomenclature

GPIO General Purpose Input/Output
H2020 Horizon 2020
HDMI High-Definition Multimedia Interface
HTTP HyperText Transfer Protocol
HVAC Heating, Ventilation and Air Conditioning
IAQ Indoor Air Quality
IDF Input Data File
IP Internet Protocol
IR InfraRed
KPI Key Performance Indicator
LLS Linear Least Squares
MAPE Mean Absolute Percentage Error
MBE Mean Bias Error
MPC Model Predictive Control
MQTT MQ Telemetry Transport
OS Operating System
POST "REST method used to request that the origin server accept the entity enclosed in the request as a new subordinate of the resource identified by the Request-URI in the Request-Line" [36]
PREDYCE Python semi-Realtime Energy DYnamics and Climate Evaluation
PRELUDE Prescient building Operation utilizing Real Time data for Energy Dynamic Optimization
REST REpresentational State Transfer
RMSE Root Mean Squared Error
SARS-CoV-2 Severe Acute Respiratory Syndrome CoronaVirus 2
SBDCV Sensor-Based Demand-Controlled Ventilation
SBS Sick Building Syndrome
SBV Smart Building Visualizator
SHGC Solar Heat Gain Coefficient
SOAP Simple Object Access Protocol
SSH Secure SHell
TVOC Total Volatile Organic Compounds
UART Universal Asynchronous Receiver-Transmitter
URL Uniform Resource Locator
VC Ventilative Cooling
VNC Virtual Network Computing
VOC Volatile Organic Compound
VPN Virtual Private Network
W3C World Wide Web Consortium
XML eXtensible Markup Language

3. State of the art

In the following paragraphs, state-of-the-art methods for both dilutions of bioeffluents and other indoor pollutants and ventilative cooling techniques will be inspected, aiming at understanding the most recent solutions for these kinds of applications in order to be exploited in this work.

3.1 Indoor Air Quality

Different control strategies can be used to ventilate interior spaces through mechanical ventilation systems in order to ensure a healthy environment for occupants.

Sensor-based demand-controlled ventilation use sensors to monitor the environment and decide related actions based on sensed values. SBDCV has been proved to be more effective with the following conditions [32]:

- a single or a limited group of contaminants is predominant in the considered space so that by controlling them it is possible to provide a healthy indoor condition;
- rooms with highly variable occupancy that can not be predicted;
- places with lots of needs for heating or cooling;
- places with very expensive energy.

The main methodologies are usually based on:

- bioeffluents emitted by people through breathing, whose indicator is the CO_2;
- pollutants produced by other sources within the indoor space, like radon or VOCs;
- building's occupancy detected through IR-sensors [51].

In the school studied by the E-DYCE project, only CO_2 sensors are present in all rooms with mechanical ventilation, so the main focus of this work will be on CO_2-based control techniques to improve indoor air quality. In addition, in one of the monitored classrooms, the sensor for VOC is present, allowing complete supervision of air contaminants before and after ventilation.

3.1.1 Constant Air Volume Strategy

One of the most basic strategies to control mechanical ventilation is to provide constant air exchange from outside following a given schedule. The ventilation flow is designed for the maximum load of expected air contaminants. This technique is called CAV, and it is used in most cases because of its simplicity [51, 52, 66, 71, 75].

The ventilation rate can be calculated according to ASHRAE 62:

$$V = R_p P_z \tag{3.1}$$

where V is the outdoor air ventilation rate in L/s, R_p is the required outdoor airflow rate per person in $L/s/person$ and P_z is the expected number of people in the area. According to this standard, in classrooms, the minimum ventilation rate must be 8 $L/s/person$ [53]. It does not require a minimum amount of ventilation when the zone is unoccupied, so pollutants coming from buildings and materials may reach dangerous and uncomfortable levels. In the new version of the standard, ASHRAE 62.1, this problem is addressed by providing ventilation that depends on the room dimension. The ventilation rate V can be calculated as:

$$V = R_p P_z + R_A A_z \tag{3.2}$$

where R_A is the outdoor air ventilation rate per floor area $L/s/m^2$ and A_z is the zone floor area in m^2, R_p is set to 5 $L/s/person$ and R_A to 0.6 $L/s/m^2$ [4].

However, this method may lead to over-ventilation and waste of energy for most of the time or to under-ventilation for short periods if the space is more crowded than expected. These issues can be avoided by using suitable control solutions and making decisions based on monitored environmental values.

3.1.2 CO_2 Thresholds Control Strategies

In other widely used control approaches, CO_2 sensors are installed to monitor space conditions to decide in a more optimized way when to start and stop ventilating and the amount of airflow needed [52].

The most basic CO_2-based strategy is developed by identifying a threshold for the maximum allowable CO_2 measurement. The ventilation is started when the sensed value is above the limit, and it is stopped when the carbon dioxide concentration is below the chosen value. In most applications, the CO_2-set-point is set to $1000ppm$ [5,16,32,65,71]. To limit the number of on/off cycles of the mechanical ventilation system it is possible to use a double threshold, considering different values for activating and deactivating the ventilation flow [37,51].

3.1.3 Occupancy Detection using CO_2 Control Strategies

Another strategy is based on estimating the occupants' number when occupancy is unpredictable thanks to CO_2 measurements, given that people are the primary source of indoor carbon dioxide generation. In this case, the airflow selected is proportional to occupancy and varies between the minimum and maximum values [16,52,66,75] that can be provided by the mechanical ventilation system. In a classroom, the students' number is predictable, so it is less convenient to use this kind of control, given that the number of occupants is always known for both lesson and non-lesson time. By simply measuring the CO_2 level, it is possible to understand whether students are in the classroom or not.

3.1.4 CO_2-based Control Strategies combined with Purge

Sometimes the CO_2 based strategy is combined with a second parameter that indicates those pollutants that are not produced by the human body but are dangerous to the health [16,60], like TVOCs, VOCs, and radon. This dual-mode is composed of two different phases:

- the real-time modulation mode used when the building is occupied. In this mode, the mechanical ventilation is controlled usually by monitoring CO_2 and taking decisions according to its current level;
- the purging mode used when the building is empty. It aims to remove all air contaminants generated by space and materials. Here the fan speed selected is the maximum available, and the mechanical ventilation is activated based on levels of the chosen second parameter.

3.2 Ventilative Cooling

There are different types of control strategies that are used to provide ventilative cooling correctly. They can range from spontaneous to fully automated ventilation that can use different control algorithms.

3.2.1 Spontaneous Occupant Manual Ventilation

The simplest way to implement ventilative cooling control with no maintenance at all is based on windows' manual opening according to occupants' perceptions of indoor conditions [19]. Nevertheless, users' perceptions may not represent and follow the changing external and internal situations [17, 31]. Therefore, more complex strategies have been developed to obtain energy savings and better indoor conditions.

3.2.2 Informed Occupant Manual Ventilation

In this case, information about when to ventilate is provided to the user, who is required to perform appropriate actions [1, 10]. Even in this case, energy savings and thermal comfort were not satisfactory and not significantly improved compared to the spontaneous control [17]. Moreover, performance is dependent on the responsiveness of occupants, and the worst results are achieved when the responsiveness is smaller. Finally, if the number of requests is very high, it may be a burden for the user to follow instructions in the long term. To solve this last point fixed operation schedule can be used [17]. In this case, occupants check instructions at fixed points during the day to complete suggested actions and ignore them for the rest of the time.

3.2.3 Fully Automated Ventilation

These kinds of controls are the ones that provide better performances considering energy consumption and thermal comfort [10, 35]. According to [17] it is possible to save up to 80% of energy without sacrificing comfort at the cost of a large initial investment and high maintenance requirements. There are two different possibilities to control ventilation to cool the environment automatically:

- by using automatic control of windows opening through heuristics [11, 17], advanced model predictive control [17, 39, 43], and machine-learning techniques [45];
- by pumping air from outside using a mechanical ventilation system where the most common strategies are heuristic controls [19].

3.2.4 Rule-based Heuristics Control

One of the most used heuristics for HVAC systems is the rule-based one [19]. It is based on a decision tree where, at each stage, a sensed parameter is compared with a predefined nominal value to decide which branch to follow [12]. Leaves contain specific actions to be taken based on environmental conditions questioned before.

3.2.5 Model Predictive Control

MPCs are less used compared to heuristic methods because of their complexity [19]. They need a physical building model to simulate the evolution of parameters under observation [35].

3.2.6 Reinforcement Learning Control

They are less complex when compared to MPCs because they do not need the building's model to find the optimal action to perform [19], but they require a lot of data.

3.2.7 Parameters Monitored for Ventilative Cooling

For developing a correct control strategy for ventilative cooling, the most important parameters that should be monitored are [1, 19, 35]:

- internal temperature;
- external temperature;
- CO_2;
- humidity;
- external weather conditions, just when the system is not mechanical.

3.2.8 Internal and External Temperature-based Control

There are two most common ways to implement ventilative cooling [19]:

- increase the ventilation flow rate;
- use night-time air to pre-cool indoor spaces [42], which is particularly suited for schools given that they are not occupied during the night.

One of the simplest controls is based on a single temperature threshold. If the internal temperature is lower than the set-point selected, there is no need to cool the room through ventilation. Otherwise, if the external temperature is lower than the internal one, external air can be used to cool the space inside the building, otherwise, ventilation would lead to a heating of the environment, and for this reason it is kept off. This strategy can also use two different thresholds to avoid continuous on-off cycles of the mechanical ventilation [37]. In this case, the lower threshold is used to turn off the ventilation, while the higher one is used to start ventilating spaces.

There are also more complex strategies, in particular, a correct cooling strategy should depend on the difference between the indoor temperature set as comfortable and the outdoor air temperature [12, 19]:

- if the difference is more than $10°C$, and the outdoor air temperature is lower than the indoor one, the ventilation flow rate should be kept to its minimum to avoid too cold and uncomfortable conditions in indoor spaces;
- if the difference is between $2°C$ and $10°C$, and the outdoor air temperature is still lower than the indoor one, the airflow should be set to its maximum value to cool the indoor environment to reach a comfortable condition [21, 60];
- if the difference is in the range between $-2°C$ and $+2°C$, the airflow should be set to its minimum value during daytime and to its maximum value at night. By doing this, the indoor environment is pre-cooled during night-time, and during day-time, ventilation is kept to its minimum so that fresh air is not dispersed;
- if the outdoor air is hotter and more humid compared to the indoor one, the air supply should be set to its minimum to avoid bringing outdoor heat into occupied spaces.

The comfortable indoor temperature can be set differently based on season and hour of the day, as can be seen in [30].

3.2.9 Night-time Ventilation

Night ventilation allows to pre-cool the environment so that in the morning when occupants enter the building, internal conditions are more comfortable for what concerns both air pollutants and indoor temperatures. Night-time ventilation is more effective in those buildings that are unoccupied during night hours because there is no problem of thermal discomfort. Reasonably, the higher the building's thermal mass, the more effective will be nighttime ventilation [42]. As [42] also states, ventilating during the night can affect thermal comfort in four different ways:

- reduce indoor air temperature's peaks;
- reduce the mean air temperature during the day, particularly in the morning;
- reduce slab temperatures;
- the internal maximum temperature is reached after the maximum external peak, and not at the same time.

Moreover, it is shown in [42, 48, 70] that advantages that come from using a very complex control strategy are very small if compared with a simpler fixed-rules approach as long as over-cooling control is considered in both cases. One of the most used strategies for nighttime ventilation is to keep a constant airflow for the whole duration of the selected night period if the internal temperature is higher than a threshold, otherwise, ventilation is switched off to guarantee thermal comfort in the morning [41, 42]. Usually, a threshold for the outdoor temperature value is also considered. It has been proven in [59] that through the use of this kind of ventilation it is possible to decrease the next day's peak indoor temperature up to three degrees.

3.2.10 Humidity-based Control

Another crucial factor to be monitored for comfortable indoor conditions when ventilative cooling strategies are actuated is humidity [34] as specified in 3.2.7. One of the most used and simple strategies for controlling ventilation based on this parameter [21] is by using a single threshold value. If the indoor relative humidity is higher than the selected value and the indoor humidity is higher than the external one, the environment should be ventilated using a fan speed that depends on indoor and outdoor temperatures to avoid uncomfortable thermal conditions.

3.2.11 CO_2-based Control

In some applications, in addition to temperature and humidity controls, indoor air quality is also taken into account. In those cases, the minimum amount of ventilation provided is always higher than the flow rate needed for having good indoor air quality [1, 34, 63].

4. Case of Study and Methodologies

In the secondary school in Torre Pellice have been installed, thanks to funds from the E-DYCE project, three Helty Flow M800 units to improve the school's indoor air quality and energy consumption performance. By using these units, heating energy consumption is reduced by substituting cold and polluted outdoor air that enters the room through open windows with warmer and filtered air coming from the heat recovery system of mechanical ventilation units.

4.1 Capetti Winecap System

Sensors installed in Torre Pellice school belong to Capetti company. Capetti [13] is an Italian electronic company that mainly provides wireless sensors, but it also develops monitoring user interfaces. Sensors' data can be downloaded by using SOAP protocol to be stored in an InfluxDB Database where they can be easily retrieved when needed. Sensors were installed in the school in the spring of 2021, so they already got a lot of data that can be used to calibrate school models.

4.2 SOAP Protocol

Capetti WineCap system uses Simple Object Access Protocol (SOAP) to communicate and transmit data on HTTP. SOAP protocol [6] is an open protocol based on Client/Server architecture, developed and maintained by W3C, using XML messages over HTTP services.

4.3 Helty Flow M800

In the secondary school have been installed, thanks to E-DYCE funding, three Helty Flow M800 ventilation units [38]. These units are inserted within a closet and can sanitize indoor air by pumping up to $800m^3/h$ of fresh air with ten different fan speeds. They have filters to purify incoming air from outdoor-generated pollutants like smog, particulates, and pollen and they have heat recovery units with a thermal efficiency of 82% to reduce the waste of energy needed to heat classrooms. The Helty mechanical ventilation units can be controlled on-site through a control panel on the closet and remotely using Modbus RS485 protocol.

The heat recovery bypass can be set by selecting two different values:

- a first value that must be between 5°C and 30°C that represents the beginning of the interval, X;
- a second value between 2°C and 15°C that indicates the delta Y that is summed to X to obtain the interval $[X,\ X+Y]$ in which the exchange of heat between incoming outdoor air and exiting indoor air is prevented.

In the interval $[X,\ X+Y]$, warmer indoor air can be exchanged with colder outdoor air without the heat recovery system in order to cool the indoor environment. For testing ventilative cooling strategies in the school, the X value has been set to 16°C, and the Y value to 15°C.

Exhaust and input fans of Helty units have a speed that can be adjusted over 10 different speeds, which are 100/180/260/340/420/500/580/640/720/800 m^3/h, and the declared absorbed power at maximum speed is 188W.

4.4 Classrooms with Mechanical Ventilation Units

One room for each different floor is chosen for installing mechanical ventilation units for the demo school building in Torre Pellice. The selected room's area on the first floor, whose chosen nomenclature code is $act201bc$, is equal to the second floor's one, $act201cc$, which is 58.85 m^2. On the contrary, the area of the third-floor room, $act208da$, is bigger, and its value is 98.93 m^2, so ventilation will be less effective because of the bigger space volume, but CO_2 concentration will be also lower because it is more diluted in the bigger amount of air. All three selected rooms are designed for around 17 to 22 people and are used as classrooms during the school year, so they hold equivalent activities. In this thesis, 18 people are considered within each room.

4.5 Modbus RS485 Protocol

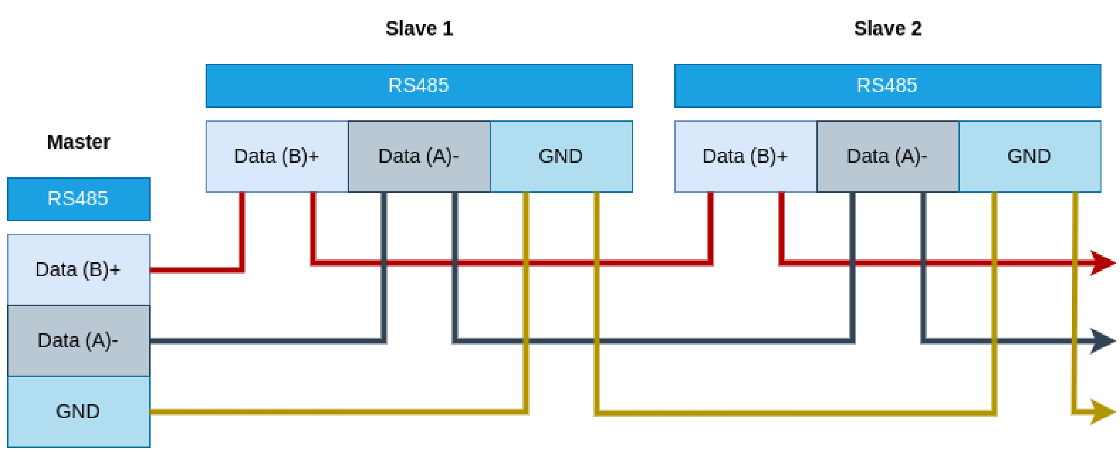

Figure 4.1: Modbus RS485 connection scheme

Helty Flow M800 units can be controlled by setting an hourly schedule from the command monitor equipped on the unit case or by changing the values of registers by using Modbus. The Modbus version supported by these systems is the wired RS485, which in this application is characterized by:

- baud rate of 4800 or 9600 based on the considered configuration;
- stop bit of 1;
- parity bit of None;
- starting registers address of 00;
- address size of 8 bit.

Modbus RS485 [49] is a wired protocol that uses a two or four-wire physical interface to transfer information. It allows both point-to-point and multi-point communications, having a Master Device as coordinator of communications and one or more Slave Devices that receive instructions. The connection scheme can be seen in 4.1, where the ground wire is optional.

4.6 Software Tools Used

In this thesis, different software tools are used in addition to Python programming, particularly for managing and modeling the school demo-building. All these software will be briefly listed in this paragraph.

4.6.1 DesignBuilder

DesignBuilder [22] is a licensed tool that has been used thanks to the license provided by Politecnico di Torino. It is a simulation tool that can perform optimizations and dynamic simulations of buildings. It allows 3D modeling of structures through a user-friendly interface, enabling also graphical visualization of results. It can export the model in various formats, among which there is the EnergyPlus one.

It will be used to model the school demo-building and export models in the above-mentioned format to obtain an editable IDF.

4.6.2 EnergyPlus

EnergyPlus [26] has been founded by the U.S. Department of Energy in 1997. It is a building performance-driven simulation program that allows, in addition to the simulation of building dynamics, also the one of water usage and energy consumption. It is free, open-source, and works in different operating systems. It includes an IDF Editor that allows editing files in IDF format.

It is used, by giving as input the IDF file containing the school demo-building model, to simulate it and to obtain environmental parameters and consumption as output.

IDF Format

Even Input Data Files have been developed by the U.S. Department of Energy with the EnergyPlus tool. IDFs [7] are ASCII files that model the building and its HVAC system to simulate it through EnergyPlus to obtain the values of the most relevant environmental and consumption parameters.

The rules that characterize an IDF file are:

- it is structured only by commas, which are used to separate fields of objects, and semicolons, that instead separate each object from others;
- the relationship between fields and data is defined only by the latter's positions;
- spaces and returns are used only for better visualization and do not influence information contained in the IDF;
- comments are inserted with the "!" character and are ignored from the simulation program;
- it is case insensitive.

4.6.3 PREDYCE Python Library

PREDYCE [54] is a Python library that has been developed by Politecnico di Torino and which is part of two European H2020 projects: E-DYCE and PRELUDE.

In this thesis, it is used for obtaining functions needed to modify IDFs and for calibrating them.

4.6.4 Eppy

Eppy [28] is a scripting language written in Python that is used for the management of EnergyPlus IDFs and output files. It allows navigation and modification of IDF files directly from programming interfaces.

It is used to run EnergyPlus simulations in parallel directly from Python by passing IDF files as building models.

4.6.5 *PyModbus* Python Library

PyModbus [55] is a Python library used to implement the Modbus protocol to establish a communication that can be synchronous or asynchronous. It supports different Modbus types of communications, among which there is the one supported by the chosen mechanical ventilation units: the serial RS485. It is very lightweight and can run even on basic interfaces, so it is perfect to be implemented on Raspberry Pi.

In this thesis, the ***PyModbus*** Python library is used to write scripts that simulate both the Modbus Master simulator that will run on Raspberry Pi and the Slave simulator, used to test strategies with the laptop before the implementation in the school.

5. Models Calibration

5.1 Models of the Classrooms

For the thesis' simulation part, the school DesignBuilder model (Fig. 5.1) was modified to obtain IDF files that will allow the calibration of the environmental behavior of rooms with mechanical ventilation.

To obtain these IDFs, the steps followed starting from the original DesignBuilder model are:

- for each different room with the mechanical ventilation, create a different DesignBuilder model so that they can be modified independently;
- for each DB model, every element is deleted except for the floor corresponding to the room of interest. If the room is on the third floor, also the roof is kept to have a more accurate model to be simulated. In this way, the simulation will be much lighter, and it will run faster. So a larger number of simulations can run in parallel to find optimal calibration parameters in a reasonable time;
- all the surfaces that were adjacent to some removed object were made adiabatic to avoid heat dispersion. Given that the mechanical ventilation units are placed on different floors, after these steps, the three different models that contain just a single floor can be seen in 5.2, 5.3 and 5.4, where the dark pink room is the one with the mechanical ventilation unit;
- IDFs are then exported from models in the EnergyPlus 8.9 version.

5.2 Data Needed for the Calibration

5.2.1 Weather Data

Thanks to E-DYCE funding, a real-time weather data station has been installed in Torre Pellice on the roof of the "Liceo Valdese" high school. In this way, it is possible to obtain accurate weather data to be used in

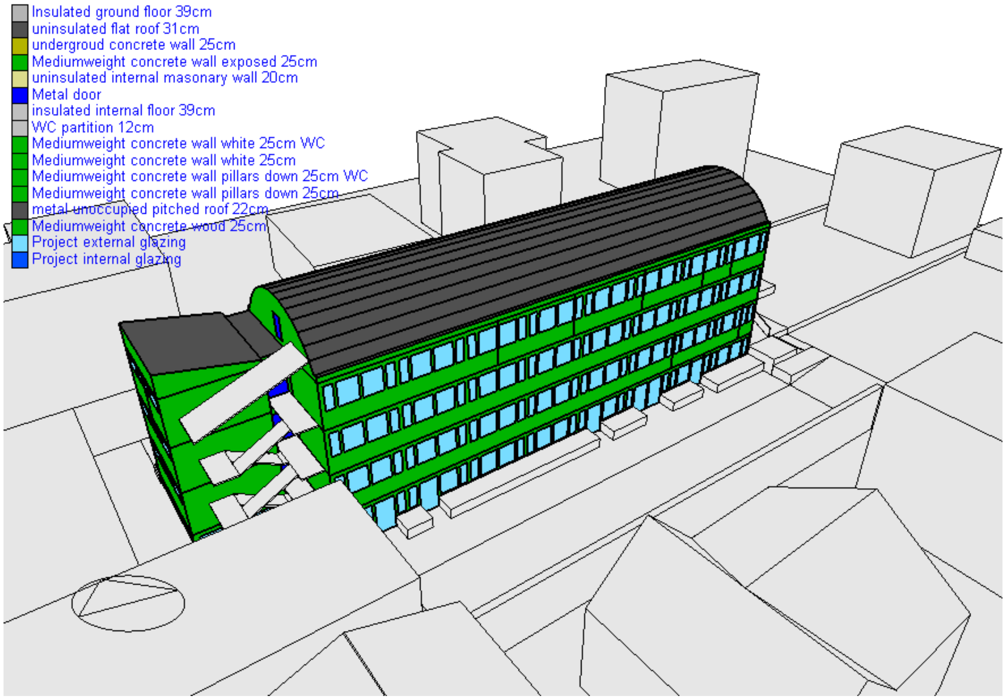

Figure 5.1: Model of the school in DesignBuilder

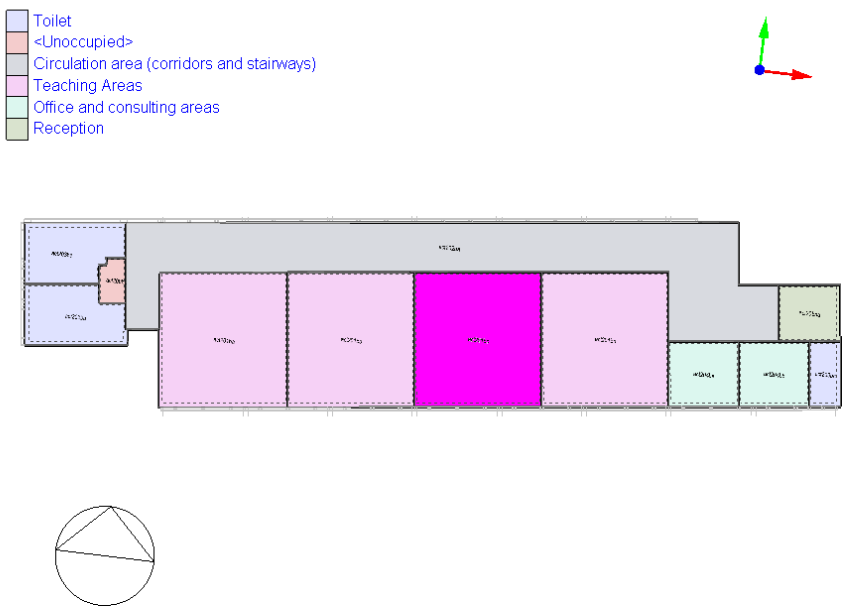

Figure 5.2: Model of the first floor in DesignBuilder, with the room *act*201*bc*

EnergyPlus simulations to get more reliable results. Data are downloaded and stored in EPW files thanks to the EPW compiler developed in the PREDYCE project.

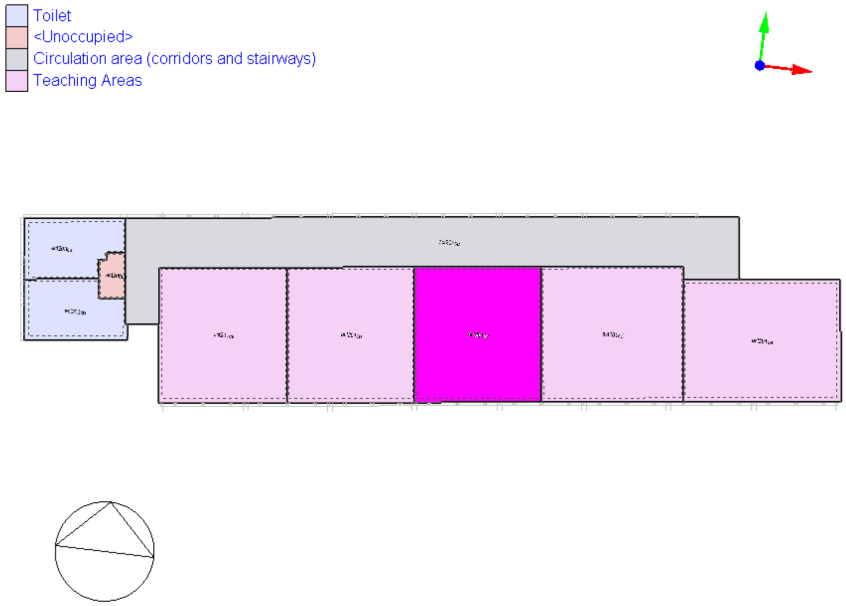

Figure 5.3: Model of the second floor in DesignBuilder, with the room *act*201*cc*

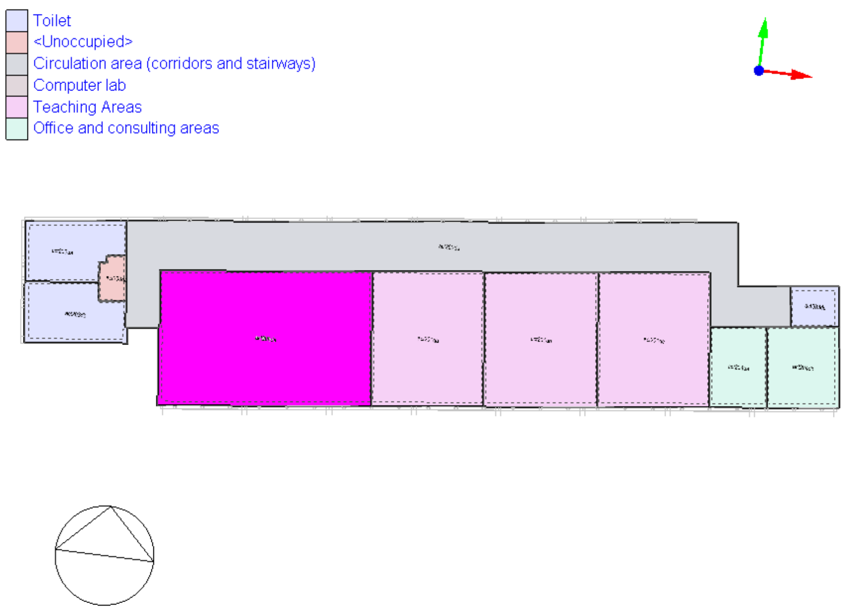

Figure 5.4: Model of the third floor in DesignBuilder, with the room *act*208*da*

5.2.2 Sensors' Data

To correctly calibrate the models, school data taken from sensors are needed. The software developed to retrieve them will be comprehensively described in section 7.

The first calibration step aims at sizing indoor temperatures of the rooms under study while temperatures of the other rooms are fixed using values retrieved from sensors. The selected calibration period is from 01/07/2021 to 31/07/2021 because the absence of people removes environmental parameters' uncertainties due to occupation, but the EnergyPlus simulator requires data for the whole year. For this reason, all 2021 data was downloaded and the unavailable ones from the beginning of the year, when sensors had not yet been installed, were filled with the value 20°C. Therefore, for all areas of the same floor except for the one that contains the mechanical ventilation system, temperature measurements are retrieved from sensors, filled, aggregated hourly, and then stored in a CSV file. The data of the room under study are also collected for the whole calibration period, except for the first six days that EnergyPlus considers as warm-up days, to compare simulation results with actual measured data to evaluate the error between the calibration output and the school environment behavior.

The second step is to calibrate the CO_2 of the target room for the whole year. In this case, CO_2 values of the other rooms are not relevant for the sizing, so just the data of the room with mechanical ventilation are downloaded, filled, aggregated hourly, and stored in a CSV file.

Eventually, the temperature calibration validity over time is tested, considering all the available data for 2021 and 2022. Therefore, a file that contains all the available temperature data of 2022 aggregated hourly is also needed.

5.3 IDFs Modifications Before Calibration

After the generation from DB models, IDFs are not ready to be calibrated, and some modifications are necessary:

- for all the rooms, except for the one that should be calibrated, heating and cooling set-point schedules are changed from *Schedule:Compact* to *Schedule:File*. The new schedules take as input the column of the CSV file that contains all the retrieved temperature data from the sensor of the corresponding room;
- for all the rooms, except the one with mechanical ventilation, heating and cooling availability schedules are modified to be always on. The result of these two last points is that the temperature of all the rooms, except the one to calibrate, is fixed to the monitored value for each simulation time step;
- to further increase the simulation's speed, all unused outputs are deleted from the IDFs;
- for the same reason, all the objects *OtherEquipment* and the associated schedules are deleted;
- for all the rooms, except for the target one, *People* and *ZoneVentilation:DesignFlowRate* objects are deleted because monitoring them does not add any improvement to the calibration given that the temperature in those areas is fixed;
- occupancy and lighting schedules of the room of interest are changed into more realistic ones;
- the number of $people/m^2$ is changed considering 18 people in classrooms;
- in the *ZoneVentilation:DesignFlowRate* of the room to calibrate, remove the minimum indoor temperature limit and the maximum temperature difference for the operation leaving default values. In this way, the occupants' behavior is more similar to the real one, that is to ventilate a lot regardless of internal environmental conditions also because of the COVID-19 normative.

5.4 Temperature Calibration

5.4.1 Method

The temperature was calibrated by exploiting the script *run_calibration.py* that is included in the library PREDYCE [54] developed by Politecnico di Torino and that is part of H2020 projects E-DYCE and PRE-

LUDE. The configuration file that is used to run the script contains the information needed for calibration. In particular, it contains the following main settings:

- the run period over which IDFs will be calibrated. 01/07/2021 has been set as starting day, while 31/07/2021 is the ending date. This period has been chosen because the school is empty and, in this way, the calibration process can be done more easily because variabilities introduced by occupation, heating, and ventilation are not present;
- the name of the zone to be calibrated and the corresponding floor;
- the name of the file that contains data collected from sensors for the whole run period except warm-up days, and the column's name of the CSV file that contains the target zone's temperature. These data are used as ground truth for temperature calibration in the area with mechanical ventilation;
- the calibration actions, that are used to modify simulation parameters to find the optimal configuration that minimizes the difference between measured and simulated data over the selected period.

The calibration actions can change the original values contained in IDFs of a selected percentage or substitute them with new chosen values that can be also varied in percentage. Parameters that should be calibrated for a correct temperature behavior are:

- U-value of walls. U-value is the amount of heat loss through a one square meter surface that can be composed of one or more layers of materials divided by the temperature difference across the structure, hence it is measured in W/m^2K. The lower the U-value, the more insulating the structure [47];
- roof's U-value, if the room is on the third floor and the roof has been included in the model;
- U-value of windows;
- solar heat gain coefficient of windows, that is the part of solar radiation that passes through glass layers, heating inside spaces. The lower the SHGC, the less heat is transmitted into the indoor environment [25];
- air infiltration;
- internal building mass, that acts as a thermal capacitance, hence it is the ability to store thermal energy within the system [72];
- slat shading angle.

These parameters have been calibrated in pairs to limit the number of simulations that were needed to find the sub-optimal configuration.

5.4.2 Results

For all the three rooms, selected sub-optimal parameters are shown in tables 5.1 and 5.2, while in 5.3 relative errors are shown.

Room	Floor	U-value wall	U-value roof	air infiltration	internal mass
$act201bc$	1	70%	-	-15%	30%
$act201cc$	2	55%	-	-50%	15%
$act208da$	3	45%	45%	10%	20%

Table 5.1: Optimal percentage change for each parameter of the room with mechanical ventilation with respect to IDF values

Room	Floor	SHGC	U-value windows	angle slat shading
$act201bc$	1	0.69	2.37 W/m^2K	90°
$act201cc$	2	0.621	1.3846 W/m^2K	125°
$act208da$	3	0.966	1.7802 W/m^2K	115°

Table 5.2: Optimal parameters chosen for each room with mechanical ventilation from new selected values varied in percentage

Room	Floor	RMSE	MBE	RMSE_MBE
$act201bc$	1	0.233°C	0.104°C	0.255°C
$act201cc$	2	0.258°C	-0.010°C	0.258°C
$act208da$	3	0.511°C	-0.008°C	0.511°C

Table 5.3: Calibration errors

The absolute U-values, obtained from the percentage changes seen in Table 5.1, can be seen in Table 5.4. A typical wall U-value in Italian buildings is usually between 0.1 W/m^2K and 0.54 W/m^2K, while for roofs, it is usually in the range from 0.1 W/m^2K to 0.42 W/m^2K [68], thanks to insulation materials used in constructions. Hence, 0.1 W/m^2K corresponds to a very high level of insulation, while 0.54 W/m^2K and 0.42 W/m^2K are related to low insulation. In absence of insulation, the U-value can reach an average value of 1.49 W/m^2K for walls and 1.40 W/m^2K for roofs, meaning that heat dispersion is relevantly high. From Table 5.4, it can be seen that walls and roofs' U-values are higher than the optimal upper threshold of the Italian buildings' U-value range. However, this result is not concerning since this is the optimal result that allows the behavior of the simulated building to be in line with the actual one.

The same conclusions are valid even for the windows U-value since Torre Pellice is part of the Italian climatic zone F [2, 14], hence the minimum requirement for the windows' U-value is 1.10 W/m^2K [27].

In Table 5.4 can be even seen the optimal air infiltration absolute values for each room under study.

Room	Floor	U-value wall	U-value roof 1	U-value roof 2	air infiltration [ACH]
$act201bc$	1	0.68 W/m^2K	-	-	0.017
$act201cc$	2	0.62 W/m^2K	-	-	0.016
$act208da$	3	0.59 W/m^2K	1.74 W/m^2K	3.29 W/m^2K	0.059

Table 5.4: Optimal absolute U-values and air infiltration

The error is evaluated in the following way:

$$RMSE\_MBE = \sqrt{RMSE^2 + MBE^2} \tag{5.1}$$

in which RMSE [74] is the root mean squared error and it is obtained as:

$$RMSE = \sqrt{\frac{1}{N}\sum_{k=1}^{N}(data\_predicted_k - data\_true_k)^2} \tag{5.2}$$

in which N is the total number of samples. It is one of the most considered metrics given that by squaring the difference it is possible to remove the errors' sign. In this way, the magnitude of every single error influences the final average of all the errors, and larger differences influence it more than smaller ones.

MBE [74], the Mean Bias Error, is

$$MBE = \frac{1}{N}\sum_{k=1}^{N}(data\_predicted_k - data\_true_k) \tag{5.3}$$

that indicate the model bias, so it shows if predictions tend to be higher or lower than true measurements. It underestimates the error magnitude given that errors with signs can be compensated. By summing the square of RMSE and the one of MBE it is possible to reduce during calibration both the error magnitude and the bias of the temperature trend.

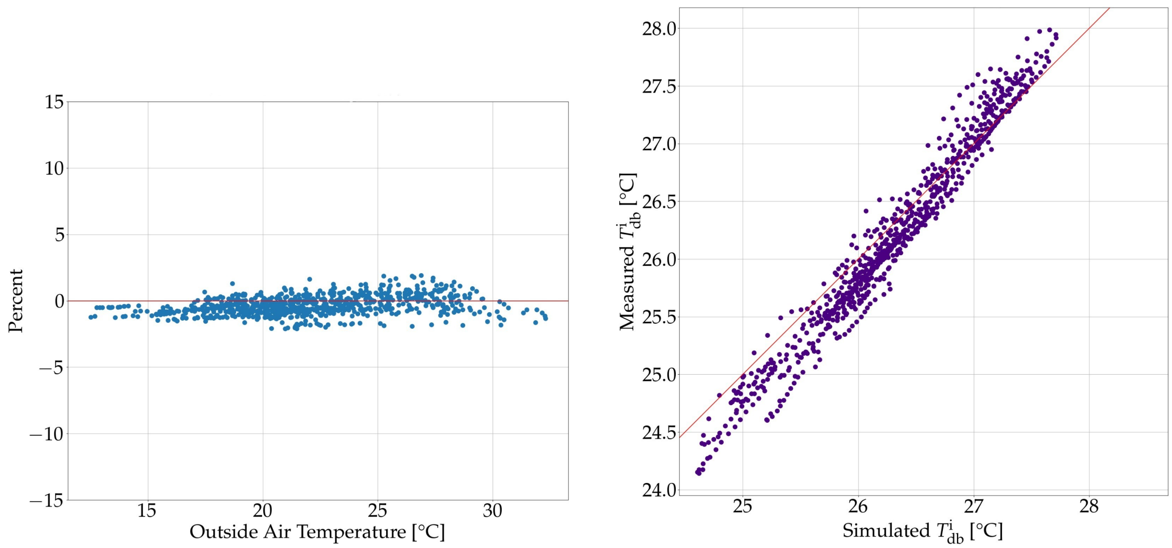

Figure 5.5: Calibration signature on the left and measured vs simulated data on the right for the room *act*201*bc*

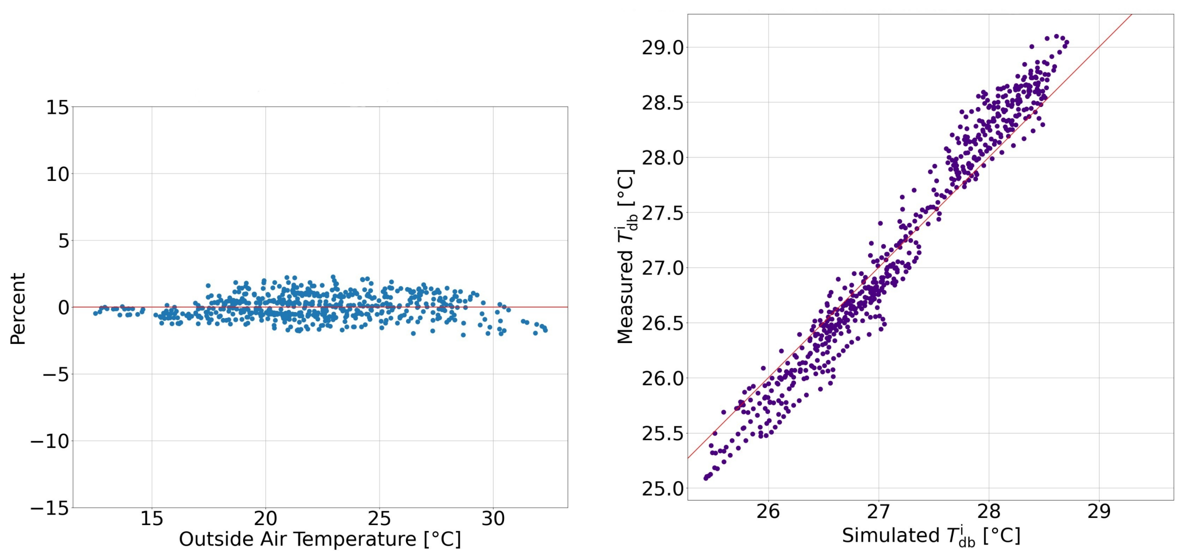

Figure 5.6: Calibration signature on the left and measured vs simulated data on the right for the room *act*201*cc*

In Figs. 5.5, 5.6, and 5.7 can be seen both the calibration signature and measured vs simulated data of the indoor dry-bulb temperature. The calibration signature is the plot of the percentage error variation

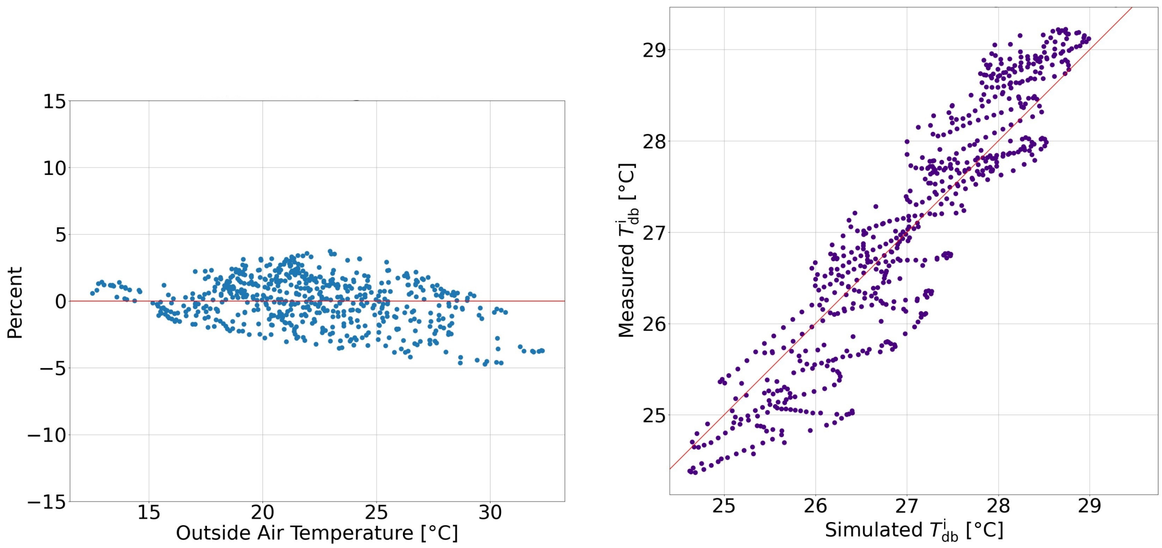

Figure 5.7: Calibration signature on the left and measured vs simulated data on the right for the room *act*208*da*

with the outside air temperature. It is calculated as:

$$calibration\_signature = 100\frac{data\_true - data\_predicted}{data\_true_{max}} \tag{5.4}$$

While the second plot indicates the difference between measured and simulated data, and in perfect conditions, points should all be overlapped to the red line that indicates where measured and simulated data have the same value.

From all three first plots, it can be seen that the percentage error is always less than 5%, so the calibration model can be considered valid [3, 15].

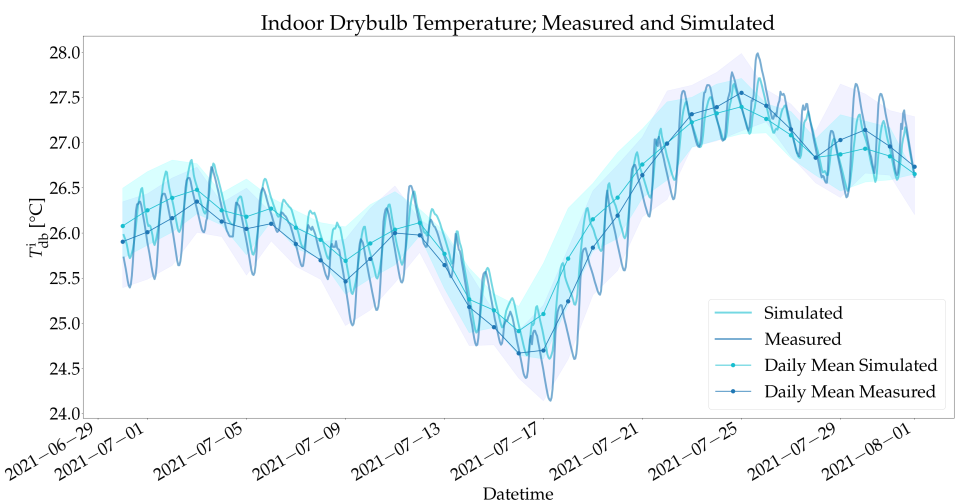

Figure 5.8: Simulated vs measured temperature behavior in the calibration period for the room *act*201*bc*

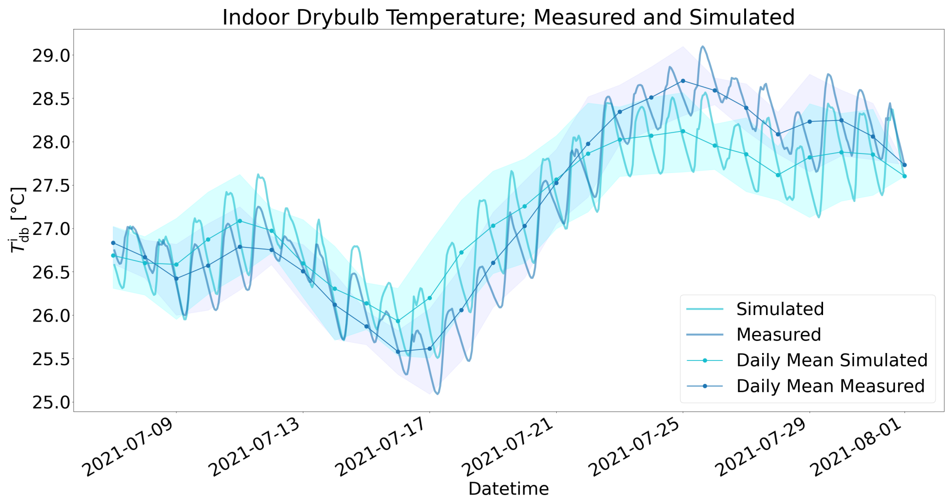

Figure 5.9: Simulated vs measured temperature behavior in the calibration period for the room *act*201*cc*

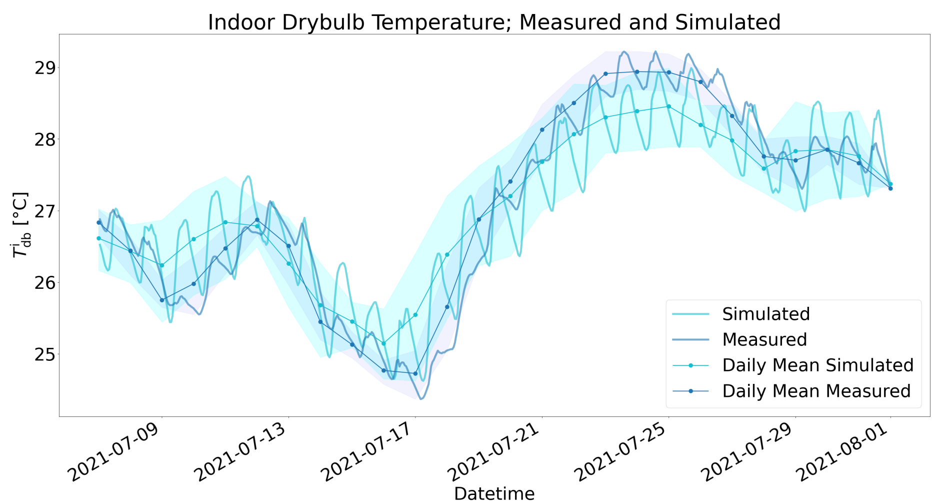

Figure 5.10: Simulated vs measured temperature behavior in the calibration period for the room *act*208*da*

The actual behavior of the temperature in the calibration period can be seen in Figs. 5.8, 5.9, and 5.10.

5.4.3 Validity Over Time

Method

The temperature calibration was checked with the complete available dataset for 2021 and 2022 to see how calibrated models work over time. It is expected that the further the data is away from the chosen calibration period, the more the model will deviate from the actual behavior.

To verify the temperature calibration validity over time, data available from 25/04/2021 to 06/07/2022 are retrieved by using the code explained in 7.4 and 7.6, to be then compared with simulation results. All the obtained data are filtered so that all wrong temperature measurements coming from sensors, which are due to sensor errors, are replaced with a more reasonable value.

To measure the goodness of the calibration validity over time both RMSE_MBE and MAPE errors are evaluated.

RMSE_MBE is used to compare the calibration precision over time with the one in the calibration period.

MAPE [9] is calculated as:

$$MAPE = \frac{1}{N}\sum_{k=1}^{N}\frac{\mid data\_predicted_k - data\_true_k \mid}{data\_true_k} * 100 \quad (5.5)$$

It is one of the most used metrics to understand the goodness of forecasted values with respect to real ones. It is a unit-free index whose values can be interpreted by referring to Table 5.5, taken from [9].

MAPE	Interpretation
< 10	Highly accurate forecasting
$[10, 20]$	Good forecasting
$[20, 50]$	Reasonable Forecasting
> 50	Inaccurate Forecasting

Table 5.5: Interpretation of MAPE metric

Results

The results obtained from the calibration over time of the three different selected rooms are shown in Tables 5.6 and 5.7.

Room	RMSE	MBE	RMSE_MBE	MAPE
$act201bc$	1.439°C	1.038°C	1.775°C	5.90
$act201cc$	1.395°C	0.976°C	1.703°C	5.44
$act208da$	1.130°C	0.409°C	1.202°C	4.19

Table 5.6: Error results from the calibration over 2021

Room	RMSE	MBE	RMSE_MBE	MAPE
$act201bc$	1.161°C	0.504°C	1.266°C	4.65
$act201cc$	1.165°C	0.287°C	1.200°C	4.30
$act208da$	1.601°C	-0.551°C	1.694°C	5.43

Table 5.7: Error results from the calibration over 2022

As expected, from RMSE_MBE, it is possible to see that predictions are a lot worse than the ones in the calibration period. The more the measurements are far from dates contained in the interval of calibration, the less effective will be the building parameters calibration to follow the actual school temperature behavior.

By looking at MAPE, it can be seen that the calibration is always highly accurate, and predictions follow accurately the actual building behavior for both 2021 and 2022.

Plots showing 2021 temperature behavior in the three different target rooms are shown in Figs. 5.11, 5.13 and 5.15. The ones of 2022 are shown in 5.12, 5.14 and 5.16.

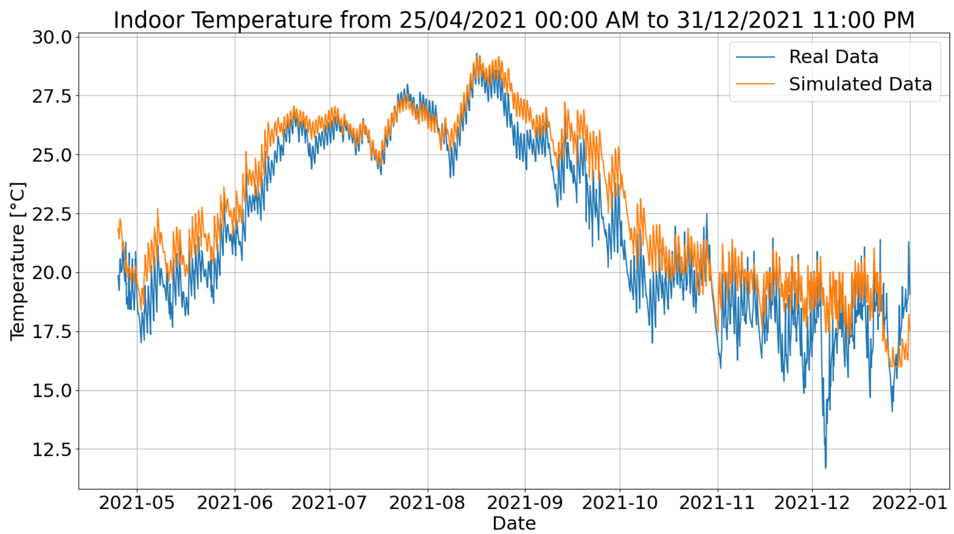

Figure 5.11: Simulated temperature behavior of the room *act*201*bc* in 2021

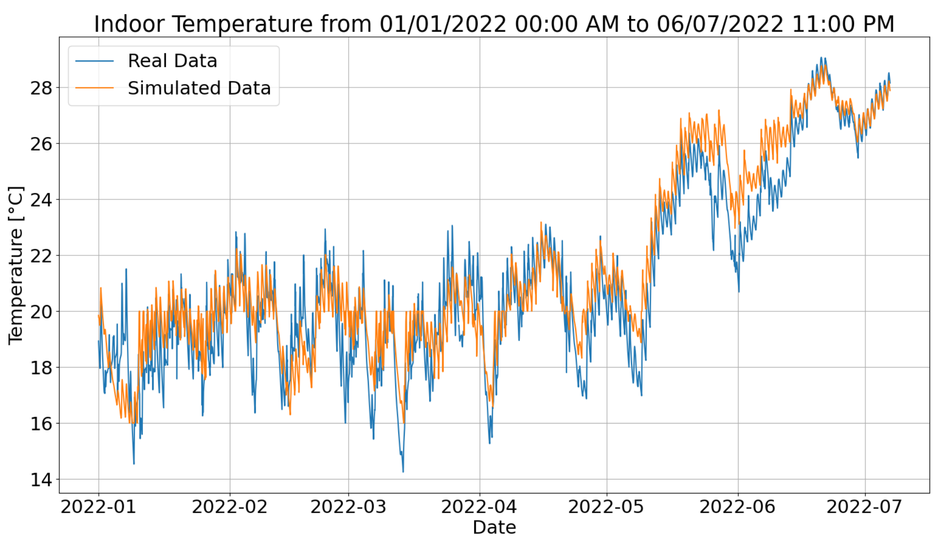

Figure 5.12: Simulated temperature behavior of the room *act*201*bc* in 2022

5.5 Carbon Dioxide Calibration

5.5.1 Method

Objects needed for enabling the carbon dioxide behavior simulation have been inserted in the IDF using the software that will be exhaustively explained in Section 6.

The carbon dioxide behavior has been calibrated just for the room *act*201*bc* because, in this way, all the CO_2 related strategies can be tested in the same room to compare the efficiency of different techniques

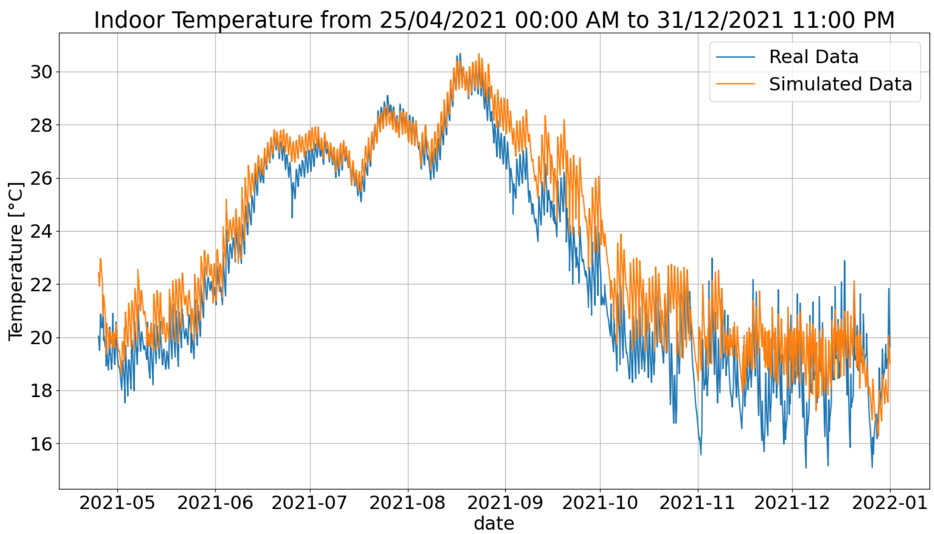

Figure 5.13: Simulated temperature behavior of the room *act*201*cc* in 2021

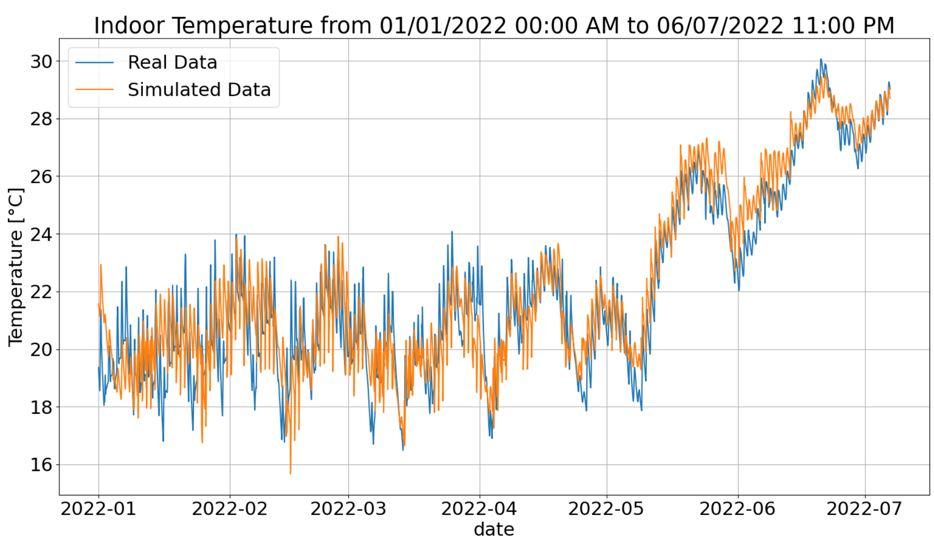

Figure 5.14: Simulated temperature behavior of the room *act*201*cc* in 2022

under the same conditions.

To calibrate the CO_2 behavior different parameters of the IDF are considered:

- the schedule of the object *ZoneVentilation:DesignFlowRate* related to the operation of the windows that influences the target zone ventilation. This schedule has been hypothesized from the monitored data because there is no information about the opening of the windows in the school. Moreover, people's behavior in opening and closing windows changes day by day, so the error in assuming a schedule with the same values for all the days over a given period will not be negligible. The hypothesized schedule can be seen in Algorithm 1;

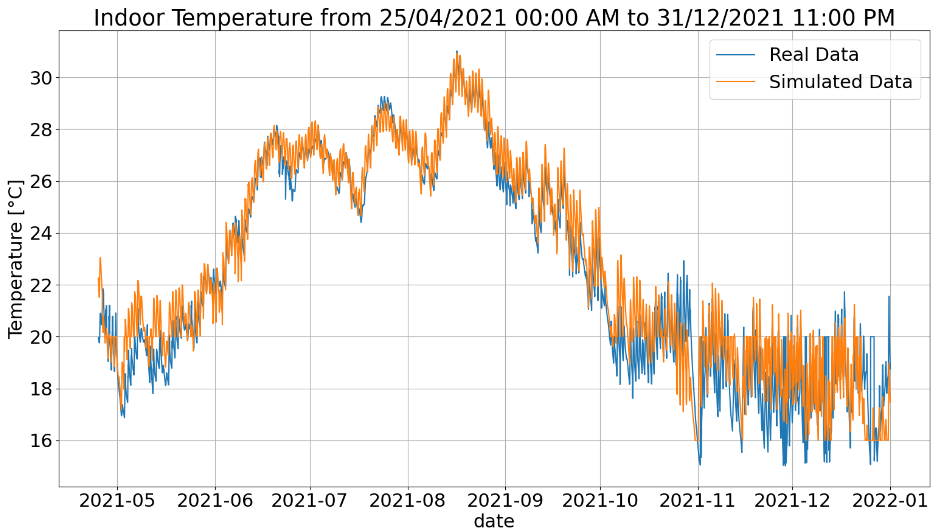

Figure 5.15: Simulated temperature behavior of the room *act*208*da* in 2021

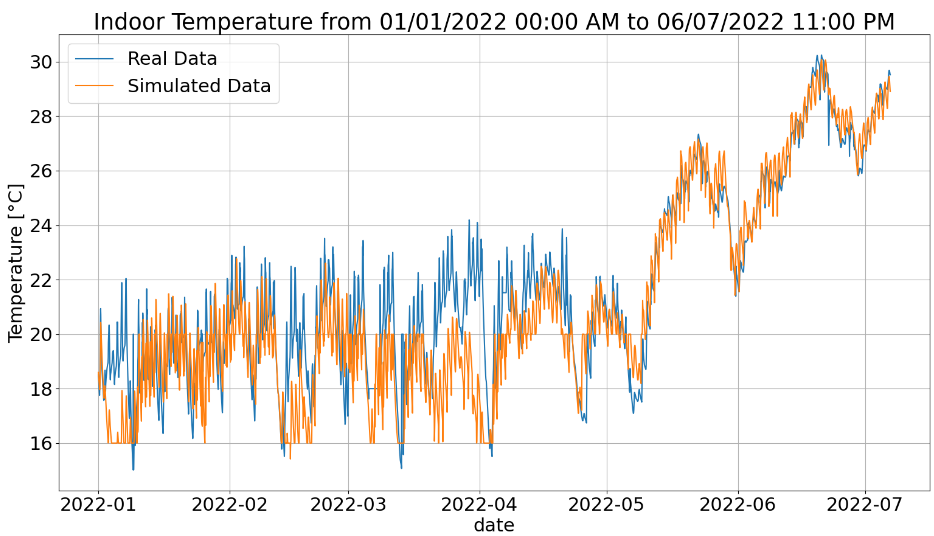

Figure 5.16: Simulated temperature behavior of the room *act*208*da* in 2022

- in the *People* object of the selected room, the people's carbon dioxide generation rate is left to the default value $3.82 * 10^{-8} m^3/s - W$;
- the number of people within the classroom for the CO_2 calibration has been tested in the range from 17 to 20, and the optimal chosen value is 17;
- in the *People* object of the selected room, the ratio between the number of people and the zone floor area is set to $0.29 person/m^2$, which is a more reasonable value considering the chosen number of people;

- the outdoor CO_2 schedule is modified according to local measured values, which on average are equal to $412.5 ppm$.

Algorithm 1 Schedule of the object $ZoneVentilation : DesignFlowRate$

Ventilation is expressed in percentage of the maximum nominal value of the ventilation unit

From 01/01 to 03/01: 0% all day long
For 04/01: 100% from 8:00 AM to 2:00 PM, 0% for the rest of the day
From 05/01 to 09/01: 0% all day long
From 10/01 to 20/01: 20% from 8:00 AM to 10:00 AM, 100% until 10:45 AM, 50% until 11:45 AM, 100% until 00:15 PM, 90% until 2:00 PM, 0% for the rest of the day
From 21/01 to 05/03: 35% from 8:00 AM to 10:00 AM, 100% until 10:45 AM, 50% until 11:45 AM, 100% until 00:15 PM, 90% until 2:00 PM, 0% for the rest of the day
From 06/03 to 19/03: 5% from 8:00 AM to 10:00 AM, 100% until 10:45 AM, 20% until 11:45 AM, 100% until 00:30 PM, 10% until 1:30 PM, 80% until 2:00 PM, 0% for the rest of the day
From 20/03 to 31/03: 10% from 8:00 AM to 10:00 AM, 100% until 10:45 AM, 20% until 11:45 AM, 100% until 00:30 PM, 20% until 1:30 PM, 80% until 2:00 PM, 0% for the rest of the day
From 01/04 to 06/06: 20% from 8:00 AM to 10:00 AM, 100% until 10:45 AM, 20% until 11:45 AM, 100% until 00:30 PM, 20% until 1:30 PM, 80% until 2:00 PM, 0% for the rest of the day
From 07/06 to 23/09: 100% from 8:00 AM to 2:00 PM, 0% for the rest of the day
From 24/09 to 02/10: 80% from 8:00 AM to 10:00 AM, 100% until 10:45 AM, 90% until 11:45 AM, 100% until 00:15 PM, 90% until 2:00 PM, 0% for the rest of the day
From 03/10 to 26/10: 60% from 8:00 AM to 10:00 AM, 100% until 10:45 AM, 60% until 11:45 AM, 90% until 2:00 PM, 0% for the rest of the day
From 27/10 to 30/10: 30% from 8:00 AM to 10:00 AM, 90% until 10:45 AM, 30% until 11:45 AM, 100% until 00:30 PM, 70% until 2:00 PM, 0% for the rest of the day
For 31/10 and 01/11: 0% all day long
From 02/11 to 08/11: 30% from 8:00 AM to 10:00 AM, 90% until 10:45 AM, 30% until 11:45 AM, 100% until 00:30 PM, 70% until 2:00 PM, 0% for the rest of the day
From 09/11 to 06/12: 15% from 8:00 AM to 10:00 AM, 100% until 10:45 AM, 30% until 11:45 AM, 100% until 00:15 PM, 15% until 1:30 PM , 80% until 2:00 PM, 0% for the rest of the day
From 07/12 to 16/12: 100% from 8:00 AM to 2:00 PM, 0% for the rest of the day
From 17/12 to 23/12: 10% from 8:00 AM to 10:00 AM, 100% until 10:45 AM, 30% until 11:45 AM, 100% until 00:15 PM, 20% until 1:30 PM , 80% until 2:00 PM, 0% for the rest of the day
From 24/12 to 31/12: 0% all day long

5.5.2 Results

The CO_2 calibration results goodness is evaluated by using two different indicators. The first one is MAPE which indicates the predictions' quality, and the second one is an indicator developed specifically for this situation which is based on the difference between simulated daily peaks and measured ones. It is used because CO_2 peaks are dangerous for the occupants' health, as highlighted in section 2, so it is needed that the calibrated model imitates them in the best possible way to see the real control strategies' impact in the reduction of the value of these peaks. It is measured by using the following equation:

$$peak\_error = \frac{1}{N_d} \sum_{k=1}^{N_d} \frac{| peak\_predicted_k - peak\_true_k |}{peak\_true_k} * 100 \tag{5.6}$$

where $peak\_true_k$ and $peak\_predicted_k$ are respectively the daily maximum measured and forecasted CO_2 values for each day in which the CO_2 value reaches a maximum value greater than $450ppm$, which is an indicator of the room occupation. In this way, just the days in which there is someone in the room are considered. N_d is the total number of peaks considered. The obtained results are shown in Table 5.8.

Year	MAPE	Peak Error
2021	6.64	13.48
2022	8.85	18.94

Table 5.8: Error results from the CO_2 calibration

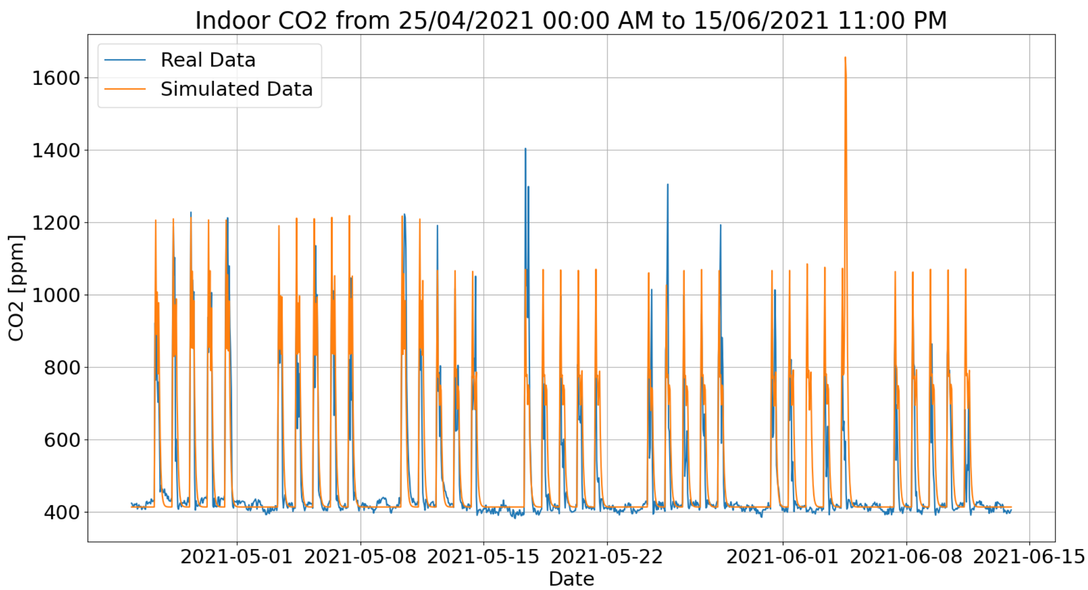

Figure 5.17: Simulated CO_2 behavior of the room $act201bc$ in the first part of 2021

The CO_2 calibration results in 2021 are really good, considering that there are no clues on the operation of the windows in the school. MAPE of less than 10 indicates that the forecasting is highly accurate, and also the percentage of the peak error is relatively small, leading to a good forecast of the maximum CO_2 values reached during the days.

In 2022 the predictions' accuracy drops even though, according to MAPE, they remain highly accurate. The drop in peak predictions is instead higher, making results less reliable than those of the previous year. For these reasons, it is better to test the control strategies by using the 2021 weather file to have a behavior more compatible with reality.

The plot of both measured and predicted data is shown in Figs. 5.17 and 5.18 for 2021 and in Fig. 5.19 for 2022 period. It can be seen that a lot of times measured CO_2 values have peaks over $1000ppm$ during the lesson time, which can have negative health consequences. For this reason, control strategies and mechanical ventilation units are really necessary.

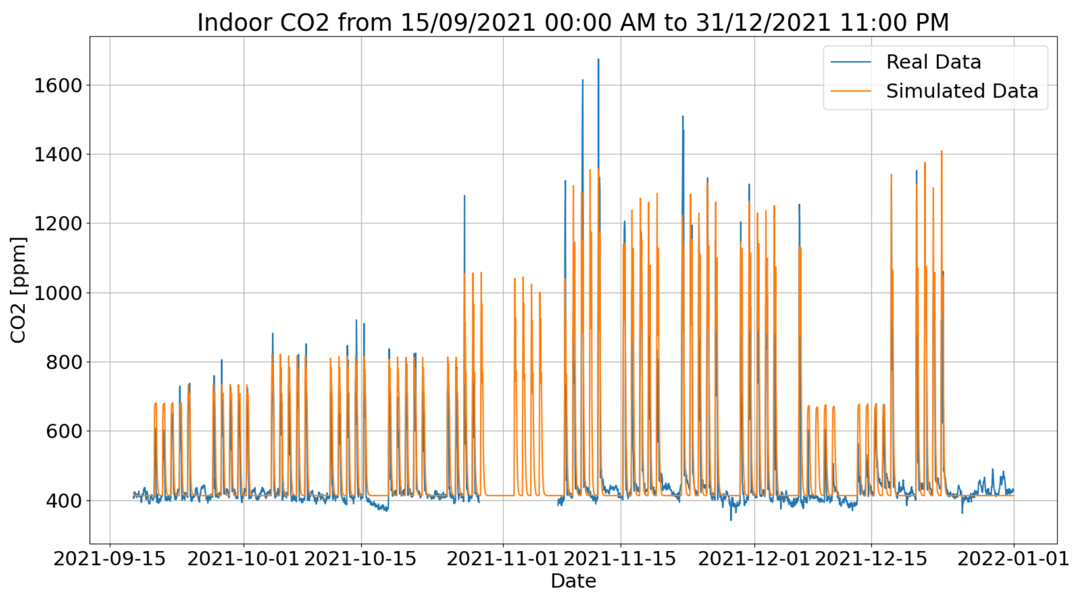

Figure 5.18: Simulated CO_2 behavior of the room $act201bc$ in the second part of 2021

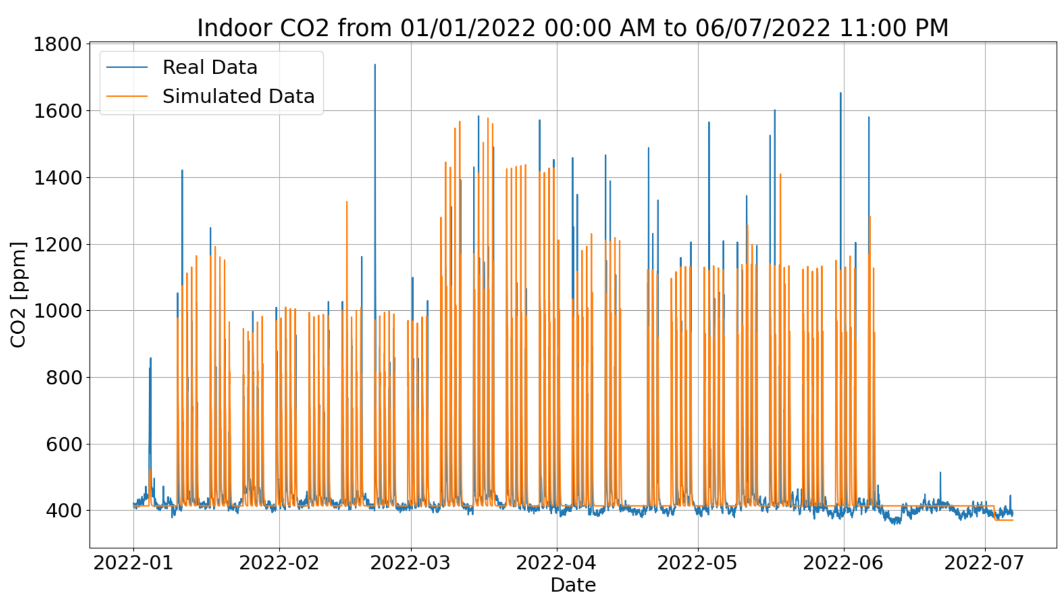

Figure 5.19: Simulated CO_2 behavior of the room $act201bc$ in 2022

5.6 Electric Consumption Calibration

The mechanical ventilation units have a declared consumption of $188W$ at full fan speed. For a correct simulation, given that other fan speeds are used, it is needed to characterize overall the system power absorption.

5.6.1 Characterization of the Consumption Curve

The characterization of the power absorption curve's main points was asked to the Helty manufacturer. The points provided by the manufacturer are shown in Table 5.9.

Fan speed $[m^3/h]$	Power absorbed $[W]$
800	188
700	84
540	50
370	30

Table 5.9: Characterized points obtained from the manufacturer

These points are then interpolated linearly to create the curve that shows the power absorption with respect to the amount of fan-injected air.

The absorbed power value that corresponds to a given amount of injected air is then calculated by projecting the flow measurement on the curve to see the related power value. The characterization curve and operation points of interest can be seen in Fig. 5.20.

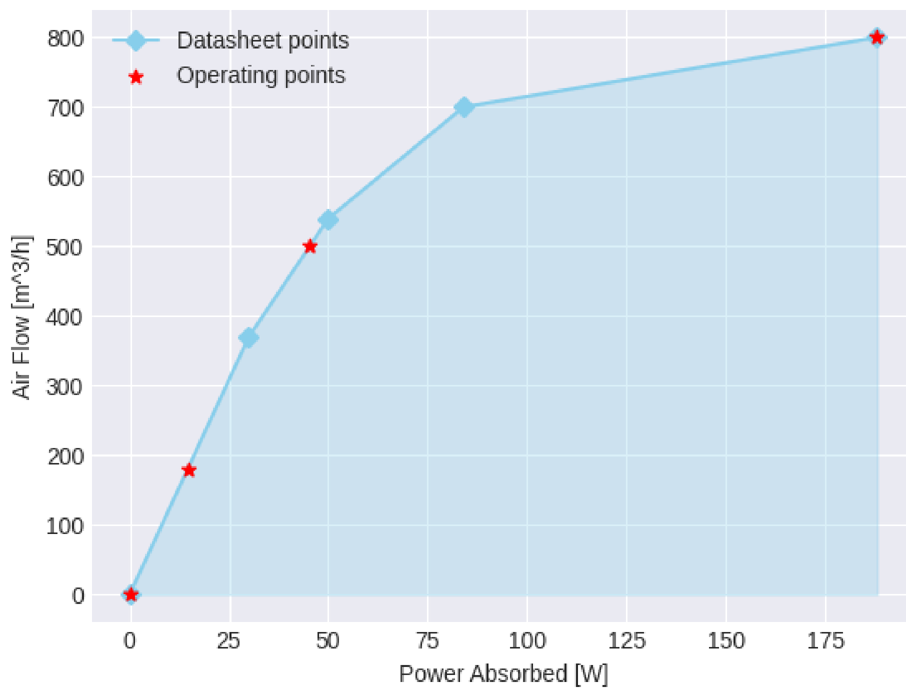

Figure 5.20: Air flow with respect to the absorbed power

5.6.2 Calculation Method

To calculate the total amount of energy used in the building, the value obtained as output from the *Electricity:Facility [J](RunPeriod)* EnergyPlus Output, transformed from joule into Kilowatt, should be summed with the energy that is consumed by the mechanical ventilation unit. To calculate this last contribution, the power absorbed from all the fan speeds used in the simulation is obtained as shown in Fig. 5.20, and then the following formula is used:

$$Fan\_Total\_Consumption[kWh] = \sum_{k=1}^{N_t} \Delta t * P_a(v) \tag{5.7}$$

where N_t is the total number of timestep of the simulation, Δt is the duration of a single timestep in hours, which is obtained by dividing the 10 minutes duration of each timestep by 60 minutes, and $P_a(v)$ is the absorbed power at the fan speed v.

5.7 Mechanical Ventilation Calibration

5.7.1 Method

The objects needed for adding the mechanical ventilation simulation have been inserted in the IDF using the software that will be completely explained in Section 6.

The mechanical ventilation is added in this way to the model with calibrated CO_2, and it is calibrated over the period from 02/04/2022 to 08/05/2022. This interval has been chosen because in the selected period mechanical ventilation units were already installed in the school. They have been programmed to run every weekday from 8:00 AM to 2:00 PM with the minimum flow rate using heat recovery.

The mechanical ventilation system in the model has been designed through an *Ideal Loads Air System* object, which has been calibrated by copying the settings of classrooms' real units. In this way, simulated data can be compared with real ones to understand the accuracy of the calibrated model.

5.7.2 Results

Results evaluate both the temperature predictions accuracy and the carbon dioxide one, to check that the inclusion of ventilation does not modify drastically temperature behavior. Concerning temperature, the accuracy is measured using the MAPE metric, while for carbon dioxide both MAPE and peak metrics are computed. Results are shown in Table 5.10.

Room	MAPE Temperature	MAPE CO_2	Peak CO_2 error
$act201bc$	5.20	6.83	17.59

Table 5.10: Results of the mechanical ventilation calibration

Temperature and CO_2 predictions are highly accurate, given that MAPE is significantly smaller than 10, and the peak information is also good. Moreover, it is possible to note that the accuracy of both CO_2 and peak behavior increases if compared with the model with just the carbon dioxide calibration in 2022. Therefore, the introduction of the mechanical ventilation system in the model increases the overall performance of the predictions.

The plot of simulated data compared with real ones can be seen in Figs. 5.21 and 5.22.

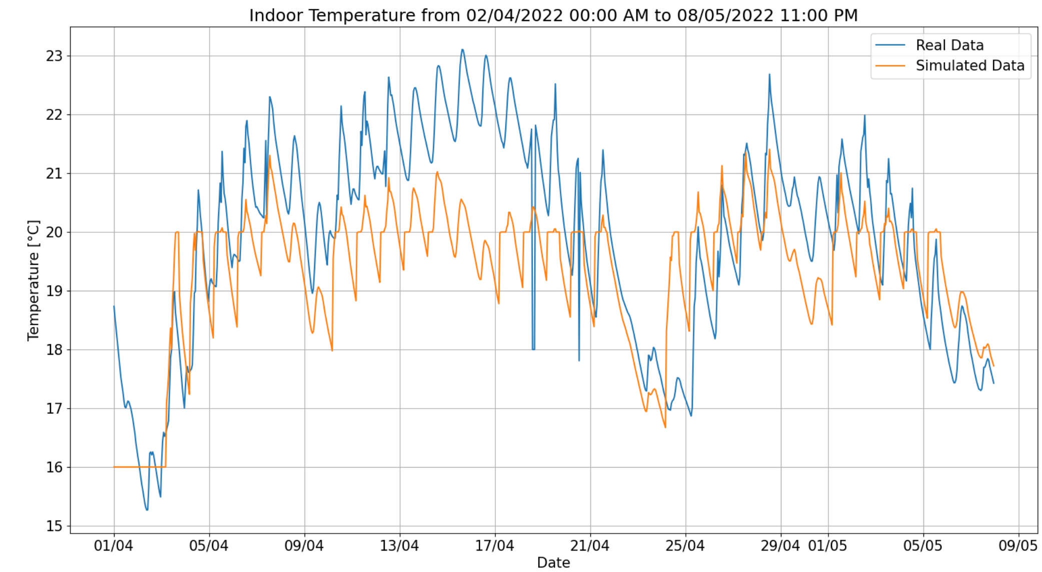

Figure 5.21: Simulated temperature behavior of the room *act*201*bc* after mechanical ventilation calibration

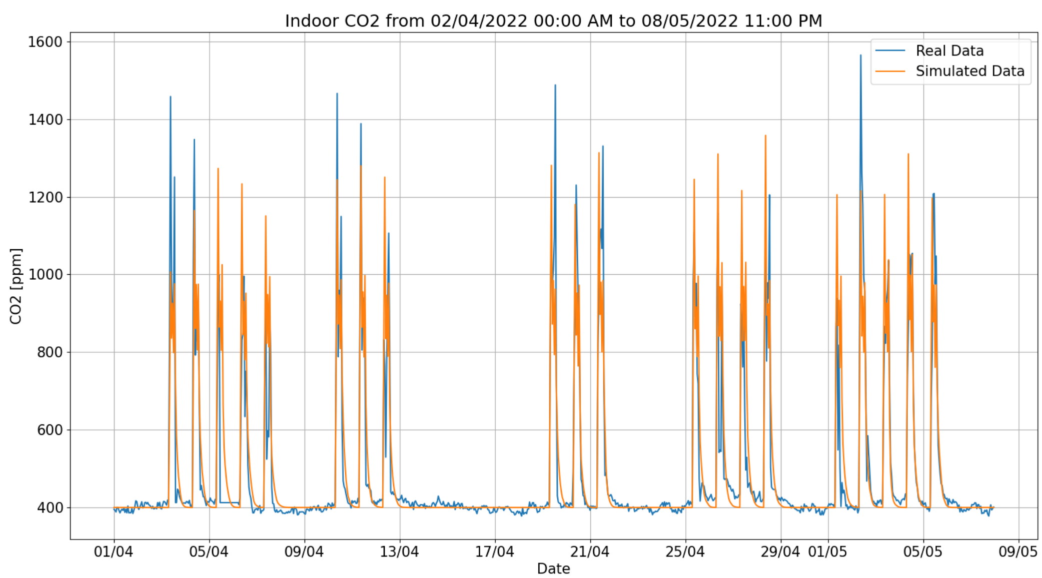

Figure 5.22: Simulated CO_2 behavior of the room *act*201*bc* after mechanical ventilation calibration

6. Software for IDFs Modifications

6.1 PREDYCE *idf_editor.py*

The script *idf_editor.py* is taken from the PREDYCE python library [54] and is partially modified to be used in this thesis. This library provides two useful functions that can be exploited in the IDFs modification, which are:

- *set_outdoor_co2*;
- *add_mechanical_ventilation*.

6.1.1 *set_outdoor_co2*

This function is used to introduce the carbon dioxide simulation in the IDF. It takes two different input parameters:

- the IDF to be modified;
- the outdoor CO_2 schedule as a *Schedule:Compact* object of EnergyPlus.

6.1.2 *add_mechanical_ventilation*

The *add_mechanical_ventilation* function is used to modify all the concerned EnergyPlus objects to include the mechanical ventilation unit in the IDF simulation. It asks as input:

- the IDF to be modified;
- the zone name in which the unit will be inserted;
- the ventilation schedule in the format of a *Schedule:Compact* EnergyPlus object.

This function has been modified to take as input three more parameters, which are used to modify the settings of the *DesignSpecification:OutdoorAir* object:

- *Outdoor Air Method*, that indicates the method for calculating the airflow rate volume;
- *Outdoor Air Flow per Person*, which indicates the airflow rate volume per person in $m^3/(s * person)$;
- *Outdoor Air Flow per Zone*, which is the total outdoor airflow rate for the whole zone in m^3/s.

6.2 Add Carbon Dioxide Simulation to IDFs

A dedicated script has been created to add the carbon dioxide simulation to IDFs. It imports the eppy modeleditor IDF class to create a virtual IDF object, and the *idf_editor.py* script to call the function *set_outdoor_co2* over the newly created IDF object, to then save it into a new file.

Given that *set_outdoor_co2* takes as input a schedule in the format *Schedule:Compact*, a dedicated secondary script has been created and imported into the main one to parse the schedule correctly. This last script takes as input a file containing the schedule in the format of an IDF object, and then it creates the Python dictionary needed for the required *Schedule:Compact* format.

6.3 Add Mechanical Ventilation Unit to IDFs

The script used to add the mechanical ventilation works in the same way as the one described in the previous paragraph 6.2. It uses the same secondary script to parse the schedule of the mechanical ventilation unit and set the parameters *Outdoor Air Method* to *Flow/Zone*, *Outdoor Air Flow per Person* to 0 $m^3/(s * person)$, and *Outdoor Air Flow per Zone* to 0.22 m^3/s, which is the maximum available ventilation declared by the system manufacturer. To reach the minimum amount of ventilation that is used in the calibration of the ventilation unit in the IDF (see paragraph 5.7.1), the weight factor in the mechanical ventilation schedule is set to 10% of the nominal airflow value.

7. Downloading Calibration Data

7.1 General Software Structure

The general software structure used to retrieve data for calibration is shown in Fig. 7.1, highlighting communication strategies between different parts of the software and the most relevant pieces of information that are exchanged.

The whole architecture is developed following the micro-service approach instead of the monolithic structure. Therefore, it is characterized by scalability, modularity, and easy debugging and upgrading capabilities. In particular, the Catalog can be considered as the software glue, in fact, through its REST interface, it provides to all the other scripts the needed information for interacting successfully. So it can be considered the coordinator of the whole system, allowing smooth operations between different software parts.

7.2 Data Retrieval, Filling, Smoothing and Storage

The data retrieval, filling, smoothing, and storage had already been created by a project developed in parallel in which I was one of five developers, called “SBV - Smart Building Visualizator”. It is designed for the same demo buildings in Torre Pellice, and it is part of the E-DYCE project too. It aims at providing users with an application that allows them to be continuously aware of building conditions, giving them a complete overview of the most valuable environmental information, ranging from instantaneous measurements to elaborated KPIs, as well as some predictions of both internal and external conditions, like indoor temperature and weather. The mobile application has been tailored for different user-type and allows simple interaction such as adding new sensors or changing room naming conventions.

7.2.1 Catalog

The Catalog is the software glue providing all other processes with needed pieces of information about locations and communication strategies of other software parts, thus being the real coordinator for smooth operations of the whole software.

7.2.2 Retrieval and forwarding

The data retrieval code connects to WineCap Capetti gateways by using the SOAP protocol to get the list of available sensors to download one hour of data. Then the code queries the Catalog to get for each sensor the corresponding standardized name to correctly assign it to the downloaded data. Named data are sent to the InfluxDB database storage through the MQTT protocol, creating a first bucket that contains raw data. Data are updated every hour, and most sensors have 10 minutes granularity.

7.2.3 Naming Convention

The used sensors naming convention chosen to simplify queries and aggregations of data is:

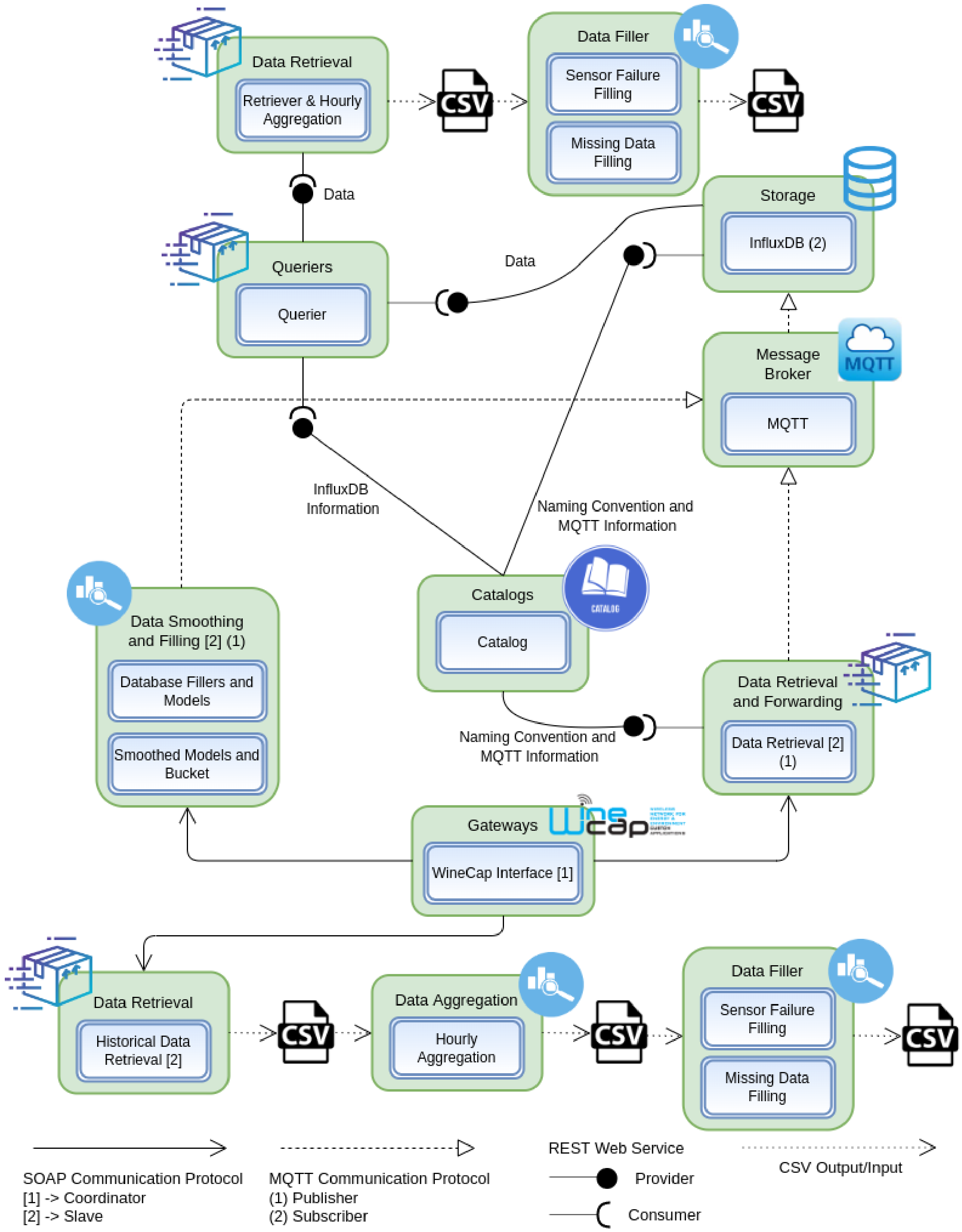

Figure 7.1: General software structure for retrieving data to calibrate the models

$$demoName\_floor\_activityIdentifier\_MACAddress\_Orientation\_typeOfVariable$$

The $demoName$ field contains the demo building name, $floor$ is the floor where the sensor is located, $activityIdentifier$ is a code that represents activities that are carried out in the room in which the sensor is located, $MACAddress$ is the sensor MAC, $Orientation$ contains the value in degrees of the sensor position from the north direction counterclockwise, and $typeOfVariable$ contains the information of the measurement and its unit.

7.2.4 Filling and Smoothing Algorithm

Filling and smoothing algorithms retrieve data from Capetti gateways using the SOAP protocol and associate them to the correct name by retrieving it from the Catalog. Data are later processed and, in particular, they are filled and smoothed by using appropriate models. At this point, data are sent to the InfluxDB database by using the MQTT protocol to create a second bucket of processed data. Even this bucket is updated every hour with new data.

Filling Algorithm

The filling algorithm provides missing data based on two different approaches:

- LLS regression for temperature and relative humidity. If the predicted value varies more than 20% compared to the previous one, the change is considered too high. In this case, the estimated value is discarded, and the missing value is obtained by up-sampling the previously measured value, simply repeating the old value at the new timestamp;
- up-sampling for CO_2 and heat meters.

Smoothing Algorithm

The smoothing algorithm is used to remove outliers caused by wrong sensor measurements. The smoothing is done using a moving average filter for each two-hours interval.

7.2.5 Storage

The database used to store data is InfluxDB because data from sensors are timestamped, and a time series database is the best choice for tracking and organizing them. Moreover, time-series databases can perform queries whose performances are independent of the quantity of stored data within the database, which is particularly useful for the massive amount of data that comes from sensors. The Influx client asks the catalog the information on how to connect to the database and the MQTT topic to subscribe to for getting data and finally collects and stores them, as can be seen in 7.3, using as keys fields of the sensor naming 7.2.

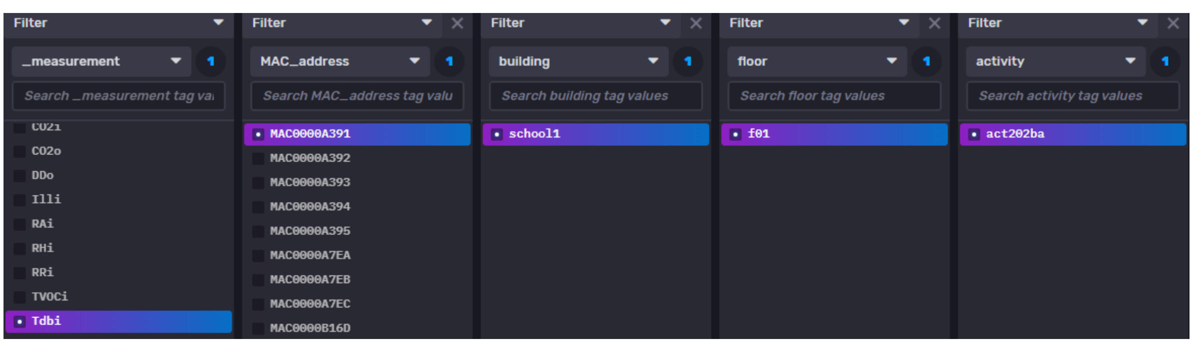

Figure 7.2: InfluxDB example of the keyed fields of the database

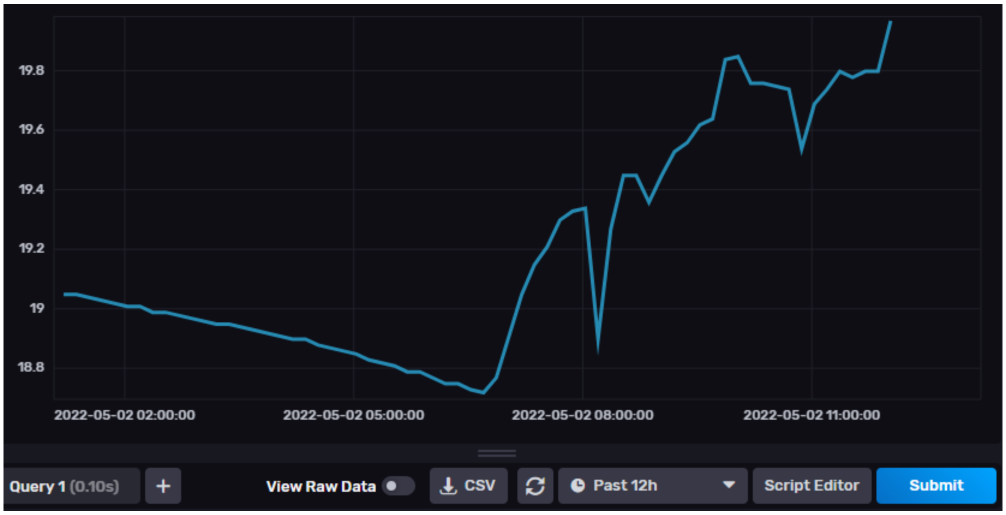

Figure 7.3: Example of the raw temperature measurements taken from the sensor MAC0000A391

7.3 Querier

The querier is used to retrieve data and their timestamps from InfluxDB, organizing them to be subsequently handled. Data can be aggregated according to:

- sensor name;
- name of building zones;
- building name.

Moreover, data can be collected for any date by providing the wished start and end timestamps. The querier can also return statistical metrics for a selected period using the above-mentioned aggregation levels.

7.4 Data Retriever

The Data Retriever script requests data from the querier to store them in a CSV output file. It takes as input a configuration file whose main fields are:

- the querier aggregation level;
- the starting and ending date and hours to get all the data stored in the period of interest;
- the sensors' names from which data should be retrieved.

Then it sends a GET request to the querier to obtain selected data and aggregates them hourly. Eventually, it saves hourly aggregated data into a CSV file.

7.5 Data Filler

The Data Filler algorithm is composed of two scripts with different main aims:

- the first one is used to fill missing values that are due to software, sensors, or Capetti gateways failure;

- the second is instead used to add fake data at the beginning of 2021 when sensors were not installed yet in the school.

At the end of these two steps, the output will be of two CSV files which have a column with the average measured data for every hour of 2021 and 2022 respectively.

Missing Values due to Sensors Failure

This script is used to fill all those missing values that are due to some malfunction that can be caused by software, sensors, or Capetti gateways.

It takes as input the CSV coming from the Data Retriever script and checks if all the hours within the chosen period of interest are present. If not, it adds missing dates, and for each lacking hour, the last previously measured value is duplicated and considered as the lacking one. Finally, newly filled data are saved in a new CSV file that contains a value for each hour without any absence for the whole requested period.

Missing Values due to Absence of Sensors

Temperature and CO_2 data for the beginning of 2021 are unknown since sensors have been installed in the school in the spring of that year. To work correctly, the EnergyPlus simulation needs data from the beginning of the year, and for this reason, it is needed to fill missing data with fake ones. Each lacking hourly average is fixed to $20°C$ for temperature and $412.5ppm$ for CO_2. The output of the script is a CSV file with data ready to be used for the calibration process.

7.6 Historical Data Retriever from Capetti

The querier script, as can be seen in the general software structure, fetches data from the InfluxDB database that has been developed in the SBV project. The development period of the SBV project was from November 2021 to June 2022, so the database contains data from approximately the spring of that year. For this reason, the historical data retriever script can be used to get the CSV containing the 2021 and the beginning of 2022 data, which are not present in the database. This script has been also developed as part of the SBV project to retrieve all the data directly from the Capetti database to train regression and neural network models that require more data.

7.7 Data Aggregation per Hour

Data obtained through the historical data retriever script have a time resolution of 10 minutes, so it is necessary to create a new script that aggregates them to get hourly data. The output of this script is a CSV that is given as input to the Data Filler algorithm shown in 7.5 to fill all the missing data with the chosen value.

8. Simulated Strategies

Most of the strategies that are simulated are CO_2-based because during the first round of tests carbon dioxide controls could not be tested in the school. After all, the first testing period in the demo building is during July, which falls during the holiday period, so the school is empty, and the main sources of CO_2, people, are absent. Ventilative cooling strategies, instead, can be tested the same, so they were the first to be monitored in the school.

8.1 Energy Management System of EnergyPlus

To add control strategies to IDFs, the Energy Management System of EnergyPlus [8] must be used. The EMS is based on two different types of EnergyPlus objects:

- *EnergyManagmentSystem:Sensor*, which are used to declare variables linked to EnergyPlus outputs. They are used to retrieve the current value of a given internal parameter to make decisions based on its value;
- *EnergyManagementSystem:Actuator*, which is an object that is used to map a variable used in the control program with an internal EnergyPlus variable. In this way, the value of the linked EnergyPlus variable can be changed during the simulation by changing the actuator value.

By using these two objects, it is possible to emulate within EnergyPlus the behavior of digital energy management systems used for controlling real buildings.

The other two fundamental objects that are needed to run IDFs with EMS controls are:

- *EnergyManagementSystem:ProgramCallingManager*, which specifies when the EMS program will run within the simulation;
- *EnergyManagementSystem:Program*, which contains all the instructions needed for control actions, expressed in the EnergyPlus Runtime Language. Lines of the program are run in order at a specific point of the simulation when conditions expressed in the *EnergyManagementSystem:ProgramCallingManager* are satisfied.

8.2 Integration of EMS in the PREDYCE *idf_editor.py* Script

In the PREDYCE *idf_editor.py* script, the possibility of adding EMS controls is not present. For this reason, an additional function has been added to the script which inserts all the objects needed for controlling the mechanical ventilation based on CO_2 and temperature values. It takes the following input parameters:

- the IDF to be modified;
- the zone name that contains the mechanical ventilation unit;
- a dictionary containing the EMS program;
- a list of dictionaries, where each element is a dummy *Schedule:Constant* of type *Any Number*. One of these schedules is added every time it is necessary to keep the value of a variable or counter over different simulation timesteps. The name of these schedules must be *flag_n*, where n is an integer number that increases, starting from 0, for each added schedule. Its value will be linked to a sensor, called *flag_n_sens*, and to an actuator, *flag_n_act*, to be read and updated from the EMS program every time it is needed. In this way, the variable contained in the schedule will not be initialized every time a new timestep begins, allowing to keep the value throughout the simulation.

The function then performs the following actions:

1. inserts in the IDF an *Output:EnergyManagementSystem* object, which is used to report the details of Energy Management System operations in a simulation output file;
2. adds as IDF outputs EnergyPlus internal variables *Zone Outdoor Air Drybulb Temperature [C]* and *Zone Mean Air Temperature [C]* for the zone with the mechanical system that is passed to the function. These variables indicate respectively the outdoor air dry-bulb temperature at the height of the selected zone centroid and the average indoor zone air temperature at each system timestep;

3. adds three *EnergyManagementSystem:Sensor* for EnergyPlus variables *Zone Air CO_2 Concentration*, *Zone Outdoor Air Drybulb Temperature* and *Zone Mean Air Temperature*. These are needed to read values of current internal variables, and respectively the carbon dioxide value of the selected zone, the outdoor temperature value, and the indoor air temperature of the target zone;

4. adds one actuator connected to the *Outdoor Air Mass Flow Rate* of the *Ideal Loads Air System* of the zone with the mechanical ventilation so that it is possible to modify the air supplied by fans during the simulation running;

5. adds the *EnergyManagementSystem:ProgramCallingManager* with *BeginTimestepBeforePredictor* as *EnergyPlus Model Calling Point*. This calling point allows running the EMS program at the beginning of each timestep but before the calculation of the model zone's loads. It is particularly useful when, as in this case, there is a need of controlling some HVAC components;

6. adds the *EnergyManagementSystem:Program*;

7. for each element in the list of dictionaries which contains variables that keep their value over different timesteps passed as parameter to the function, a *Schedule:Constant* and its linked *EnergyManagementSystem:Sensor* and *EnergyManagementSystem:Actuator* are created. The schedule is also added as an output to the IDF so that changes in its value throughout the simulation can be monitored.

8.3 Add EMS Controls to the IDFs

A dedicated script has been created to add EMS controls to IDFs with the calibrated temperature, carbon dioxide, and mechanical ventilation. It imports:

- the script used to parse *Schedule:Compact* schedules explained in detail in paragraph 6.2;
- the class IDF from the eppy modeleditor Python library;
- the script $idf\_editor.py$;
- a new script that is used to parse correctly the EMS program. This script takes as input the zone name with the mechanical ventilation and a file with the EMS program written in ERL but using a simplified nomenclature. In particular, to refer to the sensor of outdoor air temperature, the word *sensor_out* should be used, *sensor_in* for the indoor air temperature sensor, *sensor_co*2 for the carbon dioxide sensor, and the word *actuator* for the mechanical ventilation airflow. In this way, it is possible to always use the same simplified nomenclature, and the parser translates these names into the ones that are used in the IDF, which depend on the zone name passed as a parameter of the function. If it is needed to keep some variables over different timesteps, as said in paragraph 8.2, it is necessary to use the nomenclature $flag\_n\_sens$ to read and $flag\_n\_act$ to modify them. Moreover, the script transforms the ERL program into the dictionary needed for the function that adds the *EnergyManagementSystem:Program* object to the IDF, keying every line of the program with the string *Program Line n*, where *n* is the number of the line, starting from 1.

Then the script performs the following operations:

1. creates a first virtual version of the IDF using the EPW weather file of 2021 and changes the run period from 25/04/2021 to 02/06/2021, which is the period with the best accuracy of the CO_2 calibration and with the presence of people. Given the chosen period, the heat recovery system is set to be off;

2. the IDF is simulated before the addition of the EMS control, with the mechanical ventilation unit always off. In this way, it is possible to have results related to the free-running building to compare all the results with natural conditions;

3. then EMS controls and all the related EnergyPlus objects are added by exploiting the function inserted into the script *idf_editor.py*, explained in paragraph 8.2;

4. then the modified IDF with the EMS program is run to obtain simulation results of the controlled environment.

8.4 Constant Air Flow Controls based on ASHRAE Standards

The most simple control approach for CO_2-based strategies is ventilation at a constant airflow rate. To guarantee that the selected airflow is sufficient to ensure the environment's healthiness, ventilation rates suggested by standards are used, and in particular, ASHRAE 62 and 62.1 standards are considered.

8.4.1 ASHRAE 62

The ASHRAE 62 standard does not ventilate when the room is empty, while it uses proportional ventilation to the number of occupants when the classroom is occupied. The formula used to calculate the airflow can be seen in paragraph 3.1.1. The coefficient R_p that multiplies the number of people is, for classrooms, set to $8L/s/person$ according to the standard. The complete flow of the algorithm can be seen in Fig. 8.1.

8.4.2 ASHRAE 62.1

The ASHRAE 62.1 standard is the evolution of the previous one, and it ventilates even when there is no occupancy in the room. In this way, it is possible to reduce all those pollutants which are not produced by humans. The formula used for the airflow rate calculation can be seen in paragraph 3.1.1, using $5L/s/person$ as R_p and $0.6L/s/m^2$ as R_A. The complete flow of the algorithm can be seen in Fig. 12.7.

8.5 CO_2 Single Threshold Controls

This strategy is mostly used because of its effectiveness and simplicity. Threshold values have been decided by consulting the review paper cited in [46]. In particular, the selected limit values are:

- $600ppm$: under this value, the CO_2 has a negligible effect on almost all health problems;
- $800ppm$: over this threshold value, it is more likely to show the mildest SBS symptoms;
- $1000ppm$: carbon dioxide values over this threshold are significantly associated with moderately severe diseases, like dry cough and rhinitis, specifically in children. Moreover, it is related to a decrease in pupils' attention, but without affecting their school performances. $1000ppm$ is also the limit value that is suggested by the ASHRAE standard;
- $1500ppm$: a value greater than $1500ppm$ is associated with a decrease in the number of correct answers given by students, also increasing the risk of more severe symptoms.

Two different constant air volume strategies are considered, which are both based on the main algorithm that can be seen in the flow chart in Fig. 8.2.

The first one is based on the following principles:

- there is no injected airflow when the CO_2 is under $600ppm$ since room environmental conditions are considered healthy;
- when the carbon dioxide level is between $600ppm$ and $1000ppm$, the ventilation flow rate is set to 1/5 of the nominal value declared by the manufacturer. In this way, a small amount of ventilation can bring back environmental conditions to be healthy in a relatively long time, given that conditions are still not dangerous and do not considerably affect health;

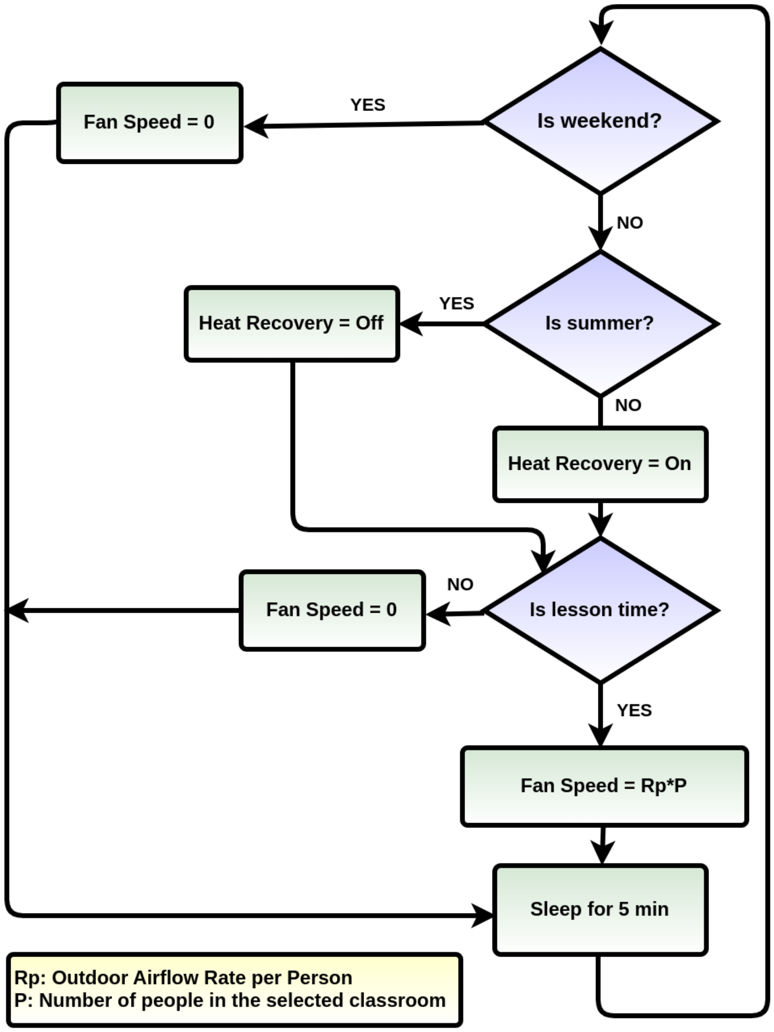

Figure 8.1: Ventilation algorithm recommended from the ASHRAE 62

- when the CO_2 is between $1000ppm$ and $1500ppm$, the ventilation value is 3/5 of the nominal value. The ventilation increases in this range because conditions start to be worse, so it is needed to increase the ventilation to bring conditions back to normal in a shorter time;
- above $1500ppm$ the mechanical ventilation flow rate is the maximum allowed, to try to reduce the indoor carbon dioxide concentration as fast as possible, to avoid the worst health effects.

The second strategy is equal to the first one, except that the lower threshold value is $800ppm$ instead of $600ppm$. This is done to save some energy as effects on the health and concentration of students of the carbon dioxide between $600ppm$ and $800ppm$ are not so impacting.

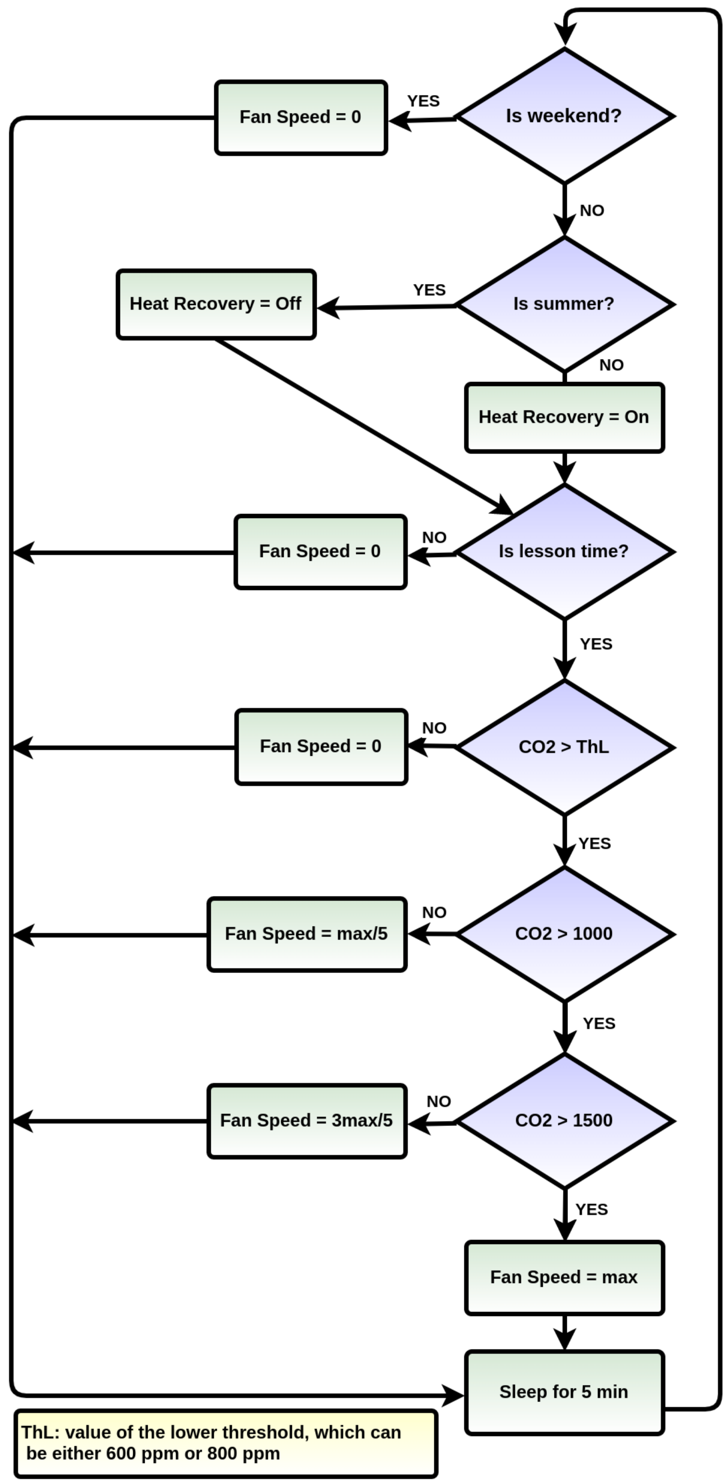

Figure 8.2: Ventilation algorithm based on a single CO_2 threshold

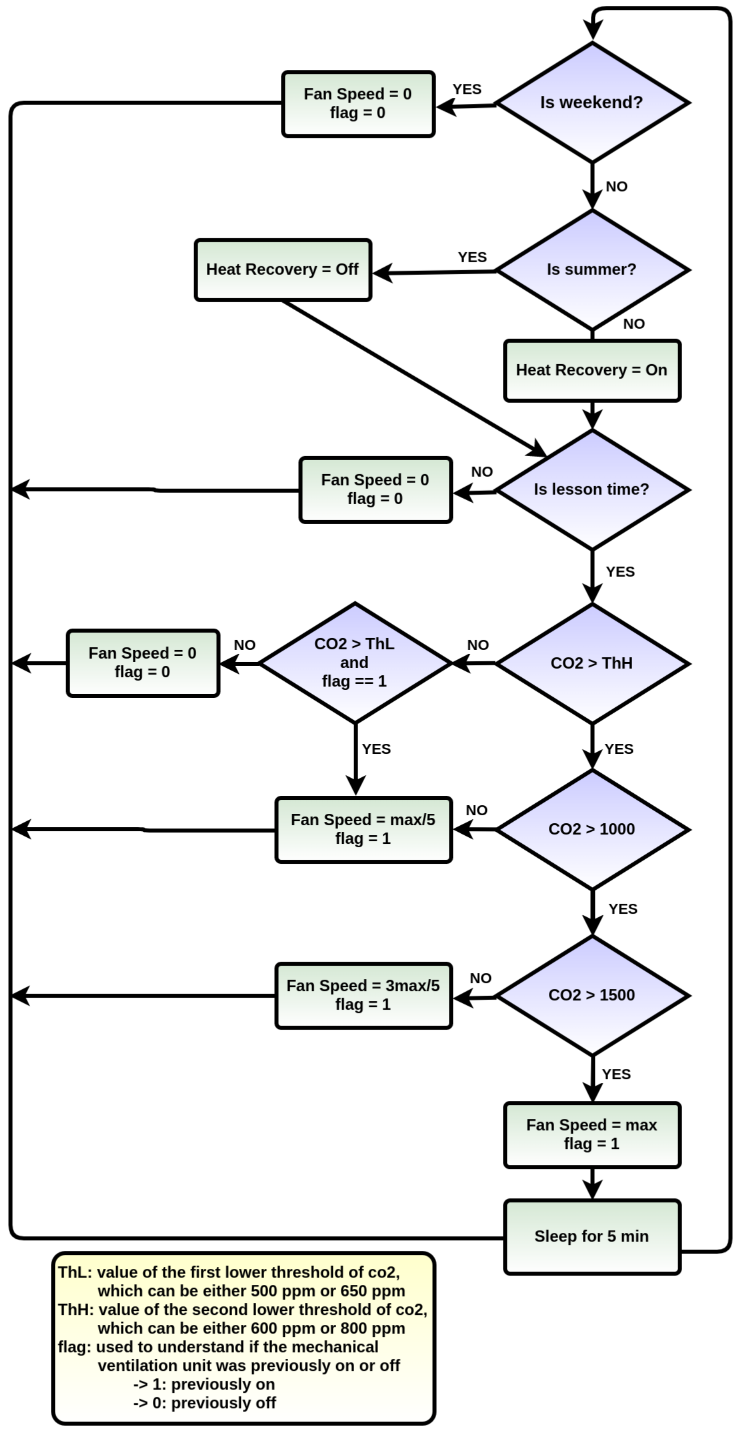

Figure 8.3: Ventilation algorithm based on a double CO_2 threshold

8.6 CO_2 Double Threshold Controls

Double threshold controls have been developed to reduce the number of switches on and off of the unit if the value of CO_2 is fluctuating around the threshold value. Selected values used as thresholds are the same specified in 8.5, and even the general algorithm, which can be seen in Fig. 8.3, is similar to the one of the single threshold case. The only exception is when the mechanical ventilation unit was already on, and the CO_2 value drops below $600ppm$ or $800ppm$, depending on the case. In these cases, the airflow is not set to zero, but it is kept at 1/5 of the nominal value until the carbon dioxide concentration drops under $500ppm$ and $650ppm$ respectively.

9. Simulated Strategies Results

9.1 Free-Running Building Results

At first, the complete IDF has been simulated without EMS controls to see the free-running building behavior.

The temperature behavior can be seen in Fig. 9.1, while the carbon dioxide behavior is shown in Fig. 9.2. This last figure shows that without control, in the selected period, the maximum CO_2 value overpasses every weekday the suggested ASHRAE value of $1000ppm$, sometimes also of a relevant amount, so controls are needed to bring environmental parameters back to healthiness.

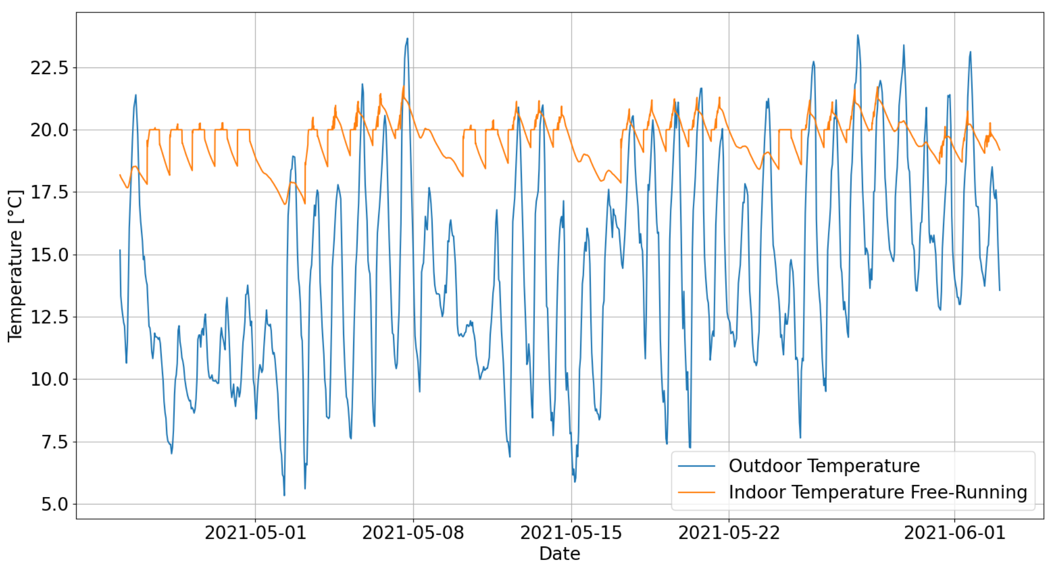

Figure 9.1: Indoor and outdoor temperature behavior of the free-running building over the selected period

Results of relevant environmental parameters are shown in Table 9.1.

9.2 Constant Air Flow based on ASHRAE Standards Results

9.2.1 ASHRAE 62

Simulations' results of the ASHRAE 62 control strategy can be seen in Table 9.2.

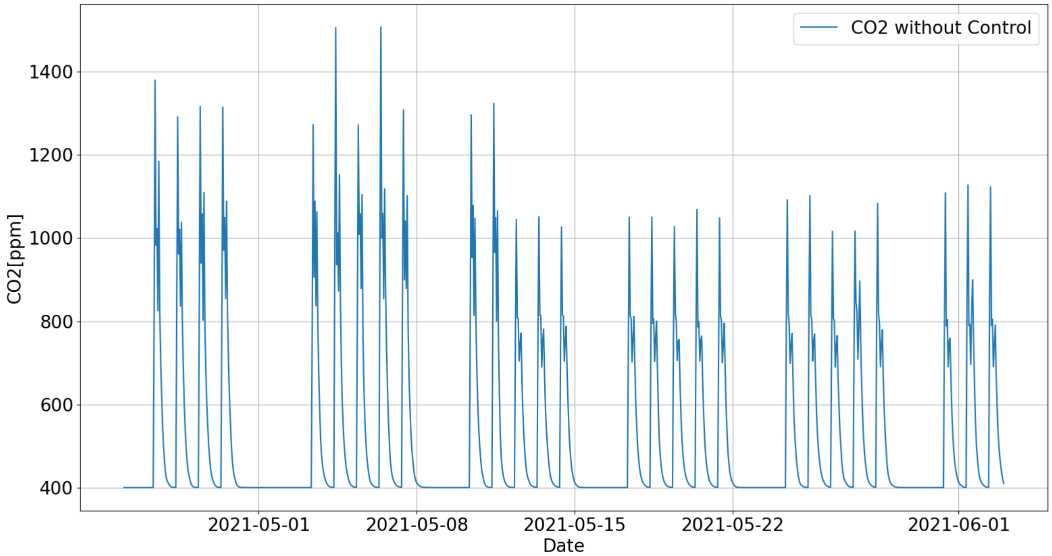

Figure 9.2: Indoor CO_2 behavior of the free-running building over the selected period

Total electric consumption	1188 kWh
Average outdoor temperature	14.3 °C
Average indoor temperature	19.6 °C
Average indoor CO_2	524 ppm
Average indoor CO_2 considering just when there is occupation	748 ppm
Average indoor CO_2 peak value	1179 ppm

Table 9.1: Results of the free-running building simulation

Mechanical ventilation airflow total consumption	8 kWh
Total electric consumption	1196 kWh
Average indoor temperature	19.5 °C
Average indoor CO_2	460 ppm
Average indoor CO_2 considering just when there is occupation	593 ppm
Average indoor CO_2 peak value	713 ppm
Total on/off cycles of the mechanical ventilation unit	28

Table 9.2: Results of the ASHRAE 62 control strategy simulation

The behavior of the CO_2 can be seen in Fig. 9.3, the one of the indoor temperature in Fig. 9.4, and the used airflow rate in Fig. 9.5.

From these results, it can be seen that the average indoor temperature does not drop relevantly because of the ventilation, so there will not be an increase in the heating consumption even though the heat recovery is off.

Both peaks and average carbon dioxide values when there is occupation are consistently smaller than the measurements in the free-running simulation, so the control is correctly working, limiting the concentration of the CO_2 in the room to be under $800ppm$.

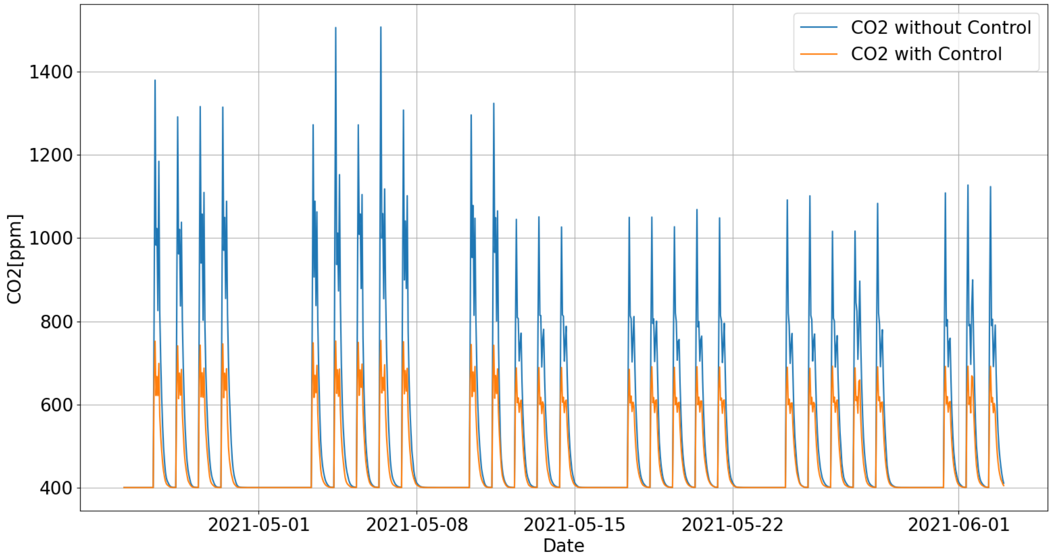

Figure 9.3: Indoor CO_2 behavior of the free-running building compared with the controlled one over the selected period

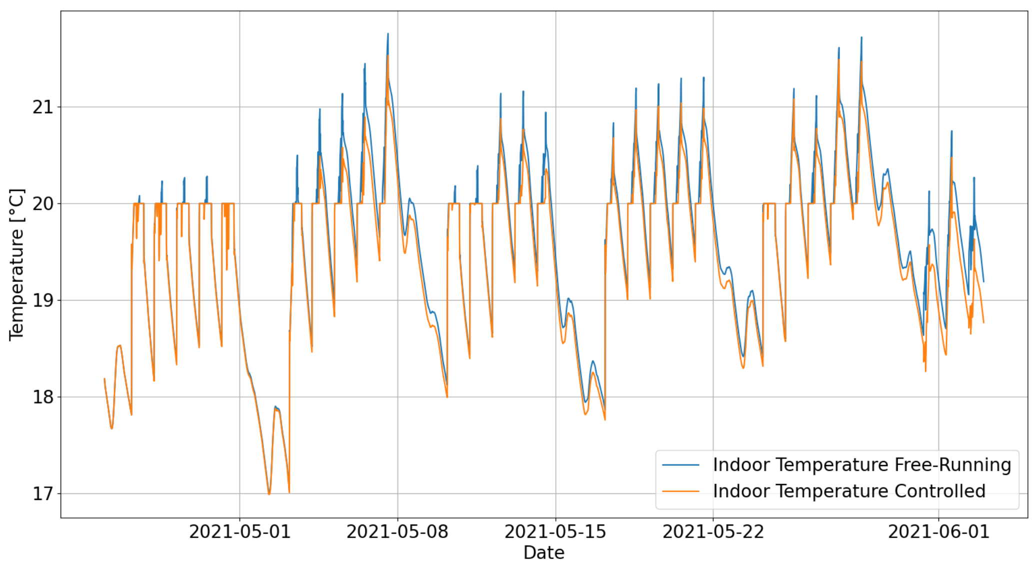

Figure 9.4: Indoor temperature behavior of the free-running building compared with the controlled one over the selected period

From the ventilation plot in Fig. 9.5, it can be seen that the ventilation is set to the value recommended by the ASHRAE 62 standard during occupation periods, which for schools correspond to all the weekdays

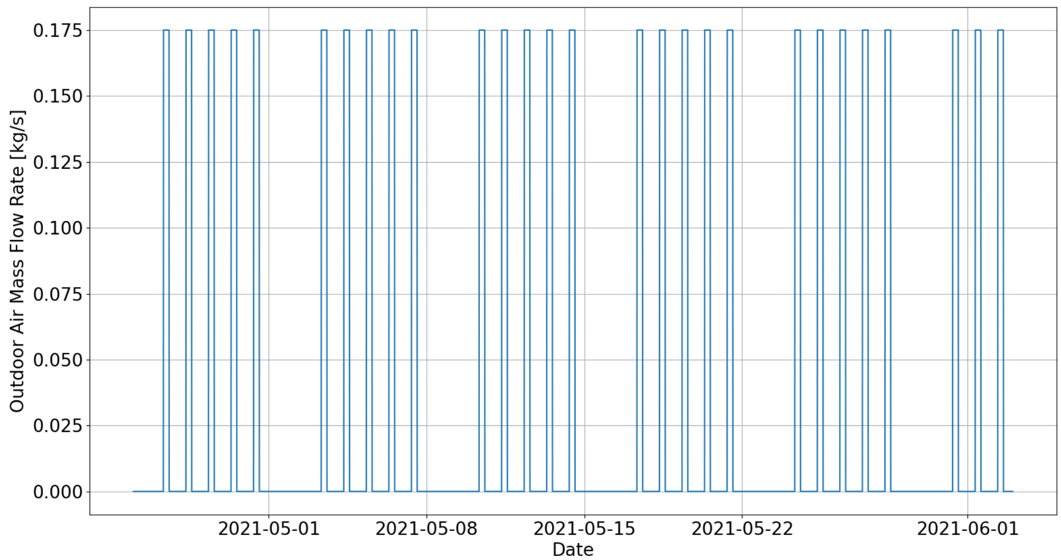

Figure 9.5: Ventilation airflow rate over the selected period

from 8:00 AM to 2:00 PM, else it is turned off. For these reasons, the mechanical ventilation unit turns on and off exactly once per day.

9.2.2 ASHRAE 62.1

ASHRAE 62.1 simulations' results can be seen in Table 9.3.

Mechanical ventilation airflow total consumption	19 kWh
Total electric consumption	1207 kWh
Average indoor temperature	19.1 °C
Average indoor CO_2	453 ppm
Average indoor CO_2 considering just when there is occupation	624 ppm
Average indoor CO_2 peak value	742 ppm
Total on/off cycles of the mechanical ventilation unit	1

Table 9.3: Results of the ASHRAE 62.1 control strategy simulation

The CO_2 behavior can be seen in Fig. 9.6, the indoor temperature one in Fig. 9.7, and the used airflow rate in Fig. 9.8.

It can be seen that the average indoor temperature drops overall by a small amount due to the ventilation, so there might be an increase in the heating consumption specifically in the morning, where this drop in temperature is not negligible. In fact, by ventilating all night with the outdoor air at a colder temperature, which reaches a minimum value of 5°C, the indoor temperature also drops during the night, taking its minimum value in the morning when students arrive at school. The indoor temperature reaches minimum peaks of 16°C during occupation hours, at the very beginning of school days, overpassing the minimum indoor temperature established by Italian laws, which indicates that the temperature in classrooms should not be lower than 18°C. For these reasons, an increased heating consumption must also be considered when using this control approach.

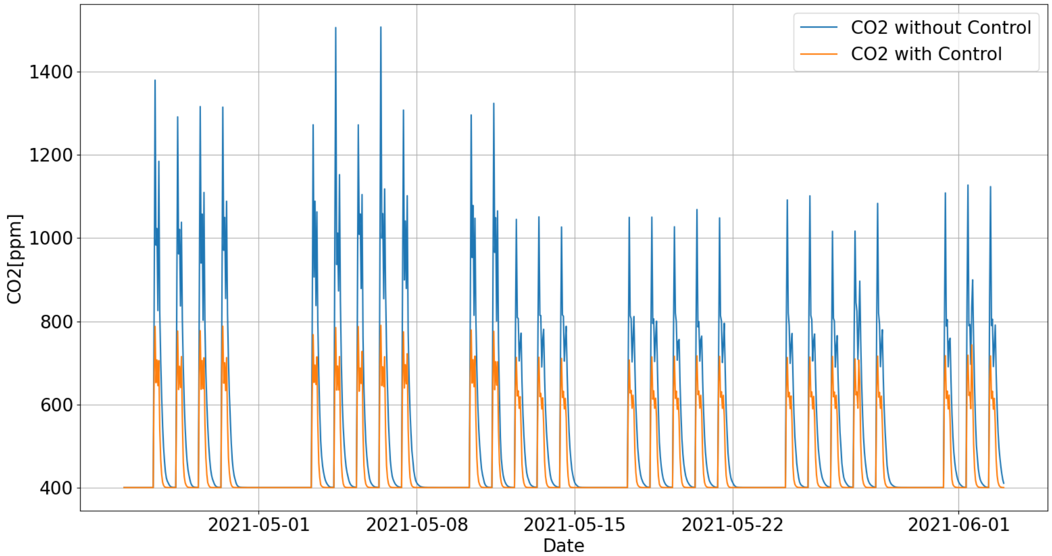

Figure 9.6: Indoor CO_2 behavior of the free-running building compared with the controlled one over the selected period

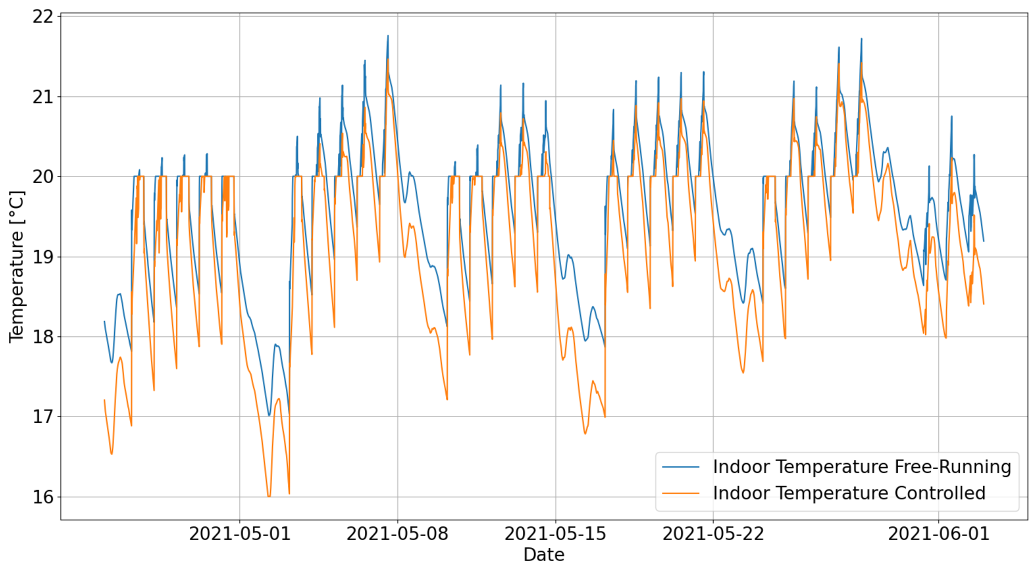

Figure 9.7: Indoor temperature behavior of the free-running building compared with the controlled one over the selected period

Both peaks and average carbon dioxide values when there is occupation are limited to be under $800ppm$, without any relevant advantage if compared with the previous version of the standard ASHRAE 62. The

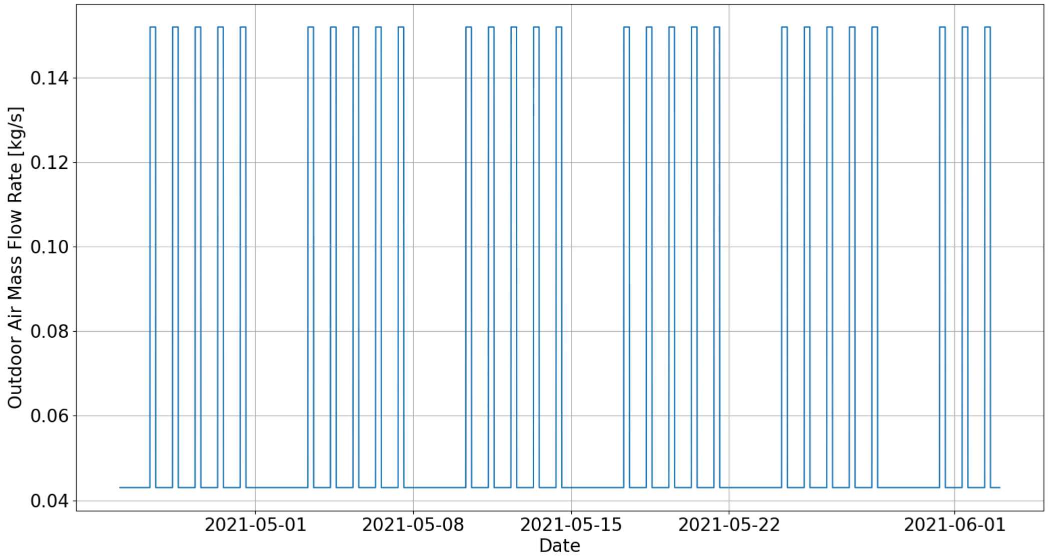

Figure 9.8: Ventilation airflow rate over the selected period

main advantage is related to pollutants that are not human-produced, which are removed by the minimum ventilation rate during the night, while in the previous standard they cumulate till the morning when students come in.

From the ventilation plot in Fig. 9.8, it can be seen that the ventilation is set to the value recommended by the ASHRAE 62.1 standard during both occupation and empty periods, so the mechanical ventilation unit is always on, even during weekends. For this reason, even the electric consumption of the mechanical ventilation unit is more than double the one obtained by using the ASHRAE 62 standard.

9.3 CO_2 Single Threshold Results

9.3.1 Threshold of $600ppm$

Simulations' results of the single threshold control strategy with $600ppm$ as the lower threshold value can be seen in Table 9.4.

Mechanical ventilation airflow total consumption	2 kWh
Total electric consumption	1190 kWh
Average indoor temperature	19.5 °C
Average indoor CO_2	490 ppm
Average indoor CO_2 considering just when there is occupation	669 ppm
Average indoor CO_2 peak value	913 ppm
Total on/off cycles of the mechanical ventilation unit	27

Table 9.4: Results of the single threshold control strategy simulation with $600ppm$ as the lower threshold value

The behavior of the CO_2 can be seen in Fig. 9.9, the one of the indoor temperature in Fig. 9.10, and the used airflow rate in Fig. 9.11.

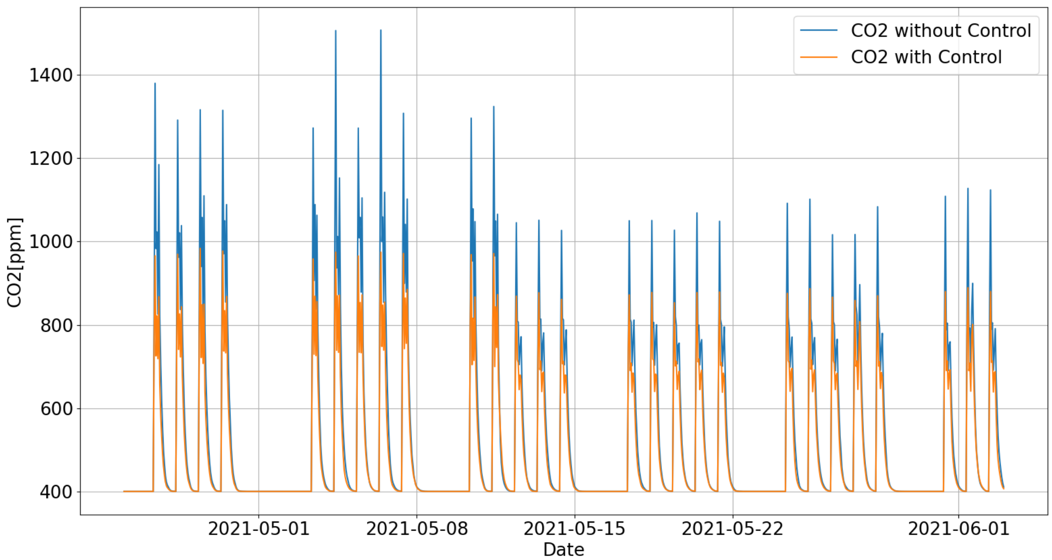

Figure 9.9: Indoor CO_2 behavior of the free-running building compared with the controlled one over the selected period

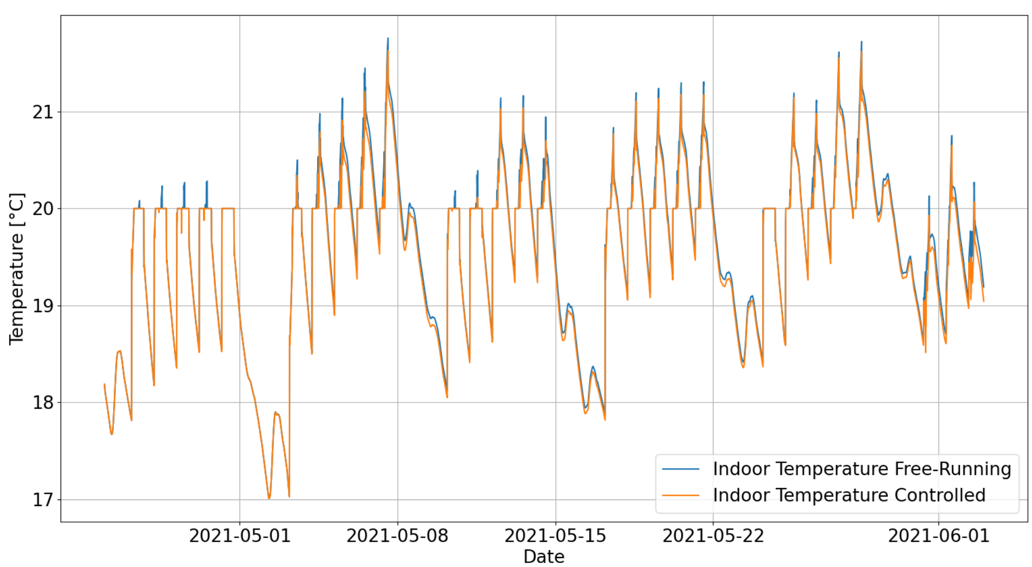

Figure 9.10: Indoor temperature behavior of the free-running building compared with the controlled one over the selected period

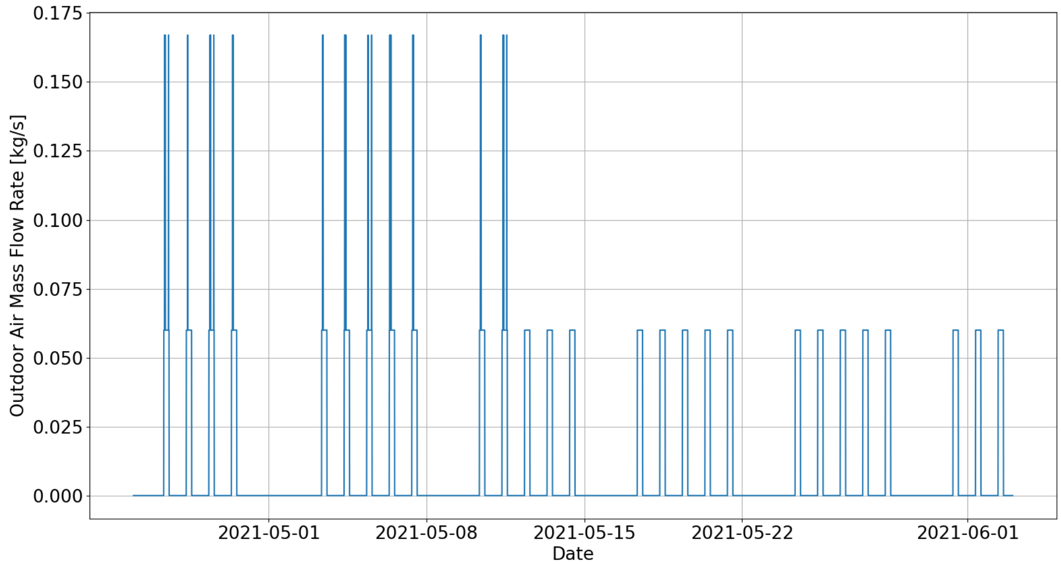

Figure 9.11: Ventilation airflow rate over the selected period

From these results, it can be seen that even here, as in the control strategy seen in paragraph 9.2.1, the indoor temperature is very similar to the one of the free-running building. Even in this case, there will not be an increase in heating consumption to compensate for the colder air introduced with ventilation.

Both peaks and average carbon dioxide values when there is occupation are reduced if compared with the free-running simulation. The CO_2 value is limited to be under $1000ppm$, which is the value suggested by ASHRAE as the limit for guaranteeing healthiness. The reduction in the carbon dioxide concentration is smaller if compared with constant ventilation strategies discussed in 9.2. It happens because the single threshold strategy ventilates just when there is the need to, while fixed ventilation approaches inject a constant airflow rate every day at every hour, which can lead most of the time to over-ventilation. Thanks to its on-demand nature, electric consumption of the threshold strategy is four times smaller than the fixed ventilation strategy which consumes less, as seen in 9.2.1, and it consumes nine-time less than the ASHRAE 62.1 ventilation standard seen in 9.2.2.

From the ventilation plot in Fig. 9.11, it can be seen how the ventilation rate evolves during occupation periods. While in unoccupied moments, ventilation is turned off. The mechanical ventilation unit turns on/off 27 times, which means that once the mechanical ventilation unit is set on for a given school day, it remains on till the end of that day because the CO_2 concentration never returns under $600ppm$.

9.3.2 Threshold of $800ppm$

Simulations' results of the single threshold control with $800ppm$ as the lower threshold can be seen in Table 9.5.

The behavior of the CO_2 can be seen in Fig. 9.12, the one of the indoor temperature in Fig. 9.13, and the used airflow rate in Fig. 9.14.

The temperature behavior is similar to the one of the $600ppm$ threshold strategy previously explained in paragraph 9.3.1. Therefore, conclusions on heat dispersion of the previous strategy can be drawn here as well.

The same thing is valid even for the level of carbon dioxide concentration, which is similar to the $600ppm$

Mechanical ventilation airflow total consumption	1 kWh
Total electric consumption	1189 kWh
Average indoor temperature	19.5 °C
Average indoor CO_2	500 ppm
Average indoor CO_2 considering just when there is occupation	690 ppm
Average indoor CO_2 peak value	918 ppm
Total on/off cycles of the mechanical ventilation unit	92

Table 9.5: Results of the single threshold control strategy simulation with 800ppm as the lower threshold value

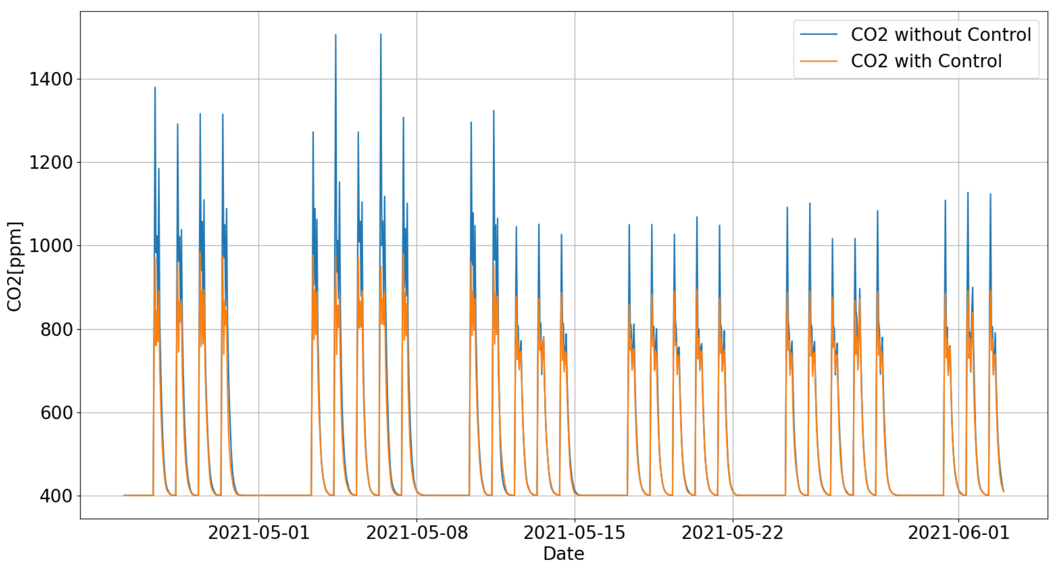

Figure 9.12: Indoor CO_2 behavior of the free-running building compared with the controlled one over the selected period

threshold strategy seen in 9.3.1. Peaks and average CO_2 values are reduced if compared with the free-running building, given that they are limited under 1000ppm, but are higher than the ones of fixed ventilation strategies presented in 9.2, for the same reasons explained in 9.3.1. Given that the threshold value is 800ppm instead of 600ppm, the ventilation unit will be off for more time, and for this reason, it consumes half of the energy of the strategy with 600ppm.

From the ventilation plot in Fig. 9.14, it can be seen how the ventilation rate evolves during occupation periods. In particular, the ventilation unit turns on and off multiple times during the day because the value of CO_2 concentration returns several times under 800ppm. While in unoccupied moments, ventilation is set to zero. The mechanical ventilation unit turns on/off 92 times, which is more than three times per day on average. Continuous on and off of the mechanical ventilation system may shorten its lifetime, so it is preferable to use a control strategy that limits these switching, so double thresholds strategies are investigated.

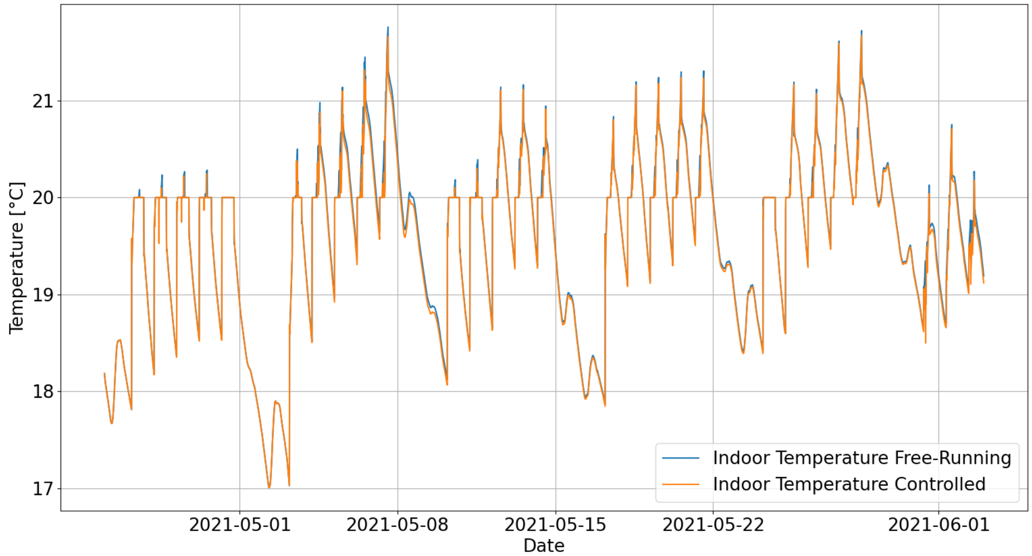

Figure 9.13: Indoor temperature behavior of the free-running building compared with the controlled one over the selected period

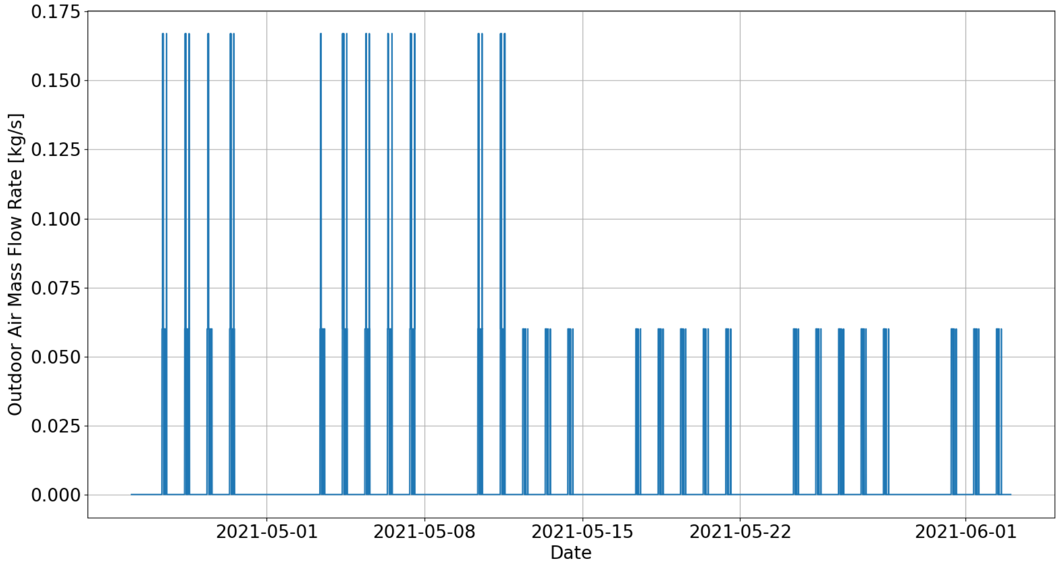

Figure 9.14: Ventilation airflow rate over the selected period

9.4 CO_2 Double Threshold Results

9.4.1 Threshold of $500ppm$ and $600ppm$

Simulations' results of the double threshold control strategy with $500ppm$ as the lower threshold can be seen in Table 9.6.

Mechanical ventilation airflow total consumption	2 kWh
Total electric consumption	1190 kWh
Average indoor temperature	19.5 °C
Average indoor CO_2	490 ppm
Average indoor CO_2 considering just when there is occupation	669 ppm
Average indoor CO_2 peak value	913 ppm
Total on/off cycles of the mechanical ventilation unit	27

Table 9.6: Results of the double threshold control strategy simulation with $500ppm$ as the lower threshold value

CO_2 behavior can be seen in Fig. 9.15, the indoor temperature one in Fig. 9.16, and the used airflow rate in Fig. 9.17.

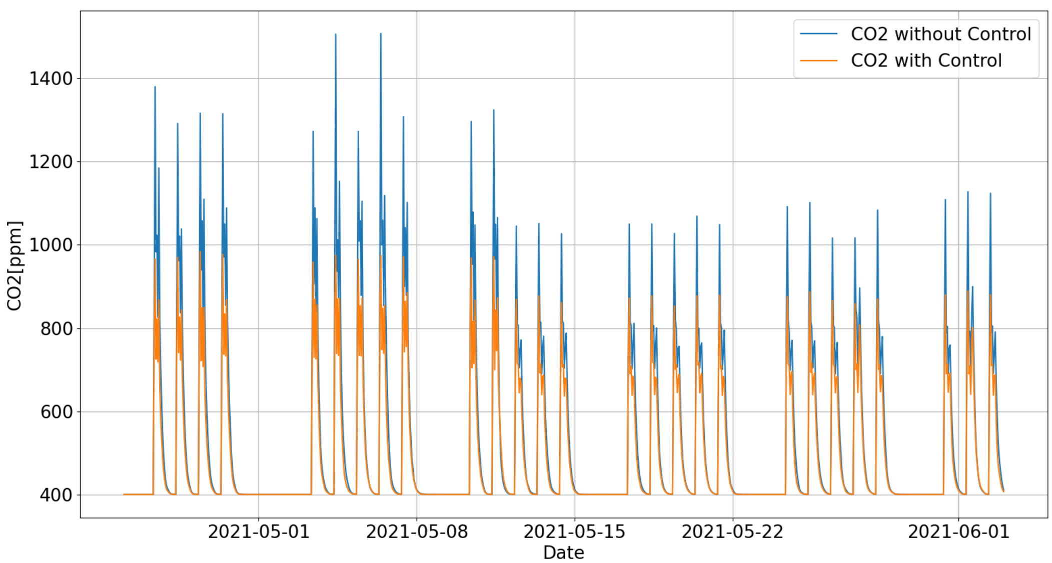

Figure 9.15: Indoor CO_2 behavior of the free-running building compared with the controlled one over the selected period

All results are identical to the ones obtained for the single threshold strategy with $600ppm$ as the lower threshold value already analyzed in 9.3.1. This happens because the ventilation turns on, even in this case, once every weekday, and the CO_2 concentration never returns under $600ppm$ before the end of the school period in which ventilation is then turned off. Therefore, the only difference between the two strategies is that the one with a single threshold turns off when the CO_2 reach at the end of the day the value $600ppm$, while the one with two thresholds is turned off when the internal carbon dioxide concentration reaches the value of $500ppm$, so a few minutes after.

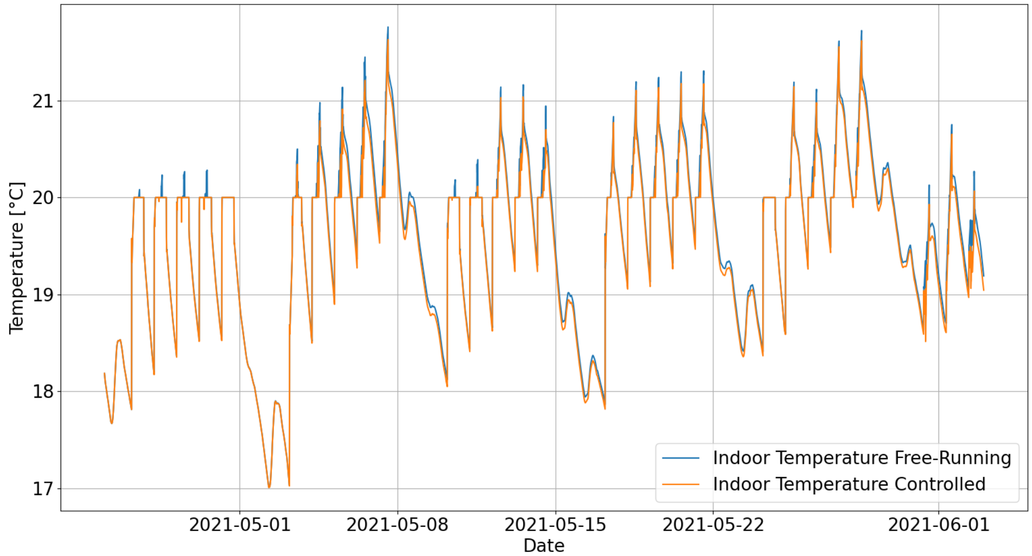

Figure 9.16: Indoor temperature behavior of the free-running building compared with the controlled one over the selected period

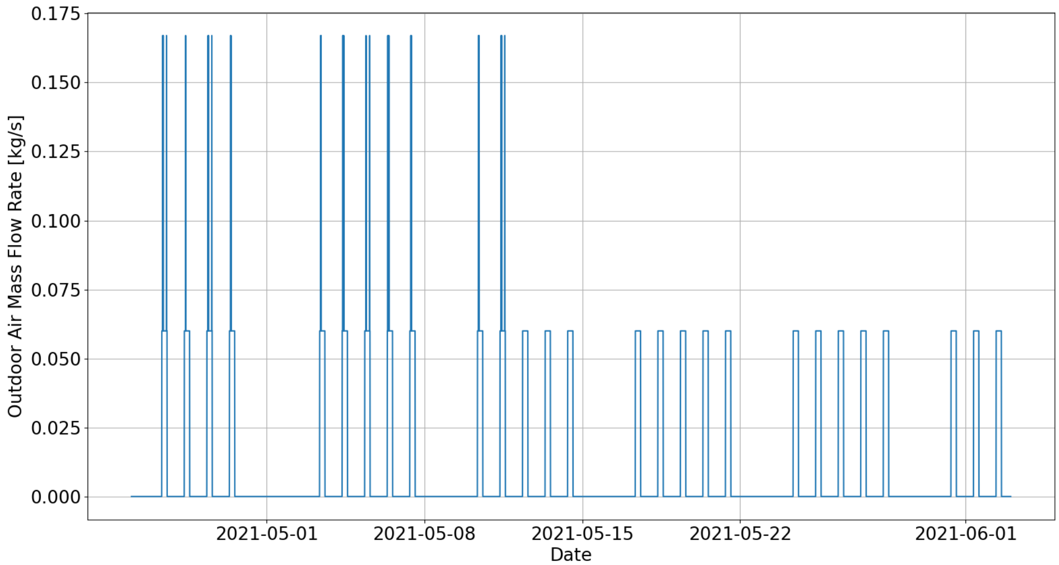

Figure 9.17: Ventilation airflow rate over the selected period

9.4.2 Threshold of $650ppm$ and $800ppm$

Simulations' results of the double threshold control strategy with $650ppm$ as the lower threshold can be seen in Table 9.7.

Mechanical ventilation airflow total consumption	2 kWh
Total electric consumption	1190 kWh
Average indoor temperature	19.5 °C
Average indoor CO_2	497 ppm
Average indoor CO_2 considering just when there is occupation	678 ppm
Average indoor CO_2 peak value	918 ppm
Total on/off cycles of the mechanical ventilation unit	58

Table 9.7: Results of the double threshold control strategy simulation with $650ppm$ as the lower threshold value

CO_2 behavior can be seen in Fig. 9.18, the indoor temperature one in Fig. 9.19, and the used airflow rate in Fig. 9.20.

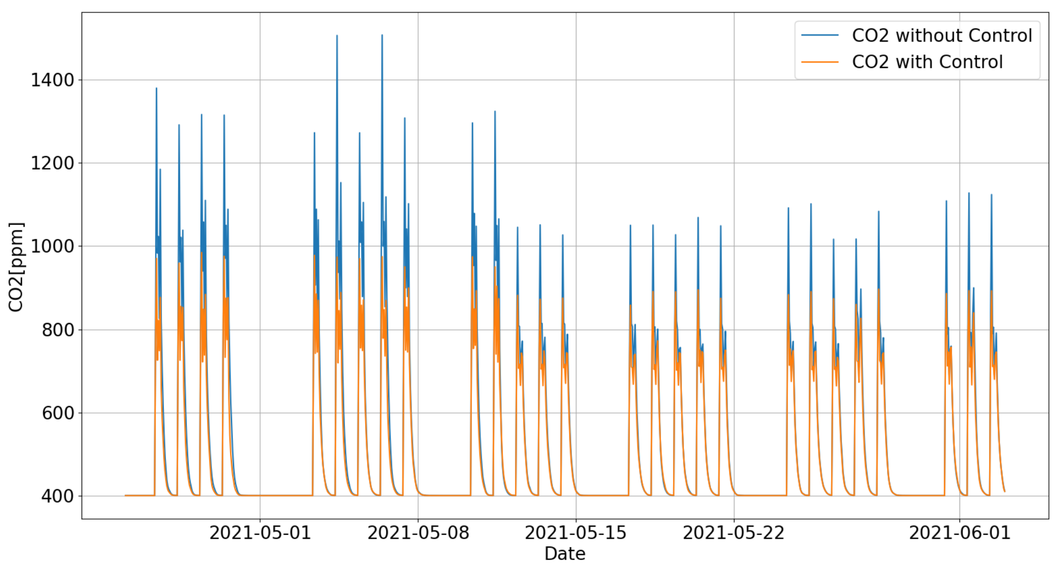

Figure 9.18: Indoor CO_2 behavior of the free-running building compared with the controlled one over the selected period

Results on both temperature and carbon dioxide behavior are equal to the ones of the single threshold control approach with $800ppm$ as the lower threshold, which has been previously explained in 9.3.2, so its conclusions are still valid even here as well.

Two main differences are introduced because of the double threshold if this approach is compared to the single $800ppm$ threshold strategy. These differences are:

- the energy consumption is higher given that ventilation stays on for more time;
- from the ventilation plot in Fig. 9.20, it can be seen that ventilation does not turn on and off as often

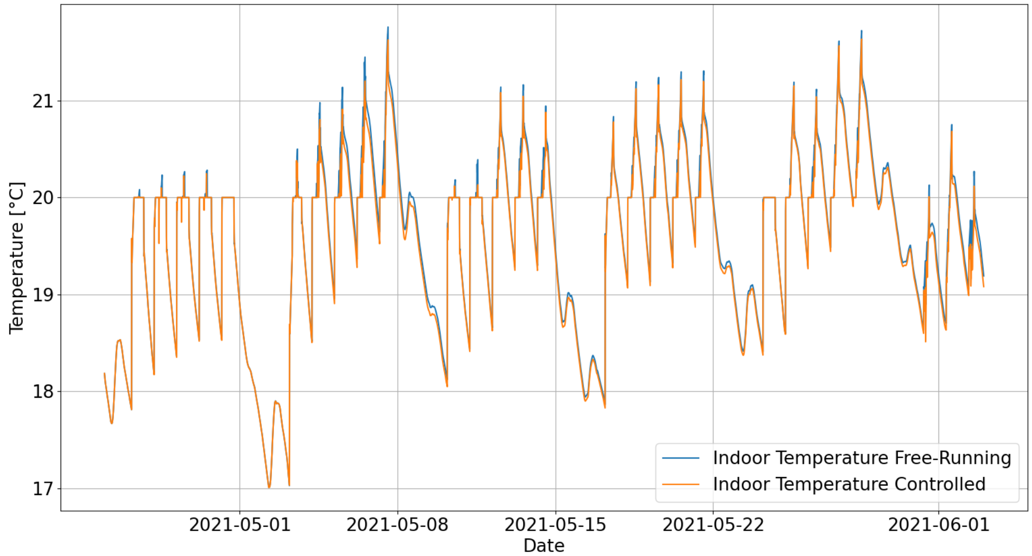

Figure 9.19: Indoor temperature behavior of the free-running building compared with the controlled one over the selected period

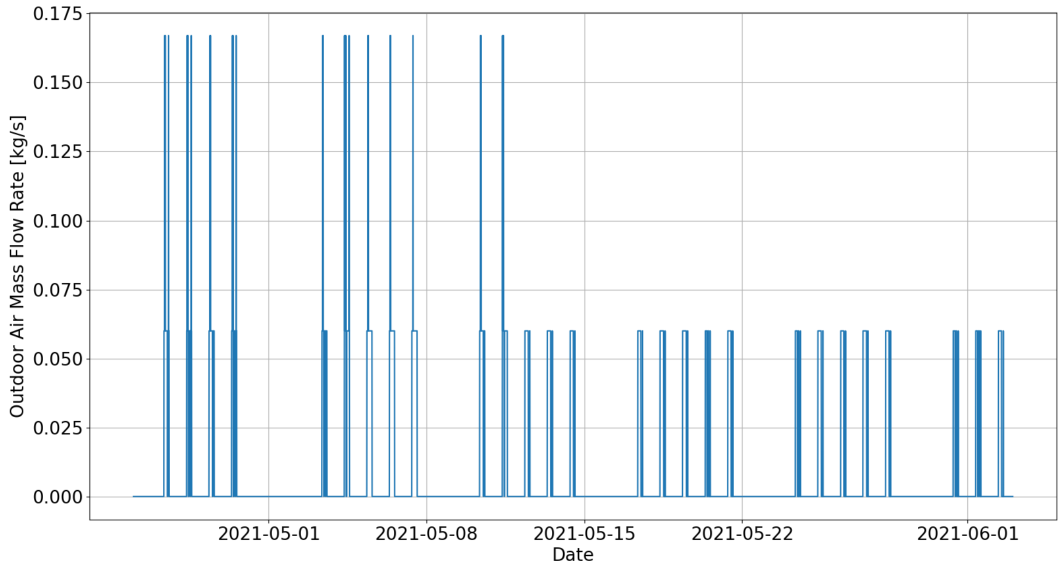

Figure 9.20: Ventilation airflow rate over the selected period

as in the single threshold approach, and the number of on/off cycles is about half. In this way, the lifetime of the mechanical ventilation unit is lengthened.

10. Hardware Structure for Modbus

10.1 Hardware Components

For testing control strategies in the school, it is necessary to have a controller that can act as a Master in the Modbus communication. For this purpose, the following hardware components are used:

- three Raspberry Pi 4 8GB KITs, one for each mechanical ventilation unit;
- three B6RS485 CAN HATs that are Raspberry Pi interfaces needed to allow the Modbus communication;
- $30m$ of $4x0.22mmq$ copper shielded cable, black sheath;
- USB to RS485 converter to test strategies with a simulator before implementing them in real units;
- a 7" touch display compatible with the Raspberry Pi used for an easier configuration of devices.

The whole structure used for testing the Modbus communication with the laptop can be seen in Fig. 10.1.

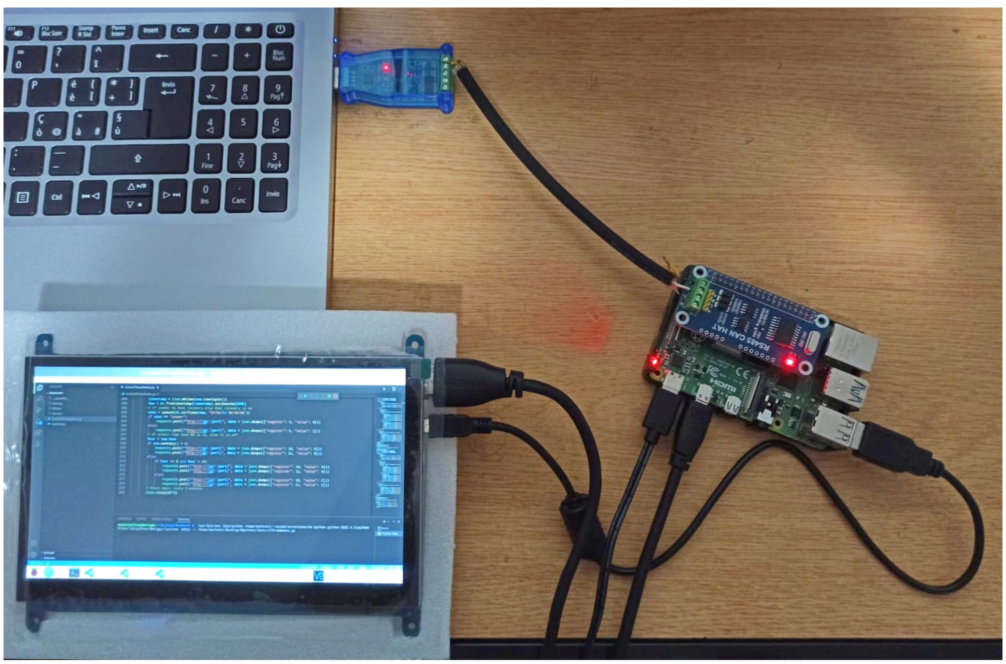

Figure 10.1: Hardware structure for testing the Modbus communication with the laptop

Moreover, in the second testing period, which is at the beginning of the school year in September, carbon dioxide-based strategies are tested in the actual mechanical ventilation units. In this case, a dedicated CO_2 sensor is installed on Raspberry Pi to have fast control strategies responsiveness. The chosen sensor is the Sensirion SEK-SCD41 CO2 Sensor Evaluation Kit because of its compatibility with Raspberry Pi, for which it also provides drivers [61].

10.2 Raspberry Pi 4 8GB KIT

The Raspberry Pi, that can be seen in Fig. 10.2, is a single-board computer used in many fields of application because it is cheap and allows the building of different architectures through open design components. In particular, in this thesis, it is used to run scripts that make it act as a Master Device in the Modbus communication. The base kit is composed of:

- one Raspberry Pi 4 8GB board;
- one power supply for powering the board;
- a Raspberry Pi HDMI Cable used to connect the board to the display;
- a 32GB Micro SD Card that is used to store the Raspberry Pi OS;
- the standard case for the Raspberry Pi board.

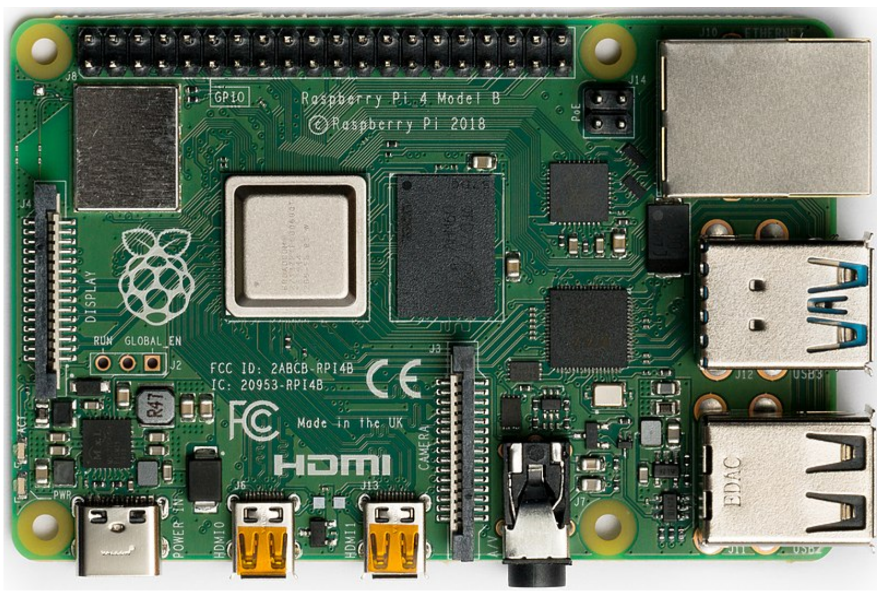

Figure 10.2: Raspberry Pi 4 B [44]

To be prepared for use, the Raspberry Pi OS has been installed on the memory card by using the Raspberry Pi Imager [56]. Then, after creating the user and corresponding credentials, SSH, VNC, serial, and Wi-Fi communications are enabled.

The Wi-Fi connection is needed both to configure boards correctly and to run scripts that need to retrieve data from the InfluxDB server.

SSH connection has been used when the display was still not available to discover the IP address of the Raspberry Pi on the network to configure the VNC connection that was used as an alternative for the missing screen. To connect to the Raspberry Pi using SSH the software PuTTY [67] has been used.

After finding IP addresses of boards, to connect the laptop to them through VNC the software VNC Viewer [58] is used. At this point, it is possible to use the board with the screen of the computer given that the 7" display did not arrive yet.

The VNC connection has been used also when the display was at the disposal for connecting the Raspberry Pi installed in the school and connected to the school network with the computer screen to control them remotely. For doing this, a VPN service ZeroTier [76] is used to put the computer and the three boards on the same virtual network.

Serial communication is needed for enabling the Modbus communication through the RS485 port of the B6RS485 CAN HAT.

10.3 B6RS485 CAN HAT

The B6RS485 CAN HAT, which can be seen in Fig. 10.3, is used to enable the Modbus communication in the Raspberry Pi through the port RS485 controlled via UART, which allows the serial transmission and reception of data without ad-hoc programming. It can be connected to the board through 40 GPIO pins. Its configuration steps can be seen in [73].

Figure 10.3: B6RS485 CAN HAT

10.4 4x0.22 mmq Copper Shielded Cable

The cable is used to physically connect the Raspberry Pi RS485 port with that of the USB to RS485 Converter or that of the mechanical ventilation unit board to allow wired communication.

10.5 USB to RS485 Converter

The USB to RS485 Converter, that can be seen in Fig. 10.4, is used to connect the B6RS485 CAN HAT of the Raspberry Pi with the laptop to simulate the Modbus communication.

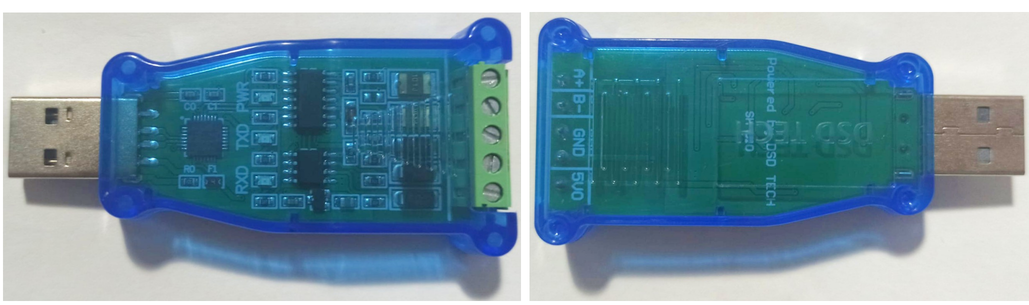

Figure 10.4: USB to RS485 Converter

10.6 7” touch display

The touch display has been added in a second moment to make the configuration of the Raspberry Pi easier, to avoid the cumbersome headless setup, done according to the official documentation that can be seen in [57].

10.7 Sensirion SEK-SCD41 CO2 Sensor Evaluation Kit

The Sensirion SEK-SCD41 CO2 Sensor Evaluation Kit [50] is used to retrieve the instantaneous value of indoor carbon dioxide to make real-time decisions on how to operate the mechanical ventilation units. It has been connected directly with RaspberryPi and retrieves current CO_2 values through the drivers written in C available in [61].

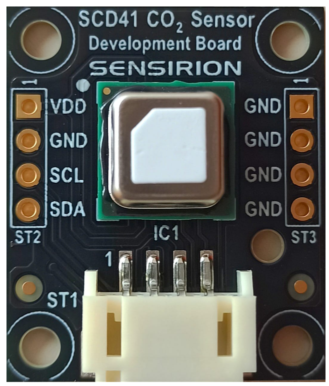

Figure 10.5: Sensirion SEK-SCD41 CO2 Sensor Evaluation Kit

11. Software for Monitored Strategies

11.1 General Software Structure

The general software structure used to control the mechanical ventilation units in the school in Torre Pellice is shown in Fig. 11.1, highlighting communication strategies between different software parts and the most relevant pieces of information that are exchanged.

Even in this case, the whole architecture is developed following the micro-service approach instead of the monolithic structure. The same Catalog explained in detail in 7.2.1 is the heart of the whole architecture.

11.2 Season Information Script

This script is used to understand if a given date is in the summer or winter period. In this way, it is possible to decide if it is needed to enable or disable the heat recovery system of mechanical ventilation units. By allowing heat recovery in winter, it is possible to save energy from the heating system because a significantly smaller amount of heat is lost because of ventilation. On the contrary, by shutting off the heat recovery in summer, it is possible to exploit the outdoor air to ventilate the indoor environment to reduce the cooling load of the conditioning system.

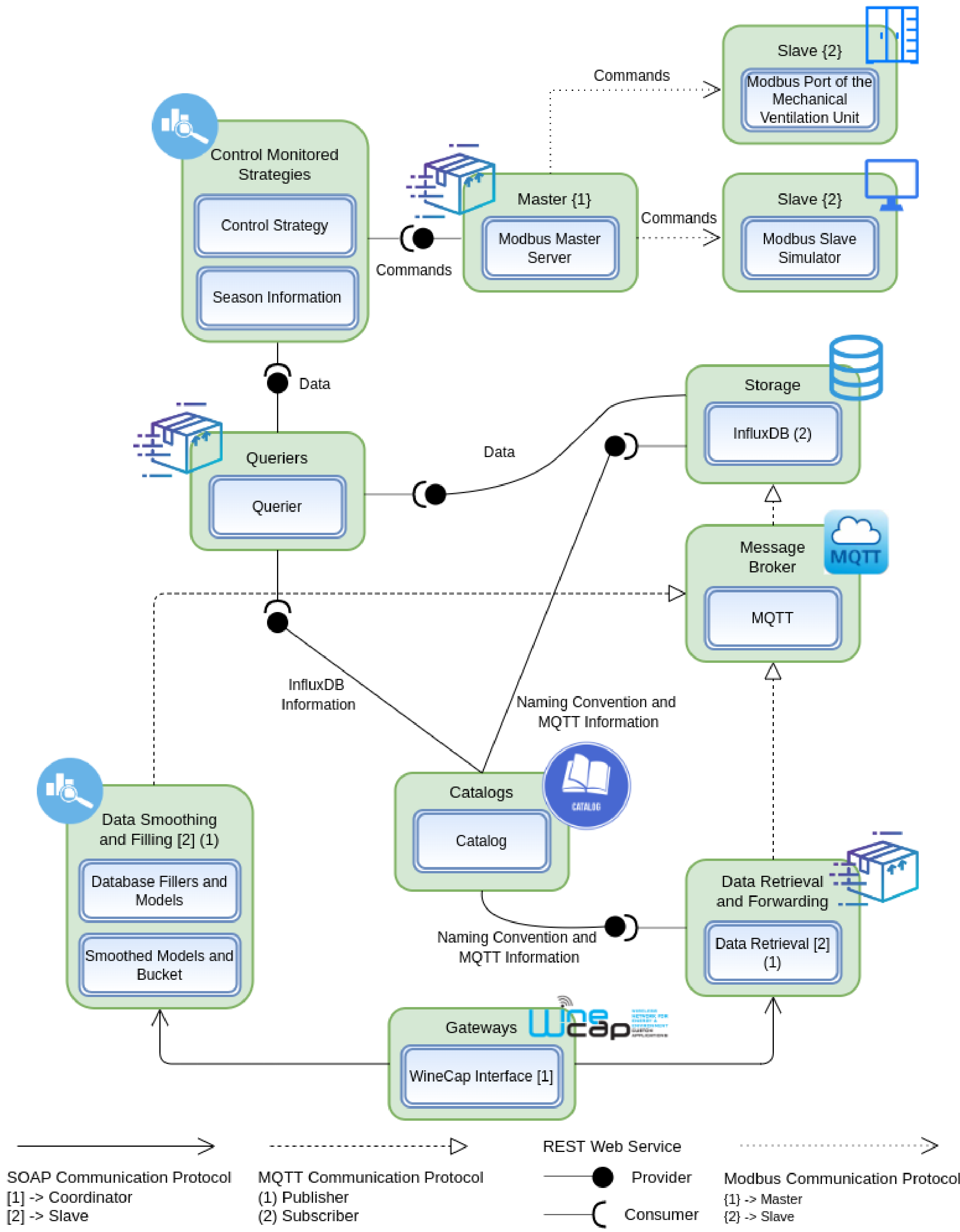

Figure 11.1: General software structure for monitored control strategies

11.3 Control Strategies

Different Control Strategies scripts have been developed to compare the results of different approaches to find the most effective. All of these scripts follow the same logical structure that is based on:

- retrieve the current date and change its timezone to *Europe/Rome*;
- open a file that will be used as a log file to save the current time and Modbus commands that are sent while the script is running;
- retrieve the season to choose if activating or deactivating the heat recovery;
- get the last collected data from sensors by connecting to the querier script explained in 7.3 through the REST interface to make decisions based on the condition of both the indoor and the outdoor environment. If the test is done on the second testing period with the carbon dioxide sensor installed on the RaspberryPi, data are taken directly from it, and the whole structure in Fig. 11.1 till the querier is not used.
- change the speed of fans of mechanical ventilation units based on sensed conditions by sending requests through the REST interface to the Modbus Master Server;
- check again conditions every 5 minutes to update the decisions.

11.4 Modbus Master

The Modbus Master is a CherryPy server that, in the initialization, enables the port of the B6RS485 CAN HAT to be correctly used for the Modbus communication and then exposes two different REST methods based on the *PyModbus* python library:

- GET, that is used to obtain the value of a specific register that is specified in the URL of the request;
- POST, which is used to change the value of a particular register by sending both the new value and the register's name in the request's body.

11.5 Modbus Slave Simulator

The Modbus Slave simulator script is used to simulate, through the *PyModbus* python library and by using the USB to RS485 Converter, the real Modbus port of the mechanical ventilation units of the school to test control strategies before implementing them in the real system. It also saves the history of received commands in a log file for debugging purposes.

12. Monitored Strategies

12.1 Ventilative Cooling Strategies

During the first testing period, the main control strategies tested in the school are seven, and their main aim is to refresh the indoor environment by exploiting ventilative cooling techniques. This objective was chosen as a priority because these methodologies were tested in July when there are no occupants in the school. Therefore, the test of a CO_2-based technique is useless given that the main sources of carbon dioxide, people, are absent. On the contrary, given that July is usually the hottest month in Italy, the ventilative cooling techniques can be tested successfully in the most favorable conditions.

For each room, three different strategies have been tested, one for each testing week. The selected weeks for running strategies are:

- from 14/07/2022 at 00:00 AM to 20/07/2022 at 11:59 PM;
- from 21/07/2022 at 00:00 AM to 27/07/2022 at 11:59 PM;
- from 28/07/2022 at 00:00 AM to 03/08/2022 at 11:59 PM.

All used strategies have in common the following actions:

- if the selected day is of the weekend, ventilation is turned off;
- if it is winter, heat recovery is turned on to limit heat losses, and a simple single threshold strategy is used to control the CO_2 concentration, using $600ppm$ as lower threshold value;
- if it is summer, heat recovery is turned off to allow the cooling of the indoor environment thanks to the lower temperature of the outdoor air, and the selected peculiar strategy is employed.

In the following sections, all tested monitored strategies are reported and explained properly.

12.1.1 Temperature Difference Ventilation

The temperature difference-based ventilation control strategy takes all its decisions according to the temperature difference between the internal and the external temperatures. The algorithm complete flow can be seen in Fig. 12.1, and in particular:

- if the difference is within the interval $[-2, 2]$ and it is night-time, the fan speed is set to the maximum value unless the indoor temperature is lower than 16°C. In this case, the airflow is set to zero to avoid unpleasant cooling;
- if the temperature difference is between 2°C and 10°C, then the fan speed is set to its maximum value if it is lesson time or immediately before it, to exploit the cooling load of the outdoor air to its maximum potential during occupation periods, else it is turned off to avoid unnecessary use of electricity;
- in every other case, it uses a simple single threshold CO_2-based control and checks if the outdoor temperature is higher than the indoor one to select the value of the lower threshold. If the external temperature is the highest, the lower CO_2 threshold is set to $800ppm$ to avoid unnecessary hot air flowing indoors from the outside. Otherwise, it is set to $600ppm$ to use the cooler outdoor air even when the CO_2 strategy is used.

12.1.2 Temperature Threshold Ventilation

The temperature threshold-based control strategy decides the airflow amount on instantaneous indoor and outdoor temperature values. The algorithm flow can be seen in Fig. 12.2. At first, this strategy checks if it is lesson time. If not, ventilation is fixed to zero. Otherwise, if the indoor temperature is higher than 21°C and the room air temperature is higher than the external one, ventilation is set to its maximum, if not, it uses a single threshold CO_2 control with $800ppm$ as the lower threshold, to avoid unnecessary heating.

12.1.3 Temperature and Humidity Thresholds Ventilation

The control strategy based on temperature and humidity thresholds is shown in Fig. 12.3. This strategy is equal to the one previously discussed in paragraph 12.1.2, except that it considers even internal humidity conditions. Actually, in addition to the single temperature threshold control, it ventilates at the maximum speed if it is lesson time and the relative humidity is higher than 60%. In this way, it is possible to see the improvement in internal temperature conditions obtained thanks to the addition of the humidity threshold, given that air humidity contributes to heat perception [64].

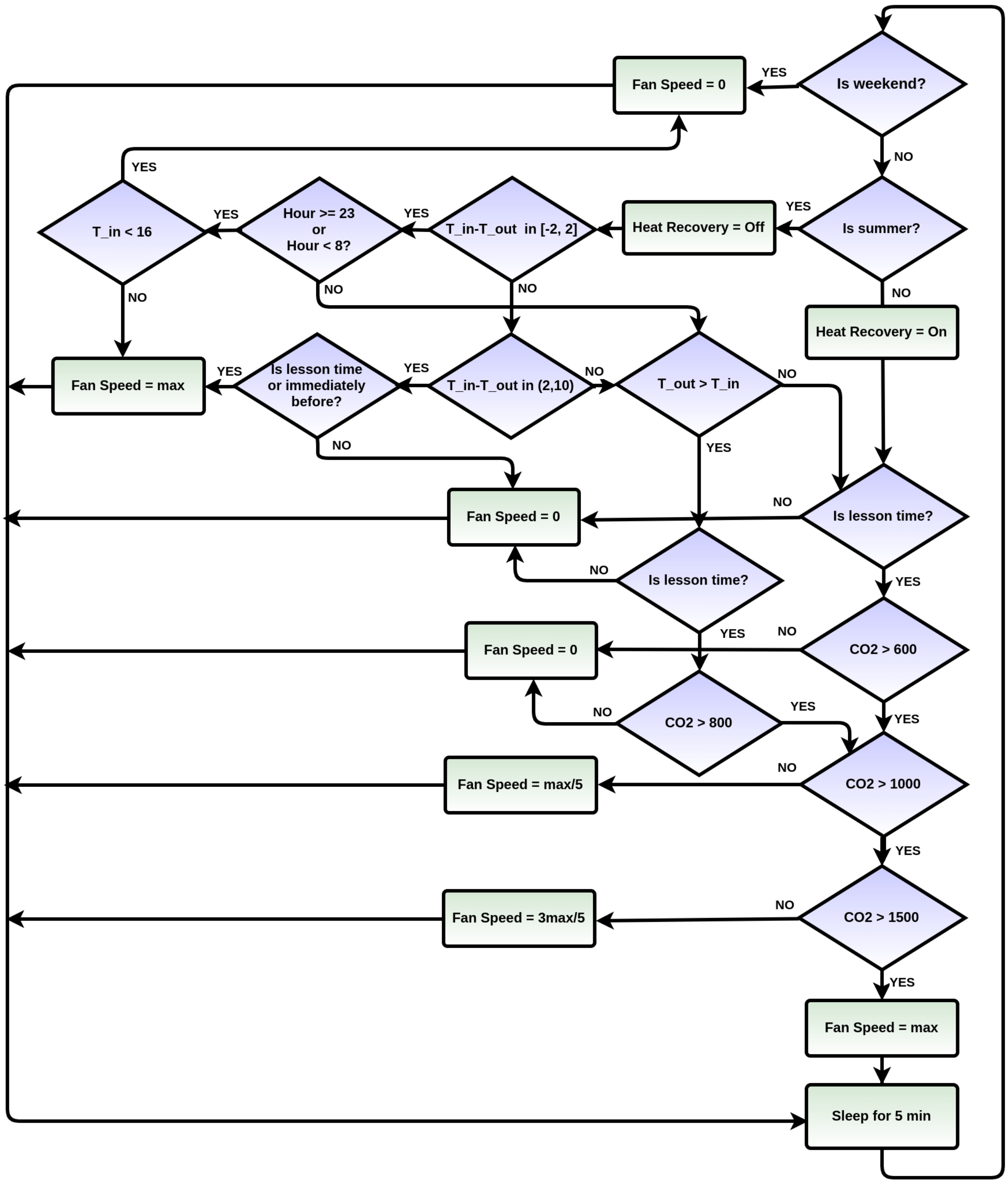

Figure 12.1: Internal and external temperature difference control for ventilative cooling and CO2-based control for correct IAQ during lessons time

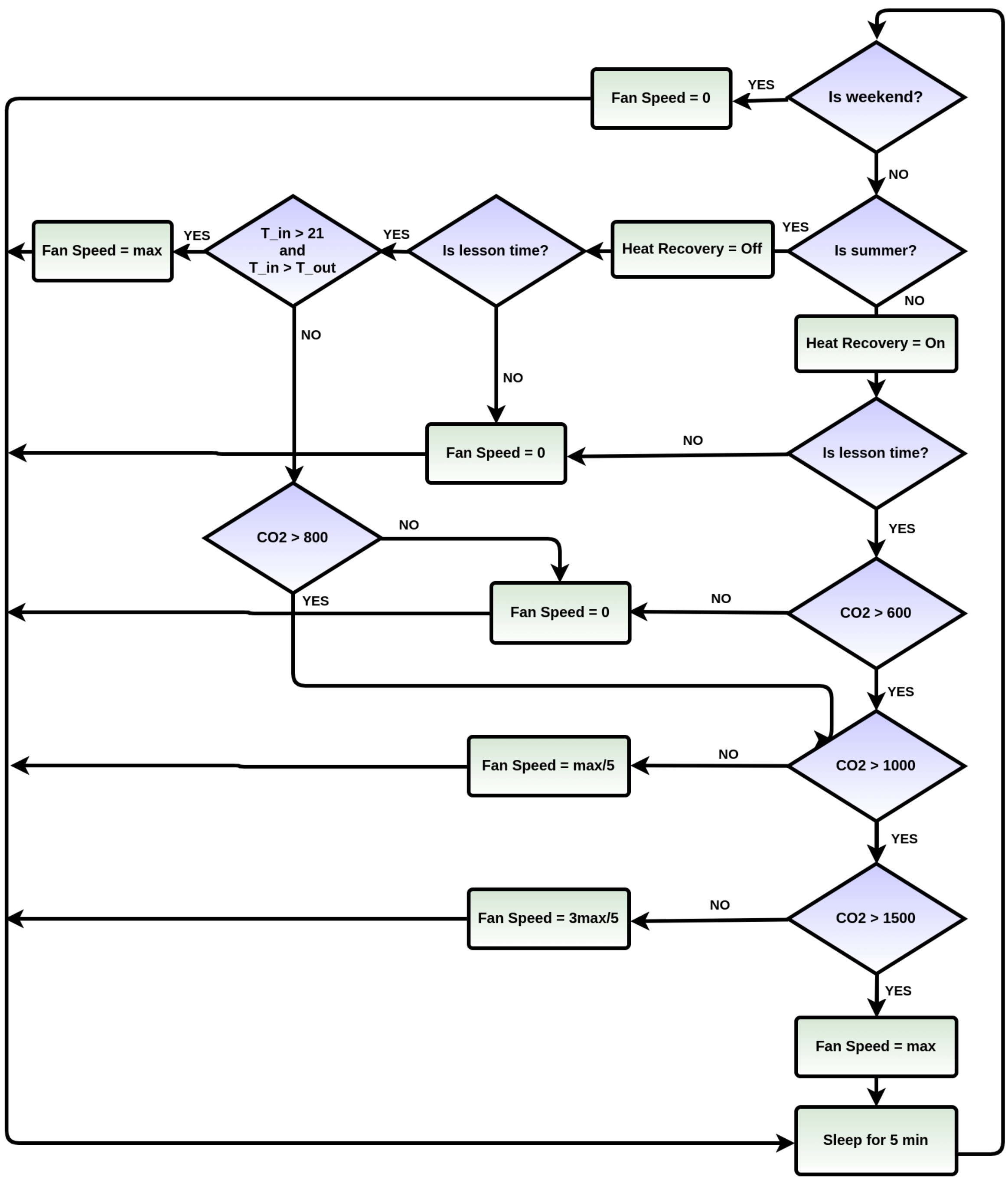

Figure 12.2: Temperature single threshold for ventilative cooling and CO2-based control for correct IAQ during lessons time

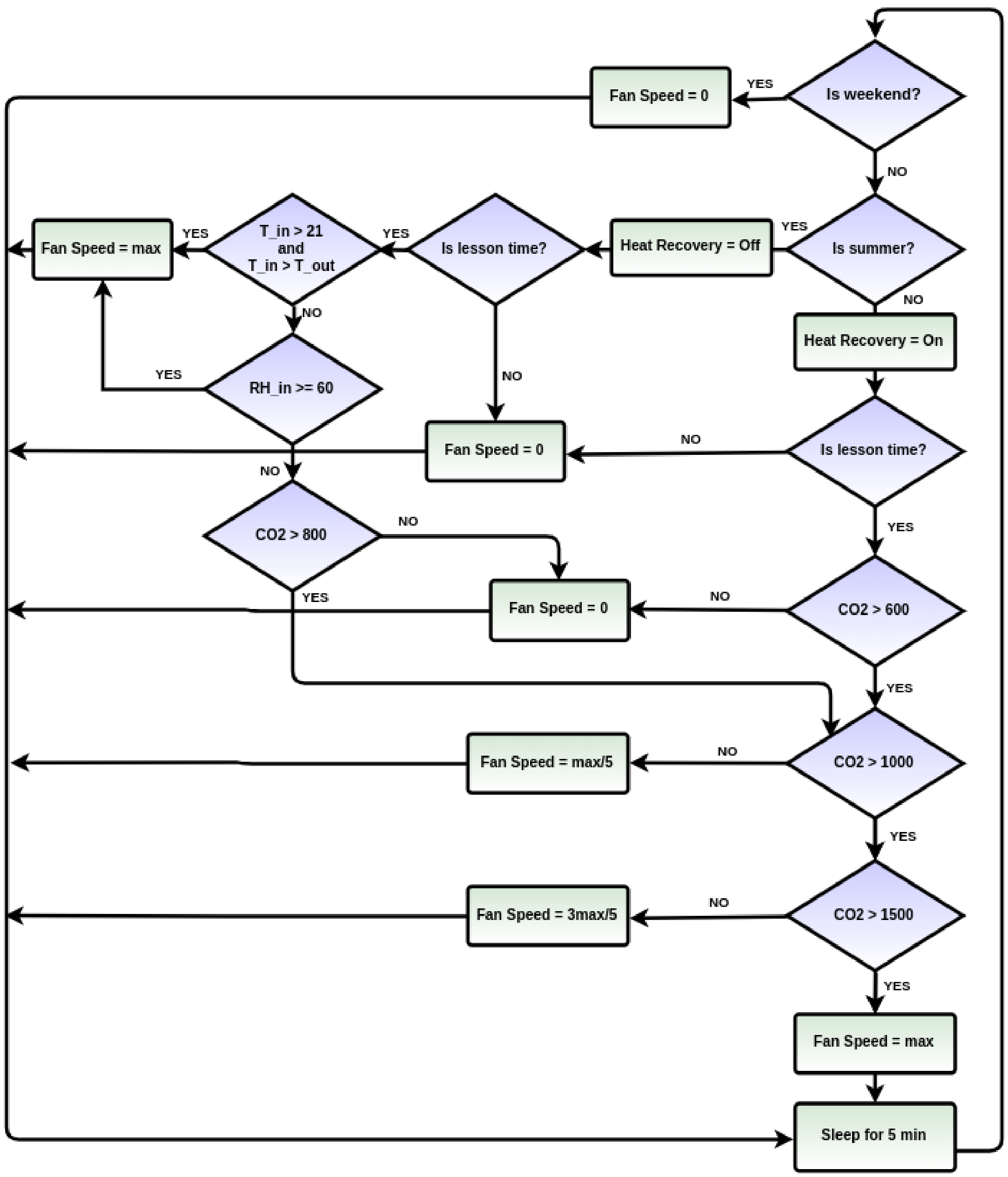

Figure 12.3: Temperature and humidity single thresholds for ventilative cooling and CO2-based control for correct IAQ during lessons time

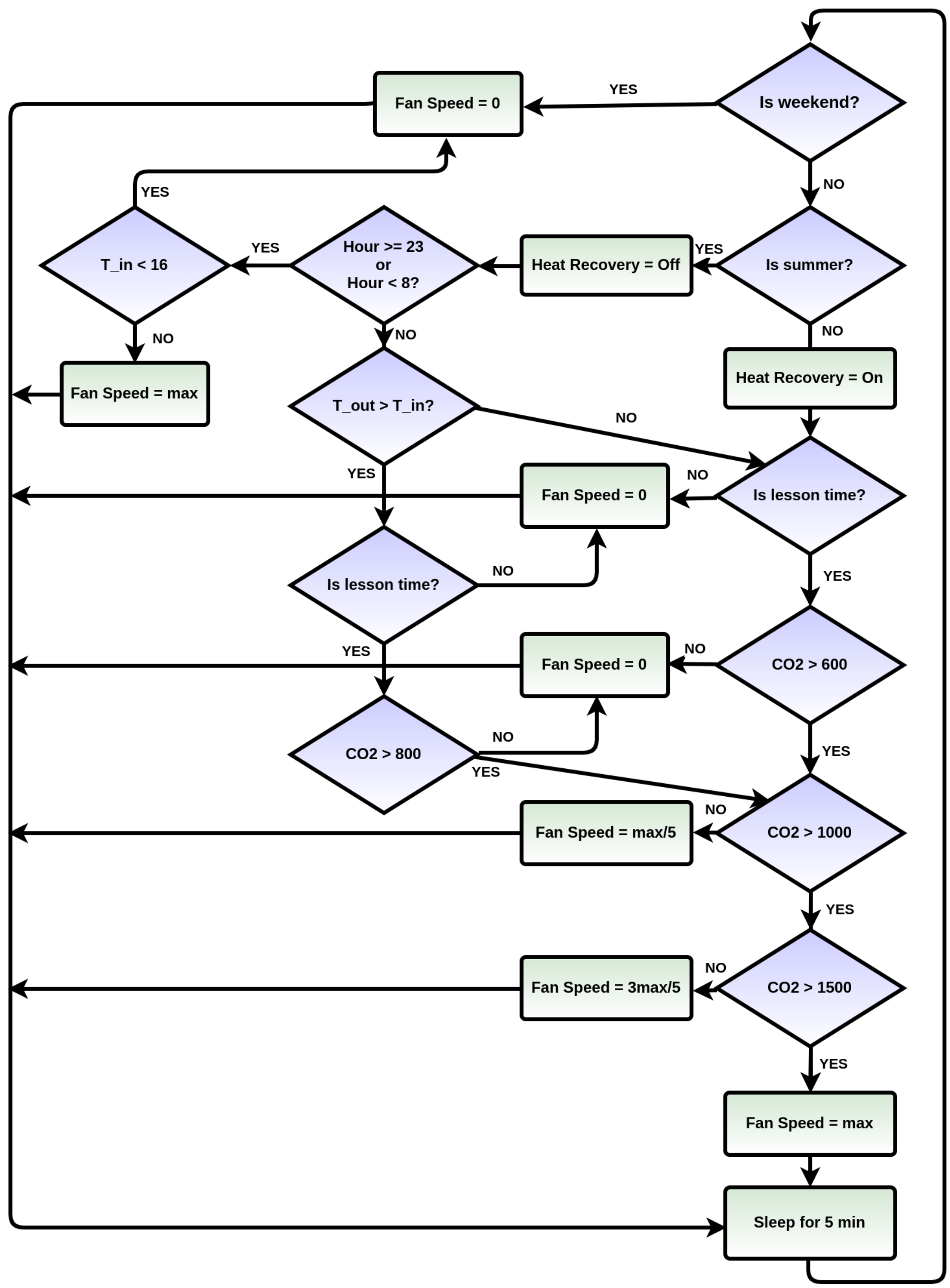

Figure 12.4: Night ventilation from 11:00 PM for ventilative cooling and CO2-based control for correct IAQ during lessons time

12.1.4 Night Ventilation from 11:00 PM

The night ventilation strategies are used to pre-cool the indoor environment by exploiting the cooler night air to obtain comfortable conditions when occupants arrive in the morning. The algorithm used to implement night ventilation is presented in Fig. 12.4. In this case, the chosen night period is from 11:00 PM to 8:00 AM. During night hours, ventilation is kept to its maximum rate unless the indoor temperature is under 16°C. If the internal condition starts to be too cold, the mechanical ventilation unit is set to be off. During daily hours, ventilation follows the single carbon dioxide threshold control with $800ppm$ as lower threshold if the outdoor air temperature is higher than the internal one, $600ppm$ if not.

12.1.5 Night Ventilation from 11:00 PM and Temperature Threshold Control

This strategy can be seen in Fig. 12.5, and it combines two approaches previously seen in paragraphs 12.1.4 and 12.1.2. In this way, it is possible to see the advantages of the combined version over the two single approaches, and if, by doing this, it is possible to obtain a relevant improvement in air temperature reduction.

12.1.6 Night Ventilation from 8:00 PM

This night ventilation strategy is equal to the one in paragraph 12.1.4, but it considers as night period the interval from 8:00 PM to 8:00 AM. In this way, it is possible to see if ventilating for three more hours leads to a higher temperature reduction or if the advantages are almost the same and there is just a higher electric consumption. This modified version is shown in Fig. 12.6.

12.1.7 ASHRAE 62.1

The ASHRAE 62.1 ventilation control was used to compare all the approaches mentioned above with the one suggested by the standard. It can be seen in Fig. 12.7 and works as explained in paragraph 8.4.2.

12.1.8 $act201bc$

In the room on the first floor $act201bc$, the following strategies have been tested:

- temperature difference-based ventilation;
- temperature threshold-based ventilation;
- temperature and humidity thresholds-based ventilation, which can be compared with the temperature threshold-based control within the same room to obtain a reliable confrontation.

12.1.9 $act201cc$

In the room on the second floor $act201cc$, the run strategies are:

- night ventilation from 11:00 PM;
- temperature threshold-based ventilation;
- night ventilation from 11:00 PM and temperature threshold control, which can be compared with the previous two because they have been verified in the same room.

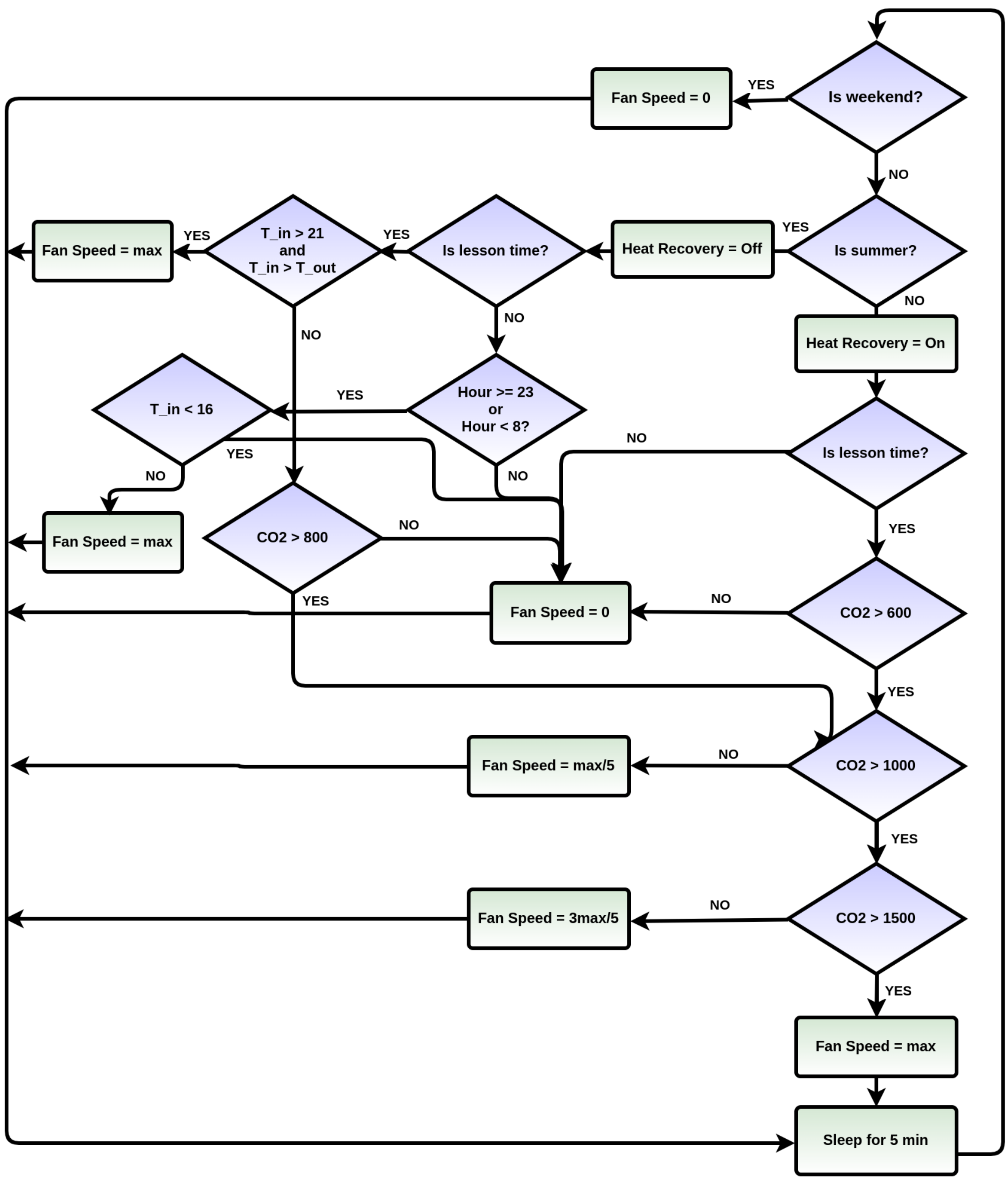

Figure 12.5: Night ventilation from 11:00 PM and temperature single threshold for ventilative cooling and CO2-based control for correct IAQ during lessons time

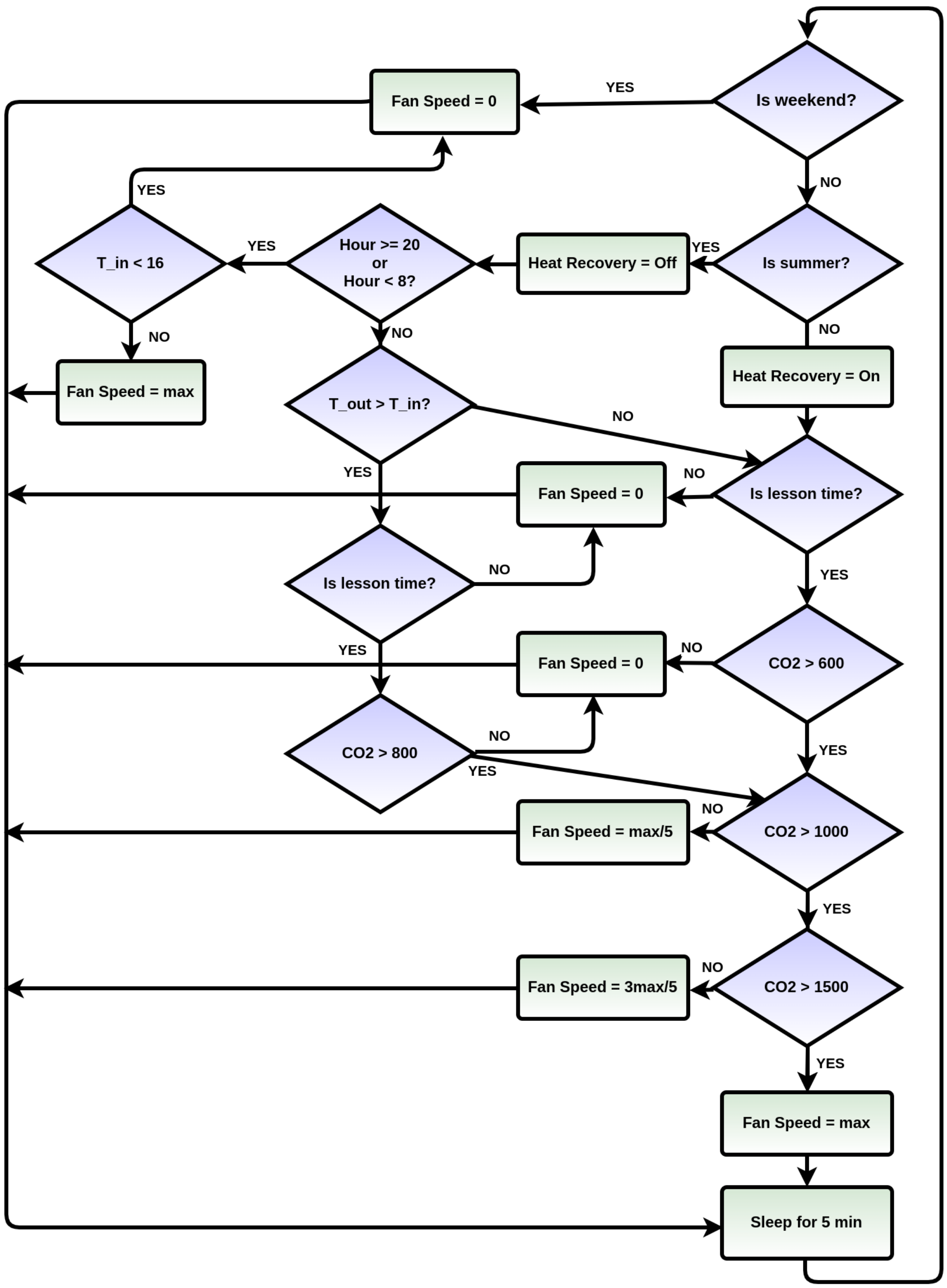

Figure 12.6: Night ventilation from 8:00 PM for ventilative cooling and CO2-based control for correct IAQ during lessons time

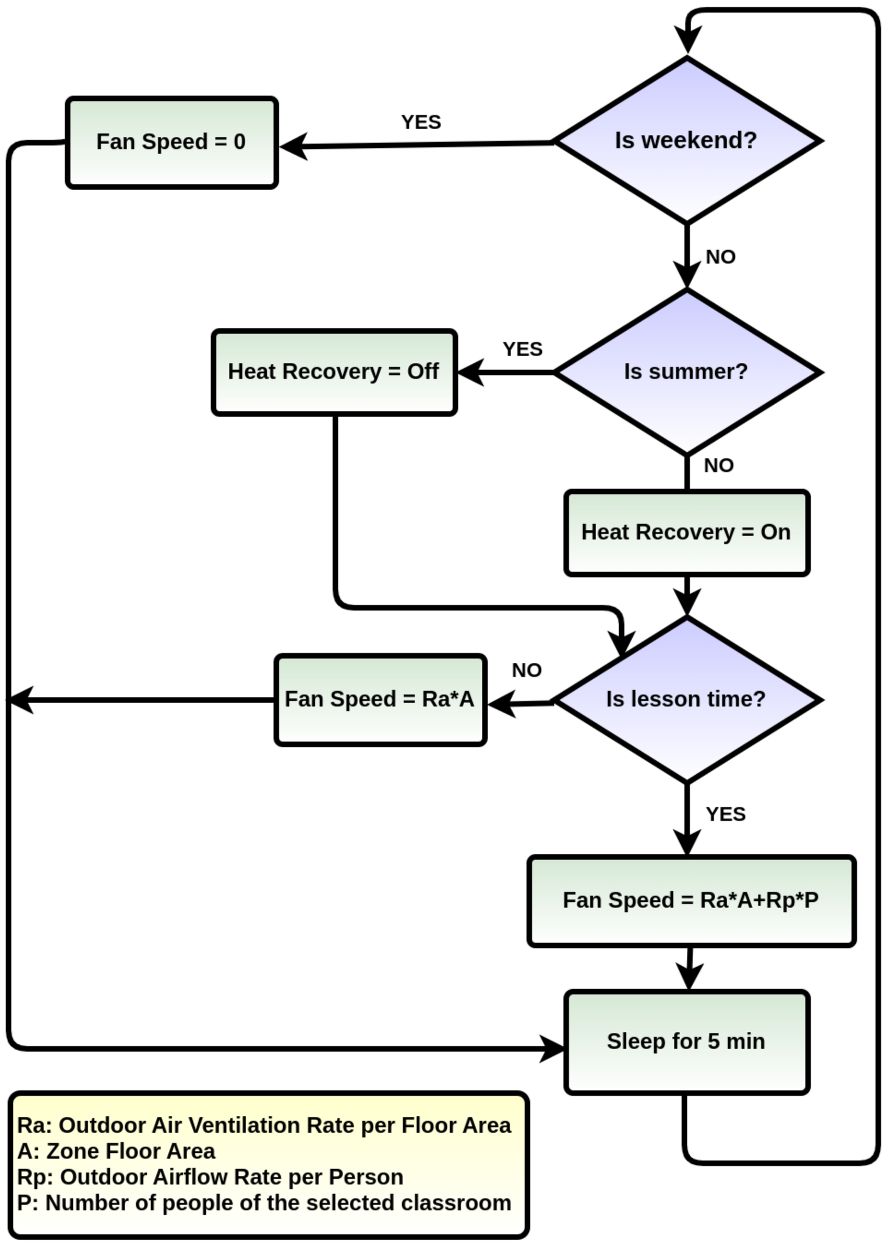

Figure 12.7: Ventilation algorithm recommended from the ASHRAE 62.1

12.1.10 *act*208*da*

The strategies analyzed on the third floor in the classroom *act*208*da* are:

- night ventilation from 11:00 PM;
- night ventilation from 8:00 PM, which can be compared with the previous one;

- ASHRAE 62.1 standard approach.

12.2 Indoor Air Quality Strategies

During the second testing period, the main tested strategies are the ones that aim at guaranteeing satisfactory indoor air quality. These controls are performed in September when students return from vacation, so the production of carbon dioxide during classes can be monitored at its usual production level.

All the tested control strategies perform the following actions:

- if the current day is of the weekend, ventilation is turned off;
- retrieve current carbon dioxide concentration from the Sensirion SEK-SCD41 CO2 sensor which is equipped on the RaspberryPi board;
- if it is a weekday set the ventilation according to the measured CO_2 concentration and the selected control strategy used.

The approaches tested in this period are the same already seen in section 8. In this way, the results of the monitored and simulated approaches can be compared to see if the conclusions are consistent.

In addition to these strategies, two other approaches are considered, which are:

- CO_2 single threshold of $1000ppm$, which has been considered since the ASHRAE standard indicates that conditions are healthy for concentrations below this value;
- CO_2 double threshold with $600ppm$ as the lower threshold and $1000ppm$ as the higher one.

12.2.1 CO_2 single threshold of $1000ppm$

The algorithm used for the single threshold control is shown in Fig. 12.8. The steps that are done are the following:

- if it is weekend, the ventilation is turned off;
- if the CO_2 concentration is lower than $1000ppm$, indoor environmental conditions are considered healthy, and the ventilation is off;
- if the carbon dioxide is between $1000ppm$ and $1500ppm$, conditions start to be unpleasant for occupants as the ASHRAE standard suggests, so the ventilation is set to 3/5 of the maximum mechanical ventilation capacity;
- if the measured CO_2 is more than $1500ppm$, effects on the children start to become more impacting, so conditions must be brought back to normal faster. Therefore, the ventilation rate of the mechanical ventilation unit is set to its maximum value.

12.2.2 CO_2 double threshold of $600ppm$ and $1000ppm$

Even here, the double threshold control has been developed to reduce the number of powering up of the mechanical ventilation unit in case the carbon dioxide concentration is fluctuating around $1000ppm$. The algorithm considered is shown in Fig. 12.9, and it can be seen that it is similar to the single threshold one. The only exception is when the mechanical ventilation is on, and the carbon dioxide value drops below $1000ppm$. In these cases, ventilation is not turned off until the internal concentration is less than $600ppm$.

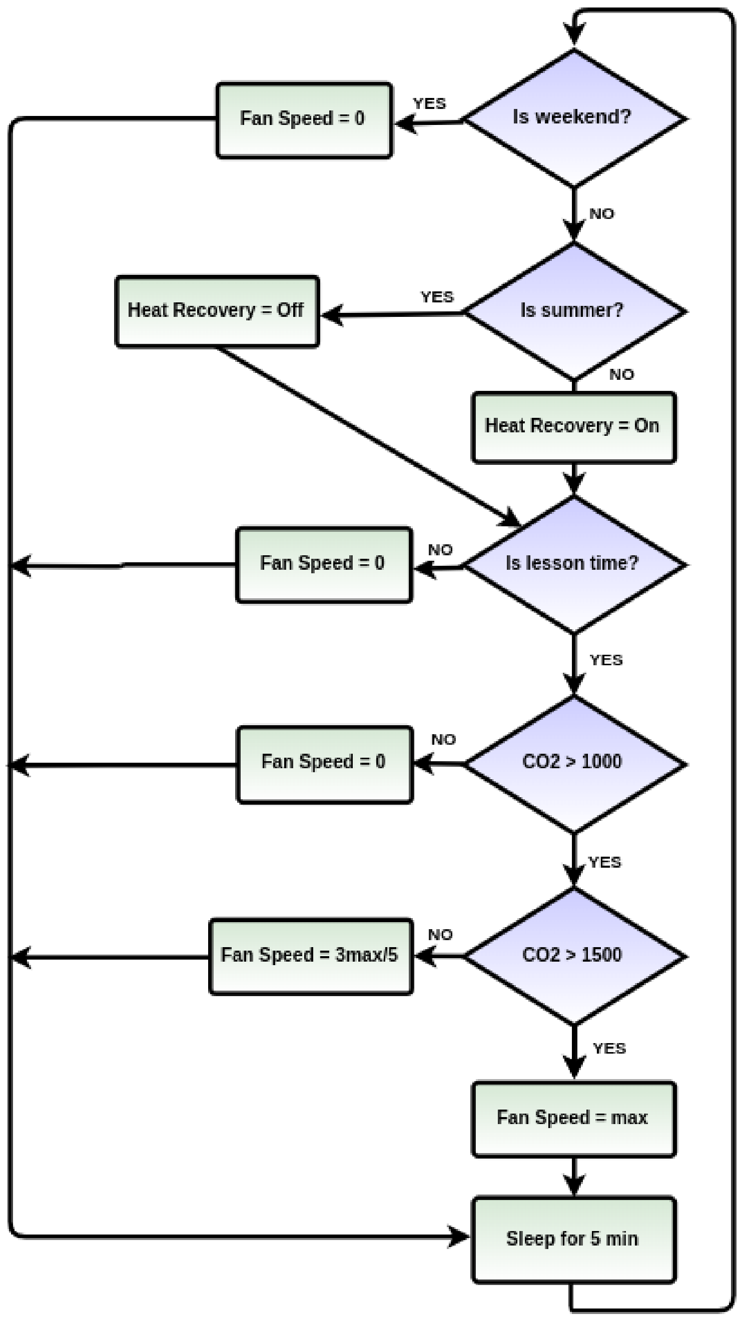

Figure 12.8: CO_2 single threshold of $1000ppm$ approach

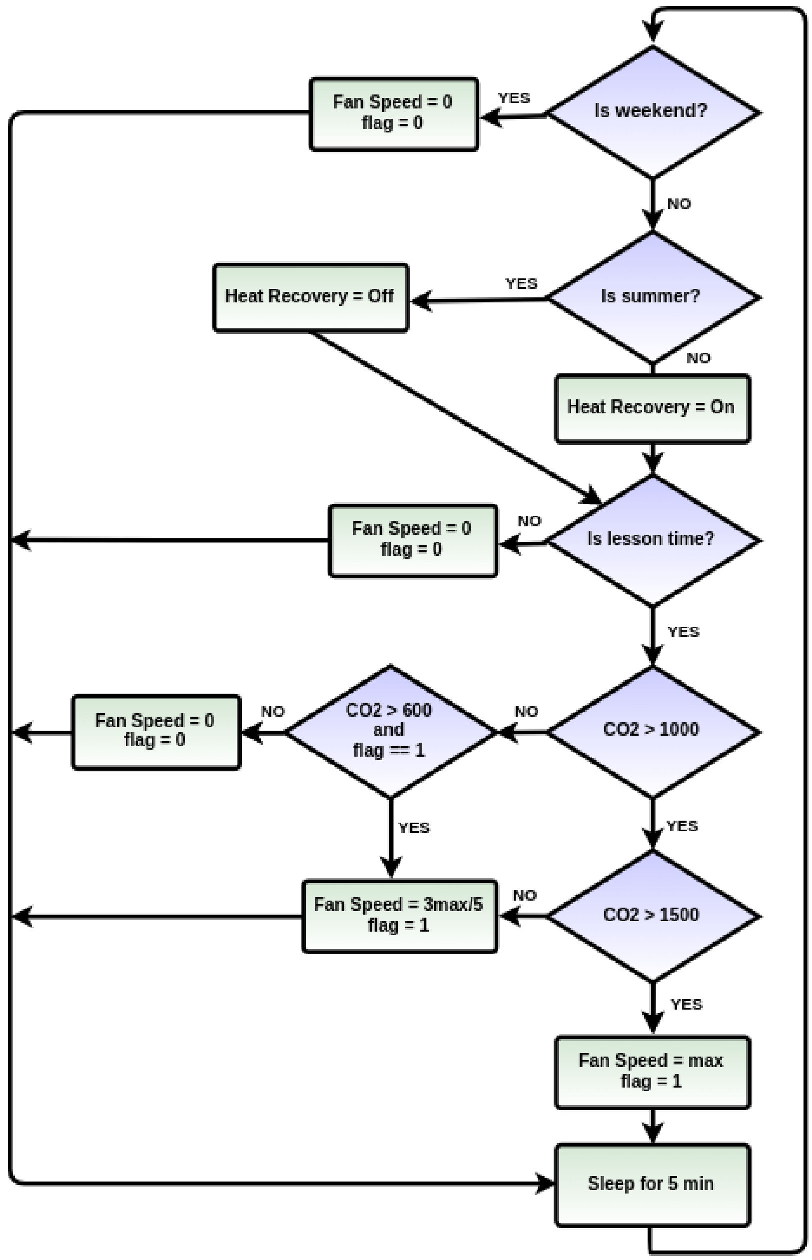

Figure 12.9: CO_2 double threshold of $600ppm$ and $1000ppm$ approach

12.2.3 $act201bc$

In the room on the first floor $act201bc$, the following strategies have been tested during the second testing period:

- $600ppm$ single threshold;
- $600ppm$ double threshold;
- ASHRAE 62;
- $1000ppm$ single threshold;

12.2.4 $act201cc$

In the room on the second floor $act201cc$, the run strategies during the second testing period are:

- $800ppm$ single threshold;
- $800ppm$ double threshold;
- ASHRAE 62.1;
- $1000ppm$ double threshold;
- $600ppm$ double threshold, to validate the results obtained during atypical days on the first floor.

13. Monitored Strategies Results

13.1 Analysis Scripts

Four scripts have been created to analyze data collected from sensors. They process and manipulate monitored data to obtain significant parameters that will allow the numerical comparison between different tested strategies.

The downloaded data processed by these two scripts to analyze ventilative cooling strategies are coming from:

- the outdoor temperature sensor;
- temperature sensors of the three selected rooms with mechanical ventilation;
- temperature sensors of rooms close to the selected ones.

The data used for the analysis of indoor air quality strategies are the ones retrieved from:

- carbon dioxide sensors of the three selected rooms with mechanical ventilation;
- carbon dioxide sensors of rooms close to the selected ones.

During the test of ventilative cooling strategies, given that the school is empty, the rooms close to the ones with mechanical ventilation are kept in the same shading and closed windows status conditions, but without mechanical ventilation, to be used as reference.

During the indoor air quality strategy tests, since the school has already been occupied, the conditions of all rooms are unknown as they depend on the occupants' behavior. Nevertheless, the average indoor conditions are still considered similar since lessons start and end at the same time and the number of students is approximately the same.

The chosen reference rooms are:

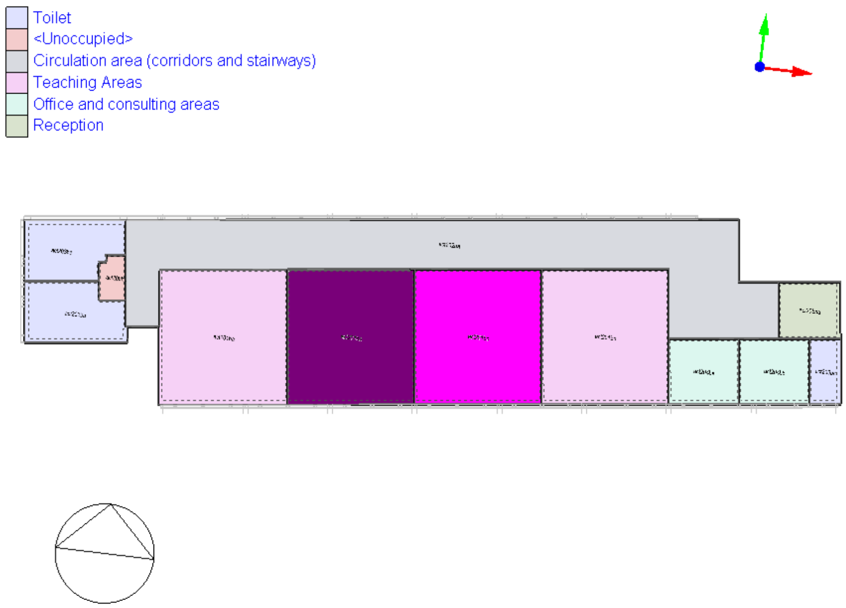

Figure 13.1: Reference room chosen on the first floor *act*201*bb*

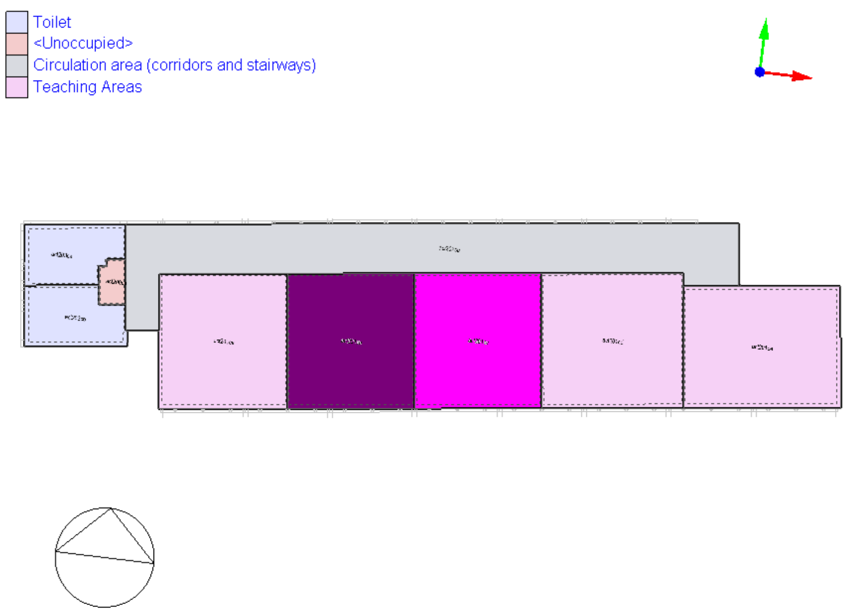

Figure 13.2: Reference room chosen on the second floor *act*201*cb*

- *act*201*bb* for the first floor;
- *act*201*cb* on the second one;
- *act*201*da* on the third one, although it is smaller than the one with the mechanical ventilation, given

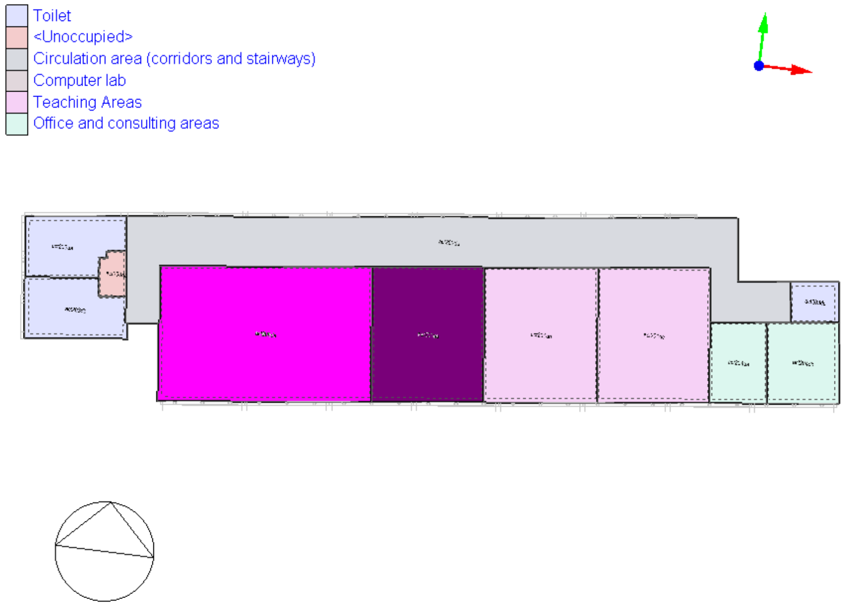

Figure 13.3: Reference room chosen on the third floor *act*201*da*

that no other room is that ample.

These rooms can be seen highlighted in purple in Figs. 13.1, 13.2, and 13.3.

One more script has been created to take outputs of control strategies scripts, which run on RaspberryPi to plot bypass status and the airflow rate of ventilation units.

13.1.1 Hourly Aggregator

This first script is used to aggregate temperature data hourly, given that their variation is slow, to have a constant granularity. It takes as input the CSV file containing raw data from sensors and gives as output a new CSV with data aggregated hourly.

13.1.2 Analyser and Plotter for Ventilative Cooling

The second script takes as input all the files aggregated hourly to extract numerical indicators and plots that are used to understand the behavior of tested approaches. It gives as output a text file containing all the requested information and even required figures. For every week selected for the running of control algorithms, the following actions are performed:

- evaluate and save in the output text file the outdoor temperature average value over all the testing week and the average indoor temperature for lesson hours (from 8:00 AM to 2:00 PM) and night hours (from 11:00 PM to 8:00 AM);
- for all three rooms with mechanical ventilation and all the ones selected as a reference, evaluate and save in the output text file the week average temperature and the average indoor temperature during lessons and night times;
- show the plot of the mechanically controlled temperature compared with the one of the reference room

13.1.3 10 Minutes Aggregator

This third script is used to aggregate carbon dioxide concentration data every 10 minutes to have a constant granularity. The chosen time span is smaller compared to the one used for the temperature data since the CO_2 concentration evolves more rapidly. Except for the time granularity, this script works exactly as the one used for temperature.

13.1.4 Analyser and Plotter for Indoor Air Quality

This script works exactly as the one of the ventilative cooling, but it evaluates the following outputs:

- for all three rooms with mechanical ventilation and all the ones selected as a reference, evaluate and save in the output text file the week's average carbon dioxide concentration and indoor temperature, the average CO_2 and indoor temperature during lessons time, and the average of the carbon dioxide peaks;
- show the plot of the mechanically controlled room's carbon dioxide behavior compared with the one of the reference room;
- show the plot of the mechanically controlled room's temperature behavior compared with the reference room's one.

13.1.5 Airflow Rate and Bypass Status Plotter

This script takes as input the output files of the control strategies tested in all the rooms and the file produced by the Modbus Master simulator, which contains heat recovery system bypass status, and it generates plots of all incoming data week by week. If the analyzed strategy controls the indoor air quality, also the following indicators are evaluated:

- the number of switches on/off of the mechanical ventilation units;
- the total electric consumption of the mechanical ventilation units.

13.2 Outdoor Temperature

The behavior of the outdoor temperature during all three selected weeks can be seen in Figs. 13.4, 13.5, and 13.6 and in Tables 13.1, 13.2, and 13.3.

Average outdoor temperature	27.8°C
Average outdoor temperature during lesson time	28.8°C
Average outdoor temperature during night	24.1°C

Table 13.1: Outdoor temperature behavior during the first testing week

Average outdoor temperature	28.2°C
Average outdoor temperature during lesson time	29.1°C
Average outdoor temperature during night	24.3°C

Table 13.2: Outdoor temperature behavior during the second testing week

From these data, it can be seen that the temperature is extreme during the daytime, even if it is a mountain city, avoiding the possibility of cooling interiors during daily hours since the temperature reaches

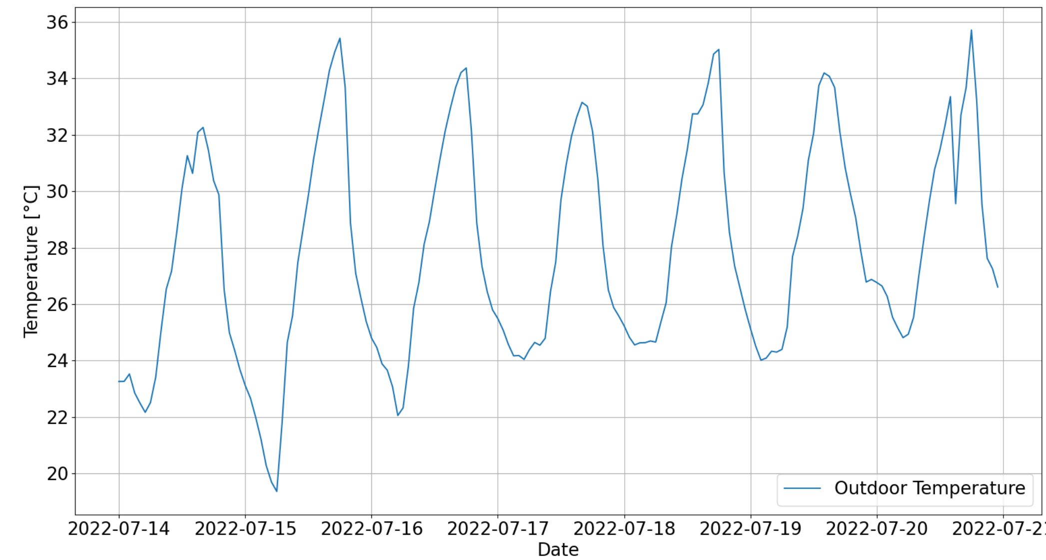

Figure 13.4: Outdoor temperature during the first testing week

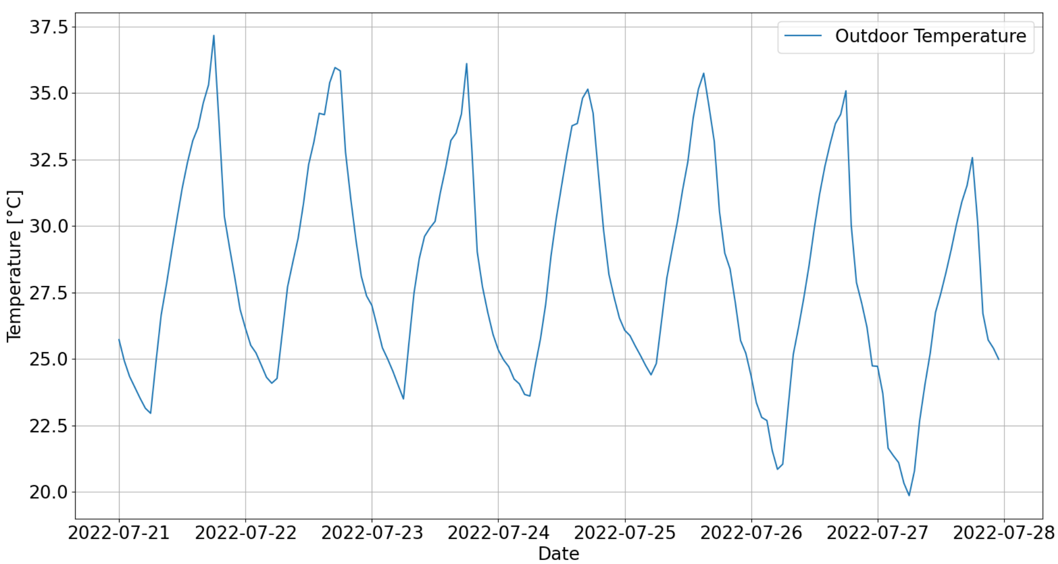

Figure 13.5: Outdoor temperature during the second testing week

peaks of 37.5°C, especially during the second week. Even at night, the average temperature is higher than expected, usually ranging from 20°C to 25°C. These temperatures characterize known tropical nights, which have poor cooling potential. For these reasons, the cooling potential will be lower than expected for a mountain city, and cooling results will be limited.

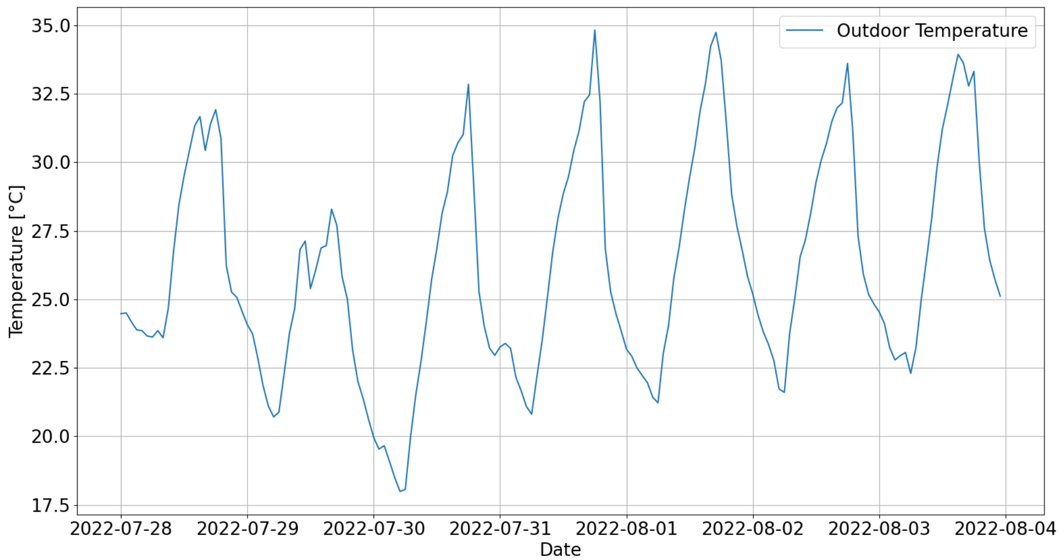

Figure 13.6: Outdoor temperature during the third testing week

Average outdoor temperature	26.2°C
Average outdoor temperature during lesson time	26.9°C
Average outdoor temperature during night	22.5°C

Table 13.3: Outdoor temperature behavior during the third testing week

13.2.1 Tropical Nights

Tropical nights are defined as those nights in which the minimum reached temperature is higher than 20°C [33]. This type of night is common in Southern European regions like Spain, Italy, and Greece [19]. In these countries, the night cooling potential is limited, and to reach indoor comfort in summer, it is needed to support night ventilation with some additional conditioning system. Nevertheless, in spring and fall, ventilative cooling can be more effective [19].

13.3 Ventilative Cooling in *act*201*bc*

13.3.1 Temperature Difference-Based Ventilation

Results of the first strategy tested in the room on the first floor are shown in Fig. 13.7 and Tables 13.4 and 13.5.

Average indoor temperature	29.4°C
Average indoor temperature during lesson time	29.2°C
Average indoor temperature during night	29.2°C

Table 13.4: Controlled temperature behavior during the first testing week

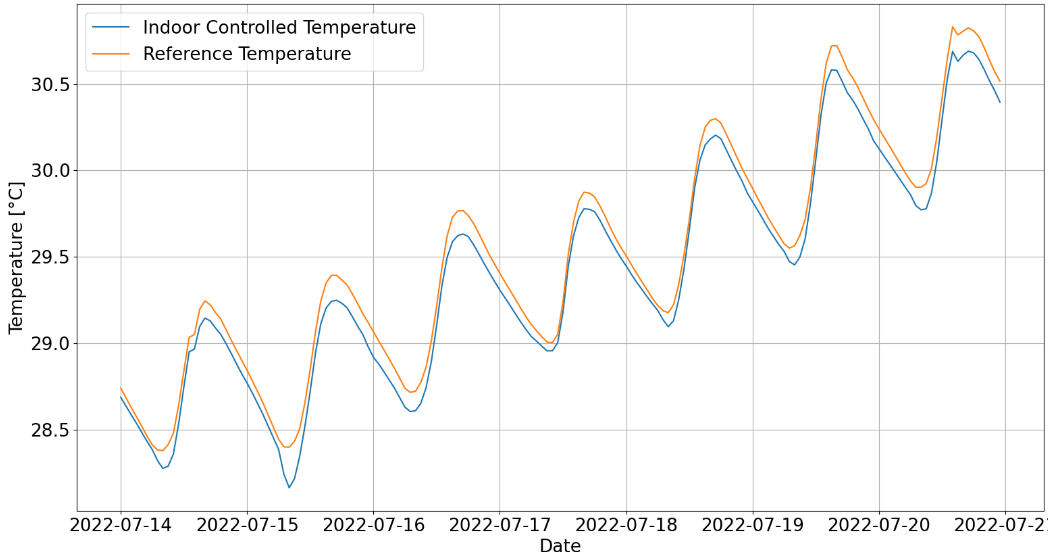

Figure 13.7: Controlled and reference temperature of $act201bc$ in the first week

Average indoor temperature	29.5°C
Average indoor temperature during lesson time	29.4°C
Average indoor temperature during night	29.3°C

Table 13.5: Reference temperature behavior during the first testing week

From the results, it can be seen that this strategy is not particularly good when it is used in the selected period of the year. The internal temperature decrease during lesson time was only 0.2°C, which is not a significant amount. This can be explained by high daytime temperatures recorded during July, which are not suited for cooling purposes. More benefits can probably be obtained by using night ventilation as temperatures are lower.

The bypass of the heat recovery behavior can be seen in Fig. 13.8, where the value 1 means that heat recovery is not used, so it avoids heat transfer between the indoor and outdoor air. The value 0 instead is set when heat recovery is on.

From the bypass figure, it can be seen that the heat recovery system is activated most during afternoons when there is a temperature peak to try to keep the cool air inside the building, while it is deactivated during nights and in the mornings to bring inside outdoor temperatures.

The airflow rate of the fan of the mechanical ventilation system can be seen in Fig. 13.9, with a unit expressed on a scale from 0 to 10, which indicates different speeds of the mechanical ventilation unit. The value 0 corresponds to an airflow equal to $0m^3/h$, while 10 to $800m^3/h$.

From this figure, it is possible to see that the ventilation is set to zero most of the time since the CO_2 level is always under $600ppm$ because of the absence of people. This conclusion on CO_2 can be considered valid even for all the other tested strategies and all the different rooms, so it will not be explained again and will be taken for granted. All the mornings, when the outside temperature is below 2 ºC compared to the indoor one, ventilation is set to its maximum value. Sometimes this condition is satisfied even in the evening, so ventilation is set to 10 also in those moments.

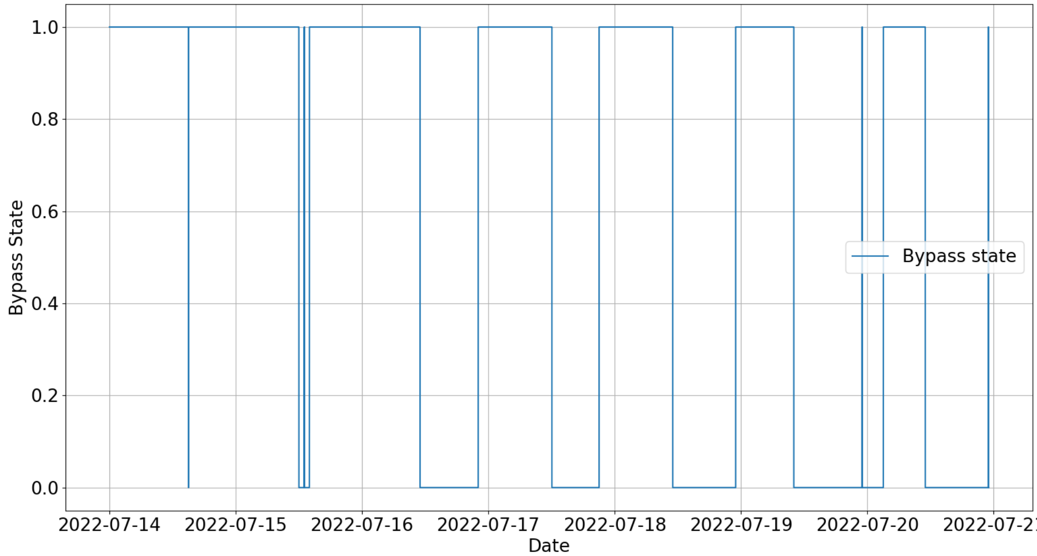

Figure 13.8: Heat recovery bypass of $act201bc$ in the first week

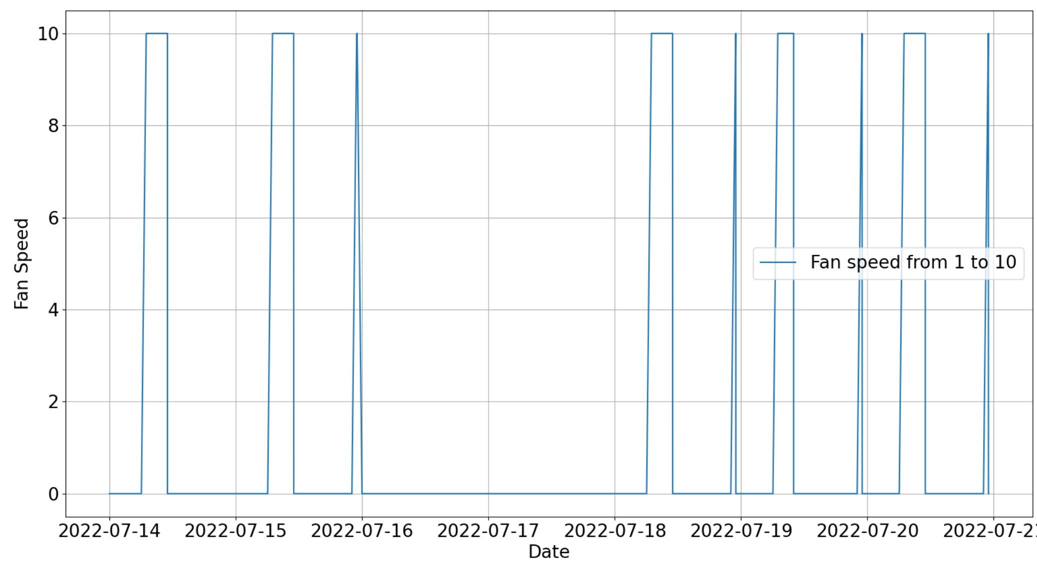

Figure 13.9: Ventilation rate of the mechanical ventilation system in the room $act201bc$ during the first week

13.3.2 Temperature Threshold-Based Ventilation

Results of the second strategy tested in room $act201bc$ on the first floor are reported in Fig. 13.10 and Tables 13.6 and 13.7.

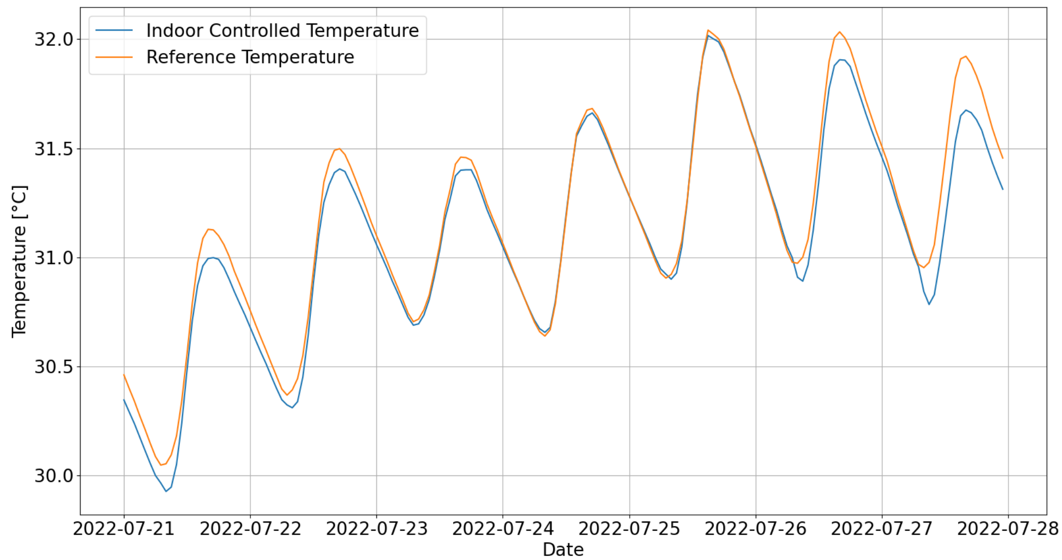

Figure 13.10: Controlled and reference temperature of $act201bc$ in the second week

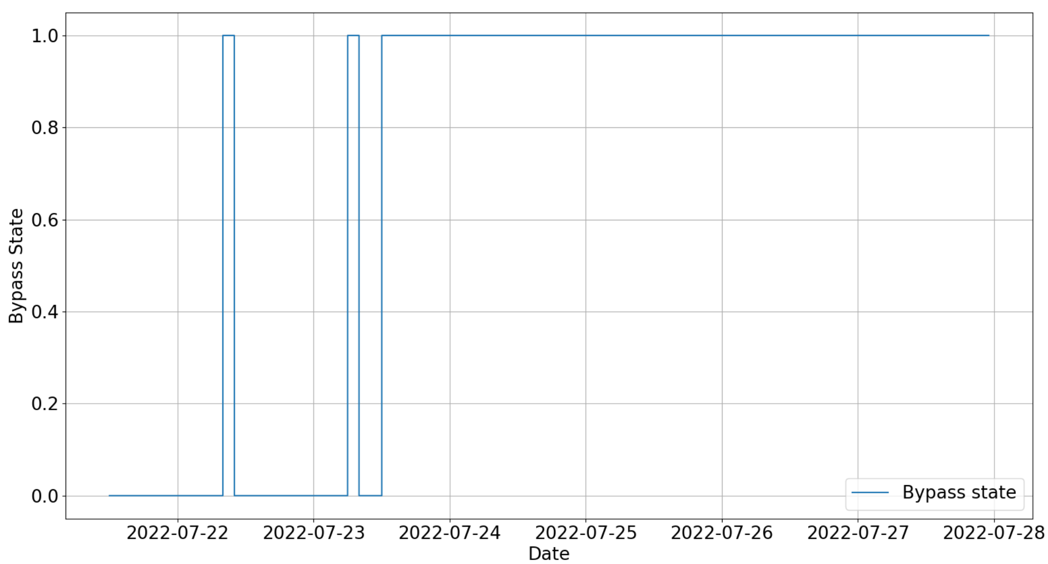

Figure 13.11: Heat recovery bypass of $act201bc$ in the second week

From the results, it can be seen that even this approach is not good when outdoor temperatures are so high during the daytime. This second strategy ventilates only during lesson time, which is when outdoor temperatures reach their peak. For this reason, the internal temperature decrease only by 0.2°C during lesson time since the mechanical ventilation unit can ventilate only in the morning, when temperatures are lower.

Average indoor temperature	31.1°C
Average indoor temperature during lesson time	30.8°C
Average indoor temperature during night	30.9°C

Table 13.6: Controlled temperature behavior during the second testing week

Average indoor temperature	31.2°C
Average indoor temperature during lesson time	31.0°C
Average indoor temperature during night	30.9°C

Table 13.7: Reference temperature behavior during the second testing week

Ventilating this small amount of hours is insufficient for cooling the room, and even in this case, nighttime ventilation can solve the problem by allowing a longer ventilation time. Given that even the strategy in paragraph 13.3.1 ventilates almost always in the mornings, the temperature reduction is similar in both cases.

The heat recovery bypass behavior can be seen in Fig. 13.11.

From the bypass figure, it can be seen that the heat recovery system is always off except for the daytime of the first two days.

The rate of the injected air can be seen in Fig. 13.12.

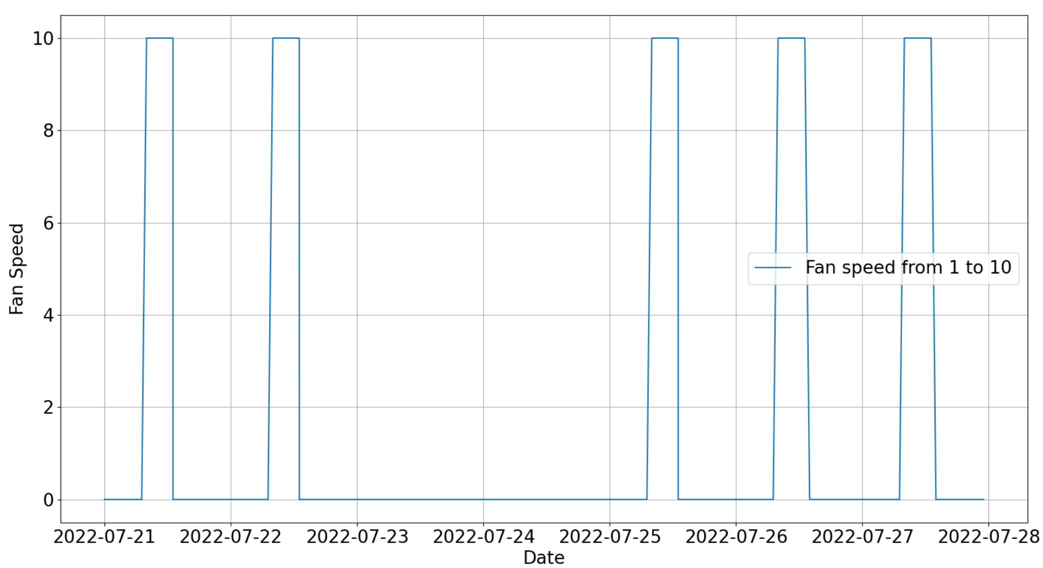

Figure 13.12: Ventilation rate of the mechanical ventilation system in the room $act201bc$ during the second week

From this figure, it can be seen that the injected air is always set to $0m^3/h$, except for a few hours in the morning of all weekdays. During these hours the ventilation is set to its maximum value to exploit the few time during lessons in which the outdoor air temperature is lower than the indoor one.

13.3.3 Temperature and Humidity Thresholds-Based Ventilation

Results of the third strategy tested on the first floor are reported in Fig. 13.13 and Tables 13.8 and 13.9.

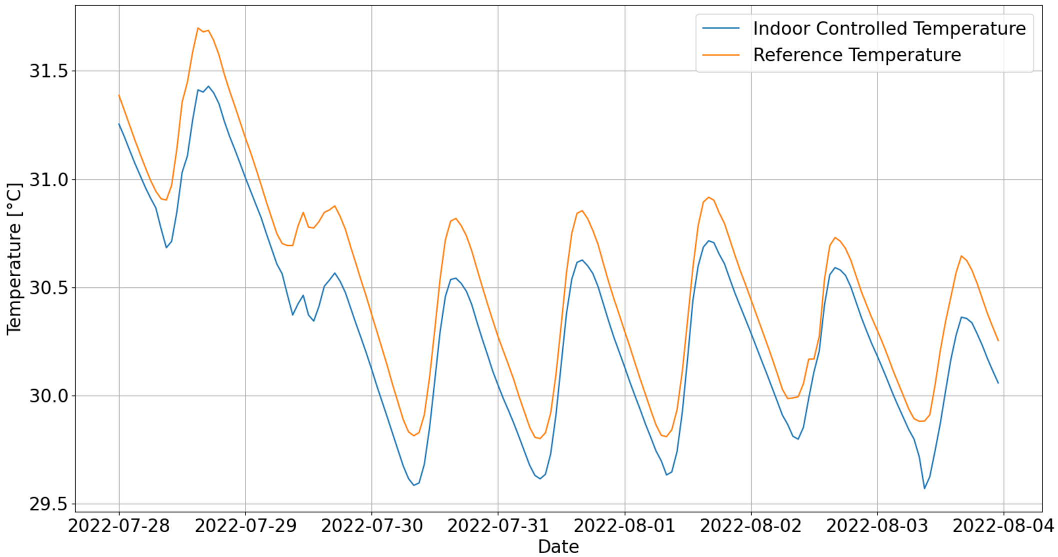

Figure 13.13: Controlled and reference temperature of *act*201*bc* in the third week

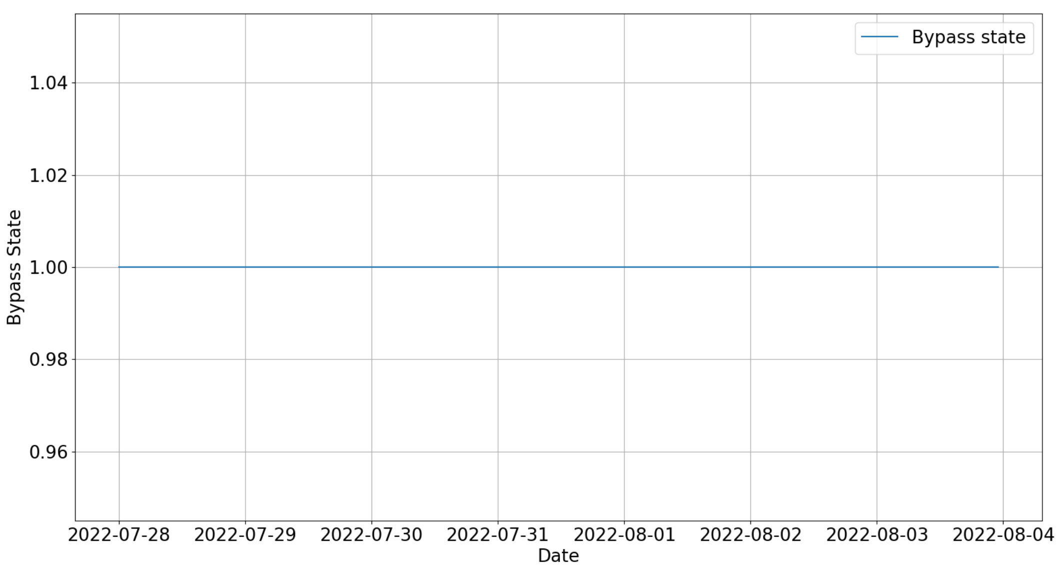

Figure 13.14: Heat recovery bypass of *act*201*bc* in the third week

Average indoor temperature	30.3°C
Average indoor temperature during lesson time	30.2°C
Average indoor temperature during night	30.4°C

Table 13.8: Controlled temperature behavior during the third testing week

Average indoor temperature	30.5°C
Average indoor temperature during lesson time	30.4°C
Average indoor temperature during night	30.5°C

Table 13.9: Reference temperature behavior during the third testing week

Gains with this strategy are similar to the ones seen in paragraph 13.3.2, but the real advantage is the human perception of indoor temperatures. If the indoor relative humidity is always kept under 60% during lessons, the perceived temperature is lower than the one sensed when the humidity is higher than this limit. Moreover, with this strategy, temperature peaks during days are lower compared with the behavior seen in 13.3.2.

From Fig. 13.14, it can be seen that the heat recovery bypass is always on in this last week, so the outdoor air temperature injected into the room is not modified by the indoor temperature.

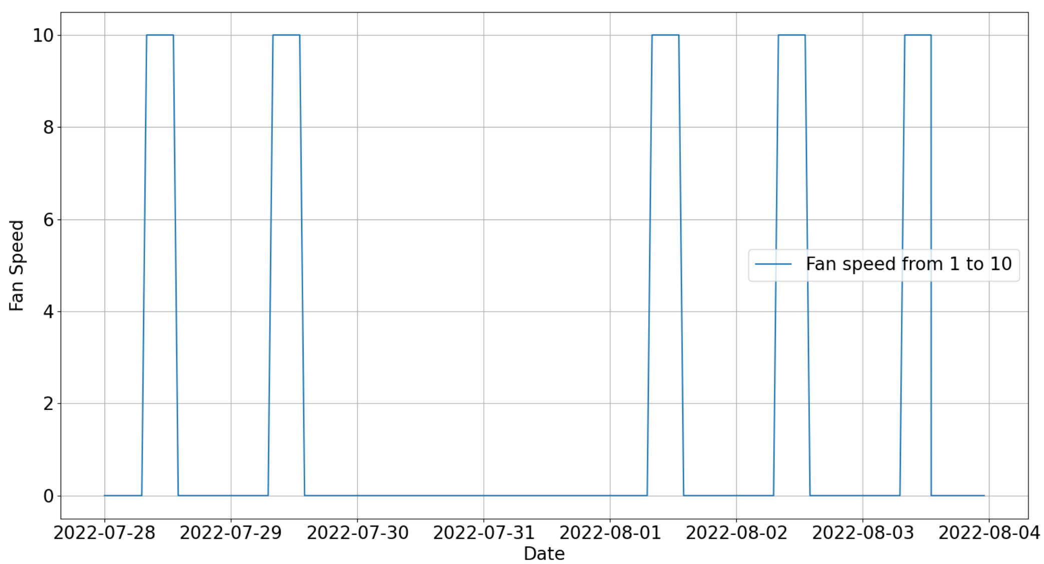

Figure 13.15: Ventilation rate of the mechanical ventilation system in the room $act201bc$ during the third week

From Fig. 13.15, it can be seen that the injected air behavior is almost equal to the one seen in paragraph 13.3.2, so it is almost always $0m^3/h$, except for some hours on weekdays mornings, where the air injection rate is $800m^3/h$.

13.4 Ventilative Cooling in *act*201*cc*

13.4.1 Night Ventilation from 11:00 PM

Results of the first strategy tested in room *act*201*cc* sited on the second floor are reported in Fig. 13.16 and Tables 13.10 and 13.11.

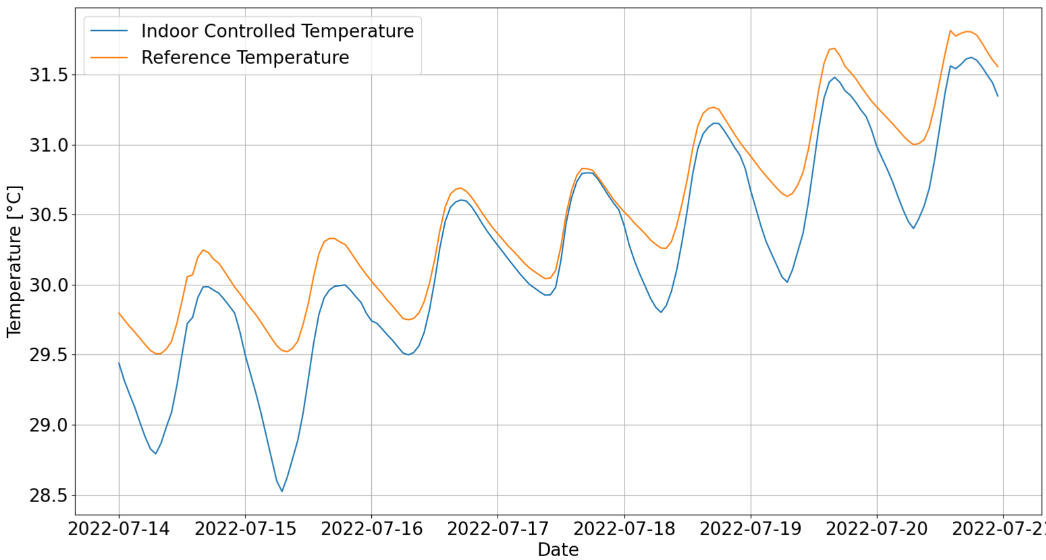

Figure 13.16: Controlled and reference temperature of *act*201*cc* in the first week

Average indoor temperature	30.2°C
Average indoor temperature during lesson time	30.0°C
Average indoor temperature during night	29.9°C

Table 13.10: Controlled temperature behavior during the first testing week

Average indoor temperature	30.5°C
Average indoor temperature during lesson time	30.4°C
Average indoor temperature during night	30.4°C

Table 13.11: Reference temperature behavior during the first testing week

From the results shown in Tables 13.10 and 13.11, it can be seen that this strategy reduces lessons' average indoor temperatures by double the value of approaches tested on the first floor. In fact, this approach ventilates for relevantly more hours, from 11:00 PM to 8:00 AM, so it injects a greater quantity of fresh air when compared to all previously mentioned approaches. Moreover, the incoming air is even colder, given that it is taken at night and not during the daytime, so its cooling potential is higher. Since nights are tropical, the temperature gain is still limited to a half degree, so the mechanical ventilation should be integrated with a conditioning system to reach a more comfortable condition.

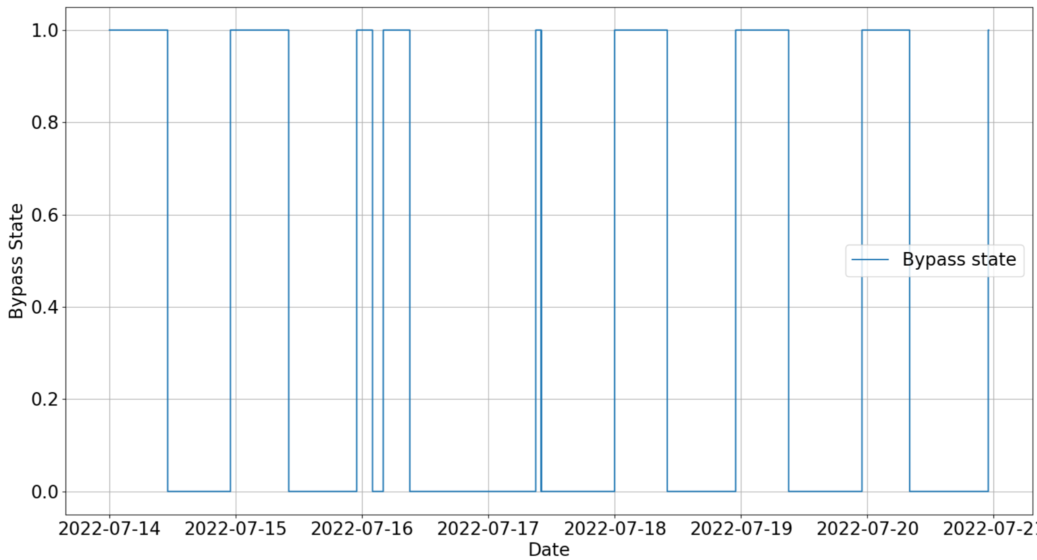

Figure 13.17: Heat recovery bypass of $act201cc$ in the first week

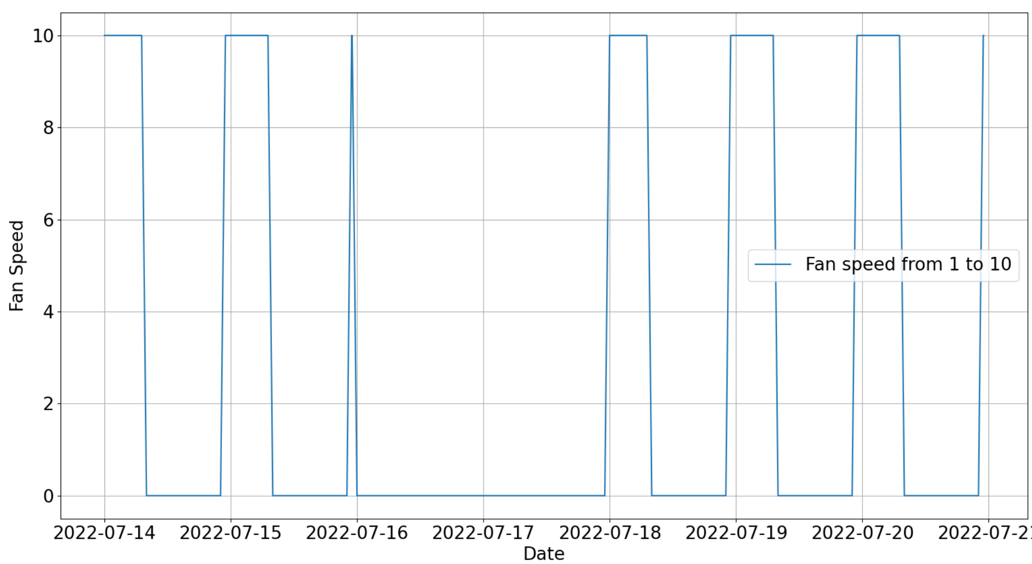

Figure 13.18: Ventilation rate of the mechanical ventilation system in the room $act201cc$ during the first week

From Fig. 13.16, it is possible to note that, in addition to previous advantages, the maximum indoor temperature difference between the room with the controlled mechanical ventilation and the reference room reaches its highest value in the mornings. At that moment of the day, it can cool the environment up to a whole degree and usually more than 0.5 degrees.

The heat recovery bypass behavior can be seen in Fig. 13.17.

The heat recovery system is switched on every afternoon and evening and sometimes at the beginning of the night. The rest of the time, including every morning, it is switched off.

The rate of the injected air can be seen in Fig. 13.18.

The injected air is set to $800m^3/h$, which is the maximum fan injection rate value, for the entire length of the period considered as night, and it is set to $0m^3/h$ otherwise. The ventilation is always off during weekends.

13.4.2 Temperature Threshold-Based Ventilation

Second strategy outputs of the room $act201cc$ are reported in Fig. 13.19 and Tables 13.12 and 13.13.

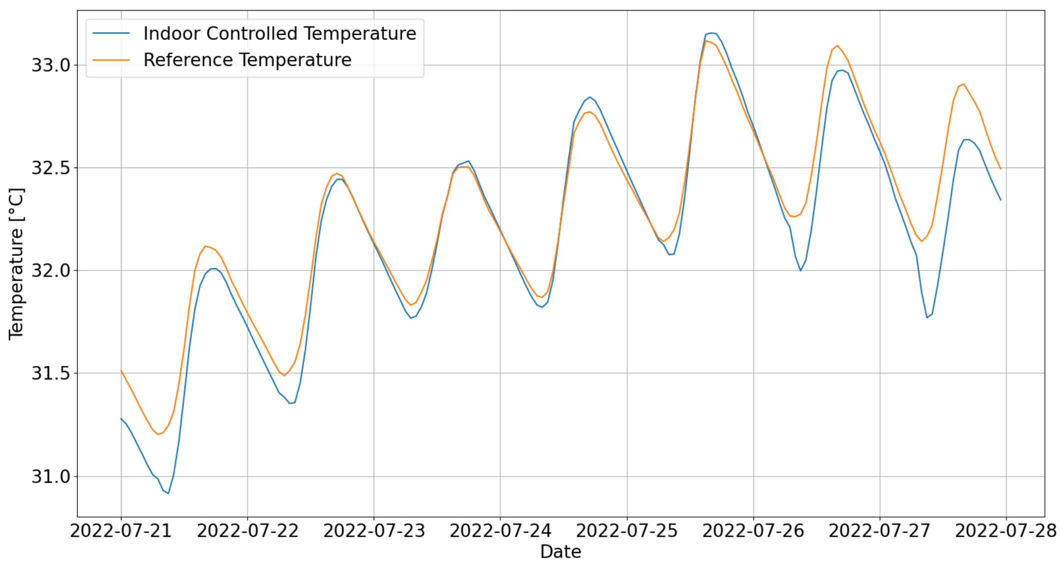

Figure 13.19: Controlled and reference temperature of $act201cc$ in the second week

Average indoor temperature	32.2°C
Average indoor temperature during lesson time	31.9°C
Average indoor temperature during night	32.0°C

Table 13.12: Controlled temperature behavior during the second testing week

Average indoor temperature	32.3°C
Average indoor temperature during lesson time	32.1°C
Average indoor temperature during night	32.1°C

Table 13.13: Reference temperature behavior during the second testing week

The heat recovery bypass behavior can be seen in Fig. 13.20.

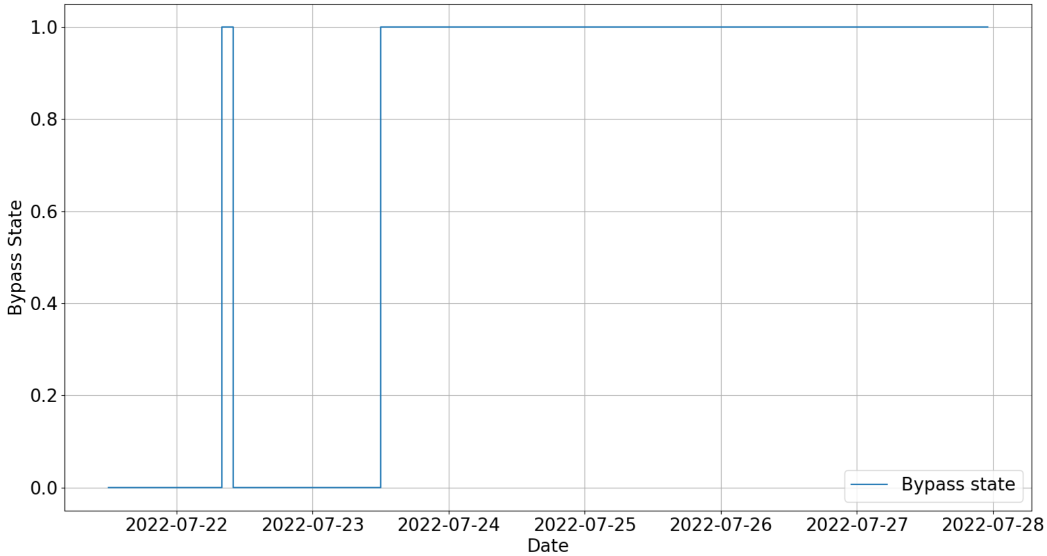

Figure 13.20: Heat recovery bypass of $act201cc$ in the second week

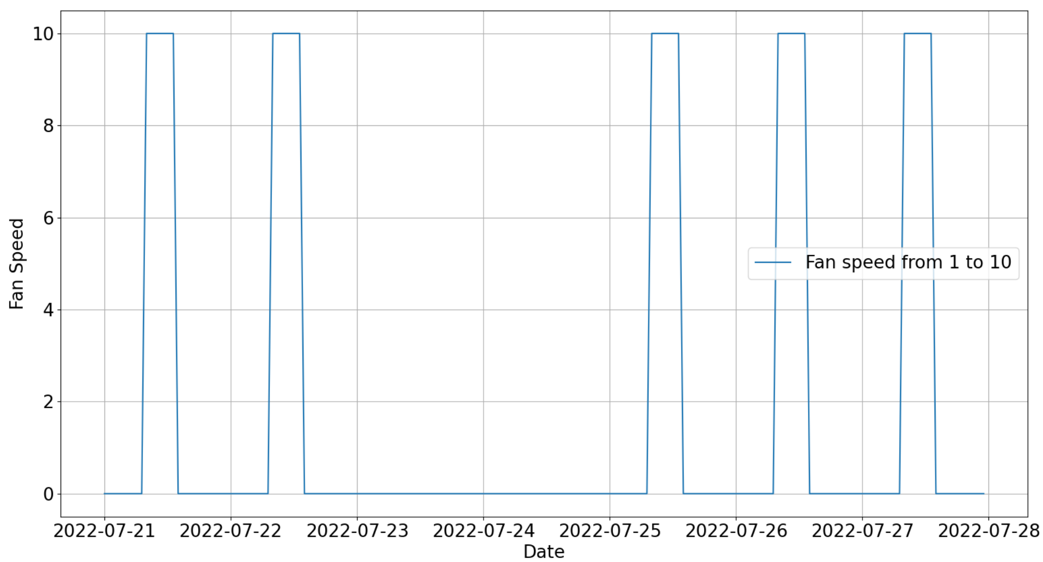

Figure 13.21: Ventilation rate of the mechanical ventilation system in the room $act201cc$ during the second week

The rate of the injected air can be seen in Fig. 13.21.

This strategy is the same as the one tested in the second week in the room $act201bc$ on the first floor already analyzed in 13.3.2. Results on this floor are comparable with those obtained in that paragraph. For this reason, to read conclusions on this approach, refer to the abovementioned paragraph.

13.4.3 Night Ventilation from 11:00 PM and Temperature Threshold Control

Results of the third approach tested in room *act*201*cc* are shown in Fig. 13.22 and Tables 13.14 and 13.15.

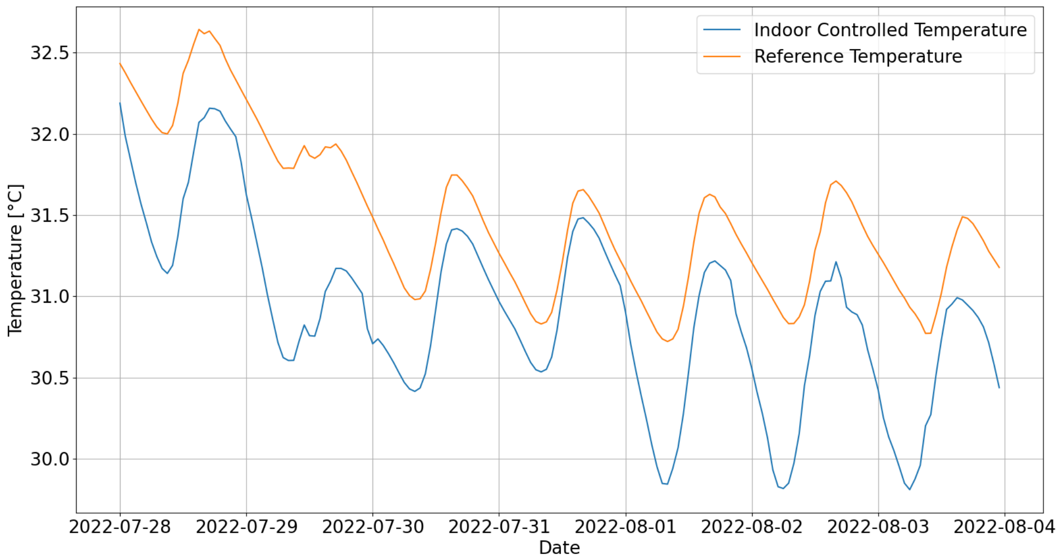

Figure 13.22: Controlled and reference temperature of *act*201*cc* in the third week

Average indoor temperature	30.9°C
Average indoor temperature during lesson time	30.7°C
Average indoor temperature during night	30.7°C

Table 13.14: Controlled temperature behavior during the third testing week

Average indoor temperature	31.5°C
Average indoor temperature during lesson time	31.4°C
Average indoor temperature during night	31.5°C

Table 13.15: Reference temperature behavior during the third testing week

From Tables 13.14 and 13.15, it can be seen that the average temperature during lessons is reduced by 0.7°C, which is more than all previously analyzed strategies. Therefore, by combining the night ventilation control with the temperature threshold-based one, the average indoor temperature reduction gives more promising results, reducing the indoor temperature by almost a whole degree.

From Fig. 13.22, it is possible to note that the minimum indoor temperature is reached in the late morning, and the difference between the controlled and the reference temperature is usually more than one degree, with a maximum value of 1.2°C.

The bypass values can be seen in Fig. 13.23, from which it can be seen that heat recovery is always set to off during this week.

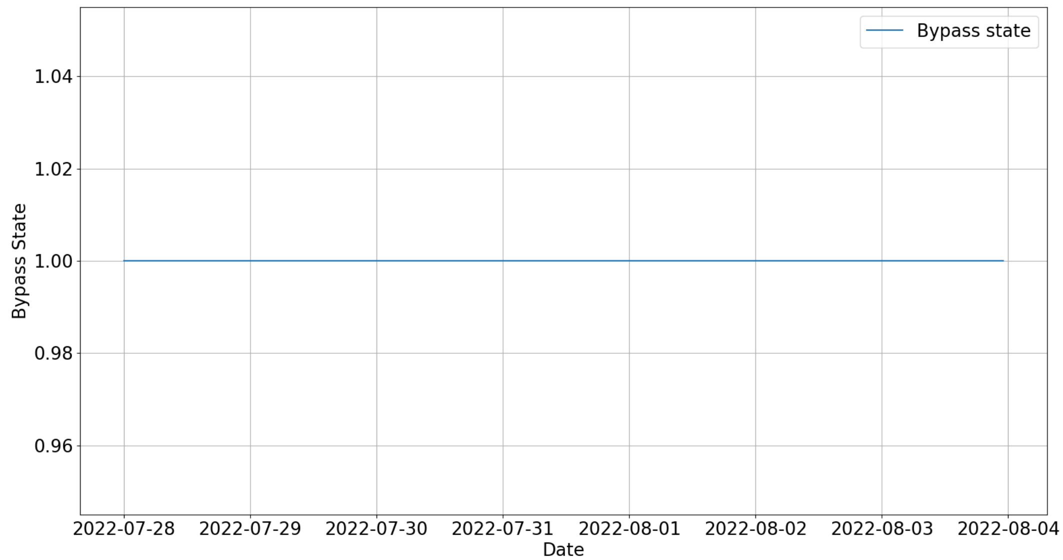

Figure 13.23: Heat recovery bypass of $act201cc$ in the third week

The injected air rate can be seen in Fig. 13.24.

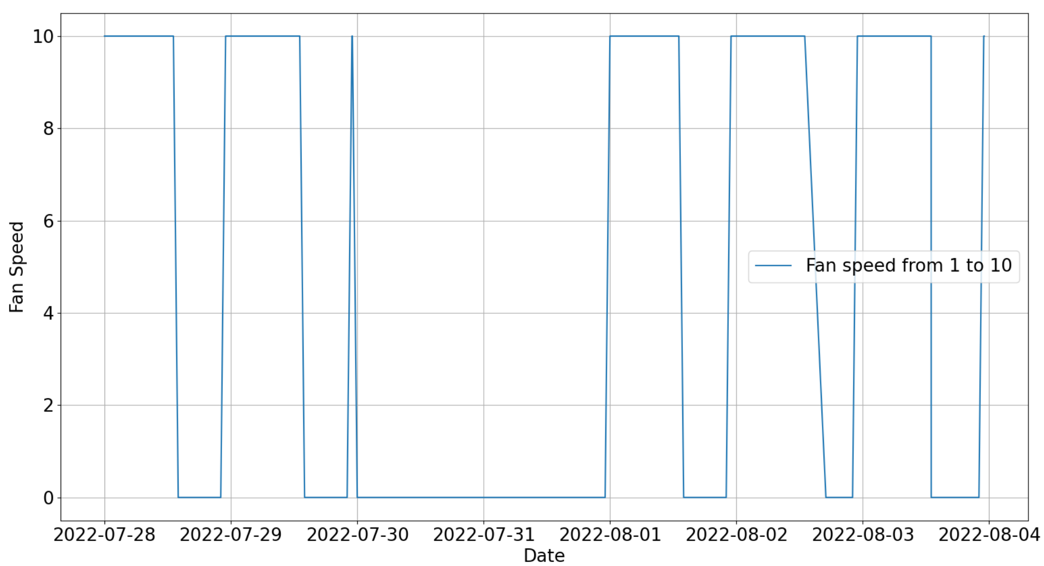

Figure 13.24: Ventilation rate of the mechanical ventilation system in the room $act201cc$ during the third week

The injected air is set to $800m^3/h$ most of the time, specifically for all the nights' durations and mornings, while the mechanical ventilation unit is turned off for the remaining part of the days and weekends.

13.5 Ventilative Cooling in *act*208*da*

13.5.1 Night Ventilation from 11:00 PM

Results of the first strategy tested in room *act*208*da* on the third floor are reported in Fig. 13.25 and Tables 13.16 and 13.17.

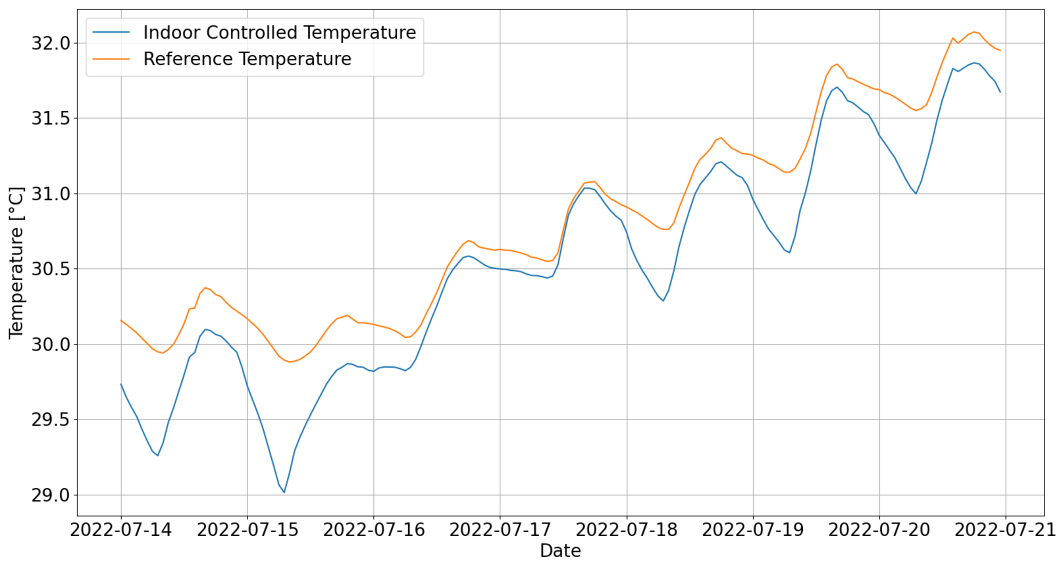

Figure 13.25: Controlled and reference temperature of *act*208*da* in the first week

Average indoor temperature	30.5°C
Average indoor temperature during lesson time	30.4°C
Average indoor temperature during night	30.3°C

Table 13.16: Controlled temperature behavior during the first testing week

Average indoor temperature	30.8°C
Average indoor temperature during lesson time	30.8°C
Average indoor temperature during night	30.8°C

Table 13.17: Reference temperature behavior during the first testing week

The heat recovery bypass behavior can be seen in Fig. 13.26.

The rate of the injected air can be seen in Fig. 13.27.

This strategy has already been tested and analyzed in paragraph 13.4.1, and the results are entirely comparable with the ones obtained there, so for their discussion, the previously mentioned paragraph should be taken as a reference.

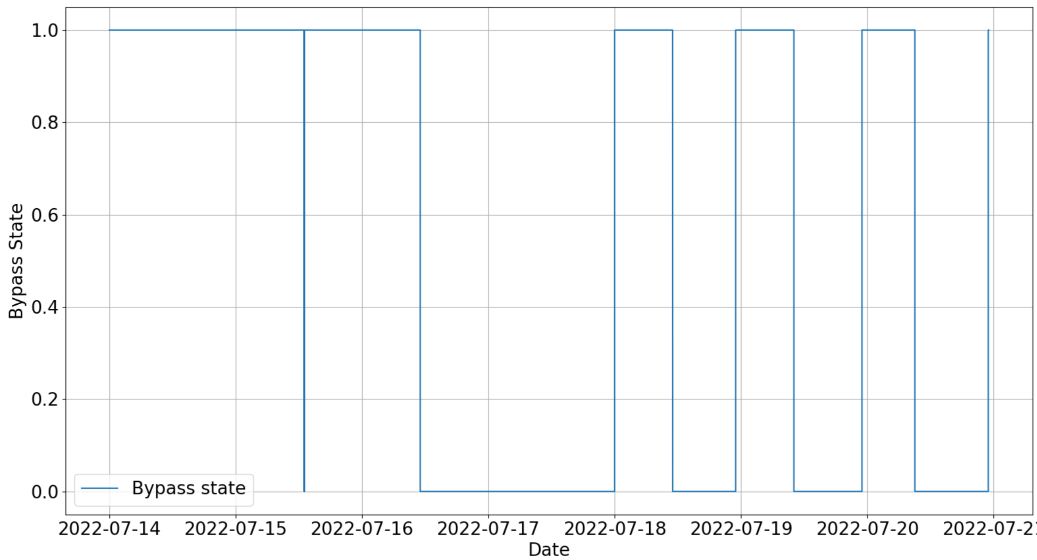

Figure 13.26: Heat recovery bypass of *act*208*da* in the first week

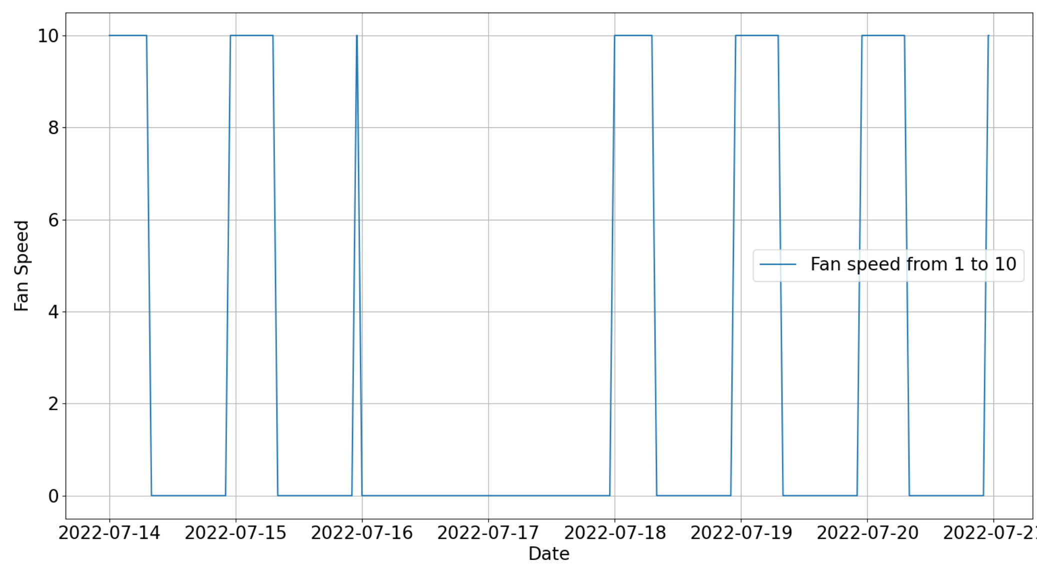

Figure 13.27: Ventilation rate of the mechanical ventilation system in the room *act*208*da* during the first week

13.5.2 Night Ventilation from 8:00 PM

Second strategy's results of room *act*208*da* are reported in Fig. 13.28 and Tables 13.18 and 13.19.

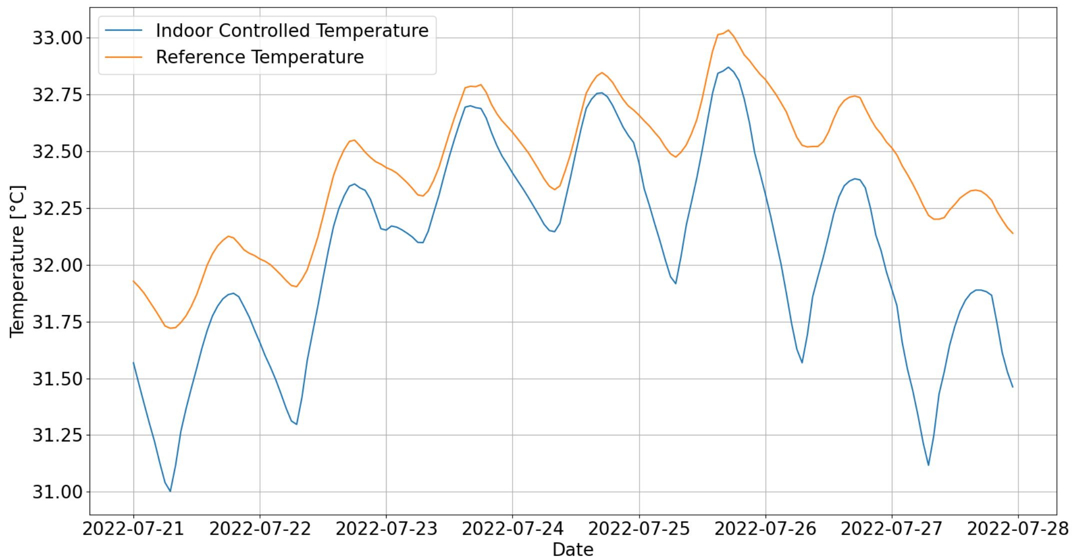

Figure 13.28: Controlled and reference temperature of *act*208*da* in the second week

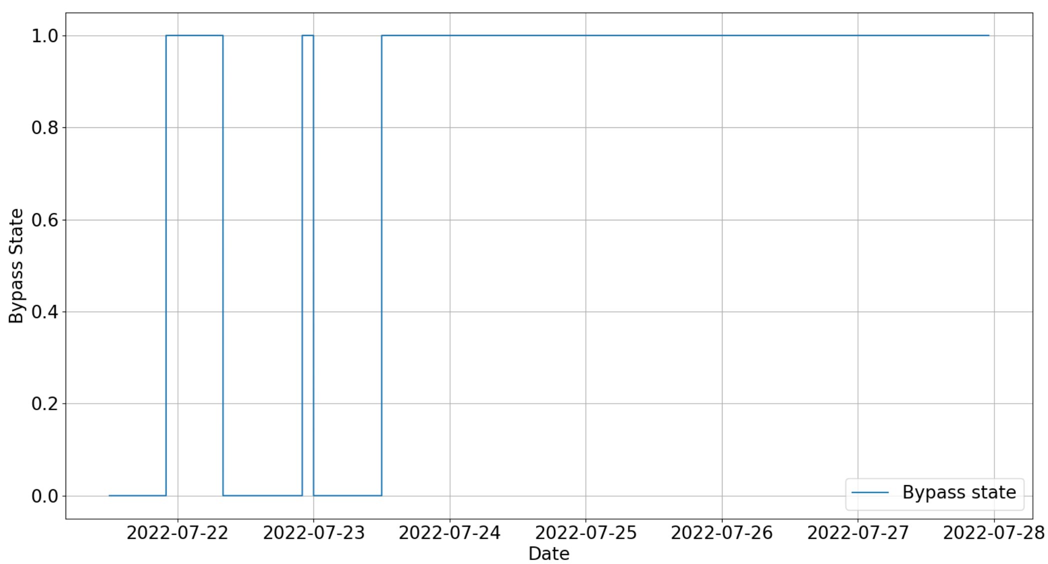

Figure 13.29: Heat recovery bypass of *act*208*da* in the second week

From the results shown in Tables 13.18 and 13.19, it can be seen that with respect to strategies that ventilate from 11:00 PM, ventilation from 8:00 PM leads to an increase in temperature reductions of 0.1 degrees, which would be probably more, given that outdoor temperatures in the second week are higher if compared to the other two weeks, especially at night. For these reasons, it can be deduced that the

Average indoor temperature	32.1°C
Average indoor temperature during lesson time	31.8°C
Average indoor temperature during night	31.7°C

Table 13.18: Controlled temperature behavior during the second testing week

Average indoor temperature	32.4°C
Average indoor temperature during lesson time	32.3°C
Average indoor temperature during night	32.3°C

Table 13.19: Reference temperature behavior during the second testing week

combination of this strategy with the single temperature threshold-based approach will lead to more savings than the strategy seen in paragraph 13.4.3, which until now has been proved to be the best way to cool the indoor environment.

From Fig. 13.28, it is possible to note that even in this case, the maximum difference between controlled and reference rooms' temperatures is reached in the mornings and has peaks of 1.2 degrees and is abundantly more than 0.5 degrees on average.

The bypass behavior can be seen in Fig. 13.29.

The heat recovery system is switched off most of the time, except for the first two days, where it is set to on usually during afternoons and evenings.

The injected air rate can be seen in Fig. 13.30.

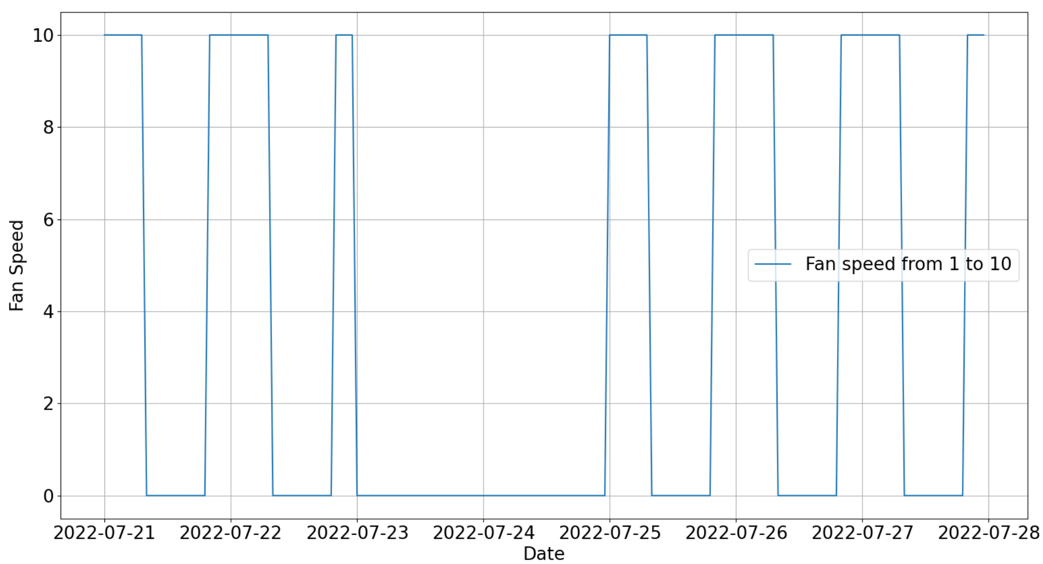

Figure 13.30: Ventilation rate of the mechanical ventilation system in the room $act208da$ during the second week

The injected air is set to $800m^3/h$ for all the night period, from 8:00 PM to 8:00 AM, $0m^3/h$ otherwise.

13.5.3 ASHRAE 62.1

Third strategy's results of room *act*208*da* are reported in Fig. 13.31 and Tables 13.20 and 13.21.

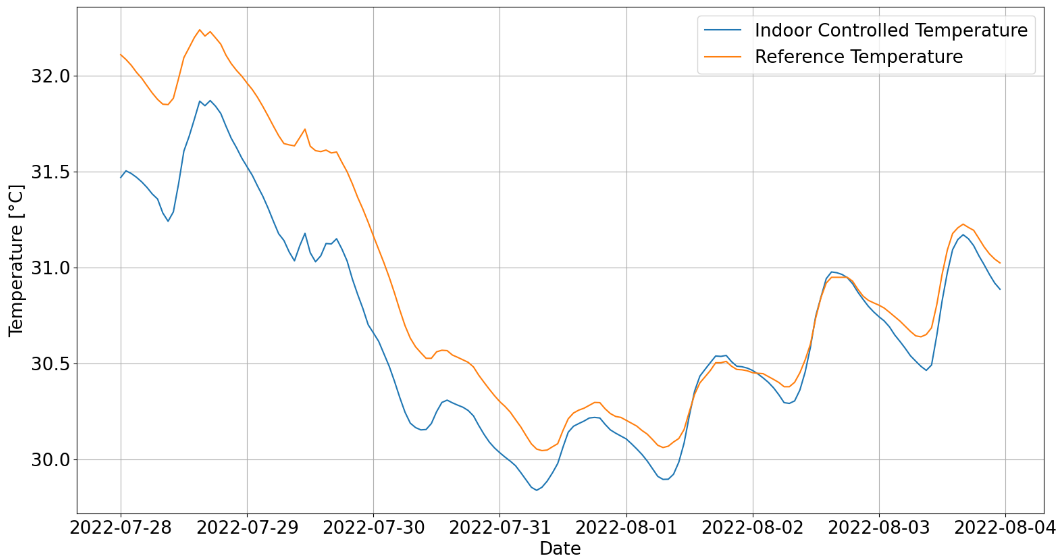

Figure 13.31: Controlled and reference temperature of *act*208*da* in the third week

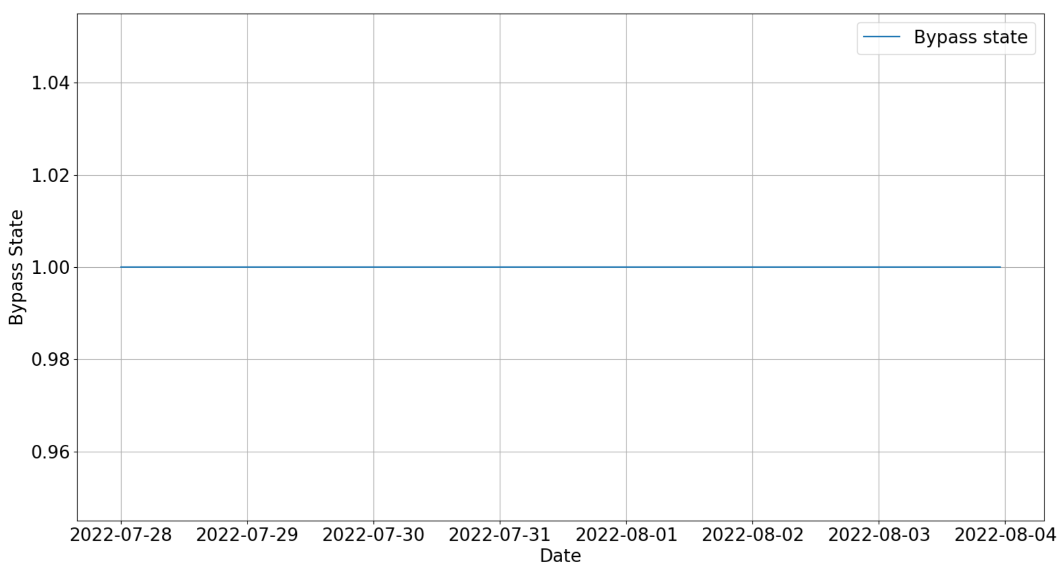

Figure 13.32: Heat recovery bypass of *act*208*da* in the third week

Average indoor temperature	30.7°C
Average indoor temperature during lesson time	30.8°C
Average indoor temperature during night	30.8°C

Table 13.20: Controlled temperature behavior during the third testing week

Average indoor temperature	30.9°C
Average indoor temperature during lesson time	31.1°C
Average indoor temperature during night	31.1°C

Table 13.21: Reference temperature behavior during the third testing week

From the results shown in Tables 13.20 and 13.21, it can be seen that the strategy proposed by the standard for classroom ventilation is more effective than all tested approaches that do not include night ventilation. In fact, ASHRAE 62.1 ventilates even during the night, exploiting lower outdoor temperatures, so it is advantageous if compared to those techniques. When the standard is compared with tested controls that include night ventilation, the advantage that it has previously is lost and performs worse than all the tested strategies as it can reduce the temperature by an average of 0.3 degrees during lesson time. It means that all the ad-hoc developed approaches for ventilative cooling which exploit night ventilation are correct and efficient.

From Fig. 13.31, it is possible to see that the maximum refreshment during lesson time is slightly more than 0.5 degrees, but it is less than this value on average.

The bypass behavior in Fig. 13.32 shows that the bypass is always on, so heat recovery is set off for the whole week.

The injected air rate can be seen in Fig. 13.33.

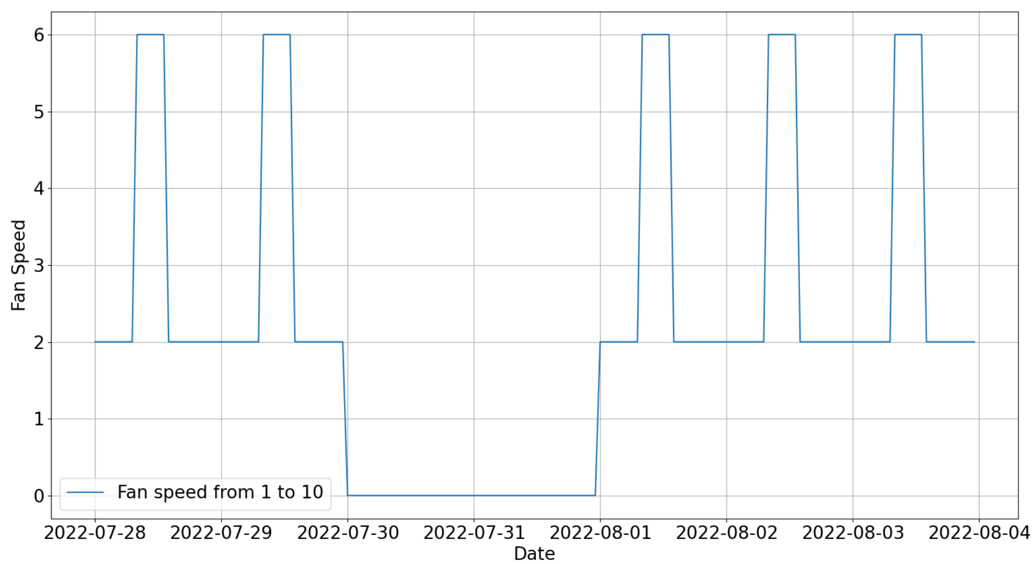

Figure 13.33: Ventilation rate of the mechanical ventilation system in the room *act*208*da* during the third week

According to the standard for classrooms, the ventilation is set to:

- $0m^3/h$ during weekends;
- $180m^3/h$ during unoccupied periods of weekdays;
- $500m^3/h$ during occupied periods of weekdays.

TVOC Reduction

The reduction of the TVOC concentration using the ASHRAE 62.1 standard compared to all the previously tested strategies in the same room is shown in Fig. 13.34, 13.35, 13.36 and 13.37.

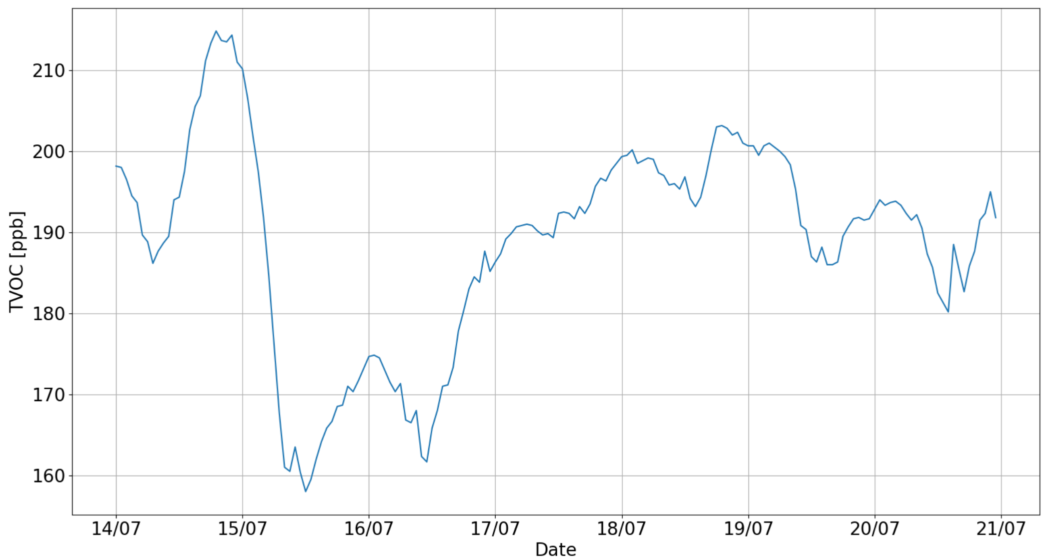

Figure 13.34: TVOC reduction in the room *act*208*da* during the first week

From these figures, it is possible to verify the ability of the ASHRAE 62.1 standard to reduce also the contaminants produced by the building and furniture materials, in addition to the ones generated by the people's breaths. Hence, from Fig. 13.37 can be seen that the concentration of TVOC in ppb is lower during the third week when the ASHRAE 62.1 standard run, while the amount of TVOC during the other two weeks is comparable and higher than one controlled with the standard approach.

13.6 Simulation of Night Ventilation from 8:00 PM

Since the combination of the night ventilation strategy from 8:00 PM to 8:00 AM with the single threshold control approach has been discovered as the best strategy for ventilative cooling, the said night ventilation has been simulated to check the consistency of the monitored results with the simulation ones. The simulation period selected is the same as the monitoring one of the same strategy in the school.

Simulation results can be seen in Tables 13.22 and 13.23, and Figs. 13.38, 13.39, and 13.40.

From Tables 13.22 and 13.23, it can be seen that in the simulation, the amount of cooling is almost six times higher than the measured one because the simulated environment is cooled by 2.8 ºC, while the actual classroom is cooled by only 0.5 ºC on average during lessons. The same conclusion is valid even for the cooling peaks, which were high up to 1.2°C in the tested approach, while, in the simulated one, they can reach values up to 5°C.

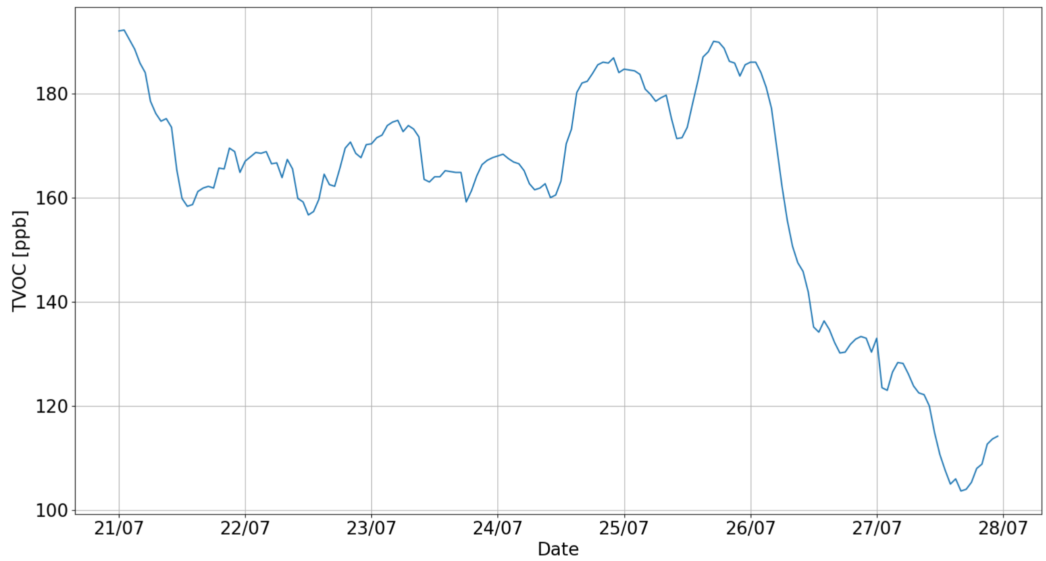

Figure 13.35: TVOC reduction in the room *act*208*da* during the second week

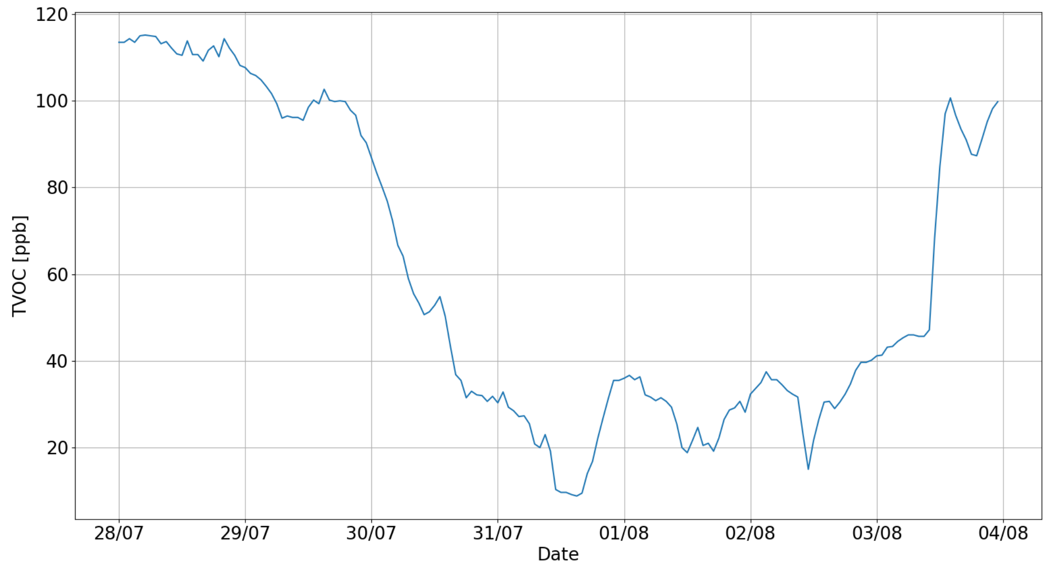

Figure 13.36: TVOC reduction in the room *act*208*da* during the third week

This discrepancy between the tests and the simulations can be due to two main reasons:

1. the position of the temperature sensor since it can be:
   - far from the airflow of the mechanical ventilation unit, since most of the sensors are located in

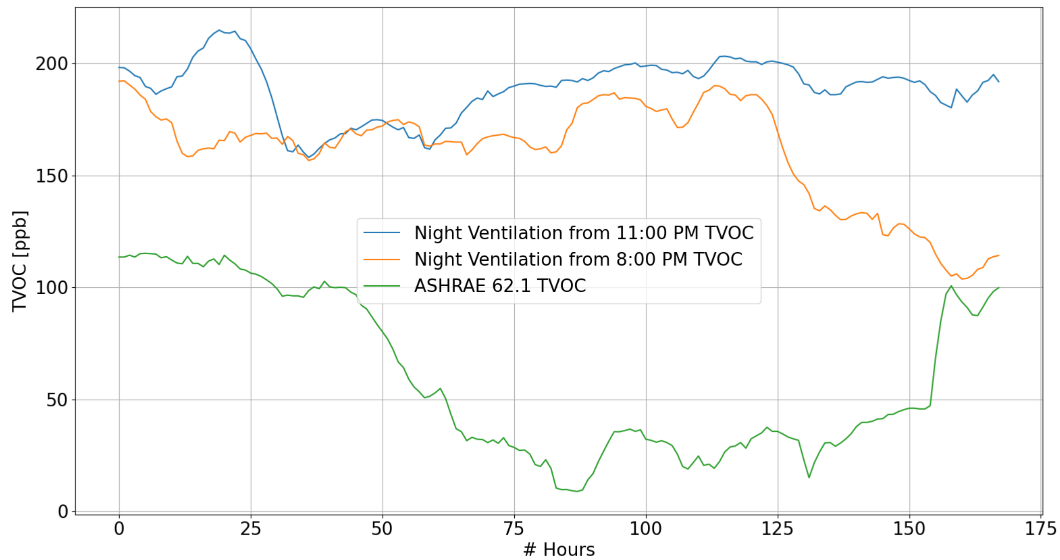

Figure 13.37: Comparison of the TVOC reduction in the room *act*208*da* in all the testing weeks

Average outdoor temperature	26.9°C
Average indoor temperature before control	31.6°C
Average indoor temperature during lessons before control	31.5°C

Table 13.22: Parameters value of the free-running building

Average indoor temperature after control	28.7°C
Average indoor temperature during lessons after control	28.7°C

Table 13.23: Parameters value of the controlled building

the wall opposite to the windows and perpendicular to the fluxes introduced from the ventilation unit. In this case, it may happen that the sensors do not measure correctly the lowering of the indoor temperatures, which affects the thermal masses close to the ventilation more;

- located on a wall not directly cooled by the ventilation and that suffers from the night re-emission of the heat accumulated in the thermal masses;
- located on a side wall, while the simulation returns results collected from a hypothetical sensor in the center of the room, where the potential temperature difference can be in the order of a couple of degrees.

2. the operation of the mechanical ventilation unit since:

- the bypass of the heat recovery may not be correctly working. This problem has also been found in other demo buildings with finer ventilation systems, and it causes a heat exchange between the colder intake airflow and the hotter emission one, reducing the ventilation cooling potential;
- the intake airflow is placed immediately below that of emission, and this could cause an unwanted backflow of warmer air;

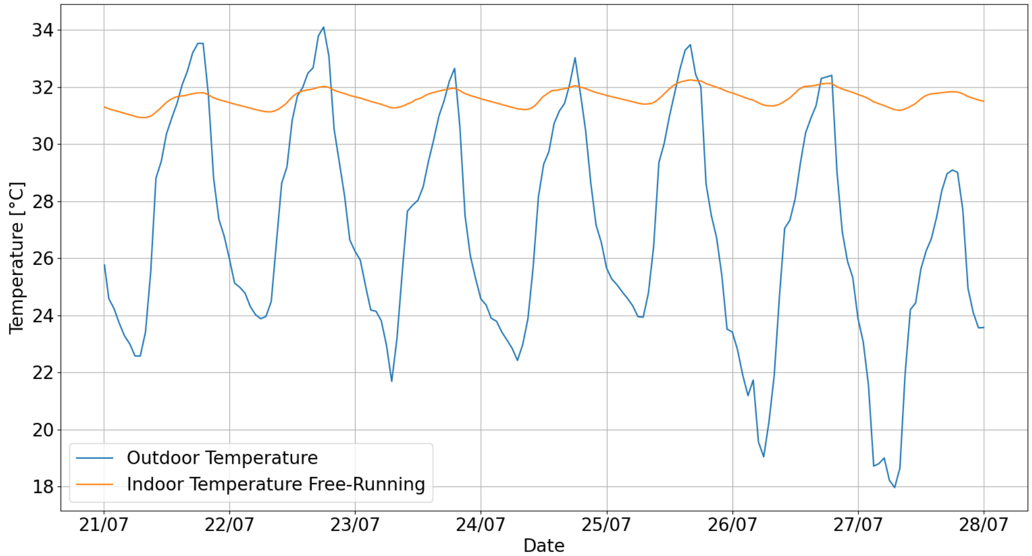

Figure 13.38: Outdoor and free-running indoor temperatures behaviors

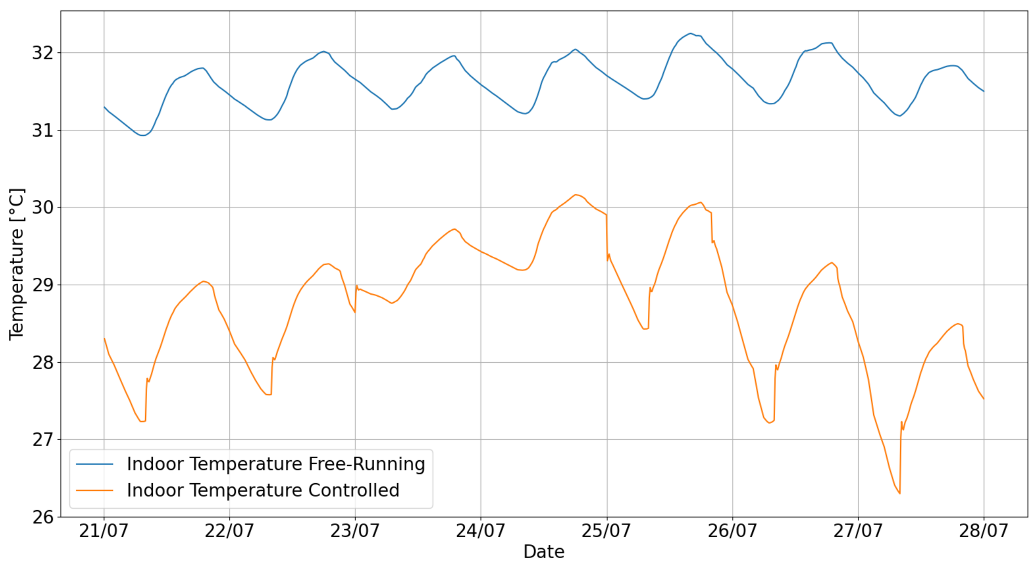

Figure 13.39: Free-running and controlled indoor temperatures behaviors

- the tested maximum airflow may be smaller than the declared nominal one.

To check if the problem is related to the said first point, the same strategy was tested on the third floor in September since, in *act*208*da*, an ad-hoc sensor was installed over the mechanical ventilation unit to see

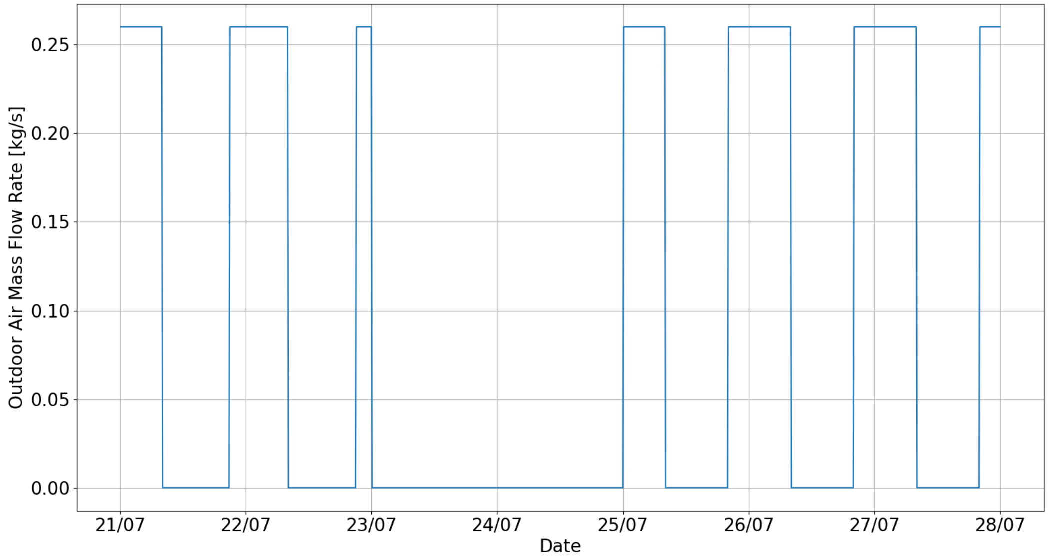

Figure 13.40: Airflow of the mechanical ventilation unit during the simulation

if the problem could be solved in this way.

Results of this monitored test can be seen in Fig. 13.41 and 13.42.

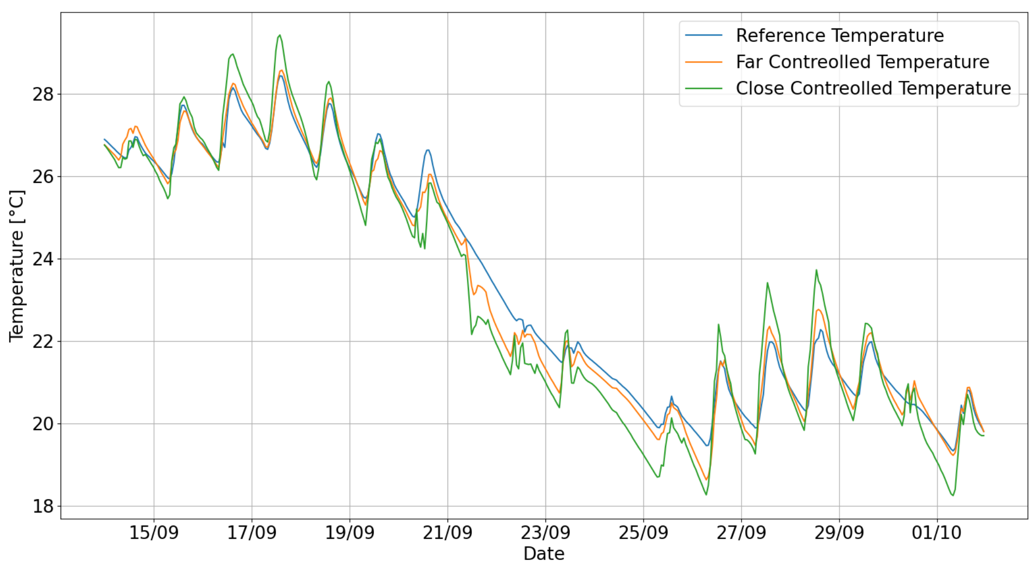

Figure 13.41: Sensor data of reference room and controlled one from far and near the mechanical ventilation unit

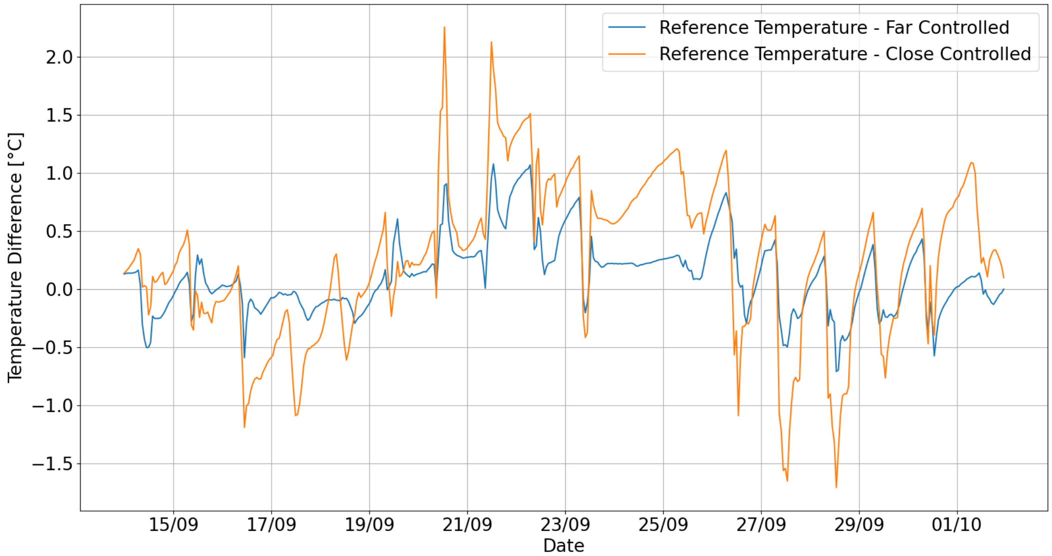

Figure 13.42: Difference between reference room temperature and controlled one from far and near the mechanical ventilation unit

Although the temperature difference in the mornings is higher when measured by the sensor close to the mechanical ventilation, and so the sensor near the ventilation unit can measure better indoor cooling than the farthest one, it should be noted that this sensor tends to react more to temperature changes, including the high-temperature peaks during the daily hours. Even if this raising in the daily temperatures is ignored, and just the morning hours are considered, it can be seen that the maximum cooling capacity reached is around 2°C, which is still far from the high values reached in the simulation. For this reason, it is more likely that the main problem of the ventilative cooling approaches is less related to the position of the sensor and more affected by the operation of the mechanical ventilation units, as said in the aforementioned second point. Hence, for future applications, it is better to install single duct ventilation units or to increase the distance between inlet and outlet air vents to avoid the heat recovery mechanisms malfunctioning if ventilative cooling techniques want to be implemented.

13.7 Indoor Air Quality in $act201bc$

13.7.1 $600ppm$ Single Threshold

The first strategy run during the second testing period in room $act201bc$ is the $600ppm$ single threshold control. It was tested for three days from 14^{th} September to the 16^{th} of the same month to collect three typical school days data. The results can be seen in Tables 13.24 and 13.25, and in Figs. 13.43, 13.44, and 13.45.

From Tables 13.24 and 13.25, it can be seen that the overall CO_2 concentration during lesson time is just slightly less than the one in the reference room. The relevant difference is thus in the discrepancy between the peaks of the two rooms. This reduction can even be seen in Fig. 13.43, where the carbon dioxide concentration in the reference room overpasses several times the $1000ppm$ threshold suggested by the ASHRAE standard, even reaching $1600pmm$. Conversely, in the classroom with mechanical ventilation, the CO_2 concentration peaks are controlled and reach lower values, never overpassing $1000ppm$.

Mechanical ventilation airflow total consumption	0.29 kWh
Average indoor temperature	26.6°C
Average indoor carbon dioxide concentration	468ppm
Average indoor carbon dioxide concentration during lesson time	638ppm
Average indoor CO_2 peak value	795ppm
Total on/off cycles of the mechanical ventilation unit	10

Table 13.24: Controlled carbon dioxide behavior for the 600ppm single threshold approach

Average indoor temperature	26.9°C
Average indoor carbon dioxide concentration	418ppm
Average indoor carbon dioxide concentration during lesson time	645ppm
Average indoor CO_2 peak value	900ppm

Table 13.25: Reference carbon dioxide behavior for the 600ppm single threshold approach

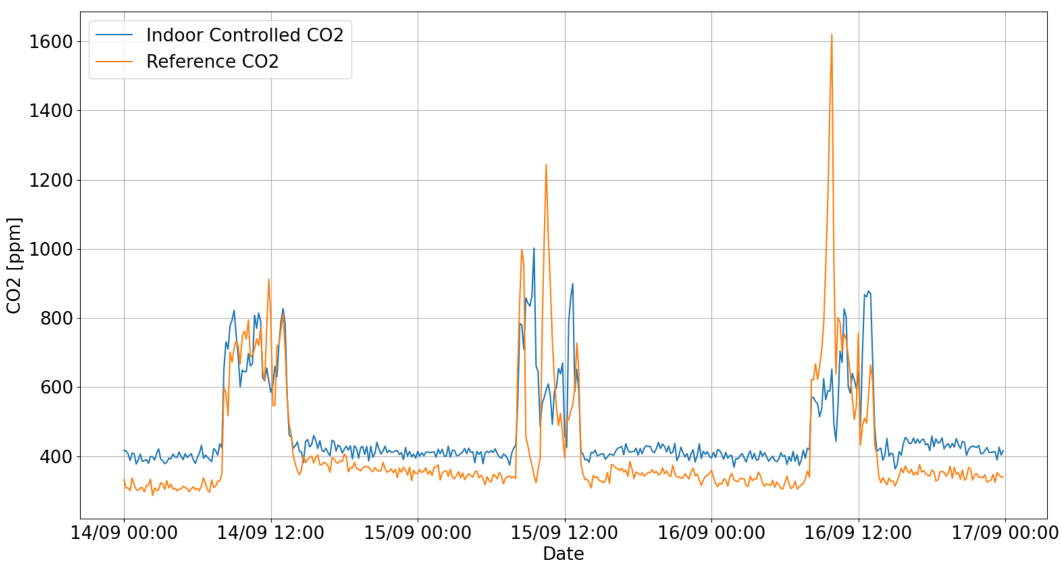

Figure 13.43: Controlled and reference carbon dioxide concentration in the room $act201bc$ with the 600ppm single threshold approach

In Fig. 13.44 it can be seen the ventilation rates used to control indoor air quality conditions. It has to be noted that said plot showing the carbon dioxide behavior has a time resolution of 10 minutes because of sensors' limitations, while the ventilation one has a resolution of 5 minutes. For this reason, sometimes ventilation and CO_2 concentration are not perfectly matched, given that within 10 minutes, the concentration of carbon dioxide in the air can change relevantly when the ventilation flow is set to a high value. This conclusion is still valid for all the other tested strategies.

The total number of switching on and off of the mechanical ventilation unit is higher than expected compared to the same simulated strategy. It can be easily explained by the occupants' behavior, which is to ventilate more during this period since it is still hot. Hence, the carbon dioxide concentration oscillates more around 600pmm instead of 800ppm as opposed to the simulation period. Since most of the year's lessons

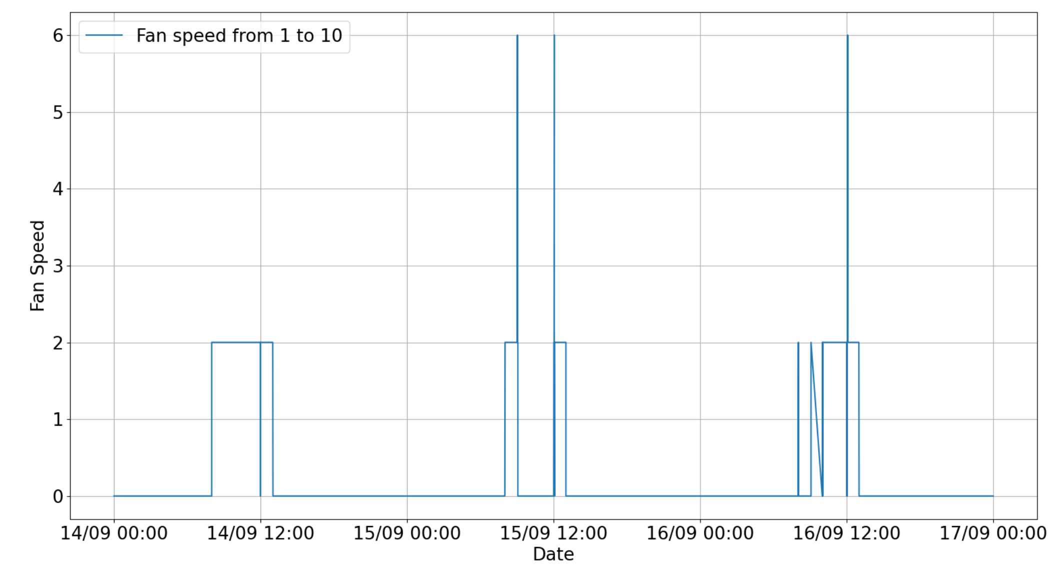

Figure 13.44: Ventilation rate of the mechanical ventilation system in the room $act201bc$ with the $600ppm$ single threshold approach

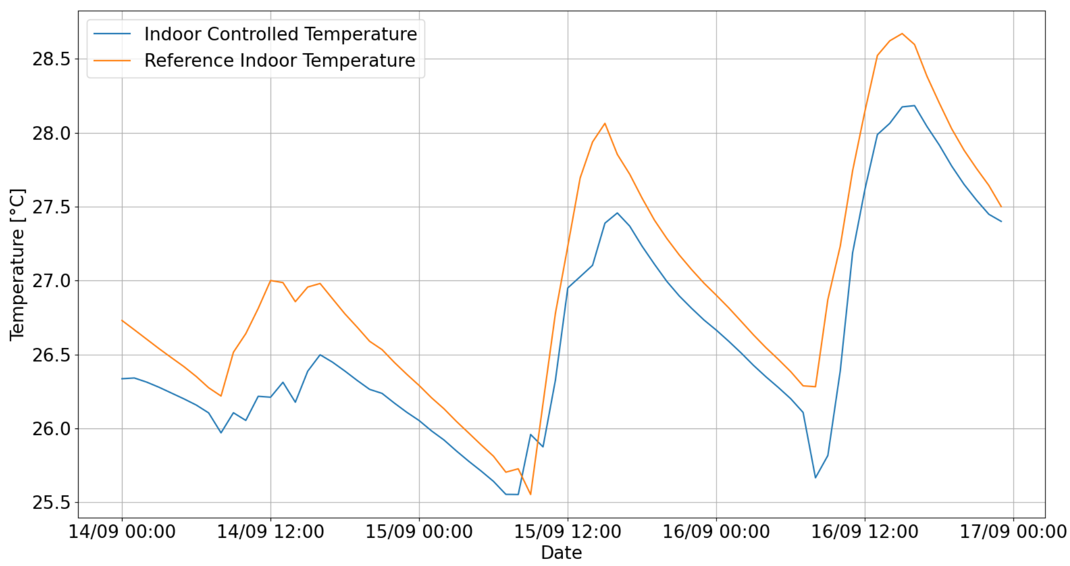

Figure 13.45: Temperature in the room $act201bc$ and in the reference one with the $600ppm$ single threshold approach

are held during winter, the result obtained from the simulation for this parameter is more relevant than this one.

The daily electric consumption is in line with the simulated one since the measured one is 0.1 kWh, and the simulated one for the same strategy is 0.08 kWh.

As already seen in the simulation of the same strategy, the indoor temperature of the controlled room is lower than the reference one of just 0.3°C, as can be seen in Fig. 13.45, so no additional heating is required to have comfortable indoor conditions.

13.7.2 600ppm Double Threshold

The second strategy in room $act201bc$ is the 600ppm double threshold control. It was also tested for three days from 20th September to the 22nd of the same month. The results can be seen in Tables 13.26 and 13.27, and in Figs. 13.46, 13.47, and 13.48.

Mechanical ventilation airflow total consumption	0.79 kWh
Average indoor temperature	24.4°C
Average indoor carbon dioxide concentration	483ppm
Average indoor carbon dioxide concentration during lesson time	784ppm
Average indoor CO_2 peak value	1156ppm
Total on/off cycles of the mechanical ventilation unit	3

Table 13.26: Controlled carbon dioxide behavior for the 600ppm double threshold approach

Average indoor temperature	24.1°C
Average indoor carbon dioxide concentration	374ppm
Average indoor carbon dioxide concentration during lesson time	623ppm
Average indoor CO_2 peak value	915ppm

Table 13.27: Reference carbon dioxide behavior for the 600ppm double threshold approach

In this case, it can be seen that the considered days are atypical since the carbon dioxide concentration and the average indoor temperature are higher in the controlled room than in the reference one. From Figs. 13.46 and 13.47, it can be deduced that this is not due to a malfunctioning of the mechanical ventilation operation since the airflows react correctly to the increase and decrease of the indoor carbon dioxide concentration but is caused by the disproportionate ventilation that is done in the reference room. This can be confirmed by looking at Fig. 13.46, where it can be seen that the peaks in the reference room are much lower than on typical days, and when the ventilation is not on, the indoor CO_2 concentration grows very fast, overpassing also 2000ppm. Conversely, the carbon dioxide concentration in the controlled room never reaches values over 1300ppm, meaning that the control is working if this value is compared to the maximum peak of the reference room. Moreover, even from Fig. 13.48, it can be proved that the reference room has been more ventilated during the testing period since the temperature has clear negative peaks during occupation periods.

As in the same simulated strategy, the double threshold avoids continuous on/off cycles of the mechanical ventilation, diminishing them to one per day.

The daily electric consumption is 0.26 kWh, which disagrees with the simulated one of 0.08 kWh because of the different year testing periods, windows operation, and the number of tests since a lower number of investigated days can bias the results more if the days are atypical.

In addition to this test, the same strategy has been tested on the second floor from the 3rd to the 5th of October to demonstrate that the strategy can work correctly and more effectively on more typical days. Results are shown in Tables 13.28 and 13.29, and in Figs. 13.49, 13.50, and 13.51.

From Tables 13.28 and 13.29, it can be seen that the peaks and the average lessons' CO_2 concentration are smaller in the controlled room when compared with the reference one, and mechanical ventilation can lower the carbon dioxide level of 300ppm for both. Mechanical ventilation is needed on the selected days since, with

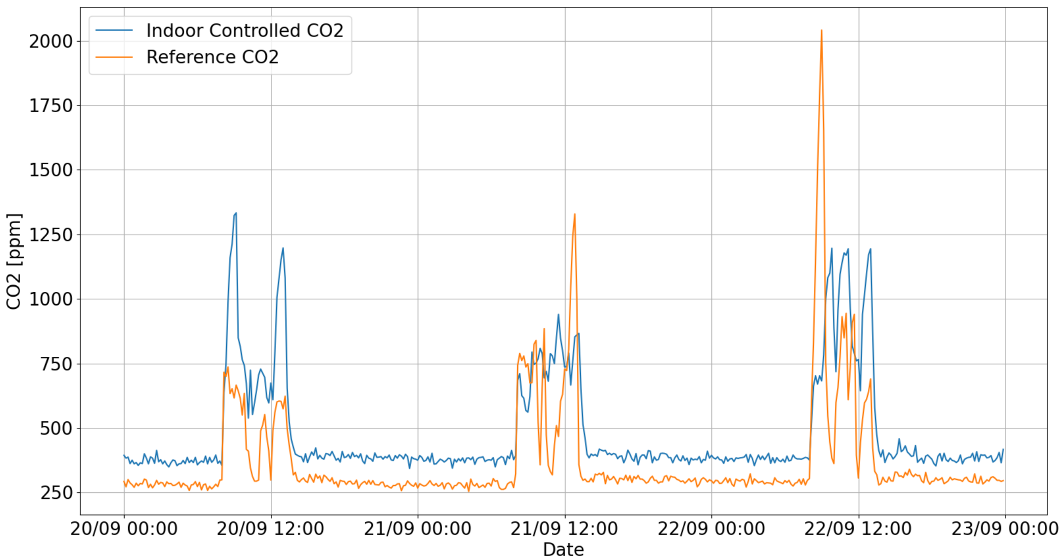

Figure 13.46: Controlled and reference carbon dioxide concentration in the room $act201bc$ with the $600ppm$ double threshold approach

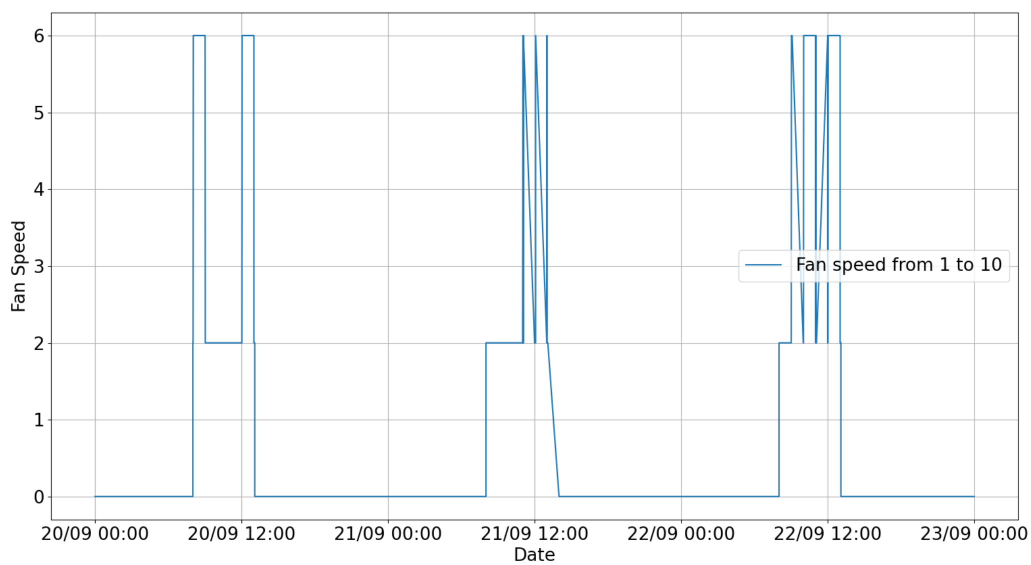

Figure 13.47: Ventilation rate of the mechanical ventilation system in the room $act201bc$ with the $600ppm$ double threshold approach

the cooling of the outdoor temperatures, windows' opening becomes rarer, and the indoor concentration tends to become higher. Hence, it can be seen from Fig. 13.49 that the maximum allowed peak in the controlled

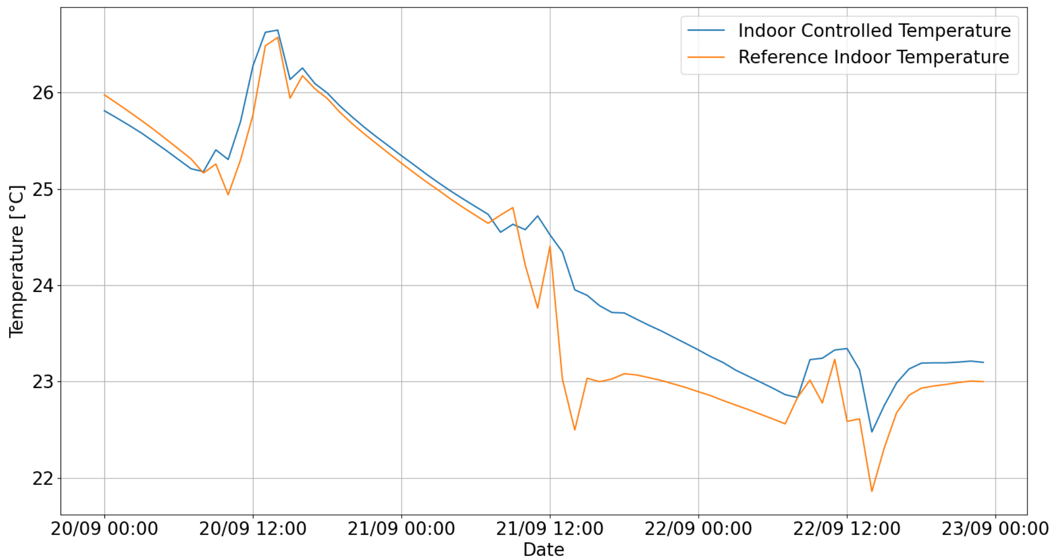

Figure 13.48: Temperature in the room $act201bc$ and in the reference one with the $600ppm$ double threshold approach

Mechanical ventilation airflow total consumption	0.69 kWh
Average indoor temperature	22.7°C
Average indoor carbon dioxide concentration	406ppm
Average indoor carbon dioxide concentration during lesson time	605ppm
Average indoor CO_2 peak value	649ppm
Total on/off cycles of the mechanical ventilation unit	3

Table 13.28: Controlled carbon dioxide behavior for the $600ppm$ double threshold approach on the second floor

Average indoor temperature	23.2°C
Average indoor carbon dioxide concentration	555ppm
Average indoor carbon dioxide concentration during lesson time	938ppm
Average indoor CO_2 peak value	980ppm

Table 13.29: Reference carbon dioxide behavior for the $600ppm$ double threshold approach on the second floor

room is under $1500ppm$, values above which the number of correct answers from the students starts to be smaller, while in the reference room, peaks of more than $2500ppm$ are reached. From all the Figs. 13.49, 13.50, and 13.51, it can be deduced that the typical behavior of the controlled room is more similar to the one on the first day, where the temperature is comparable with the one in the reference room. Conversely, during the second and third days, windows are open more often since the temperature drops more with less need for ventilation. For this reason, the higher difference in temperature values between the controlled and reference room is not due to mechanical ventilation but to the occupants' behavior which ventilates more through openings.

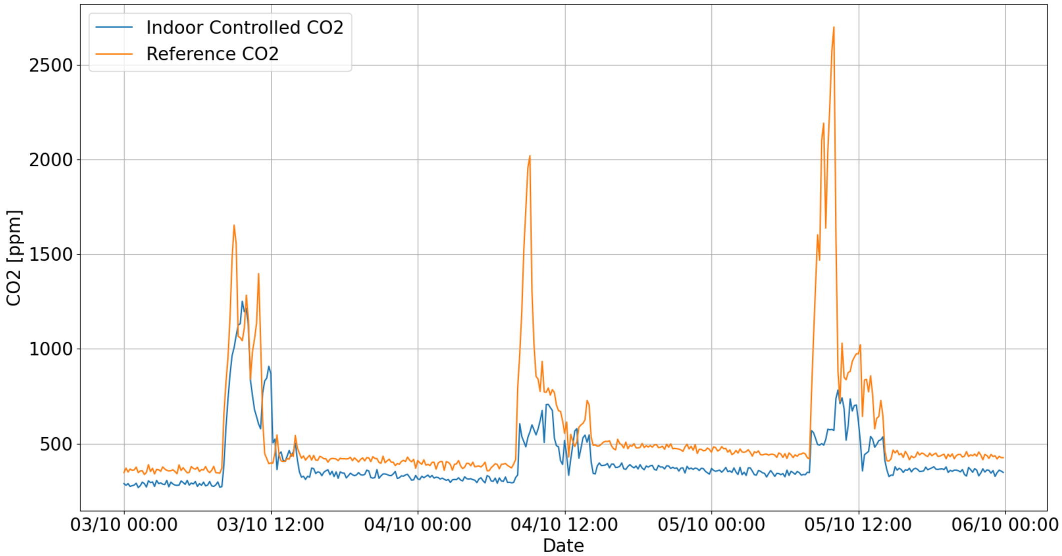

Figure 13.49: Controlled and reference carbon dioxide concentration in the room $act201bc$ with the $600ppm$ double threshold approach on the second floor

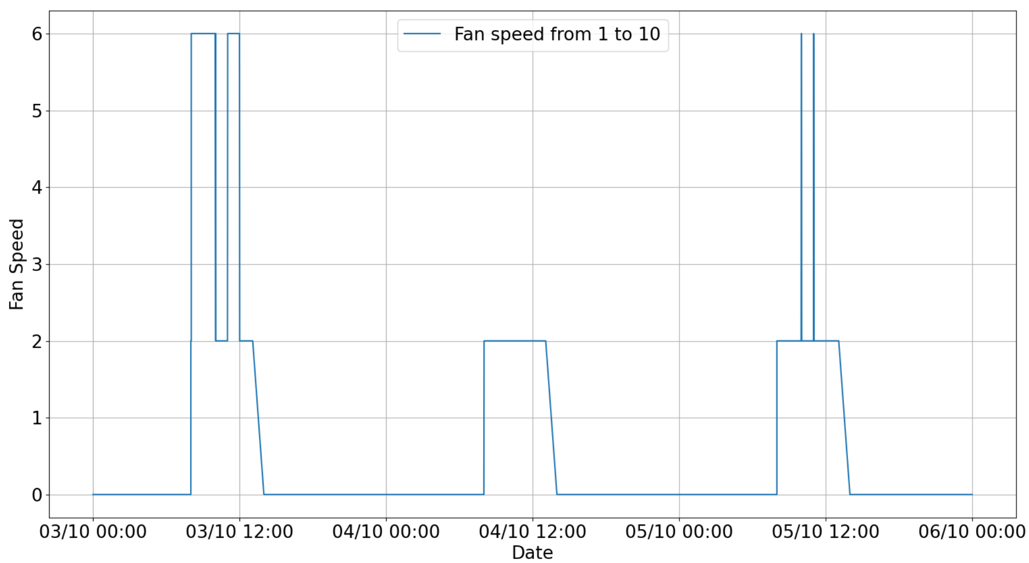

Figure 13.50: Ventilation rate of the mechanical ventilation system in the room $act201bc$ with the $600ppm$ double threshold approach on the second floor

Since the number of total on/off cycles and the consumption are comparable with the same strategy tested on the first floor, the same conclusions can be drawn here.

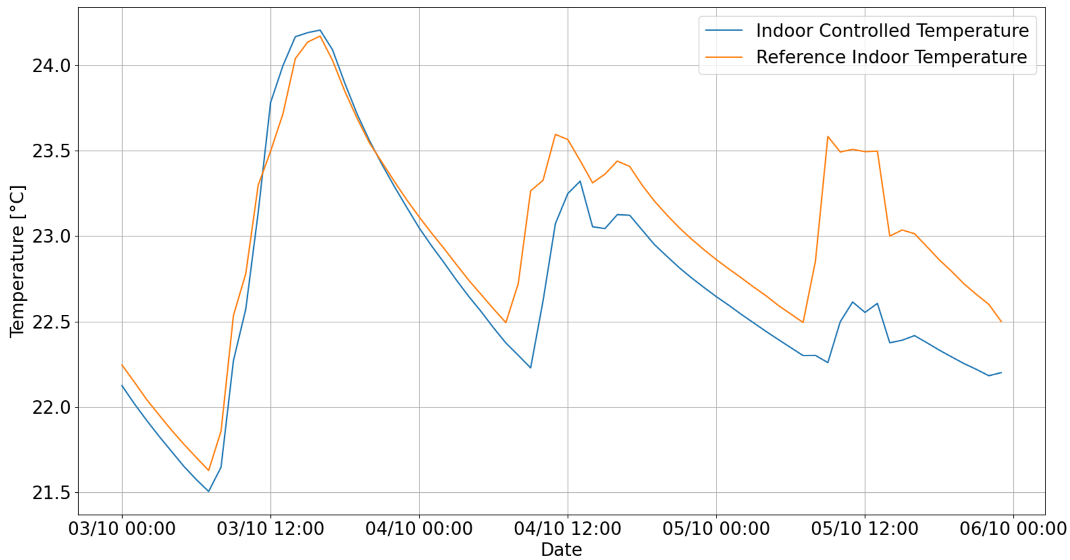

Figure 13.51: Temperature in the room $act201bc$ and in the reference one with the $600ppm$ double threshold approach on the second floor

13.7.3 ASHRAE 62

The ASHRAE 62 strategy has been tested from the 3^{rd} to the 5^{th} of October, and results are shown in Tables 13.30 and 13.31, and in Figs. 13.52, 13.53, and 13.54.

Mechanical ventilation airflow total consumption	2.49 kWh
Average indoor temperature	22.6°C
Average indoor carbon dioxide concentration	$558ppm$
Average indoor carbon dioxide concentration during lesson time	$858ppm$
Average indoor CO_2 peak value	$1118ppm$
Total on/off cycles of the mechanical ventilation unit	3

Table 13.30: Controlled carbon dioxide behavior for the ASHRAE 62 approach

Average indoor temperature	22.7°C
Average indoor carbon dioxide concentration	$517ppm$
Average indoor carbon dioxide concentration during lesson time	$940ppm$
Average indoor CO_2 peak value	$1745ppm$

Table 13.31: Reference carbon dioxide behavior for the ASHRAE 62 approach

As can be seen from Tables 13.30 and 13.31, the ASHRAE standard reduces the average indoor concentration of $100ppm$ and the peaks of $600ppm$ during a week with high values of CO_2 concentration. From Fig. 13.52, it can be seen that the maximum carbon dioxide concentration in the reference room reaches values of more than $2500ppm$, while in the room with the mechanical ventilation, peaks are confined far below $1500ppm$. As can be noted on the third testing day, this strategy can lead to overventilation when

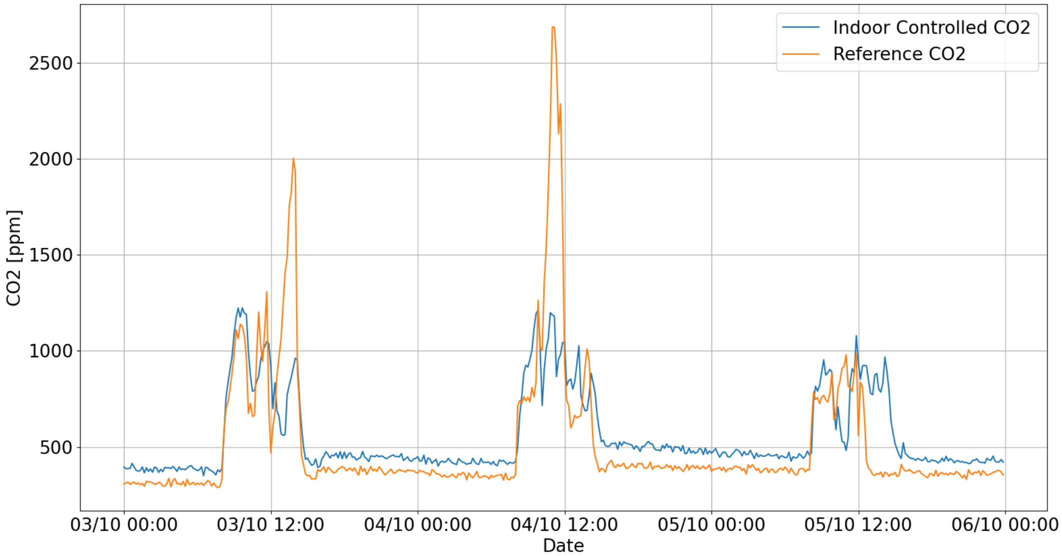

Figure 13.52: Controlled and reference carbon dioxide concentration in the room *act*201*bc* with the ASHRAE 62 approach

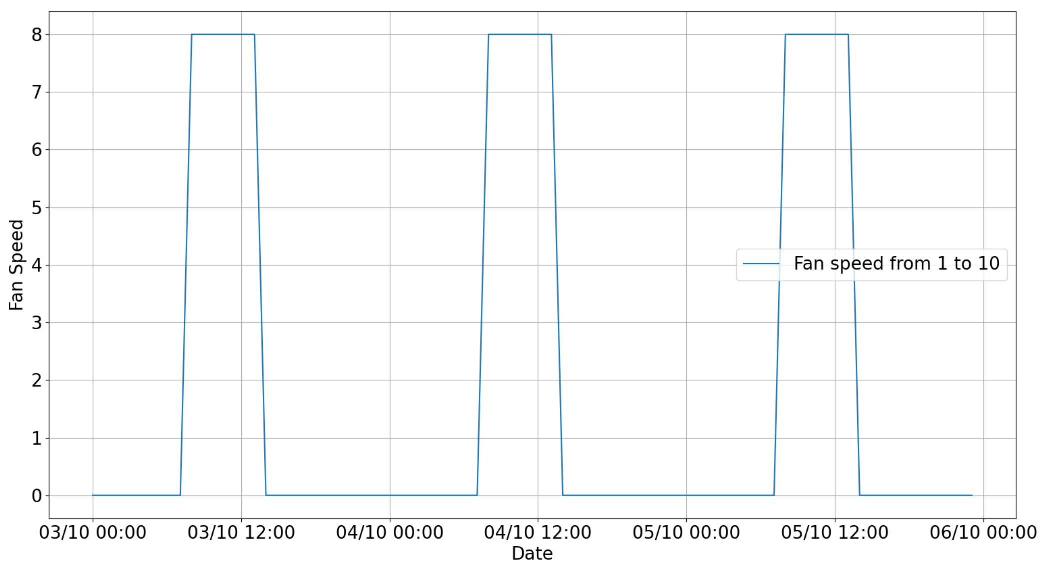

Figure 13.53: Ventilation rate of the mechanical ventilation system in the room *act*201*bc* with the ASHRAE 62 approach

the carbon dioxide concentration is lower than expected. On this day, the indoor carbon dioxide concentration reaches values comparable with outdoor conditions because of the massive unneeded ventilation. This

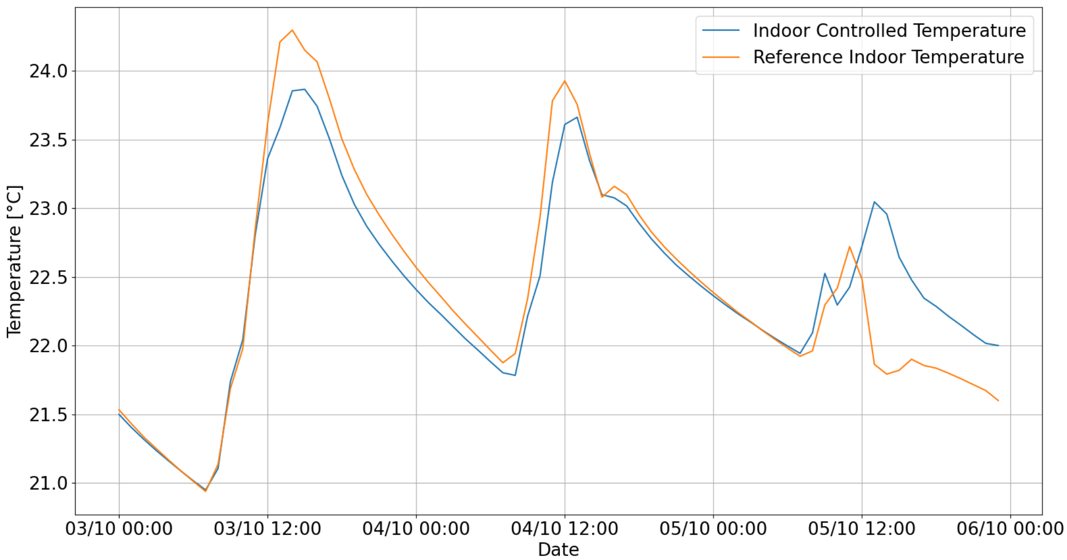

Figure 13.54: Temperature in the room $act201bc$ and in the reference one with the ASHRAE 62 approach

disproportionate ventilation may lead to additional heating consumption, which could have been saved by ventilating on demand, especially during winter when the outdoor weather is harsher.

The daily electric consumption is one of the higher since it ventilates for the whole lesson period at a power close to the maximum nominal value of the mechanical ventilation unit. It consumes 0.83 kWh per day, which is more than two times the on-demand strategy that consumes more, and even some additional heating consumption must be considered, especially in winter.

The number of on/off cycles of the ASHRAE 62 standard is precisely one per day for all the weekdays.

13.7.4 CO_2 single threshold of $1000ppm$

The fourth strategy in room $act201bc$ is the $1000ppm$ single threshold control. It was tested from 23^{rd} to 27^{th} September. The results can be seen in Tables 13.32 and 13.33, and in Figs. 13.55, 13.56, and 13.57.

Mechanical ventilation airflow total consumption	0.59 kWh
Average indoor temperature	21.8°C
Average indoor carbon dioxide concentration	$452ppm$
Average indoor carbon dioxide concentration during lesson time	$776ppm$
Average indoor CO_2 peak value	$1000ppm$
Total on/off cycles of the mechanical ventilation unit	9

Table 13.32: Controlled carbon dioxide behavior for the $1000ppm$ single threshold approach

Even here, the first and third days in the reference room are atypical since the average carbon dioxide concentration and its peaks are smaller than on typical days, as can be seen from Fig. 13.55. This can also be seen even in Tables 13.32 and 13.33 since the carbon dioxide concentration values are lower in the reference room compared to the one with the controlled mechanical ventilation. As can be deduced from Figs. 13.55 and 13.56, the ventilation in the controlled room is correctly activated when the CO_2 overpasses $1000ppm$

Average indoor temperature	21.8°C
Average indoor carbon dioxide concentration	$369ppm$
Average indoor carbon dioxide concentration during lesson time	$692ppm$
Average indoor CO_2 peak value	$948ppm$

Table 13.33: Reference carbon dioxide behavior for the $1000ppm$ single threshold approach

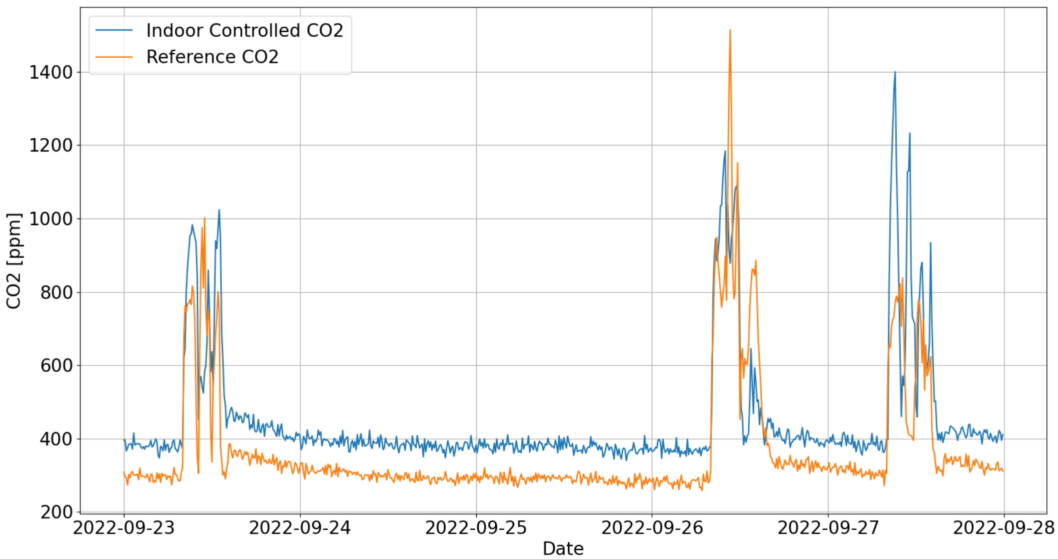

Figure 13.55: Controlled and reference carbon dioxide concentration in the room $act201cc$ with the $1000ppm$ single threshold approach

with the right airflow rate, so the difference in the carbon dioxide concentration can be due to the operation of the windows. Indeed, from Fig. 13.57 and the said Tables, it can be seen that the average temperature in the two rooms is equal, even if the controlled one is ventilated through the mechanical ventilation system. Hence, the reference room must also be ventilated. In particular, during the first day, it can be noted that the indoor temperature of the reference room is lower than the controlled one, meaning that it is more ventilated. During the second occupied day, the indoor temperature of the reference room is higher, and it can be seen that on that day, the indoor carbon dioxide has a typical behavior, so the room is poorly ventilated. On the third day, the reference room is at least as ventilated as the controlled one since the temperatures are similar.

During this test, it can be clearly noted that with the single threshold approach, the number of powering on and off of the mechanical ventilation is relevantly higher when the carbon dioxide concentration oscillates around the threshold value. This can be seen particularly during the first and third work days, where the mechanical ventilation is powered on and off four times per day. This introduces the need for a double-threshold approach to lengthen the mechanical ventilation unit's lifetime.

The daily electric consumption is 0.2 kWh, and from the said Tables, it can be seen that there is no need for additional heating consumption since the average temperature is equal to the reference room one.

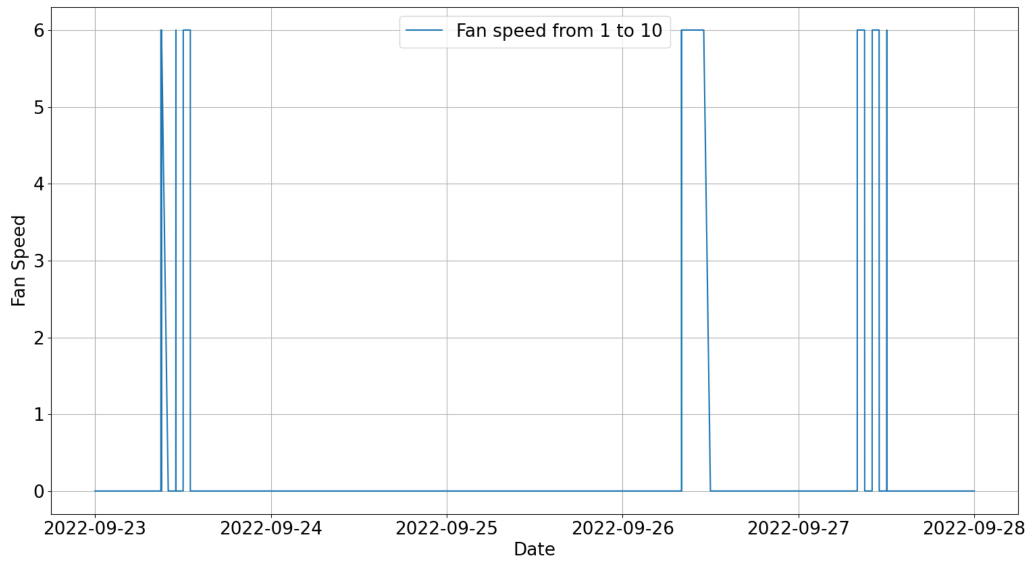

Figure 13.56: Ventilation rate of the mechanical ventilation system in the room *act*201*cc* with the 1000*ppm* single threshold approach

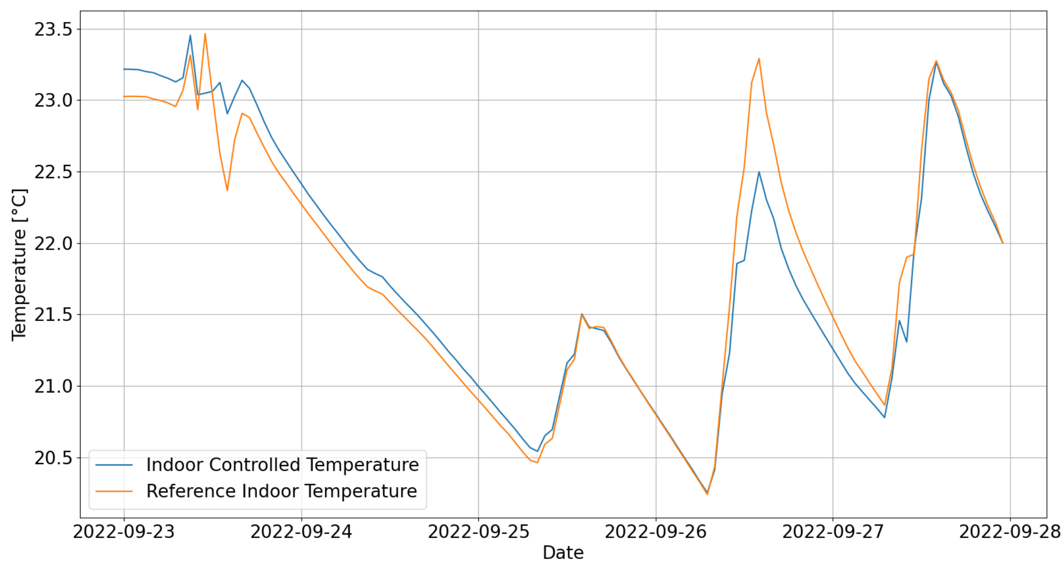

Figure 13.57: Temperature in the room *act*201*bc* and in the reference one with the 1000*ppm* single threshold approach

13.8 Indoor Air Quality in *act*201*cc*

13.8.1 800*ppm* Single Threshold

The first strategy run in the room *act*201*cc* is the 800*ppm* single threshold approach. It was tested from 14^{th} to 16^{th} September to collect, even in this case, three typical school days data. The results can be seen in Tables 13.34 and 13.35, and in Figs. 13.58, 13.59, and 13.60.

Mechanical ventilation airflow total consumption	0.08 kWh
Average indoor temperature	27.2°C
Average indoor carbon dioxide concentration	332ppm
Average indoor carbon dioxide concentration during lesson time	454ppm
Average indoor CO_2 peak value	594ppm
Total on/off cycles of the mechanical ventilation unit	5

Table 13.34: Controlled carbon dioxide behavior for the 800ppm single threshold approach

Average indoor temperature	27.4°C
Average indoor carbon dioxide concentration	432ppm
Average indoor carbon dioxide concentration during lesson time	618ppm
Average indoor CO_2 peak value	796ppm

Table 13.35: Reference carbon dioxide behavior for the 800ppm single threshold approach

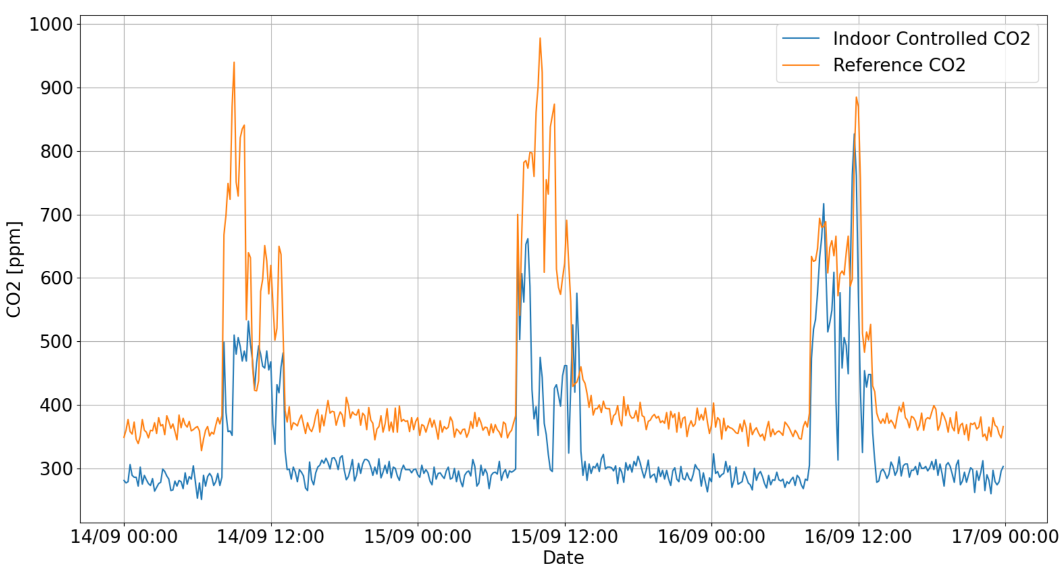

Figure 13.58: Controlled and reference carbon dioxide concentration in the room *act*201*cc* with the 800ppm single threshold approach

From Tables 13.34 and 13.35, it can be seen that both the values of the average carbon dioxide concentration during lessons and of the peaks are reduced by a significant amount. By looking at Fig. 13.58, it can be

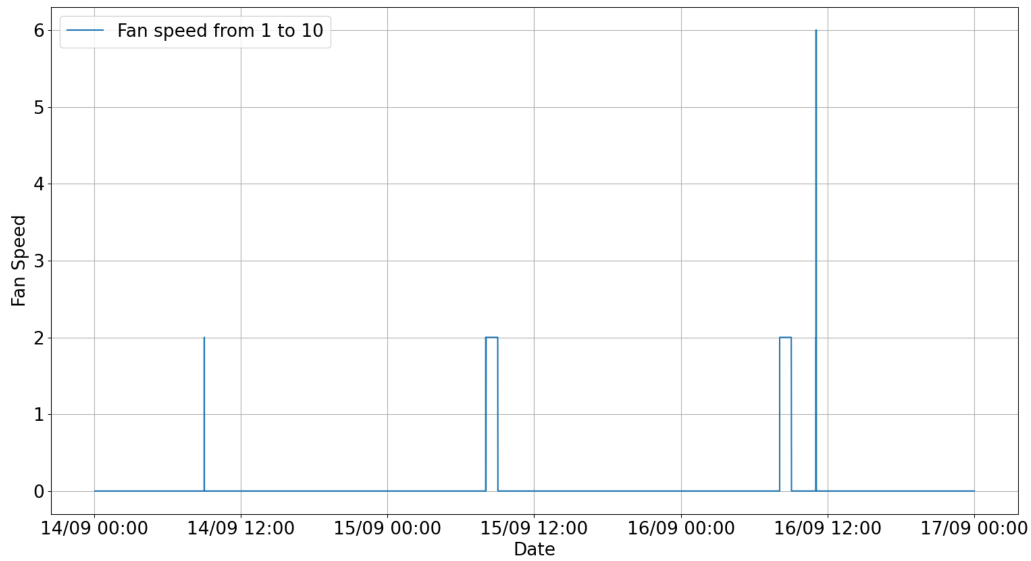

Figure 13.59: Ventilation rate of the mechanical ventilation system in the room $act201cc$ with the $800ppm$ single threshold approach

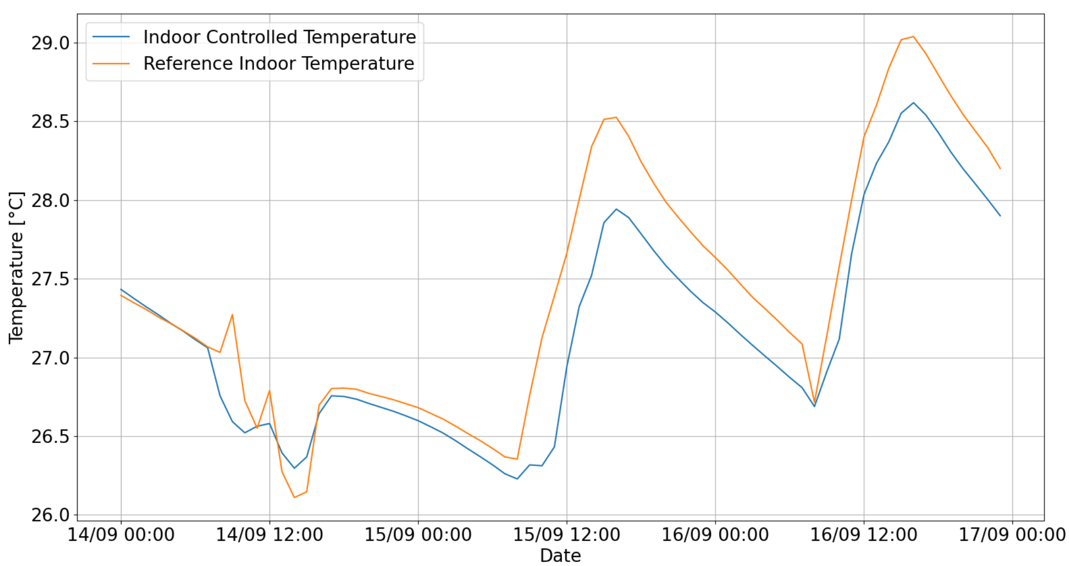

Figure 13.60: Temperature in the room $act201bc$ and in the reference one with the $800ppm$ single threshold approach

seen that the lower average of the CO_2 concentration during lesson time is not due to mechanical ventilation since the carbon dioxide concentration rarely reaches $800ppm$, which is when the airflow is activated. It is more likely that this reduction is due to the windows opening since the occupants want to cool the indoor environment. This conclusion is also confirmed by Fig. 13.59, which shows the ventilation rates during the testing period. In fact, from the afore-mentioned figure, it can be seen that, during the first two days, the ventilation is on for little time and at its minimum power. Peaks are reduced partially for the same reason but also because, on the third day, the ventilation is active for more time, reducing the maximum CO_2 concentration in the room.

The total number of on/off mechanical ventilation unit cycles is lower than expected compared to the same simulated strategy. This can be explained with the same reasoning already expressed in 13.7.1.

The daily energy consumption used for mechanical ventilation is 0.03 kWh for the monitored strategy and 0.04 kWh for the simulated one, so the results are consistent.

The indoor temperature is reduced by a negligible amount compared to the reference one, as can be seen in Fig. 13.60. The indoor temperature is on average less than 0.2°C than the reference one, as in the simulated strategy.

13.8.2 800ppm Double Threshold

The second strategy of the second testing period in the room $act201cc$ is the 800ppm double threshold approach. It was also tested for three days, from 19th to 21st September, to get three typical school days data. The results can be seen in Tables 13.36 and 13.37, and in Figs. 13.61, 13.62, and 13.63.

Mechanical ventilation airflow total consumption	0.41 kWh
Average indoor temperature	25.9°C
Average indoor carbon dioxide concentration	323ppm
Average indoor carbon dioxide concentration during lesson time	460ppm
Average indoor CO_2 peak value	703ppm
Total on/off cycles of the mechanical ventilation unit	3

Table 13.36: Controlled carbon dioxide behavior for the 800ppm double threshold approach

Average indoor temperature	26.2°C
Average indoor carbon dioxide concentration	407ppm
Average indoor carbon dioxide concentration during lesson time	592ppm
Average indoor CO_2 peak value	804ppm

Table 13.37: Reference carbon dioxide behavior for the 800ppm double threshold approach

From Tables 13.36, 13.37, and Fig. 13.61, it can be seen that both the average carbon dioxide concentration during lessons and the peaks are reduced. This time, the reduction is due to mechanical ventilation, which stays on for most classes, as shown in Fig. 13.62.

As already outlined in the simulation part of the thesis, the double threshold strategies reduce the number of mechanical ventilation unit switches on and off, passing from five to three, exactly once per day.

The daily mechanical ventilation consumption is 0.14 kWh, double the simulated consumption of 0.08 kWh. This discrepancy could be due to the lower number of days considered, which the behavior of the occupants can influence, and to the different operation of the windows compared to the simulated one since even the considered period is not the same.

Even in this case, the average temperature is not reduced significantly, as seen in 13.63, so the heating consumption does not increase when this strategy is used.

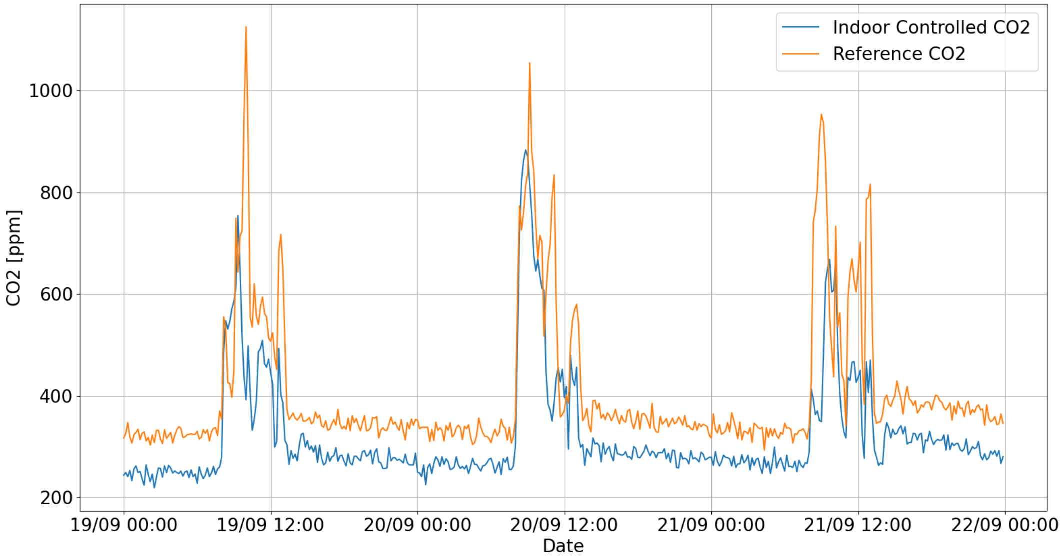

Figure 13.61: Controlled and reference carbon dioxide concentration in the room $act201cc$ with the $800ppm$ double threshold approach

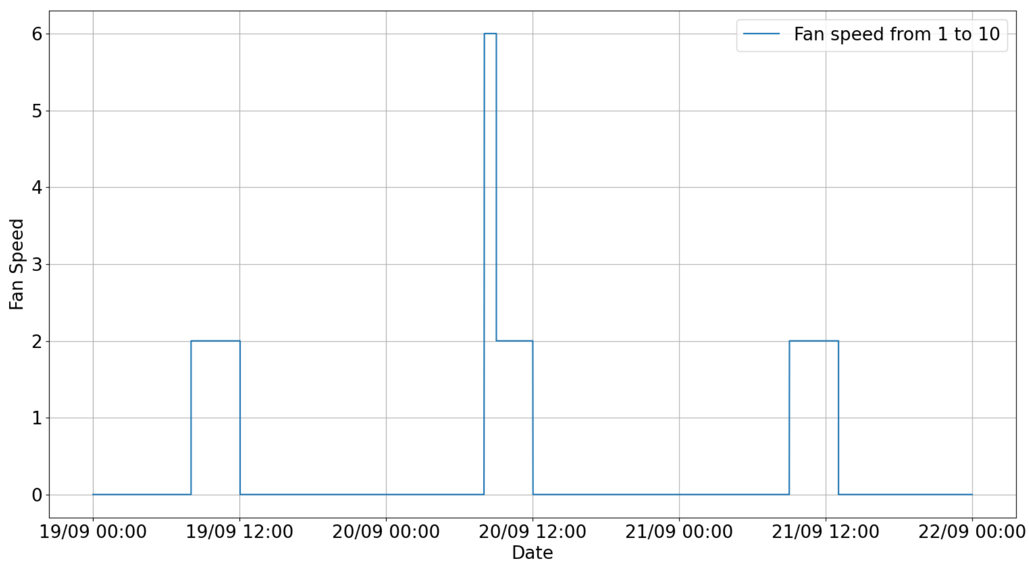

Figure 13.62: Ventilation rate of the mechanical ventilation system in the room $act201cc$ with the $800ppm$ double threshold approach

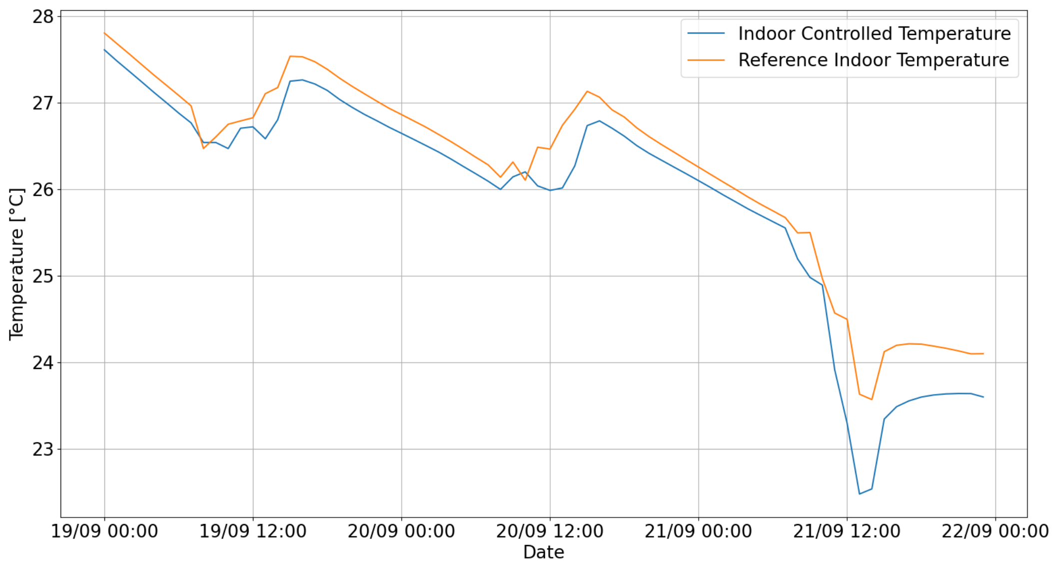

Figure 13.63: Temperature in the room $act201bc$ and in the reference one with the $800ppm$ double threshold approach

13.8.3 ASHRAE 62.1

The third strategy tested in the second period in room $act201cc$ is the ASHRAE 62.1 standard. It was tested for three days, from 22^{nd} to 26^{th} September. The results can be seen in Tables 13.38 and 13.39, and in Figs. 13.64, 13.65, and 13.66.

Mechanical ventilation airflow total consumption	3.14 kWh
Average indoor temperature	22.2°C
Average indoor carbon dioxide concentration	328ppm
Average indoor carbon dioxide concentration during lesson time	593ppm
Average indoor CO_2 peak value	707ppm
Total on/off cycles of the mechanical ventilation unit	1

Table 13.38: Controlled carbon dioxide behavior for the ASHRAE 62.1 approach

Average indoor temperature	22.5°C
Average indoor carbon dioxide concentration	407ppm
Average indoor carbon dioxide concentration during lesson time	695ppm
Average indoor CO_2 peak value	1043ppm

Table 13.39: Reference carbon dioxide behavior for the ASHRAE 62.1 approach

The ASHRAE 62.1 standard approach can significantly reduce the indoor average carbon dioxide concentration during lessons and its peaks, as can be seen in said Tables and Fig. 13.64. It achieves the best results compared to all the tested strategies, reducing the peaks of more than $300ppm$ in a week with limited CO_2 concentration and low peak values, but sacrifices the indoor temperature conditions and the consumption

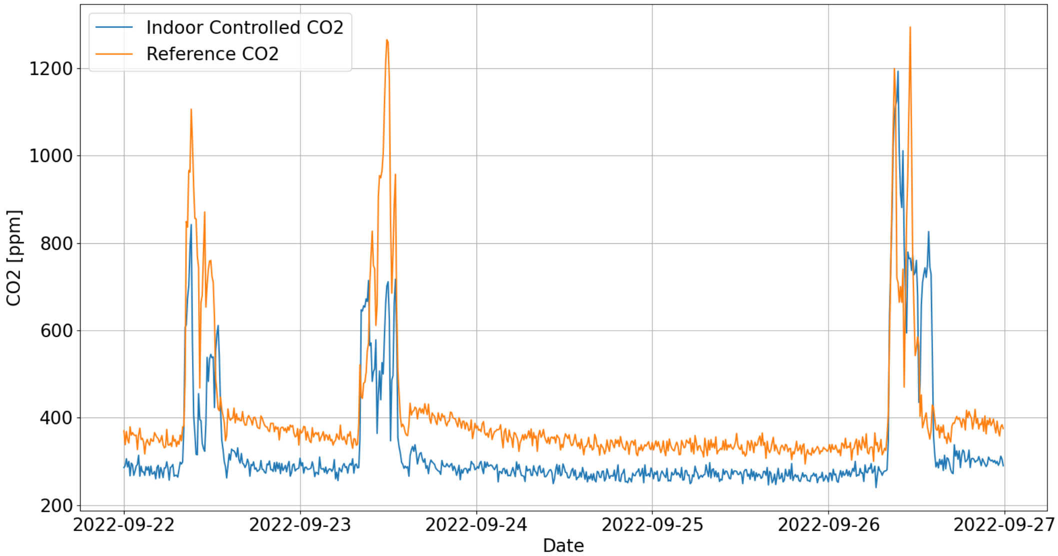

Figure 13.64: Controlled and reference carbon dioxide concentration in the room *act*201*cc* with the ASHRAE 62.1 approach

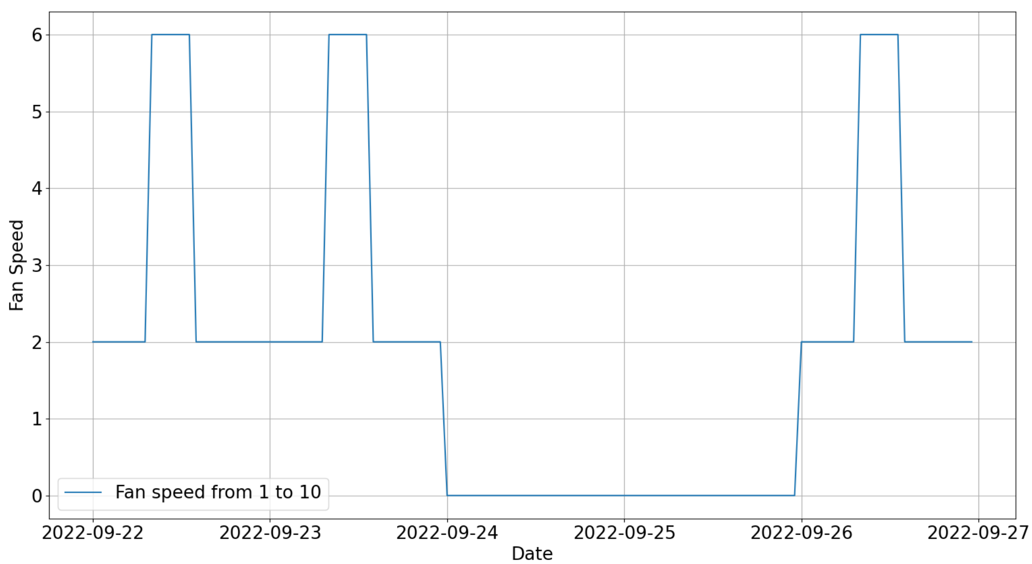

Figure 13.65: Ventilation rate of the mechanical ventilation system in the room *act*201*cc* with the ASHRAE 62.1 approach

and can lead to overventilation for some periods.

The indoor temperatures are reduced on average by 0.3°C overall, and if the weekend is not considered,

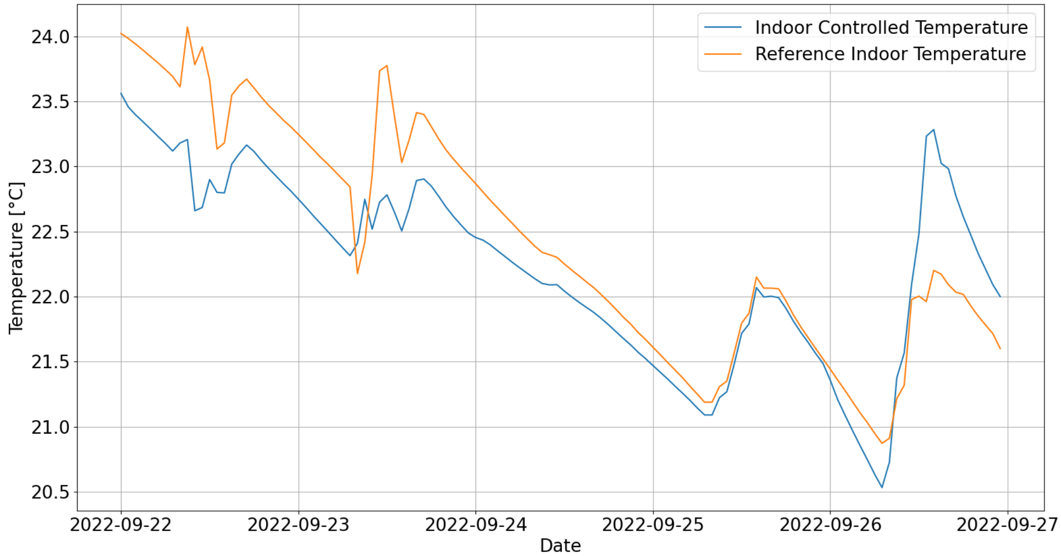

Figure 13.66: Temperature in the room $act201bc$ and in the reference one with the ASHRAE 62.1 approach

it can be seen that temperatures are reduced on average by half a degree. This lowering of the temperatures may lead to additional heating consumption if the cooling of the outdoor temperatures in the following winter months is considered.

Therefore, the daily electric consumption of mechanical ventilation is 1.05 kWh which is almost three times the higher consumption monitored during the on-demand ventilation tests since the ventilation is on even for non-lesson times. It consumes even more than the ASHRAE 62 standard, which is the other non-on-demand tested strategy since it never powers off the ventilation and even because of the higher additional heating consumptions that should be taken into account.

Moreover, this ventilation rate may lead to over-ventilation for some periods as when the occupants open the windows. This can be seen in Fig. 13.64, where on the first day, in the middle of the occupation hours, it can be seen that the carbon dioxide concentration returns for some hours to the outdoor CO_2 values. Indoor carbon dioxide values lower than $400ppm$ are a clear sign of over-ventilation, and they are due to both the tested control strategy and the opening of the windows. Over-ventilation is not problematic during the summer period since ventilation helps reduce indoor temperatures but can lead to a waste of energy during winter since the heating system is loaded more.

13.8.4 CO_2 double threshold of $600ppm$ and $1000ppm$

The fourth strategy tested in $act201cc$ is the $1000ppm$ double threshold control, with $600ppm$ as the lower threshold value. It was tested from 27^{rd} to 30^{th} September for four days since, on the second day, the ventilation has never been powered up. The results can be seen in Tables 13.40 and 13.41, and in Figs. 13.67, 13.68, and 13.69.

From Tables 13.40 and 13.41, it can be seen that the average indoor carbon dioxide concentration has been reduced of $300ppm$ during lesson time and peaks are decreased of almost $900ppm$. These highly efficient results are due to the very high concentrations during the testing days and to the opening of the windows in the controlled room starting from the second testing day. The window opening behavior can be assumed by looking at Fig. 13.69 and 13.68, where it can be seen that the temperature is reduced even if the ventilation is

Mechanical ventilation airflow total consumption	1.07 kWh
Average indoor temperature	22.3°C
Average indoor carbon dioxide concentration	409ppm
Average indoor carbon dioxide concentration during lesson time	668ppm
Average indoor CO_2 peak value	811ppm
Total on/off cycles of the mechanical ventilation unit	3

Table 13.40: Controlled carbon dioxide behavior for the 1000ppm double threshold approach

Average indoor temperature	22.6°C
Average indoor carbon dioxide concentration	538ppm
Average indoor carbon dioxide concentration during lesson time	956ppm
Average indoor CO_2 peak value	1691ppm

Table 13.41: Reference carbon dioxide behavior for the 1000ppm double threshold approach

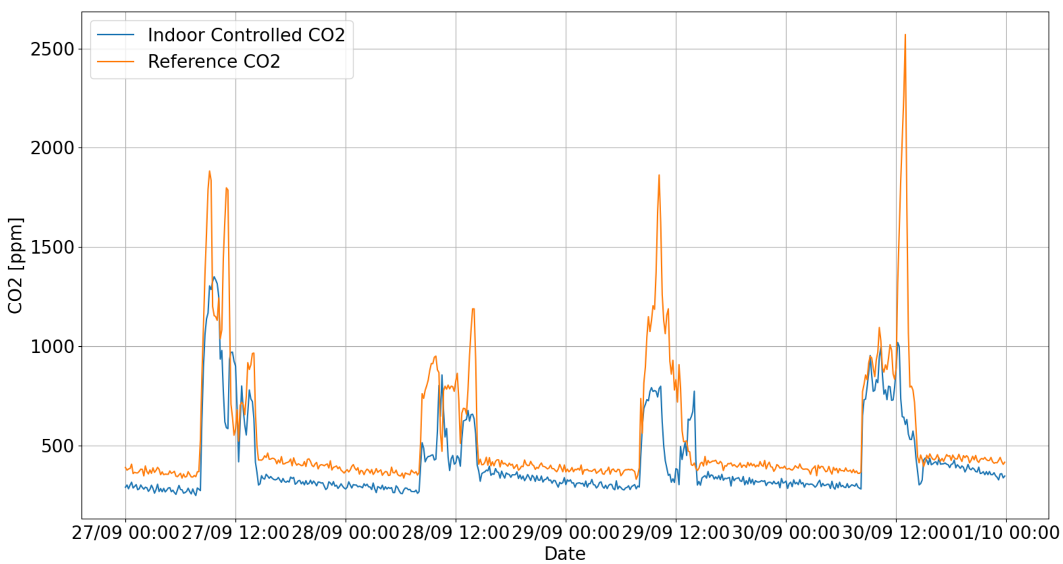

Figure 13.67: Controlled and reference carbon dioxide concentration in the room $act201cc$ with the 1000ppm double threshold approach

off or briefly powered on with a low airflow rate. For this reason, the temperature reduction in the controlled room compared to the reference one is not significant since it is due to the occupants' behavior.

Even here, the double threshold approach reduces the number of switches on and off of the mechanical ventilation unit, lowering this value to one per day.

The daily electric consumption is 0.36 kWh, which is more than all the previously tested on-demand strategies. The higher consumption can be explained by the elevated carbon dioxide concentration in the air during these testing days.

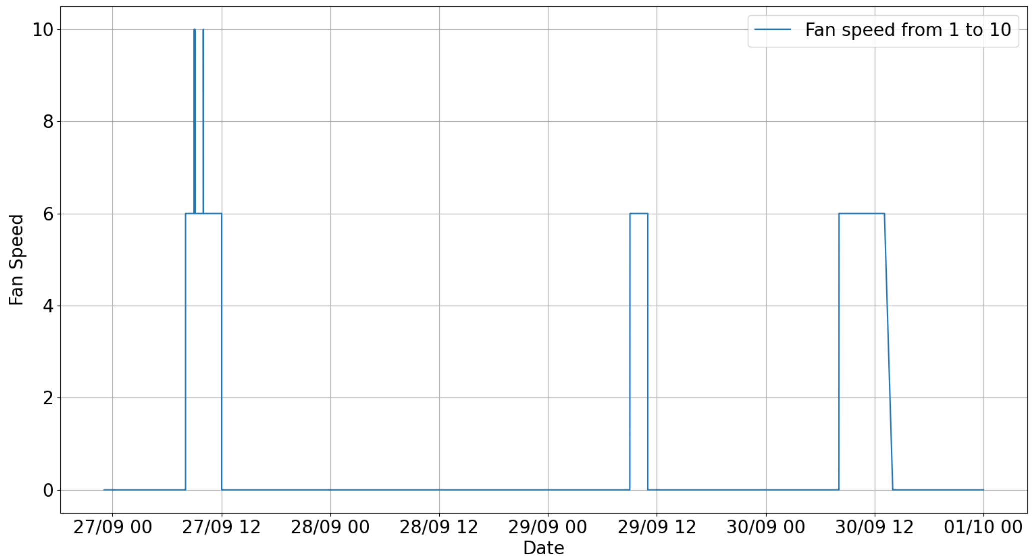

Figure 13.68: Ventilation rate of the mechanical ventilation system in the room $act201cc$ with the $1000ppm$ double threshold approach

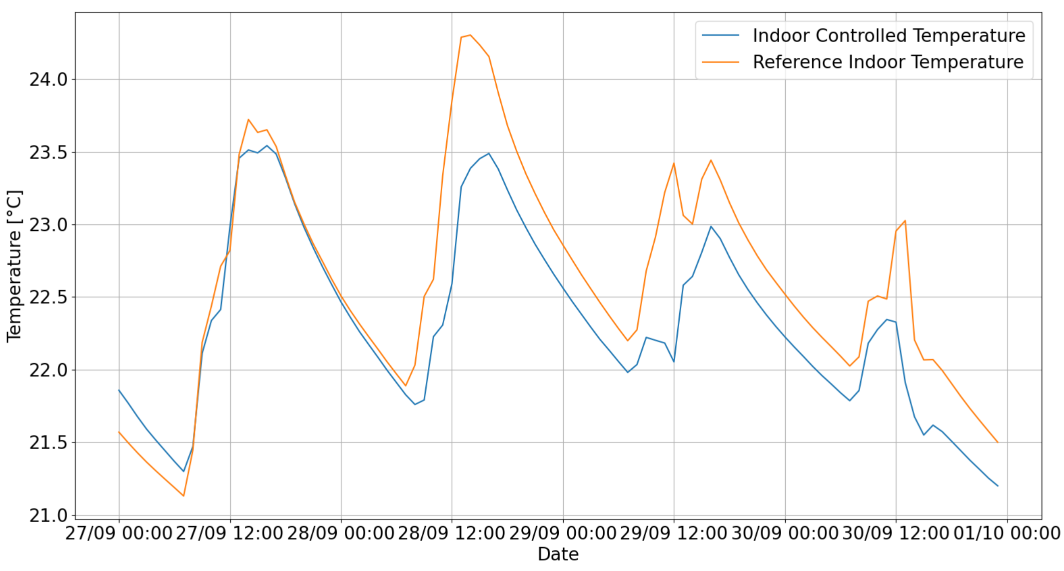

Figure 13.69: Temperature in the room $act201bc$ and in the reference one with the $1000ppm$ double threshold approach

14. Conclusions

In this thesis, several controls have been developed to simultaneously manage remotely and simulate the behavior of three mechanical ventilation units located in a school in Torre Pellice by implementing ventilative cooling and indoor air quality control strategies.

To pursue this aim, SOAP and Modbus protocols have been used as well as Python programming and EnergyPlus and DesignBuilder software.

During the first testing period, indoor air quality strategies were mainly simulated, while the ventilative cooling ones were implemented in the school with the support of a RaspberryPi board since, during July, the school was empty and the principal source of carbon dioxide production, the pupils, were absent. Conversely, the windows and shading conditions can be completely controlled, so it is well suited for ventilative cooling tests.

During the second testing period, in September, even the indoor air quality strategies were tested since the school was already occupied, so it became possible to compare the results of the simulated approaches with the monitored ones.

To simulate strategies that ensure good indoor air quality, a CO_2 concentration monitoring approach has been adopted, given that these sensors were already installed in the school. At first, the building model is exported and calibrated to follow the behavior of the actual building. Then, strategies used for indoor air quality control have been written using the EnergyPlus Runtime Language so that the resulting models can be simulated through EnergyPlus.

Monitored strategies are instead coded using Python and run through a RaspberryPi, which implements the Master of the Modbus communication, sending signals to the mechanical ventilation units to modify the fans' airflow.

14.1 Indoor Air Quality

Six different strategies based on carbon dioxide levels were simulated for indoor air quality monitoring, and two additional approaches were added during the on-site tests. For the results' analysis, the simulated strategies' outcomes were considered since the tests' environmental conditions were constant, and the uncertainty due to the occupation of the classrooms, which depends on the occupants' behaviors, was removed. Moreover, the simulated strategies were tested for long periods while the monitored ones, for thesis conclusion deadlines, were tested for only three days each, exposing the results to the influence of the randomness of atypical days, if present. In addition, the overall results obtained from the on-site tests confirm the outcomes of the simulations, which can then be used to draw the final conclusions.

It turns out that based on the intended goal, the choice of the best strategy is different. In particular:

- if the priority is to reduce the carbon dioxide as much as possible, at the expense of electric consumption, the ASHRAE 62 strategy should be chosen, given that it can keep the carbon dioxide concentration under $800ppm$, by ventilating for all the lesson time at relevantly high fluxes;
- if a healthy indoor condition is the main objective, but without wasting too much energy, all the single and double thresholds strategies can be employed, even though the single threshold ones with $800ppm$ and $1000ppm$ as lower threshold values have relevantly more on/off cycles of the mechanical ventilation unit, which can shorten its lifetime;
- if the priority is given to electrical consumption, then the single threshold strategy that uses $800ppm$ as lower threshold should be used, as it consumes at least half of the other approaches. In addition, from the tests emerged that even the $1000ppm$ single threshold strategy can be taken into account;

- if the objective is to minimize the number of switching on and off of the mechanical ventilation units, besides maintaining comfortable indoor conditions, the ASHRAE 62 or strategies that use a double threshold approach can be taken into account;
- if it is required to remove even pollutants produced by the building, the ASHRAE 62.1 standard should be used, even though it leads to a loss of internal heat and causes higher heating consumption. Moreover, this strategy is the one that consumes more compared to all the simulated and monitored ones because it never turns the mechanical ventilation off. An alternative approach that is not tested in this thesis is to ventilate even for the period before the occupation, in addition to the already scheduled ventilation used in the tested single or double threshold strategy, to remove all the pollutants before the pupils' arrival. In this way, less energy and indoor heat are wasted.

14.2 Ventilative Cooling

The main aim of ventilative cooling is to reduce the temperature of the internal environment to spare or entirely avoid higher conditioning costs. For this reason, electric consumption is not considered when considering ventilative cooling strategies. For the Italian weather in July in the location of the case study, the best approaches that guarantee an acceptable temperature reduction are the ones that include night ventilation, even though the night during that period are tropical nights and so not suited for really efficient night ventilation.

The overall best ventilation control strategy is the one that starts ventilating at 8:00 PM and keeps the ventilation rate to its maximum until 8:00 AM, while during the lesson time, it uses a single threshold temperature approach to cool the environment when the outdoor temperature is favorable. This strategy can reduce indoor temperatures by more than 1.2 degrees at maximum, while in any case, it reduces temperatures by much more than 0.5 degrees.

These results are not satisfactory if compared with the same simulated strategy during the same period, which can spare up to more than 5°C in the mornings and up to 3°C on average during lessons, so it is possible to infer some possible causes of the problem and a potential solution.

The two identified possible problems are:

1. the position of the temperature sensor within the classroom, since it can be influenced by local factors and thermal masses temperatures and since it is not sited at the center of the room as in the simulation;
2. the wrong operation of the mechanical ventilation unit, since the bypass can let the outdoor incoming air be influenced by the indoor one, or the amount of airflow actually injected within the room can be smaller, or the air of the exhaust fan can be mistakenly reintroduced by the intake fan.

After trying to figure out if the problem is the one mentioned in the first point by considering an ad-hoc sensor located above the mechanical ventilation unit, it has been found that it is more likely that the main problem of the ventilative cooling approaches is less related to the position of the sensor and more affected by the operation of the mechanical ventilation units, and by the problems expressed in the above-mentioned second point. Hence, for future applications, it is better to install single duct ventilation units or to increase the distance between inlet and outlet air vents to avoid the heat recovery mechanisms malfunctioning if ventilative cooling techniques want to be implemented.

14.3 Future Steps

In conclusion, to further improve and upgrade the studies of this thesis, the following directions are suggested:

- to overcome the limitations of the sensors update interval of one hour, real-time sensors for temperature, humidity, TVOCs, and all the other relevant environmental parameters can be installed directly on the RaspberryPi. In this way, real-time data are always available to decide control actions according to the current environmental conditions;

- add TVOC sensors in all the rooms to compare the concentration of indoor pollutants produced by building and furniture materials when using all the developed strategies and comparing the results with the reference room values. Moreover, the additional strategy of the morning purge for building-generated pollutants can be tested;
- if heat recovery bypass problems are present and ventilative cooling strategies are considered, the automatic control of the mechanical ventilation units can be integrated with an informed occupant manual ventilation approach. Using a screen to display messages or a led which turns on, it is possible to inform the user when the outdoor conditions are favorable to open the windows to cool the indoor environment more effectively;
- repeat all the indoor air quality monitored tests in a known and controlled situation, like with windows closed for the whole testing period, to have results not affected by the occupants' behavior.

Bibliography

[1] Ackerly, K., & Brager, G. (2013). Window signalling systems: control strategies and occupant behaviour. Building Research & Information, 41(3), 342-360.

[2] ANIT - Associazione Nazionale Isolamento Termico e Acustico, DPR 26 agosto 1993, n. 412 (G. U. n.96 del 14/10/1993). https://www.anit.it/wp-content/uploads/2015/03/DPR_412_93.pdf

[3] ASHRAE, A. (2002). Ashrae guideline 14: measurement of energy and demand savings. American Society of Heating, Refrigerating and Air-Conditioning Engineers, 35, 41-63.

[4] ASHRAE, (2013). Ventilation for Acceptable Indoor Air Quality. American Society of Heating, Refrigerating and Air-Conditioning Engineers.

[5] Bakó-Biró, Z., Clements-Croome, D. J., Kochhar, N., Awbi, H. B., & Williams, M. J. (2012). Ventilation rates in schools and pupils' performance. Building and environment, 48, 215-223.

[6] Bertero, M. (2020, October 30). Winecap™ data integration through SOAP web services. Capetti Elettronica.

[7] Bigladder software, EnergyPlus File Extensions, https://bigladdersoftware.com/epx/docs/8-2/getting-started/energyplus-file-extensions.html#:~:text=The%20input%20data%20file%20(IDF,descriptions%20of%20each%20file's%20features.

[8] Bigladder software, Group – Energy Management System (EMS), https://bigladdersoftware.com/epx/docs/8-0/input-output-reference/page-046.html

[9] Blasco, B. C., Moreno, J. J. M., Pol, A. P., & Abad, A. S. (2013). Using the R-MAPE index as a resistant measure of forecast accuracy. Psicothema, 25(4), 500-506.

[10] Borgeson, S., & Brager, G. (2008). Occupant control of windows: accounting for human behavior in building simulation.

[11] Breesch, H., Bossaer, A., & Janssens, A. (2005). Passive cooling in a low-energy office building. Solar Energy, 79(6), 682-696.

[12] Breesch, H., Merema, B., & Versele, A. (2018). Ventilative cooling in a school building: Evaluation of the measured performances. Fluids, 3(4), 68.

[13] Capetti, http://www.capetti.it

[14] Celsius, Climatic Zones. https://www.celsiuspanel.it/en/climatic-zones/

[15] Cerezo, C., Sokol, J., AlKhaled, S., Reinhart, C., Al-Mumin, A., & Hajiah, A. (2017). Comparison of four building archetype characterization methods in urban building energy modeling (UBEM): A residential case study in Kuwait City. Energy and Buildings, 154, 321-334.

[16] Chao, C. Y. H., & Hu, J. S. (2004). Development of a dual-mode demand control ventilation strategy for indoor air quality control and energy saving. Building and Environment, 39(4), 385-397.

[17] Chen, Y., Tong, Z., Wu, W., Samuelson, H., Malkawi, A., & Norford, L. (2019). Achieving natural ventilation potential in practice: Control schemes and levels of automation. Applied energy, 235, 1141-1152.

[18] Chiesa, G. (2020, December 18). Operational dynamic EPC specifications. E-DYCE. https://edyce.eu/wp-content/uploads/2021/01/E-DYCE_D1.2_Operational_dynamic_EPC_specifications_18.12.2020_Final.pdf

[19] Chiesa, G., Kolokotroni, M., & Heiselberg, P. (Eds.). (2021). Innovations in Ventilative Cooling. Cham, Switzerland: Springer.

[20] De Giuli, V., Da Pos, O., & De Carli, M. (2012). Indoor environmental quality and pupil perception in Italian primary schools. Building and Environment, 56, 335-345.

[21] Dell'Osso, G. R., Iannone, F., Pierucci, A., & Rinaldi, A. (2015, September). Control strategies of the natural ventilation for passive cooling for an existing residential building in Mediterranean climate. In Proceedings of the 36th AIVC-5th TightVent-3rd venticool Conference (pp. 396-405).

[22] DesignBuilder Italia, DesignBuilder V7, https://www.designbuilderitalia.it/

[23] Ding, E., Zhang, D., & Bluyssen, P. M. (2022). Ventilation regimes of school classrooms against airborne transmission of infectious respiratory droplets: A review. Building and Environment, 207, 108484.

[24] E-DYCE, E-DYCE The Dynamic Perspective of the Energy Performance Certification (EPC), www.edyce.eu

[25] Energy Saver, Energy Performance Ratings for Windows, Doors, and Skylights, https://www.energy.gov/energysaver/energy-performance-ratings-windows-doors-and-skylights#:~:text=Solar%20heat%20gain%20coefficient%20(SHGC,the%20greater%20its%20shading%20ability.

[26] EnergyPlus, https://energyplus.net/

[27] EPBD - Energy Performance of Buildings Directive, Implementation of the EPBD, Italy, Status in 2020. https://epbd-ca.eu/wp-content/uploads/2022/03/Implementation-of-the-EPBD-in-Italy-2020.pdf

[28] eppy, Welcome to eppy's documentation!, https://eppy.readthedocs.io/en/latest/

[29] European Commission, Horizon 2020: Details of the EU funding programme which ended in 2020 and links to further information, https://ec.europa.eu/info/research-and-innovation/funding/funding-opportunities/funding-programmes-and-open-calls/horizon-2020_en

[30] Fantozzi, F., Hamdi, H., Rocca, M., & Vegnuti, S. (2019). Use of automated control systems and advanced energy simulations in the design of climate responsive educational building for mediterranean area. Sustainability, 11(6), 1660.

[31] Fiorentini, M., Kokogiannakis, G., Jackson, W., Ma, Z., & Cooper, P. (2016). Evaluation methodology and implementation for natural ventilation control strategies.

[32] Fisk, W. J., & De Almeida, A. T. (1998). Sensor-based demand-controlled ventilation: a review. Energy and buildings, 29(1), 35-45.

[33] Flourentzou, F. (2021). Ventilative Cooling in Tertiary Buildings: A School Demo-Case and Parametric Analyses Under Swiss Climate Conditions (Central Europe). In Innovations in Ventilative Cooling (pp. 269-328). Springer, Cham.

[34] Foldbjerg, P., & Asmussen, T. (2013). Using ventilative cooling and solar shading to achieve good thermal environment in a Danish Active House. The REHVA European HVAC Journal, 50(3), 36-42.

[35] Gomis, L. L., Fiorentini, M., & Daly, D. (2021). Potential and practical management of hybrid ventilation in buildings. Energy and Buildings, 231, 110597.

[36] Gupta, L. (2021, September 30). REST – PUT vs POST. REST API Tutorial. https://restfulapi.net/rest-put-vs-post/

[37] Halderaker, I. D. (2016). Design and Energy Analysis of Natural and Hybrid Ventilation Strategies for Norwegian Office Buildings (Master's thesis, NTNU).

[38] Helty, Flow M800, https://www.heltyair.com/prodotti/vmc-community/flow-m800/

[39] Homod, R. Z., Sahari, K. S. M., & Almurib, H. A. (2014). Energy saving by integrated control of natural ventilation and HVAC systems using model guide for comparison. Renewable Energy, 71, 639-650.

[40] Kabirikopaei, A., & Lau, J. (2020). Uncertainty analysis of various CO_2-Based tracer-gas methods for estimating seasonal ventilation rates in classrooms with different mechanical systems. Building and Environment, 179, 107003.

[41] Kolokotroni, M., Webb, B. C., & Hayes, S. D. (1998). Summer cooling with night ventilation for office buildings in moderate climates. Energy and Buildings, 27(3), 231-237.

[42] Kolokotroni, M., & Aronis, A. (1999). Cooling-energy reduction in air-conditioned offices by using night ventilation. Applied energy, 63(4), 241-253.

[43] Kolokotsa, D., Pouliezos, A., Stavrakakis, G., & Lazos, C. (2009). Predictive control techniques for energy and indoor environmental quality management in buildings. Building and Environment, 44(9), 1850-1863.

[44] Laserlicht, (2019, July 3). File:Raspberry Pi 4 Model B - Top.jpg, Wikimedia Commons, https://commons.wikimedia.org/wiki/File:Raspberry_Pi_4_Model_B_-_Top.jpg

[45] Li, X., Wen, J., & Bai, E. W. (2016). Developing a whole building cooling energy forecasting model for on-line operation optimization using proactive system identification. Applied Energy, 164, 69-88.

[46] Lowther, S. D., Dimitroulopoulou, S., Foxall, K., Shrubsole, C., Cheek, E., Gadeberg, B., & Sepai, O. (2021). Low level carbon dioxide indoors—a pollution indicator or a pollutant? A health-based perspective. Environments, 8(11), 125.

[47] Lymath, A. (2015, February 01). What is a U-value? Heat loss, thermal mass and online calculators explained, NBS, https://www.thenbs.com/knowledge/what-is-a-u-value-heat-loss-thermal-mass-and-online-calculators-explained

[48] Martin, A., & Fletcher, J. (1996). Night cooling strategies. Final report, 11621(4).

[49] Modbus Organization. (2006). MODBUS Over Serial Line Specification & Implementation Guide: V1. 02. Modbus Organization. https://www.virtual-serial-port.org/it/article/what-is-serial-port/rs485-pinout/

[50] Mouser electronics, Sensirion SEK-SCD41 CO2 Sensor Evaluation Kit. https://www.mouser.it/new/sensirion/sensirion-sek-scd41-eval-kit/

[51] Mysen, M., Berntsen, S., Nafstad, P., & Schild, P. G. (2005). Occupancy density and benefits of demand-controlled ventilation in Norwegian primary schools. Energy and Buildings, 37(12), 1234-1240.

[52] Ng, M. O., Qu, M., Zheng, P., Li, Z., & Hang, Y. (2011). CO_2-based demand controlled ventilation under new ASHRAE Standard 62.1-2010: a case study for a gymnasium of an elementary school at West Lafayette, Indiana. Energy and Buildings, 43(11), 3216-3225.

[53] Persily, A. (2015). Challenges in developing ventilation and indoor air quality standards: The story of ASHRAE Standard 62. Building and Environment, 91, 61-69.

[54] Politecnico di Torino - E-DYCE - PRELUDE, PREDYCE documentation, PREDYCE. https://predyce.readthedocs.io/en/latest/index.html#

[55] PyModbus, Welcome to PyModbus's documentation!, https://pymodbus.readthedocs.io/en/latest/

[56] Raspberry Pi, Raspberry Pi OS, https://www.raspberrypi.com/software/

[57] Raspberry Pi, Raspberry Pi Documentation, https://www.raspberrypi.com/documentation/computers/configuration.html#setting-up-a-headless-raspberry-pi

[58] RealVNC, VNC® Connect consists of VNC® Viewer and VNC® Server, https://www.realvnc.com/en/connect/download/viewer/windows/

[59] Santamouris, M., Sfakianaki, A., & Pavlou, K. (2010). On the efficiency of night ventilation techniques applied to residential buildings. Energy and Buildings, 42(8), 1309-1313.

[60] Santos, A. Q., & Energy in Buildings and Communities Programme. Annex 67 Energy Flexible Buildings. (2019). Control strategies and algorithms for obtaining energy flexibility in buildings. Danish Technological Institute.

[61] Sensirion (2022, 24 June), Sensirion Raspberry Pi I2C SCD4x Driver. https://github.com/Sensirion/raspberry-pi-i2c-scd4x

[62] Sha, H., & Qi, D. (2020). Investigation of mechanical ventilation for cooling in high-rise buildings. Energy and Buildings, 228, 110440.

[63] Sha, H., Zhang, X., & Qi, D. (2021). Optimal control of high-rise building mechanical ventilation system for achieving low risk of COVID-19 transmission and ventilative cooling. Sustainable Cities and Society, 74, 103256.

[64] Sobolewski, A., Młynarczyk, M., Konarska, M., & Bugajska, J. (2021). The influence of air humidity on human heat stress in a hot environment. International Journal of Occupational Safety and Ergonomics, 27(1), 226-236.

[65] Stabile, L., Buonanno, G., Frattolillo, A., & Dell'Isola, M. (2019). The effect of the ventilation retrofit in a school on CO_2, airborne particles, and energy consumptions. Building and Environment, 156, 1-11.

[66] Sun, Z., Wang, S., & Ma, Z. (2011). In-situ implementation and validation of a CO2-based adaptive demand-controlled ventilation strategy in a multi-zone office building. Building and Environment, 46(1), 124-133.

[67] Tatham, S., Download PuTTY, PuTTY, https://www.putty.org/

[68] The Passive-On Project, The Passivhaus standard in European warm climates - Part 2: Italy. http://www.eerg.it/passive-on.org/CD/1.%20Technical%20Guidelines/Part%202/Passivhaus%20Italia/P-On-Part2-Italy-Guidelines-v2_1.pdf

[69] Tsai, D. H., Lin, J. S., & Chan, C. C. (2012). Office workers' sick building syndrome and indoor carbon dioxide concentrations. Journal of occupational and environmental hygiene, 9(5), 345-351.

[70] Van Paassen, A. H. C., Liem, S. H., & Groninger, B. P. (1998). Control of night cooling with natural ventilation: sensitivity analysis of control strategies and vent openings. In 19th AIVC conference ventilation technologies in urban areas: proceedings, Oslo, Norway, 28th-30th September 1998 (pp. 438-447). Air Infiltration and Ventilation Centre.

[71] Wachenfeldt, B. J., Mysen, M., & Schild, P. G. (2007). Air flow rates and energy saving potential in schools with demand-controlled displacement ventilation. Energy and buildings, 39(10), 1073-1079.

[72] Wang, S., & Xu, X. (2006). Parameter estimation of internal thermal mass of building dynamic models using genetic algorithm. Energy conversion and management, 47(13-14), 1927-1941.

[73] Waveshare, (2018, December 21). RS485 CAN HAT User Manual, https://www.waveshare.com/w/upload/2/29/RS485-CAN-HAT-user-manuakl-en.pdf

[74] Willmott, C. J., & Matsuura, K. (2005). Advantages of the mean absolute error (MAE) over the root mean square error (RMSE) in assessing average model performance. Climate research, 30(1), 79-82.

[75] Yang, X. B., Jin, X. Q., Du, Z. M., Fan, B., & Chai, X. F. (2011). Evaluation of four control strategies for building VAV air-conditioning systems. Energy and Buildings, 43(2-3), 414-422.

[76] ZeroTier, Securely Connect Any Device, Anywhere, https://www.zerotier.com/